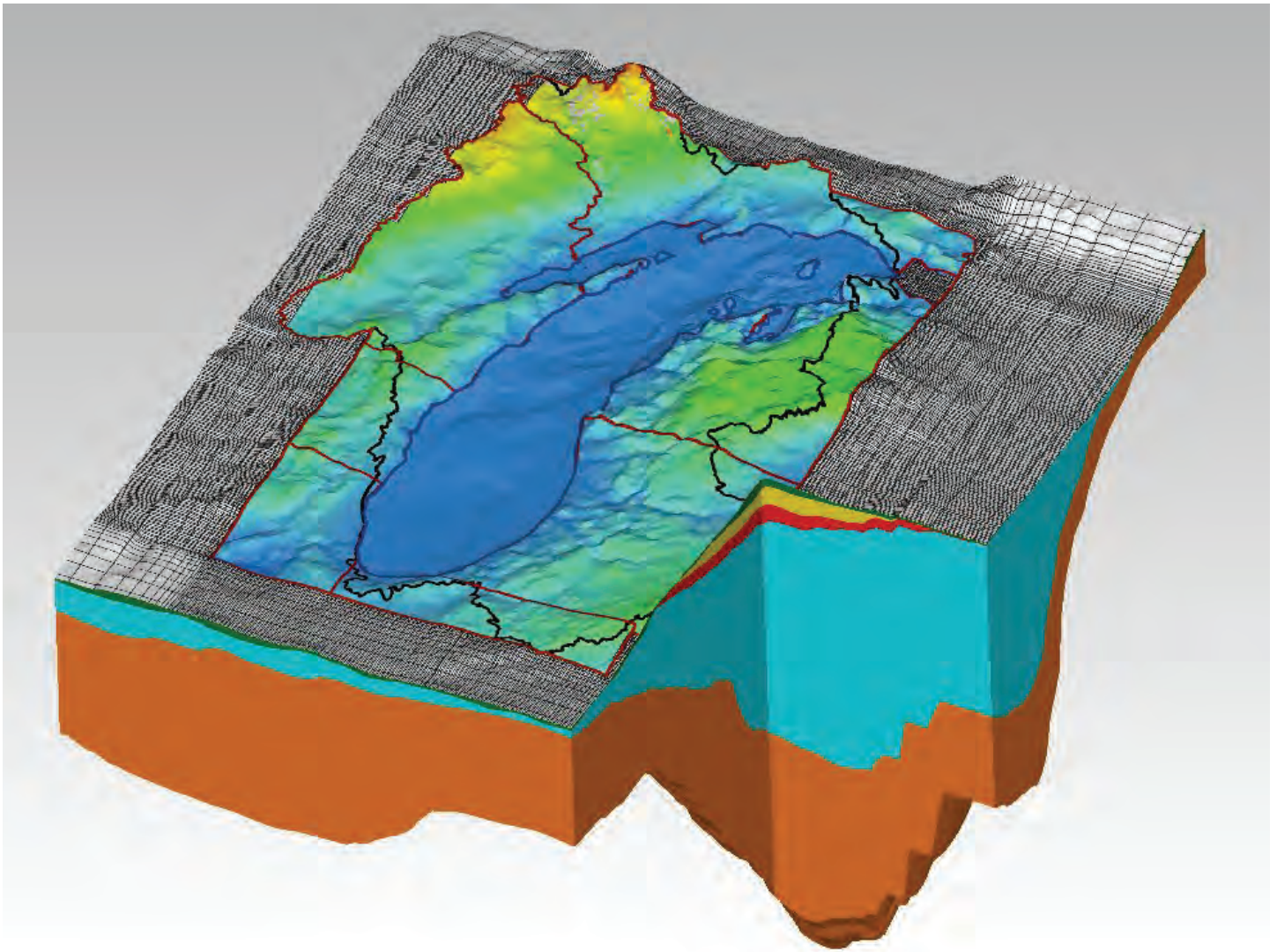


National Water Availability and Use Pilot Program

Regional Groundwater-Flow Model of the Lake Michigan Basin in Support of Great Lakes Basin Water Availability and Use Studies



Scientific Investigations Report 2010–5109

Cover: Block diagram of groundwater-flow model domain showing, in section, the aquifer systems; and in plan view, the Lake Michigan Basin drainage boundary, model subregion boundaries, simulated predevelopment nearfield water-table surface, and farfield grid. (Graphic by David C. Lampe, U.S. Geological Survey, Indianapolis, Indiana.)

Regional Groundwater-Flow Model of the Lake Michigan Basin in Support of Great Lakes Basin Water Availability and Use Studies

By D.T. Feinstein, R.J. Hunt, and H.W. Reeves

National Water Availability and Use Pilot Program

Scientific Investigations Report 2010–5109

**U.S. Department of the Interior
U.S. Geological Survey**

U.S. Department of the Interior
KEN SALAZAR, Secretary

U.S. Geological Survey
Marcia K. McNutt, Director

U.S. Geological Survey, Reston, Virginia: 2010

For more information on the USGS—the Federal source for science about the Earth, its natural and living resources, natural hazards, and the environment, visit <http://www.usgs.gov> or call 1-888-ASK-USGS

For an overview of USGS information products, including maps, imagery, and publications, visit <http://www.usgs.gov/pubprod>

To order this and other USGS information products, visit <http://store.usgs.gov>

Any use of trade, product, or firm names is for descriptive purposes only and does not imply endorsement by the U.S. Government.

Although this report is in the public domain, permission must be secured from the individual copyright owners to reproduce any copyrighted materials contained within this report.

Suggested citation:

Feinstein, D.T., Hunt, R.J., and Reeves, H.W., 2010, Regional groundwater-flow model of the Lake Michigan Basin in support of Great Lakes Basin water availability and use studies: U.S. Geological Survey Scientific Investigations Report 2010–5109, 379 p.

Acknowledgments

Because of its size and complexity, the Lake Michigan Basin model depended on contributions from a large team of geologists and hydrologists for its development. The authors were fortunate to collaborate with many other USGS scientists:

- At the Indiana Water Science Center (WSC): Dave Lampe, who developed the stratigraphic and salinity databases and many illustrations; Leslie Arihood, who developed the glacial database; and E. Randall Bayless and Bret Robinson, who characterized Lake Michigan sediments.
- At the Michigan WSC: Christopher Hoard, Edward Bissell, Stephen Aichele, and Brian Neff, who developed the surface-water network database; Carol Luukkonen, who developed part of the water-use database with the assistance of Cynthia Rachol; Lori Fuller, who lent her considerable graphics skills; and J.R. Nicholas, generous with counsel.
- At the Illinois WSC: Patrick Mills, who is especially thanked for preparing a library of references.
- At the Wisconsin WSC: Cheryl Buchwald, who developed part of the water-use database; Stephen Westenbroek, who developed the recharge database; John Walker, who provided statistical expertise; and James Kennedy, Jennifer Bruce, and Laura Nelson, who assisted with GIS and with table preparation.

Two USGS colleagues, Richard Yager (New York WSC) and Bruce Campbell (South Carolina WSC), dedicated considerable time to fashioning exceptionally thorough and thought-provoking reviews of this report. Their efforts were complemented by helpful editorial assistance from Michelle Greenwood in the USGS Wisconsin WSC and by an able editorial review from Michael Eberle of the USGS Enterprise Publishing Network, Columbus Publishing Service Center.

The USGS Office of Groundwater guided the construction and interpretation of the groundwater-flow model. We were fortunate to benefit from the advice of Arlen Harbaugh, Thomas Reilly, Kevin Dennehy, and William Alley. Equally valuable was expert guidance from senior USGS scientists Christian Langevin, Edward Banta, Claudia Faunt, Suzanne Paschke, Rodney Sheets, and Michael Fienen. We are also grateful to USGS hydrologists James Krohelski, Glenn Hodgkins, Norman Grannemann, Warren Gebert, and Eric Evenson, and to USGS scientists Steven Colman and David Foster at the Woods Hole Coastal and Marine Science Center for their extensive knowledge of surface-water and groundwater conditions in the Great Lakes Basin. With respect to the geology of the Michigan Basin, we were fortunate to benefit from ongoing interpretive studies of the sedimentary sequence by USGS geologists Christopher Swezey and Joseph Hatch.

Special thanks are due to colleagues outside the USGS who were always generous in sharing knowledge and resources. We relied on interactions with several prominent glacial geologists: David Mickelson (University of Wisconsin-Madison, emeritus), Thomas Hooyer (formerly of the Wisconsin Geological and Natural History Survey, now at the University of Wisconsin-Milwaukee), John Attig (Wisconsin Geological and Natural History Survey), Kevin Kincare (formerly Michigan Geological Survey, now at the USGS), David Lusch (Michigan State University), and Steve Brown (formerly of the Indiana Geological Survey, now at the Illinois State Geological Survey). In characterizing Lake Michigan sediments we drew heavily on exchanges with Brian Eadie (Great Lakes Environmental Research Laboratory) and Richard Cahill (Illinois State Geological Survey). The project also benefited repeatedly from collaboration with two teams of hydrogeologists: Scott Meyer, Douglas Walker, Yu-Feng Lin, and Allen Wehrmann of the Illinois State Water Survey, and Kenneth Bradbury, David Hart, and Madeline Gotkowitz of the Wisconsin Geological and Natural History Survey.

Contents

Acknowledgments	iii
Abstract	1
1. Introduction.....	2
1.1 Purpose and Scope	2
1.2 Description of Study Area	3
1.3 Water Use In and Around the Lake Michigan Basin	11
1.4 Saline Groundwater in the Lake Michigan Basin.....	11
1.5 Previous Hydrogeologic Investigations and Modeling Studies.....	17
2. Data and Methods	20
2.1 Data Sources.....	20
2.1.1 Hydrostratigraphic Units and Model Layering.....	20
2.1.2 Hydrogeologic Properties of Aquifers and Confining Units.....	20
2.1.3 Recharge	21
2.1.4 Surface-Water Network.....	21
2.1.5 Groundwater Withdrawals.....	21
2.1.6 Salinity	21
2.1.7 Water Levels.....	21
2.1.8 Groundwater Discharge to Streams and Lake Michigan	22
2.1.9 Lakebed of Lake Michigan	22
2.2 Databases and Algorithms.....	22
2.2.1 Hydrostratigraphic Units	22
2.2.2 Thickness and Properties of Quaternary Deposits	24
2.2.3 Distribution of Glacial Categories in Wisconsin and Michigan	25
2.2.4 Groundwater Withdrawals.....	25
2.2.5 Illinois Water-Use Information.....	25
2.2.6 Distribution of Salinity.....	25
2.2.7 Numerical Codes	25
2.2.7.1 Calculation of Historical Recharge	26
2.2.7.2 Simulation of Variable-Density Groundwater Flow.....	26
2.2.7.3 Parameter Estimation by Nonlinear Regression	26
3. Conceptual Model of Regional Groundwater System	26
3.1 Hydrogeologic Framework.....	27
3.2 Regional Flow System	34
3.3 Sources and Sinks	34
3.4 Groundwater/Surface-Water Interactions.....	37
3.5 Role of Salinity.....	38
3.6 Confined and Unconfined Conditions.....	38

4. Model Construction.....	39
4.1 Model Grid.....	39
4.2 Model Layering.....	41
4.3 Stress Periods	68
4.4 Farfield Boundary Conditions	69
4.4.1 No Flow.....	69
4.4.2 Constant Head	71
4.4.3 General-Head Conditions	71
4.4.4 Specified Flux	71
4.5 Nearfield Surface-Water Network	73
4.5.1 Inland Surface-Water Network.....	73
4.5.2 Lake Michigan and Lake Winnebago.....	79
4.5.3 Summary of Farfield and Nearfield Surface-Water Inputs.....	79
4.6 Recharge	79
4.7 Well Withdrawals	85
4.7.1 Database Limitations.....	85
4.7.2 Transfer of Database to Model.....	86
4.7.3 Pumping Totals in Model	86
4.8 Hydraulic Conductivity.....	90
4.8.1 QRNR Deposits Below Inland Areas	90
4.8.2 QRNR Layers Below Lake Michigan and Farfield Lakes.....	102
4.8.3 Bedrock Hydraulic Conductivity and Transmissivity of Aquifer Systems.....	108
4.9 Storage	110
4.10 Salinity	115
4.11 Model Input Packages, Program Executable, and Graphical Interface.....	118
5. Model Calibration.....	119
5.1 Linearization of Flow Equation.....	119
5.2 Calibration Parameters.....	123
5.3 Calibration Targets.....	123
5.3.1 Target Composition.....	124
5.3.2 Target Filtering.....	133
5.3.3 Target Weights and Bounds.....	133
5.4 Regularized Inversion Techniques.....	134
5.4.1 Pilot Points	134
5.4.2 Tikhonov Regularization.....	135
5.4.3 Singular Value Decomposition	135
5.4.4 Integrity of Derivatives.....	135
5.5 Calibration Results.....	137
5.5.1 Model Fit.....	137
5.5.2 Estimated Parameter Values.....	139
5.6 Parameter Sensitivity.....	147

6. Model Results.....	150
6.1 Water Levels and Drawdown	150
6.2 Lake Michigan Basin Water Budget.....	163
6.3 Groundwater Flow Rates and Patterns.....	167
6.4 Sources of Water to Pumping Wells	173
6.5 Regional Groundwater Divides.....	181
6.6 Groundwater Interactions with Lake Michigan.....	197
7. Alternative Conceptual Models and Model Sensitivity.....	208
7.1 Alternative Models	208
7.1.1 Unconfined Version of Model	208
7.1.2 Uniform-Density Simulation	215
7.1.3 Active-Transport Simulation	219
7.2 Model Sensitivity.....	221
7.2.1 Farfield Boundary Conditions	221
7.2.2 Parameter Values	221
7.2.3 Grid Spacing	225
8. Model Limitations and Suggestions for Future Work	229
9. Summary and Conclusions.....	233
10. References.....	235
Appendix 1. Geohydrologic Framework	249
Appendix 2. Inland Surface-Water Network	259
Appendix 3. Power Law for Horizontal Hydraulic Conductivity of QRNR Deposits.....	271
Appendix 4. Initial Bedrock Hydraulic Conductivity	273
Appendix 5. Calibration Parameters	283
Appendix 6. Initial and Calibrated Input for Hydraulic-Conductivity Zones	303
Appendix 7. Base-Flow Calibration Targets.....	359
Appendix 8. Comparison of Measured and Simulated Values at Calibration Targets	371
Appendix 9. Geometric Means of Hydraulic-Conductivity Values, by Aquifer System, for Initial and Calibrated Models.....	375

Figures

1.	Chart showing Great Lake Basin pilot investigations and reports structure	3
2–9.	Maps showing:	
2.	Location of study area	4
3.	Model nearfield and subregions	5
4.	Land use/land cover in model nearfield	8
5.	Population distribution in model nearfield	9
6.	Land-surface and lakebed altitude in model nearfield	10
7A.	Major surface-water basins in model domain	12
7B.	Major rivers in model domain	13
7C.	Major level 3 and 4 hydrologic units in model domain	14
8A.	Uppermost bedrock units in the study area	15
8B.	Uppermost bedrock structural features in the study area	16
9.	Estimated 1995 groundwater-withdrawal rates for major metropolitan areas in the U.S. part of the Great Lakes Basin	17
10.	Composite section showing time- and rock-stratigraphic framework and nomenclature for the Lake Michigan Basin region correlated with the hydrogeologic units and aquifer systems in the groundwater model	23
11.	Map showing principal bedrock aquifers	28
12–18.	Schematics showing:	
12.	Hydrostratigraphy in southeastern Wisconsin, northeastern Wisconsin, and northeastern Illinois	30
13.	Hydrostratigraphy in the Upper Peninsula, Michigan	31
14.	Hydrostratigraphy in northern Indiana	32
15.	Hydrostratigraphy in the northern and southern Lower Peninsula, Michigan	33
16.	Flow system and aquifer systems	35
17.	Shallow and deep parts of flow system: Predevelopment and postdevelopment	36
18.	Effect of excluding low-order streams from model input	38
19–21.	Maps showing:	
19.	Model grid	40
20A.	Thickness of hydrogeologic units: Quaternary deposits (QRNR = layers 1–3)	45
20B.	Thickness of hydrogeologic units: Jurassic red beds (JURA = layer 4)	46
20C.	Thickness of hydrogeologic units: Upper Pennsylvanian sandstone (PEN1 = layer 5)	47
20D.	Thickness of hydrogeologic units: Lower Pennsylvanian sandstone, limestones, and shales (PEN2 = layer 6)	48
20E.	Thickness of hydrogeologic units: Michigan Formation shale (MICH = layer 7)	49
20F.	Thickness of hydrogeologic units: Marshall Sandstone (MSHL = layer 8)	50
20G.	Thickness of hydrogeologic units: Devonian-Mississippian shale (DVMS = layer 9)	51

20H.	Thickness of hydrogeologic units: Silurian-Devonian carbonate and evaporites (SLDV = layers 10–12).....	52
20I.	Thickness of hydrogeologic units: Maquoketa shale (MAQU = layer 13).....	53
20J.	Thickness of hydrogeologic units: Sinnipee dolomite (SNNP = layer 14).....	54
20K.	Thickness of hydrogeologic units: St. Peter sandstone (STPT = layer 15).....	55
20L.	Thickness of hydrogeologic units: Prairie du Chien dolomite and Franconia sandstone/shale (PCFR = layer 16).....	56
20M.	Thickness of hydrogeologic units: Ironton-Galesville sandstone (IRGA = layer 17).....	57
20N.	Thickness of hydrogeologic units: Eau Claire sandstone/shale (EACL = layer 18).....	58
20O.	Thickness of hydrogeologic units: Mount Simon sandstone (MTSM = layers 19, 20).....	59
21.	Traces for two north/south and four west/east hydrogeologic cross sections.....	60
22–25.	Geologic cross sections showing:	
22A.	Layering along model column 48.....	61
22B.	Layering along model column 204.....	62
23A.	Layering along model row 80.....	63
23B.	Layering along model row 170.....	64
23C.	Layering along model row 260.....	65
23D.	Layering along model row 350.....	66
24.	Aquifer systems along model rows.....	67
25.	Major confining units along model row 170.....	68
26–29.	Maps showing:	
26.	No-flow and constant-head boundary conditions.....	70
27.	General-head and specified-flux boundary conditions.....	72
28A.	Streams represented in model.....	75
28B.	Water bodies represented in model.....	76
29A.	Example surface-water network without model RIV cells.....	77
29B.	Example surface-water network with model RIV cells.....	78
30.	Graph showing recharge trends for the inland nearfield area of the model.....	81
31A–C.	Maps showing:	
31A.	Recharge distribution: 1901–20.....	82
31B.	Recharge distribution: 1971–75.....	83
31C.	Recharge distribution: 1991–2005.....	84
32.	Graph showing total nearfield and farfield pumping through time.....	89
33.	Graphs showing nearfield pumping through time by subregion, water-use category, and aquifer system.....	91

34–37.	Maps showing:	
34A.	Spatial distribution of pumping by water-use category: 1941–50.....	92
34B.	Spatial distribution of pumping by water-use category: 1976–80.....	93
34C.	Spatial distribution of pumping by water-use category: 2001–5.....	94
35A.	Spatial distribution of shallow Quaternary, shallow bedrock, and deep bedrock wells: 1941–50.....	95
35B.	Spatial distribution of shallow Quaternary, shallow bedrock, and deep bedrock wells: 1976–80.....	96
35C.	Spatial distribution of shallow Quaternary, shallow bedrock, and deep bedrock wells: 2001–5.....	97
36A.	Glacial categories in model layer 1	99
36B.	Glacial categories in model layer 2	100
36C.	Glacial categories in model layer 3	101
37A.	Coarse fraction in model layer 1	103
37B.	Coarse fraction in model layer 2	104
37C.	Coarse fraction in model layer 3	105
38.	Graphs showing relation of initial hydraulic conductivity values to coarse fraction, by glacial category	106
39–41.	Maps showing:	
39.	Initial horizontal hydraulic conductivity distribution in nearfield area of model layer 1	107
40.	Hydraulic conductivity zones under Lake Michigan	108
41A.	Initial transmissivity distribution in aquifer system QRNR.....	109
41B.	Initial transmissivity distribution in aquifer system PENN.....	111
41C.	Initial transmissivity distribution in aquifer system MSHL	112
41D.	Initial transmissivity distribution in aquifer system SLDV.....	113
41E.	Initial transmissivity distribution in aquifer system C-O.....	114
42.	Geologic cross section showing initial vertical hydraulic conductivities in major confining units, row 170.....	115
43.	Geologic cross sections showing fixed salinity distribution along selected model rows	117
44.	Boxplots showing Jacobean derivatives for vertical hydraulic conductivity in the Maquoketa confining unit.....	121
45–48.	Maps showing:	
45A.	Spatial distribution of calibration targets: USGS network wells, household wells, and contour-derived targets, providing predevelopment water-level targets	127
45B.	Spatial distribution of calibration targets: USGS network wells, providing postdevelopment water-level targets	128
45C.	Spatial distribution of calibration targets: USGS network wells as well as RASA packer tests from the early 1980s, providing vertical-head-difference calibration targets.....	129
45D.	Spatial distribution of calibration targets: Multiple readings from USGS network wells supplemented by targets based on differences between contour maps over time, providing head change (drawdown and drawup) targets.....	130

45E.	Spatial distribution of calibration targets: USGS streamgages, providing base-flow calibration targets	131
45F.	Spatial distribution of calibration targets: household wells, providing postdevelopment water-level targets	132
46.	Pilot point locations and calibration results for vertical hydraulic conductivity of the Maquoketa confining unit.....	136
47.	Calibrated horizontal hydraulic conductivity distribution in nearfield area of model layer 1.....	140
48A.	Calibrated transmissivity distribution in aquifer system QRNR	142
48B.	Calibrated transmissivity distribution in aquifer system PENN	143
48C.	Calibrated transmissivity distribution in aquifer system MSHL.....	144
48D.	Calibrated transmissivity distribution in aquifer system SLDV	145
48E.	Calibrated transmissivity distribution in aquifer system C-O	146
49.	Geologic cross section showing calibrated vertical hydraulic conductivity values for major confining units, row 170.....	141
50.	Graphs showing composite sensitivities of calibration targets to eight parameter groups for confined (SLMB-C) calibration and unconfined (SLMB-U) calibration	147
51A–E.	Maps showing:	
51A.	Simulated predevelopment water levels for QRNR aquifer system.....	151
51B.	Simulated predevelopment water levels for PENN aquifer system.....	152
51C.	Simulated predevelopment water levels for MSHL aquifer system	153
51D.	Simulated predevelopment water levels for SLDV aquifer system.....	154
51E.	Simulated predevelopment water levels for C-O aquifer system.....	155
52.	Geologic cross sections showing simulated drawdown in 2005 along selected west/east cross sections	156
53–55A.	Maps showing:	
53A.	Simulated drawdown in Marshall aquifer, 1950	157
53B.	Simulated drawdown in Marshall aquifer, 1980	158
53C.	Simulated drawdown in Marshall aquifer, 2005	159
54A.	Simulated drawdown in Ironton-Galesville aquifer, 1950	160
54B.	Simulated drawdown in Ironton-Galesville aquifer, 1980	161
54C.	Simulated drawdown in Ironton-Galesville aquifer, 2005	162
55A.	Selected pumping centers.....	164
55B–57.	Graphs showing:	
55B.	Simulated water-levels at selected pumping centers.....	165
56.	Simulated groundwater budget, by stress period, for Lake Michigan Basin	165
57.	Simulated groundwater sources and sinks in Lake Michigan Basin for predevelopment (1864) and 2001–5 periods	166
58.	Map showing simulated flow rate (Darcy flow) in model layer 1 for predevelopment conditions	168
59.	Geologic cross sections showing simulated flow rate (Darcy flow) along selected west/east cross sections for 2005 conditions	169

60A–B.	Graphs showing:	
60A.	Simulated lateral flux by aquifer system in subregions east of Lake Michigan for predevelopment and 2005 conditions	170
60B.	Simulated lateral flux by aquifer system in subregions west of Lake Michigan for predevelopment and 2005 conditions	171
61–63.	Maps showing:	
61.	Uppermost aquifer system in deep part of flow system	172
62A.	Simulated downward leakage to uppermost aquifer system in deep part of flow system as percent of recharge: Predevelopment	174
62B.	Simulated downward leakage to uppermost aquifer system in deep part of flow system as percent of recharge: 2005.....	175
63A.	Simulated contributing areas to aquifer-system sinks in 2005	176
63B.	Simulated contributing areas to pumping wells in 2005	177
64.	Schematic showing simulated flow direction and magnitude along west/east cross section in NE_ILL: Predevelopment and 2005.....	179
65–67.	Graphs showing:	
65A.	Sources of water to wells by subregion in 2005: Shallow part of flow system.....	182
65B.	Sources of water to wells by subregion in 2005: Deep part of flow system.....	183
66.	Sources of water to wells for Lake Michigan Basin: 1941–50, 1976–80, and 2001–5	184
67.	Sources of water to wells for model nearfield: 1941–50, 1976–80, and 2001–5	185
68–69.	Maps showing:	
68A.	Simulated groundwater basins, by aquifer system, for predevelopment conditions: QRNR (layer 1)	187
68B.	Simulated groundwater basins, by aquifer system, for predevelopment conditions: PENN (layer 5)	188
68C.	Simulated groundwater basins, by aquifer system, for predevelopment conditions: MSHL (layer 8).....	189
68D.	Simulated groundwater basins, by aquifer system, for predevelopment conditions: SLDV (layer 10)	190
68E.	Simulated groundwater basins, by aquifer system, for predevelopment conditions: C-O (layer 17)	191
69A.	Simulated groundwater basins, by aquifer system, for 1991–2005 conditions: QRNR (layer 1)	192
69B.	Simulated groundwater basins, by aquifer system, for 1991–2005 conditions: PENN (layer 5)	193
69C.	Simulated groundwater basins, by aquifer system, for 1991–2005 conditions: MSHL (layer 8).....	194
69D.	Simulated groundwater basins, by aquifer system, for 1991–2005 conditions: SLDV (layer 10)	195
69E.	Simulated groundwater basins, by aquifer system, for 1991–2005 conditions: C-O (layer 17)	196

70.	Graph showing percentage of total direct discharge to Lake Michigan for nearshore rings.....	198
71–72.	Maps showing:	
71.	Simulated contributing areas for direct discharge to nearshore of Lake Michigan: Predevelopment and 1991–2005	198
72A.	Simulated shoreline outflow (from groundwater to Lake Michigan): Predevelopment.....	199
72B.	Simulated shoreline inflow (from Lake Michigan to groundwater): Predevelopment.....	200
72C.	Simulated shoreline outflow (from groundwater to Lake Michigan): 1980.....	201
72D.	Simulated shoreline inflow (from Lake Michigan to groundwater): 1980	202
72E.	Simulated shoreline outflow (from groundwater to Lake Michigan): 2005.....	203
72F.	Simulated shoreline inflow (from Lake Michigan to groundwater): 2005	204
73.	Graphs showing simulated 2005 water budgets in Lake Michigan Basin: base model (SLMB-C) versus alternative unconfined model (SLMB-U).....	210
74.	Graphs showing simulated water-level hydrographs at pumping centers: base model (SLMB-C) versus alternative unconfined model (SLMB-U) and alternative uniform-density model (MLMB-C)	212
75.	Maps showing simulated dewatering at top of Cambrian-Ordovician aquifer system as a result of pumping: base model versus alternative unconfined model for 1980 and 2005.....	214
76.	Graphs showing simulated 2005 water budgets in Lake Michigan Basin: base model (SLMB-C) versus alternative uniform-density model (MLMB-C).....	216
77A.	Map showing simulated 1991–2005 groundwater basins for C-O aquifer system: Base model	217
77B.	Map showing simulated 1991–2005 ground-water basins for C-O aquifer system: Alternative uniform-density model	218
78–81.	Graphs showing:	
78.	Simulated 2005 water budgets in Lake Michigan Basin: base model (SLMB-CF3) versus alternative active transport model (SLMB-CT3)	220
79.	Simulated water-level hydrographs at pumping centers: base model (SLMB-CF3) versus alternative active transport model (SLMB-CT3)	220
80.	Comparison of simulated predevelopment water levels at selected pumping centers: base model versus sensitivity models	224
81.	Comparison of simulated drawdown at selected pumping centers: base model versus sensitivity models.....	224
82–84.	Maps showing:	
82.	Locations and results for shoreline inset models	226
83A.	Representation of inset area in SLP_MI: regional model.....	227
83B.	Representation of inset area in SLP_MI: inset model with refined grid	227
83C.	Representation of inset area in SLP_MI: inset model with refined grid and refined surface water.....	228
84.	Demonstration area for inset models with grid refinement	232

Tables

1.	Abbreviations used in this report.....	6
2.	Altitude and relief in model nearfield.....	7
3A.	Model layering: Correlation between model layers and hydrogeologic units and aquifer systems.....	42
3B.	Model layering: Layering logic for QRNR, SLDV, and MTSM layers.....	43
4.	Thickness statistics of hydrogeologic units in model nearfield.....	44
5.	Stress period setup for model.....	69
6.	Surface-water boundary conditions.....	80
7.	Number of pumping wells by subregion, water-use category, and aquifer system.....	87
8.	Pumping by stress period and aquifer system.....	87
9A.	Shallow and deep withdrawals through time for entire model domain.....	98
9B.	Percentages of withdrawals by state for 2001–5 in model nearfield.....	98
10.	Percentage of model nearfield that is saline west and east of Lake Michigan.....	118
11A.	Calibration target sets and target groups for model calibration: Confined conditions.....	125
11B.	Calibration target sets and target groups for model calibration: Unconfined conditions.....	126
12.	Confined and unconfined model calibration statistics for weighted targets and for driller-log targets.....	138
13A.	Composite sensitivities by parameter groups for confined calibration (SLMB-C).....	148
13B.	Composite sensitivities by parameter groups for unconfined calibration (SLMB-U).....	149
14.	Relative magnitude of recharge, simulated direct discharge to Lake Michigan, and withdrawals by pumping, predevelopment through 2005.....	166
15.	Time of travel to pumping wells, by aquifer system.....	178
16.	Sources of water to pumping wells within Lake Michigan Basin.....	180
17.	Predevelopment groundwater discharge to offshore Lake Michigan.....	197
18.	Effect of nearfield pumping on simulated direct groundwater discharge to Lake Michigan.....	206
19.	Effect of nearfield pumping on total (direct plus indirect) groundwater discharge to Lake Michigan.....	207
20A.	Percentage of nearfield active cells in aquifer system with predevelopment water level more than 20 feet HIGHER in alternative models relative to SLMB-C.....	211
20B.	Percentage of nearfield active cells in aquifer system with predevelopment water level more than 20 feet LOWER in alternative models relative to SLMB-C.....	211

21A. Percentage of nearfield active cells with 2005 drawdown more than 20 feet GREATER in alternative models relative to SLMB-C.....212

21B. Percentage of nearfield active cells with 2005 drawdown more than 20 feet LESS in alternative models relative to SLMB-C.....212

22. East and west components of flow under shores of Lake Michigan between latitude of cities of Green Bay and Chicago: comparison of SEAWAT-2000 to MODFLOW-2000216

23A. Percentage of nearfield active cells in aquifer system with predevelopment water level more than 20 feet HIGHER in model sensitivity simulations relative to SLMB-C.....222

23B. Percentage of nearfield active cells in aquifer system with predevelopment water level more than 20 feet LOWER in model sensitivity simulations relative to SLMB-C.....222

24A. Percentage of nearfield active cells in aquifer system with 2005 drawdown more than 20 feet GREATER in model sensitivity simulations relative to SLMB-C223

24B. Percentage of nearfield active cells in aquifer system with 2005 drawdown more than 20 feet LESS in model sensitivity simulations relative to SLMB-C223

Appendix Figures

1–2 to 2–1. Maps showing:	
1–1. Glacial lobes in model area.....	250
1–2. Texture of surficial tills.....	251
2–1. Location of USGS streamgages in Michigan used to determine relation between Arbolate sum (upstream distance) and stream width.....	265
2–2. Graph showing relation between Arbolate sum (upstream distance) and observed stream width at USGS streamgages in Michigan	266
6A–1A to 6B–9B. Maps showing:	
6A–1A. Horizontal hydraulic conductivity, upper QRNR including Lake Michigan lakebed: zonation	305
6A–1B. Horizontal hydraulic conductivity, upper QRNR including Lake Michigan lakebed: calibrated input	306
6A–2A. Horizontal hydraulic conductivity, middle QRNR: zonation.....	308
6A–2B. Horizontal hydraulic conductivity, middle QRNR: calibrated input	309
6A–3A. Horizontal hydraulic conductivity, lower QRNR: zonation	311
6A–3B. Horizontal hydraulic conductivity, lower QRNR: calibrated input	312
6A–4A. Horizontal hydraulic conductivity, PEN1: zonation.....	314
6A–4B. Horizontal hydraulic conductivity, PEN1: calibrated input.....	315
6A–5A. Horizontal hydraulic conductivity, MSHL: zonation	317
6A–5B. Horizontal hydraulic conductivity, MSHL: calibrated input	318
6A–6A. Horizontal hydraulic conductivity, upper SLDV: zonation	320
6A–6B. Horizontal hydraulic conductivity, upper SLDV: calibrated input	321
6A–7A. Horizontal hydraulic conductivity, STPT: zonation	323
6A–7B. Horizontal hydraulic conductivity, STPT: calibrated input	324
6A–8A. Horizontal hydraulic conductivity, IRGA: zonation	326
6A–8B. Horizontal hydraulic conductivity, IRGA: calibrated input	327
6A–9A. Horizontal hydraulic conductivity, upper MTSM: zonation.....	329
6A–9B. Horizontal hydraulic conductivity, upper MTSM: calibrated input	330

6B-1A.	Vertical hydraulic conductivity, upper QRNR including Lake Michigan lakebed: zonation	332
6B-1B.	Vertical hydraulic conductivity, upper QRNR including Lake Michigan lakebed: calibrated input	333
6B-2A.	Vertical hydraulic conductivity, middle QRNR: zonation	335
6B-2B.	Vertical hydraulic conductivity, middle QRNR: calibrated input	336
6B-3A.	Vertical hydraulic conductivity, lower QRNR: zonation	338
6B-3B.	Vertical hydraulic conductivity, lower QRNR: calibrated input	339
6B-4A.	Vertical hydraulic conductivity, PEN2: zonation	341
6B-4B.	Vertical hydraulic conductivity, PEN2: calibrated input	342
6B-5A.	Vertical hydraulic conductivity, MICH: zonation	344
6B-5B.	Vertical hydraulic conductivity, MICH: calibrated input	345
6B-6A.	Vertical hydraulic conductivity, DVMS: zonation	347
6B-6B.	Vertical hydraulic conductivity, DVMS: calibrated input	348
6B-7A.	Vertical hydraulic conductivity, middle SLDV: zonation	350
6B-7B.	Vertical hydraulic conductivity, middle SLDV: calibrated input	351
6B-8A.	Vertical hydraulic conductivity, MAQU: zonation	353
6B-8B.	Vertical hydraulic conductivity, MAQU: calibrated input	354
6B-9A.	Vertical hydraulic conductivity, EACL: zonation	356
6B-9B.	Vertical hydraulic conductivity, EACL: calibrated input	357
8-1 to 8-22.	Graphs showing:	
8-1 to 8-8.	Relation between measured and simulated values for 22 calibration-target groups	372
8-9 to 8-16.	Relation between measured and simulated values for 22 calibration-target groups	373
8-17 to 8-22.	Relation between measured and simulated values for 22 calibration-target groups	374

Appendix Tables

2-1.	Surface-water network database organized by GAP processing units.....	261
2-2.	Relation between stream order and measured stream width at USGS streamgage locations in Michigan	266
2-3.	Nearfield distribution of surface-water cells for different selection criteria.....	266
3-1.	Inputs to power law for assigning horizontal hydraulic conductivity of QRNR deposits in model layers 1, 2, and 3.....	271
5-1.	Parameters with fixed values	284
5-2.	Parameters estimated in calibration process.....	286
6A-1.	Horizontal hydraulic conductivity of QRNR-L1.....	304
6A-2.	Horizontal hydraulic conductivity of QRNR-L2.....	307
6A-3.	Horizontal hydraulic conductivity of QRNR-L3	310
6A-4.	Horizontal hydraulic conductivity of PEN1-L5.....	313
6A-5.	Horizontal hydraulic conductivity of MSHL-L8	316
6A-6.	Horizontal hydraulic conductivity of SLDV-L10.....	319
6A-7.	Horizontal hydraulic conductivity of STPT-L15.....	322
6A-8.	Horizontal hydraulic conductivity of IRGA-L17	325
6A-9.	Horizontal hydraulic conductivity of MTSM-L19.....	328
6B-1.	Vertical hydraulic conductivity of QRNR-L1	331
6B-2.	Vertical hydraulic conductivity of QRNR-L2.....	334
6B-3.	Vertical hydraulic conductivity of QRNR-L3.....	337
6B-4.	Vertical hydraulic conductivity of PEN2-L6).....	340
6B-5.	Vertical hydraulic conductivity of MICH-L7	343
6B-6.	Vertical hydraulic conductivity of DVMS-L9	346
6B-7.	Vertical hydraulic conductivity of SLDV-L11	349
6B-8.	Vertical hydraulic conductivity of MAQU-L13.....	352
6B-9.	Vertical hydraulic conductivity of EACL-L18	355
7-1.	Base-flow calibration targets.....	362
9-1.	Quaternary aquifer layers	376
9-2.	Pennsylvanian aquifer layers	377
9-3.	Marshall aquifer layers.....	377
9-4.	Silurian-Devonian aquifer layers	378
9-5.	Cambrian-Ordovician aquifer layers	379

Conversion Factors and Datums

Multiply	By	To obtain
Length		
foot (ft)	0.3048	meter (m)
mile (mi)	1.609	kilometer (km)
Area		
square foot (ft ²)	0.09290	square meter (m ²)
square mile (mi ²)	259.0	hectare (ha)
square mile (mi ²)	2.590	square kilometer (km ²)
Volume		
gallon (gal)	3.785	liter (L)
gallon (gal)	0.003785	cubic meter (m ³)
million gallons (Mgal)	3,785	cubic meter (m ³)
cubic foot (ft ³)	0.02832	cubic meter (m ³)
Flow rate		
cubic foot per second (ft ³ /s)	0.02832	cubic meter per second (m ³ /s)
cubic foot per day (ft ³ /d)	0.02832	cubic meter per day (m ³ /d)
gallon per minute (gal/min)	0.06309	liter per second (L/s)
million gallons per day (Mgal/d)	0.04381	cubic meter per second (m ³ /s)
Hydraulic conductivity		
foot per day (ft/d)	0.3048	meter per day (m/d)
Hydraulic gradient		
foot per mile (ft/mi)	0.1894	meter per kilometer (m/km)

Temperature in degrees Celsius (°C) may be converted to degrees Fahrenheit (°F) as follows:

$$^{\circ}\text{F}=(1.8\times^{\circ}\text{C})+32$$

Temperature in degrees Fahrenheit (°F) may be converted to degrees Celsius (°C) as follows:

$$^{\circ}\text{C}=(^{\circ}\text{F}-32)/1.8$$

Vertical coordinate information is referenced to the North American Vertical Datum of 1929 (NAVD 29), except for Great Lake levels, which are referenced to the International Great Lakes Datum of 1985 (IGLD 85).

Altitude and elevation, as used in this report, refer to distance above the respective vertical datum.

Horizontal spatial reference for the model grid is in Universal Transverse Mercator projection Zone 16, North American Datum of 1983 (NAD 83). The grid coordinates are in units of feet.

Specific conductance is given in microsiemens per centimeter at 25 degrees Celsius (µS/cm at 25°C).

Concentrations of chemical constituents in water are given in milligrams per liter (mg/L).

The standard unit for transmissivity is cubic foot per day per square foot times foot of aquifer thickness [(ft³/d)/ft²]ft. In this report, the mathematically reduced form, foot squared per day (ft²/d), is used for convenience.

Regional Groundwater-Flow Model of the Lake Michigan Basin in Support of Great Lakes Water Availability and Use Studies

By D.T. Feinstein, R.J. Hunt, and H.W. Reeves

Abstract

A regional groundwater-flow model of the Lake Michigan Basin and surrounding areas has been developed in support of the Great Lakes Basin Pilot project under the U.S. Geological Survey's National Water Availability and Use Program. The transient 2-million-cell model incorporates multiple aquifers and pumping centers that create water-level drawdown that extends into deep saline waters. The 20-layer model simulates the exchange between a dense surface-water network and heterogeneous glacial deposits overlying stratified bedrock of the Wisconsin/Kankakee Arches and Michigan Basin in the Lower and Upper Peninsulas of Michigan; eastern Wisconsin; northern Indiana; and northeastern Illinois. The model is used to quantify changes in the groundwater system in response to pumping and variations in recharge from 1864 to 2005. Model results quantify the sources of water to major pumping centers, illustrate the dynamics of the groundwater system, and yield measures of water availability useful for water-resources management in the region.

This report is a complete description of the methods and datasets used to develop the regional model, the underlying conceptual model, and model inputs, including specified values of material properties and the assignment of external and internal boundary conditions. The report also documents the application of the SEAWAT-2000 program for variable-density flow; it details the approach, advanced methods, and results associated with calibration through nonlinear regression using the PEST program; presents the water-level, drawdown, and groundwater flows for various geographic subregions and aquifer systems; and provides analyses of the effects of pumping from shallow and deep wells on sources of water to wells, the migration of groundwater divides, and direct and indirect groundwater discharge to Lake Michigan. The report considers the role of unconfined conditions at the regional scale as well as the influence of salinity on groundwater flow. Lastly, it describes several categories of limitations and discusses ways of extending the regional model to address issues at the local scale.

Results of the simulations portray a regional groundwater-flow system that, over time, has largely maintained its natural predevelopment configuration but that locally has been strongly affected by well withdrawals. The quantity of rainfall in the Lake Michigan Basin and adjacent areas supports a dense surface-water network and recharge rates consistent with generally shallow water tables and predominantly shallow groundwater flow. At the regional scale, pumping has not caused major modifications of the shallow flow system, but it has resulted in decreases in base flow to streams and in direct discharge to Lake Michigan (about 2 percent of the groundwater discharged and about 0.5 cubic foot per second per mile of shoreline).

On the other hand, well withdrawals have caused major reversals in regional flow patterns around pumping centers in deep, confined aquifers—most noticeably in the Cambrian-Ordovician aquifer system on the west side of Lake Michigan near the cities of Green Bay and Milwaukee in eastern Wisconsin, and around Chicago in northeastern Illinois, as well as in some shallow bedrock aquifers (for example, in the Marshall aquifer near Lansing, Mich.). The reversals in flow have been accompanied by large drawdowns with consequent local decrease in storage. On the west side of Lake Michigan, groundwater withdrawals have caused appreciable migration of the deep groundwater divides. Before the advent of pumping, the deep Lake Michigan groundwater-basin boundaries extended west of the Lake Michigan surface-water basin boundary, in some places by tens of miles. Over time, the pumping centers have replaced Lake Michigan as the regional sink for the deep flow system.

The regional model is intended to support the framework pilot study of water availability and use for the Great Lakes Basin (Reeves, in press). To that end, the model is designed as a platform to

- allow evaluation of broad sustainability indicators for the overall groundwater regime;
- address the effects of future changes in water use and in climate on water availability; and

- host embedded refined models needed to address water-supply and ecologic issues at the local scale.

The regional model is commensurate in size and scope with other groundwater-availability models recently or currently under development by the USGS in different parts of the country, and contributes to a national perspective on groundwater availability by providing information required for regional comparison and analysis.

1. Introduction

In 2005, at the request of Congress, the U.S. Geological Survey (USGS) began a national program called the National Assessment of Water Availability and Use (Grannemann and Reeves, 2005) to provide citizens, communities, and natural-resource managers with

- clearer knowledge of the current status of the Nation's water resources,
- documentation of trends in water availability and use over recent decades, and
- improved ability to forecast the availability of water for future economic and ecological uses.

Groundwater is an important component of water use nationally, and groundwater-flow models are a powerful method of integrating a wide variety of hydrogeologic data and analyzing the varied responses of a groundwater system to changes in pumping and climate. A groundwater-flow model was developed of the Lake Michigan Basin as part of the National Assessment of Water Availability and Use to assess water availability in the western part of the Great Lakes Basin. The groundwater model is part of a larger set of studies integrated under the Great Lakes Basin Pilot project (fig. 1); collectively, the studies are designed to evaluate water availability and use in the Great Lakes Basin as a whole from the standpoint of both groundwater and surface water. Water availability is assessed in terms of fluxes and storage of water in water bodies and aquifers and in terms of rates of withdrawal, consumption, and return of water to surface and subsurface natural systems. The analyses support summary indicators reflecting the degree to which human activities have modified the natural system; they also allow for further examination of how future pumping and climate conditions might affect water supply and ecological requirements. The Lake Michigan Basin groundwater-flow model—referred to hereafter as the “LMB model”—contributes to each of these objectives in the context of groundwater availability. The comprehensive framework and findings for groundwater and surface water based on all the Great Lakes Pilot project studies are summarized in USGS Professional Paper 1778 (Reeves, in press, which serves as an overview of the status and sustainability of surface and subsurface fresh-water resources in the Great Lakes region.

1.1 Purpose and Scope

This report documents the development of a regional groundwater-flow model (the LMB model) used to evaluate the past and current (2010) availability of groundwater for an 83,000-mi² study area in and surrounding the Lake Michigan Basin. The status and trends of water availability across all or parts of Michigan, Wisconsin, Indiana, and Illinois are quantified by means of model simulations of historical water levels from 1864 to 2005, past and current drawdown around pumping centers, sources of water to shallow and deep wells, and interactions of groundwater with surface water, particularly with Lake Michigan. The report

1. defines sources and sinks of groundwater (including recharge—the primary source of water; and pumping and discharge of groundwater to surface-water features—the primary sinks for groundwater; each is an element of the groundwater budget that varies with time);
2. presents maps showing the direction and magnitude of flow in several aquifer systems (including the location of groundwater divides and their movement in response to pumping); and
3. describes the ways in which the flows and storage of the natural groundwater system in the western half of the Great Lakes Basin are largely unchanged since the advent of pumping in the late 19th century, and the ways in which pumping produced appreciable changes by the beginning of the 21st century.

The LMB model is designed to provide

- a forecasting tool to assess the regional effects of future changes in water use and climate in the western part of the Great Lakes Basin;
- a platform for development of embedded, higher-resolution models used to address water-management issues at smaller (local) scales;
- a means of documenting and archiving information from a wide variety of sources on the hydrogeology and water use in the region; and
- a basis for developing indicators of sustainability of water resources.

The application of the model to each of these aspects of water-availability is presented in the USGS Professional Paper that summarizes the findings of the Great Lakes Basin pilot studies (Reeves, in press).

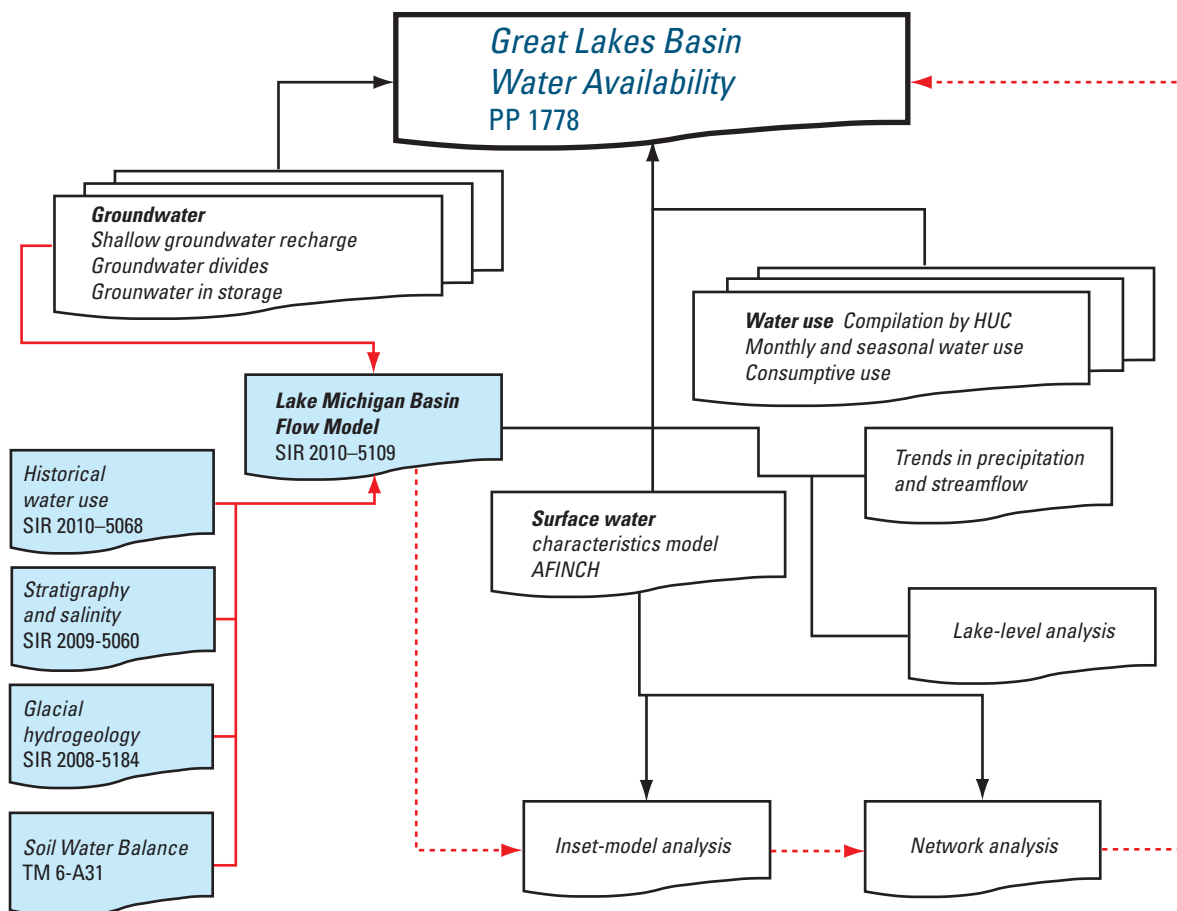


Figure 1. Great Lake Basin pilot investigations and reports structure. (Shaded boxes are reports that discuss aspects of model construction. Red lines indicate investigations contributing to or partly based on the flow model.)

1.2 Description of Study Area

The study area (model domain) includes the western part of the Great Lakes Basin in the Upper Midwestern United States (fig. 2). It is centered on Lake Michigan and extends to parts of Lake Superior, Lake Huron, Lake St. Clair, and Lake Erie. It encompasses eastern Wisconsin, northern Indiana, northern Illinois, northwestern Ohio, and nearly all of Michigan. The model domain is divided into the *nearfield*, which corresponds to the principal area of interest in which the hydrogeology is well defined, and the *farfield*, which incorporates less detail and functions as a boundary for the nearfield area (fig. 3). The nearfield is divided into seven subregions (fig. 3) that facilitate model calibration and discussion of model results. The subregions (with abbreviations) are as follows:

1. Southern Lower Peninsula, Michigan (SLP_MI)
2. Northern Lower Peninsula, Michigan (NLP_MI)
3. Upper Peninsula, Michigan (UP_MI)
4. Northeastern Wisconsin (NE_WI)

5. Southeastern Wisconsin (SE_WI)
6. Northern Indiana (N_IND)
7. Northeastern Illinois (NE_ILL)

All abbreviations used in this report are listed in table 1.

Most of the nearfield area lies within the Lake Michigan Basin (the combined area of the lake and its surface drainage). However, certain areas outside the Lake Michigan Basin, particularly on the west side of the lake, are important to include in the model nearfield because they host pumping centers that have an appreciable effect on groundwater flow within and near the basin boundaries. It is also important to include these areas because of their relation to groundwater and surface-water divides: water-level records from the early 20th century, plus results of models in southeastern Wisconsin and northeastern Illinois, indicate that, before and shortly after groundwater-resource development, groundwater divides in the deep part of the flow system did not coincide with surface-water divides defining the Lake Michigan drainage but extended west of the Lake Michigan Basin into Wisconsin and Illinois (Feinstein and others, 2005; Sheets and Simonson, 2006).

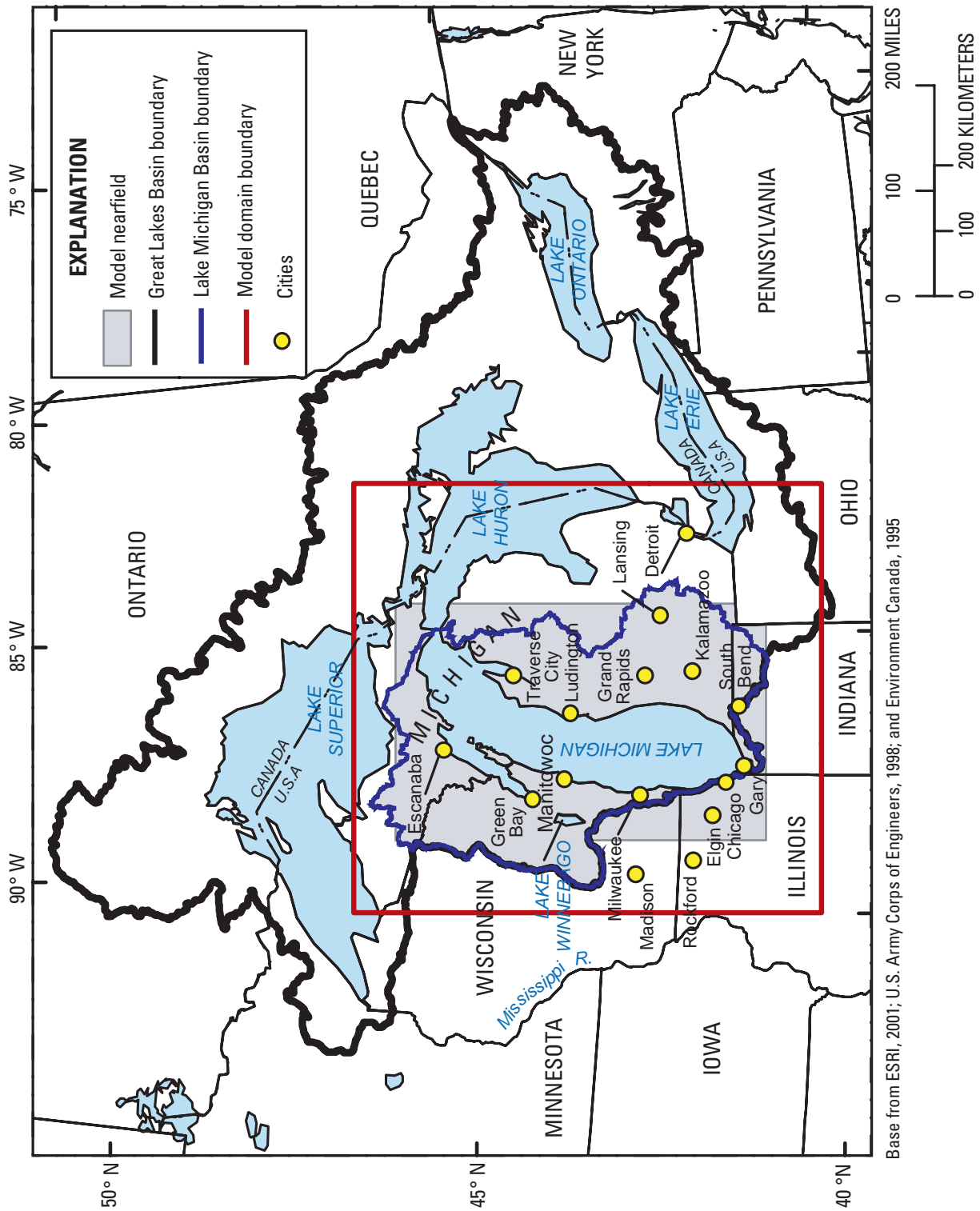


Figure 2. Location of study area.

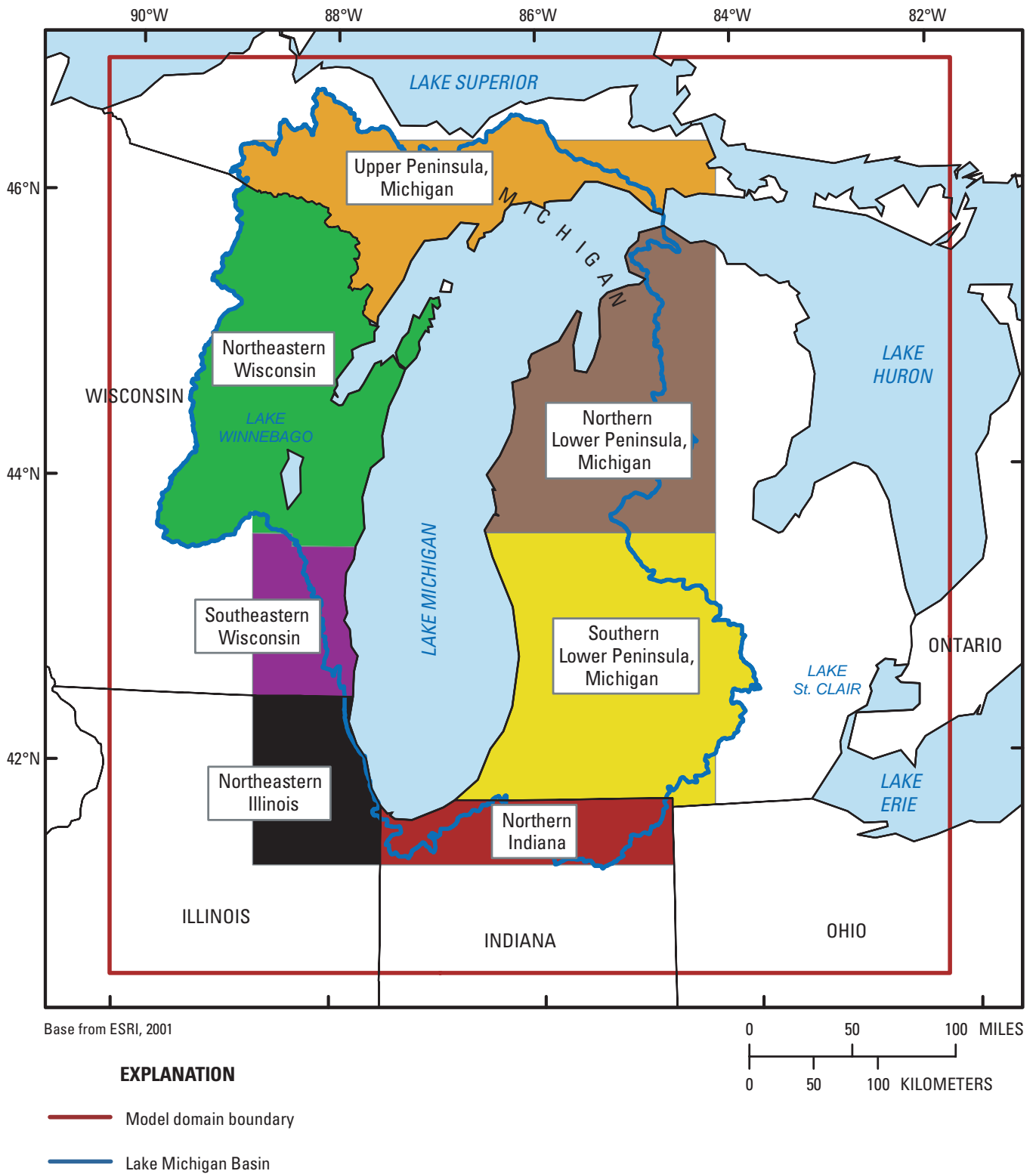


Figure 3. Model nearfield and subregions. (The combined area of the colored blocks representing model subregions constitutes the model nearfield.)

6 Regional Groundwater-Flow Model, Lake Michigan Basin, in Support of Great Lakes Water Availability and Use Studies

Table 1. Abbreviations used in this report.

Lake Michigan Basin and Subregions		
LMB	Lake Michigan Basin	
SLP_MI	Southern Lower Peninsula, Michigan	
NLP_MI	Northern Lower Peninsula, Michigan	
UP_MI	Upper Peninsula, Michigan	
NE_WI	Northeastern Wisconsin	
SE_WI	Southeastern Wisconsin	
N_IND	Northern Indiana	
NE_ILL	Northeastern Illinois	
Hydrogeologic units and aquifer systems		
QRNR	Quaternary hydrogeologic unit	Quaternary aquifer system
JURA	Jurassic hydrogeologic unit	
PEN1	Upper Pennsylvanian hydrogeologic unit	
PEN2	Lower Pennsylvanian hydrogeologic unit	
PENN	--	Pennsylvanian aquifer system
MICH	Michigan hydrogeologic unit	
MSHL	Marshall hydrogeologic unit	Marshall aquifer system
DVMS	Devonian-Mississippian hydrogeologic unit	
SLDV	Silurian-Devonian hydrogeologic unit	Silurian-Devonian aquifer system
MAQU	Maquoketa hydrogeologic unit	
SNNP	Sinnipee hydrogeologic unit	
STPT	St. Peter hydrogeologic unit	
PCFR	Prairie du Chien/Franconia hydrogeologic unit	
IRGA	Ironton-Galesville hydrogeologic unit	
EACL	Eau Claire hydrogeologic unit	
MTSM	Mount Simon hydrogeologic unit	
C-O	--	Cambrian-Ordovician aquifer system
Parameters		
K	Hydraulic conductivity (foot per day (ft/d))	
K_h	Horizontal hydraulic conductivity (foot per day (ft/d))	
K_v	Vertical hydraulic conductivity (foot per day (ft/d))	
S_s	Specific storage (1/foot (1/ft))	
S_y	Specific yield (dimensionless)	
S	Storage coefficient (dimensionless)	
MODFLOW boundary-condition cells		
CHD	Constant head	
GHB	General head boundary	
RIV	River	
RCH	Recharge	
WEL	Well	
MNW	Multinode well	

The area of the entire LMB model domain is 180,963 mi². Less than half of this area falls within the Lake Michigan Basin, which covers 66,843 mi², of which 44,922 mi² is land and 21,921 mi² is waters of Lake Michigan (National Geophysical Data Center, 1998). As discussed above, the model nearfield includes all the Lake Michigan Basin and some neighboring areas. The inland part of the model nearfield not covered by Lake Michigan is 60,785 mi².

The climate of the Lake Michigan Basin and adjacent areas is controlled by movement of air masses from the Arctic and from the Gulf of Mexico and also is moderated by the size and position of the Great Lakes within a large continental land mass (Sheets and Simonson, 2006). In winter, cold, arctic air moves across the basin and absorbs moisture from the comparatively warmer Great Lakes; condensation as the air masses reach land creates heavy snowfalls on the leeward sides of the Great Lakes, including along the western shore of Michigan. In summer, most of the Great Lakes Basin is dominated by warm, humid air from the Gulf of Mexico, and only the most northern part of the basin receives cooler and drier air from the Canadian northwest (Government of Canada and U.S. Environmental Protection Agency, 1995). These conditions create a range of climatic conditions for the part of the Great Lakes Basin occupied by the model nearfield, as reflected in 30-year average data for that area from 1971 to 2000 (PRISM Group, 2008). The average winter temperature ranges from 3.1 °F (16.0 °C) in the northern part of the model nearfield to 21.1 °F (−6.1 °C) in the southern part of the model nearfield, with an overall mean of −10.4 °C (13.2 °F). The corresponding range in summer is from 71.2 °F (21.8 °C) to 84.0 °F (28.9 °C), with an overall mean for the model nearfield of 79.0 °F (26.1 °C). The 30-year averages for precipitation in the model nearfield range from 27.4 in/yr (695 mm/yr) to

40.5 in/yr (1,029 mm/yr), with an overall mean of 33.5 in/yr (851.2 mm/yr). The precipitation pattern, in conjunction with the intensity of evapotranspiration—itsself partly a function of temperature—influences distribution of recharge to the groundwater system, which is an important input to the LMB model. The variation of precipitation and temperature with time causes variation in the rate of recharge.

Land-use/land-cover patterns also influence recharge; for example, rates of infiltration across the land surface, all other factors being equal, are generally greater in forested areas than in cropped areas (Seybold and others, 2003). In the model nearfield, the dominant land-use/land-cover types are forest, agriculture, and urban (fig. 4), which correlate with the distribution of population density (fig. 5). Groundwater use historically is greatest in urban areas served by public-supply and industrial pumping, but it has long been important in rural areas for public and domestic supply and for irrigation.

The physiography of the Great Lakes Basin is the result of a series of continental glaciers that scoured the area, the latest of which was the Laurentide Ice Sheet of the Wisconsin-stage glaciation during the Pleistocene Epoch (Sheets and Simonson, 2006). Most of the Great Lakes Basin is covered by glacial landforms such as moraines and till plains (Fenneman and Johnson, 1946). The surface topography of the model nearfield includes the higher elevations at the drainage boundaries of the Lake Michigan Basin and the lower elevations near the shoreline of the lake itself (fig. 6). The nearfield subregions of the LMB model differ in degree of topographic relief (table 2); relief is greatest in the Northern Lower Peninsula of Michigan and least in Northern Indiana. The water-table surface at the top of the groundwater system, which is the driving force for groundwater flow, generally is a subdued reflection of the land-surface topography.

Table 2. Altitude and relief in model nearfield.

[All altitudes relative to prevailing vertical datum. (See explanation in “Conversion Factors and Abbreviations” section at front of report.) Sources: National Geophysical Data Center, 1998, GEODAS Gridded data format, accessed April 2008 at http://www.ngdc.noaa.gov/mgg/gdas/gd_designagrid.html?dbase=grdglb. U.S. Bureau of the Census, 2006, County boundaries, accessed April 2008 at http://gis.glin.net/ogc/services.php#mi_county_boundaries_2000]

Nearfield subregions	Area (square miles)	Minimum altitude (feet)	Maximum altitude (feet)	Range of relief (feet)	Mean altitude (feet)
Southern Lower Peninsula, Michigan	14,159	479	1,280	801	836
Northern Lower Peninsula, Michigan	11,689	376	1,732	1,356	972
Upper Peninsula, Michigan	9,400	482	1,975	1,493	978
Northeastern Wisconsin	13,242	433	2,014	1,581	976
Southeastern Wisconsin	3,497	440	1,345	906	865
Northern Indiana	4,209	377	1,201	824	730
Northeastern Illinois	4,589	520	1,214	694	819
Total nearfield	60,785	376	2,014	1,638	907
Lake Michigan bed (excluding islands)	21,921	−327.4	577.4	905.5	294.3

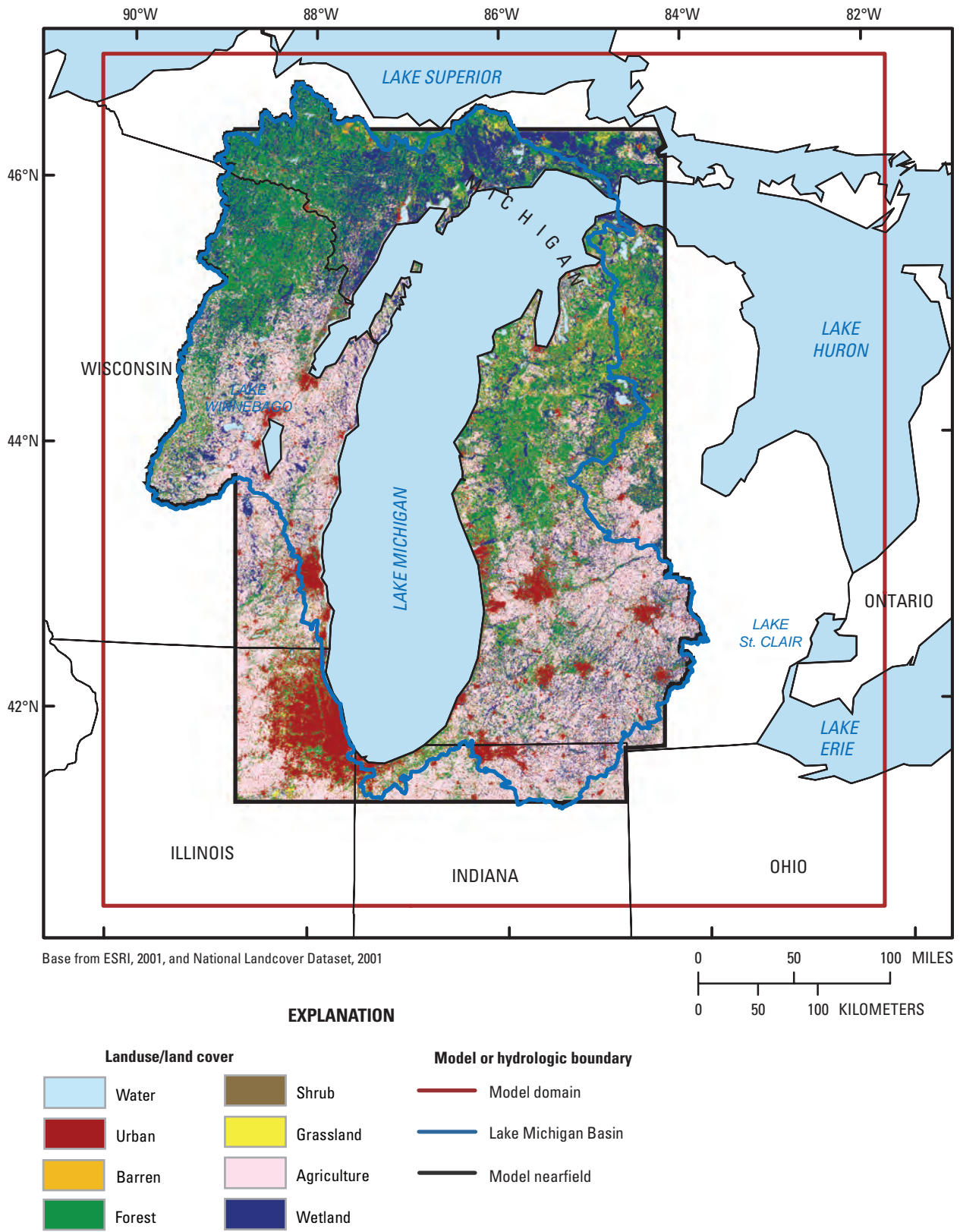


Figure 4. Land use/land cover in model nearfield.

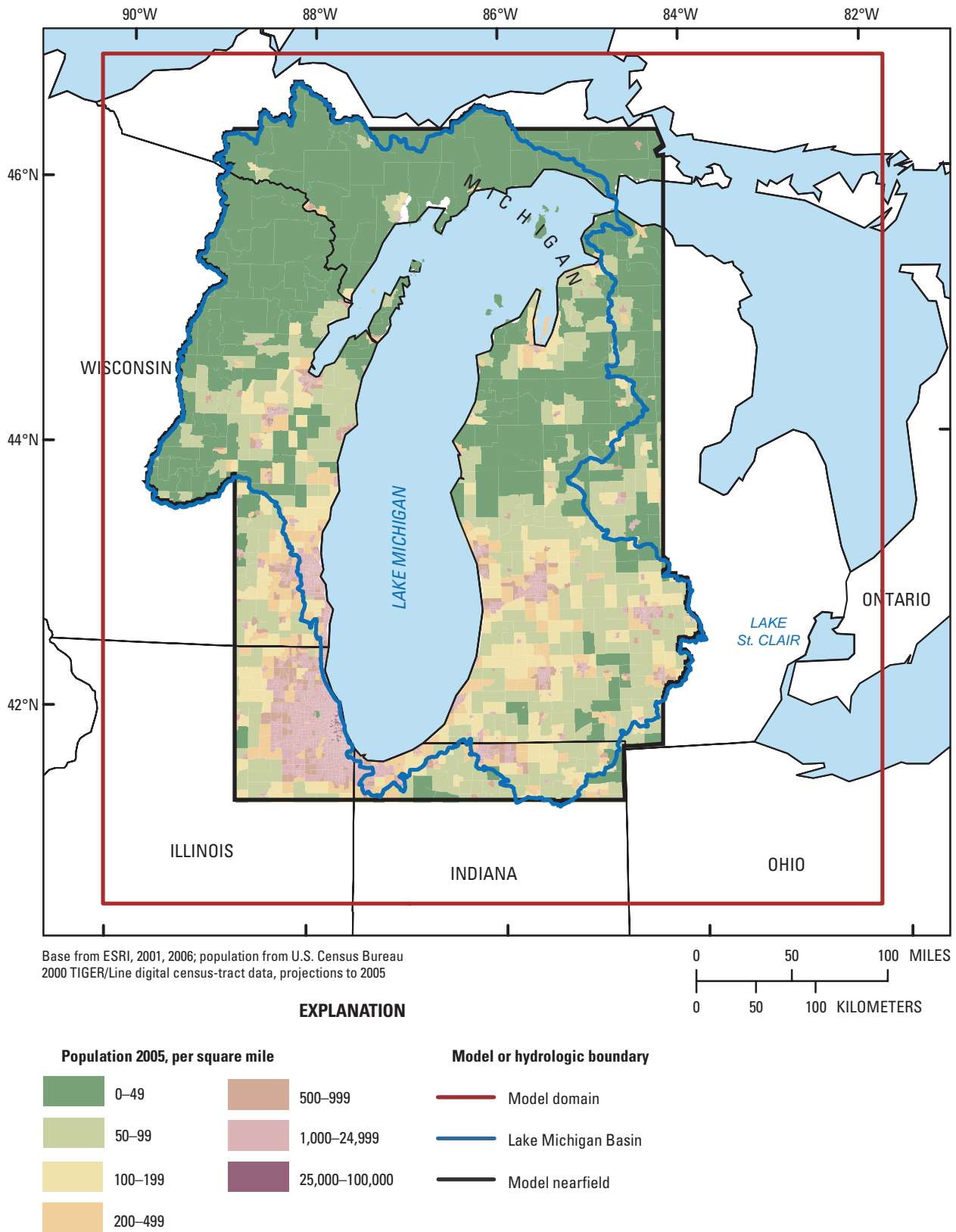


Figure 5. Population distribution in model nearfield.

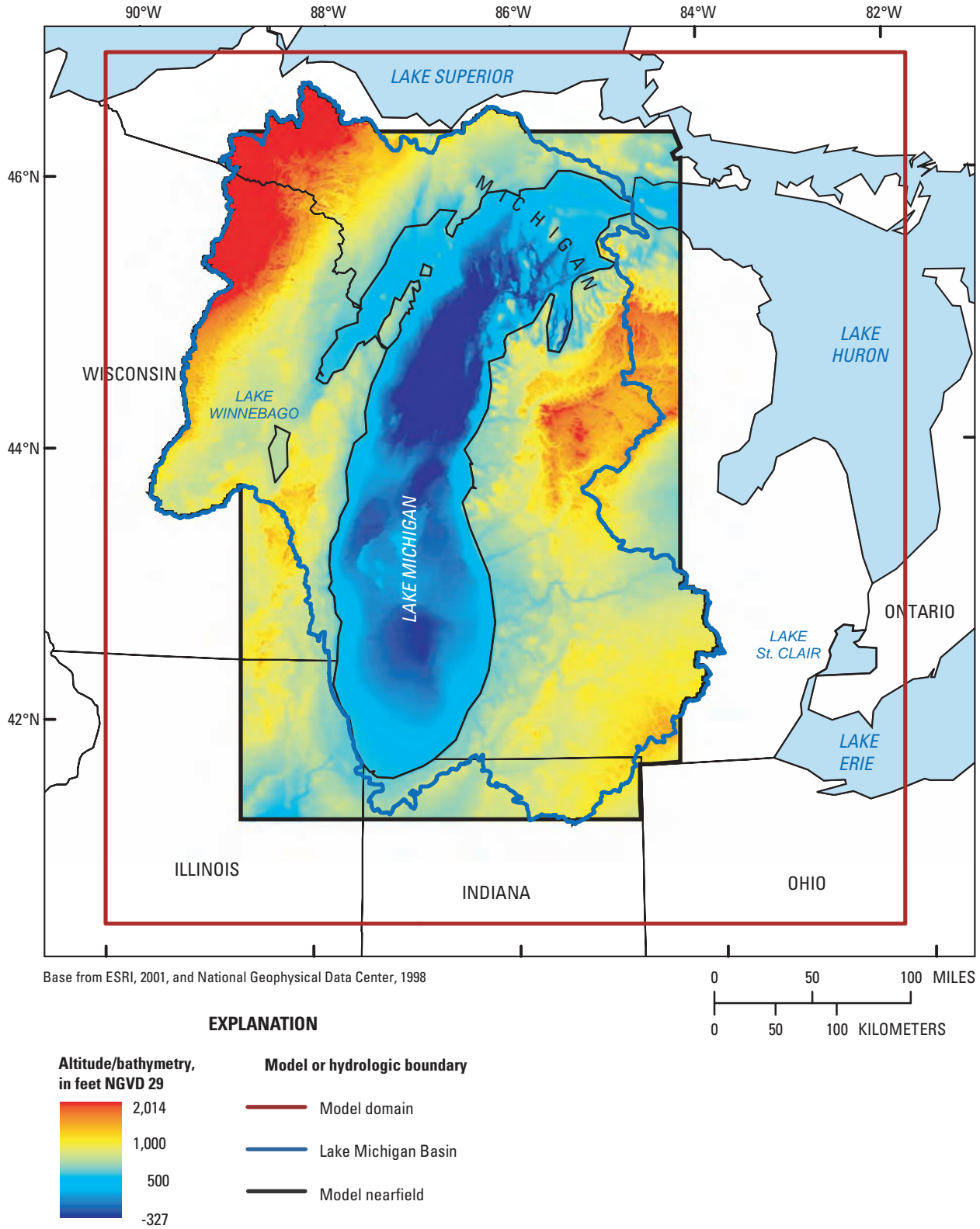


Figure 6. Land-surface and lakebed altitude in model nearfield.

The surface-water network also affects groundwater flow; under natural conditions, streams and lakes often serve as discharge areas for groundwater. The surface-water basin draining to Lake Michigan is surrounded by other major drainage basins inside the model domain associated with the Mississippi River, Lake Superior, Lake Huron, Lake St. Clair, and Lake Erie (fig. 7A). The surface-water features within these basins, in particular the major rivers (fig. 7B), constitute an important input to the groundwater-flow model. The boundaries of the hydrologic basins around major surface-water features (fig. 7C) tend to correspond to the major shallow groundwater divides.

The bedrock surface that underlies the glacial and alluvial deposits has a generally subdued topography because of glacial scouring. Bedrock units in the model nearfield range from Precambrian to Jurassic in age (fig. 8A). Precambrian units consist of crystalline rocks and metamorphosed sedimentary rocks. Precambrian bedrock of the Canadian Shield, approximately 3.5 billion years old, crops out on the northern boundary of the model domain. The overlying Paleozoic and Mesozoic rocks are sedimentary in origin. These bedrock units dip away from the crests of the Wisconsin, Kankakee, Findlay, and Algonquin Arches into the Michigan Basin, a structural basin consisting of an ovate-shaped accumulation of sedimentary rocks (fig. 8B). This series of large-scale structural basins and arches control the position and extent of bedrock units in the northern Midwest in general and in the model domain in particular (fig. 8B). The Wisconsin Arch, Kankakee Arch, Findlay Arch, and Algonquin Arch all dip radially into the Michigan Basin; the rocks are relatively thin along the arches and thicken dramatically toward the center of the Michigan Basin. The Michigan Basin is centered in the Lower Peninsula of Michigan and reaches a maximum thickness of about 15,000 ft.¹ An overview of the Paleozoic and Mesozoic units that constitute the bedrock follows in section 3.1; more detailed discussion by subregion is in appendix 1.

1.3 Water Use In and Around the Lake Michigan Basin

Although water demand in the Great Lakes Basin is predominantly met through surface-water withdrawals, the population in the Lake Michigan Basin uses appreciable amounts of groundwater at an estimated rate of 1,500 million gallons per day (Sheets and Simonson, 2006). There are several areas of concentrated withdrawals (fig. 9). The areas of largest groundwater withdrawals in the Great Lakes Basin are on the west side of Lake Michigan around Chicago in the Northeastern Illinois subregion (NE_ILL) and around Waukesha and Milwaukee in the Southeastern Wisconsin subregion (SE_WI).

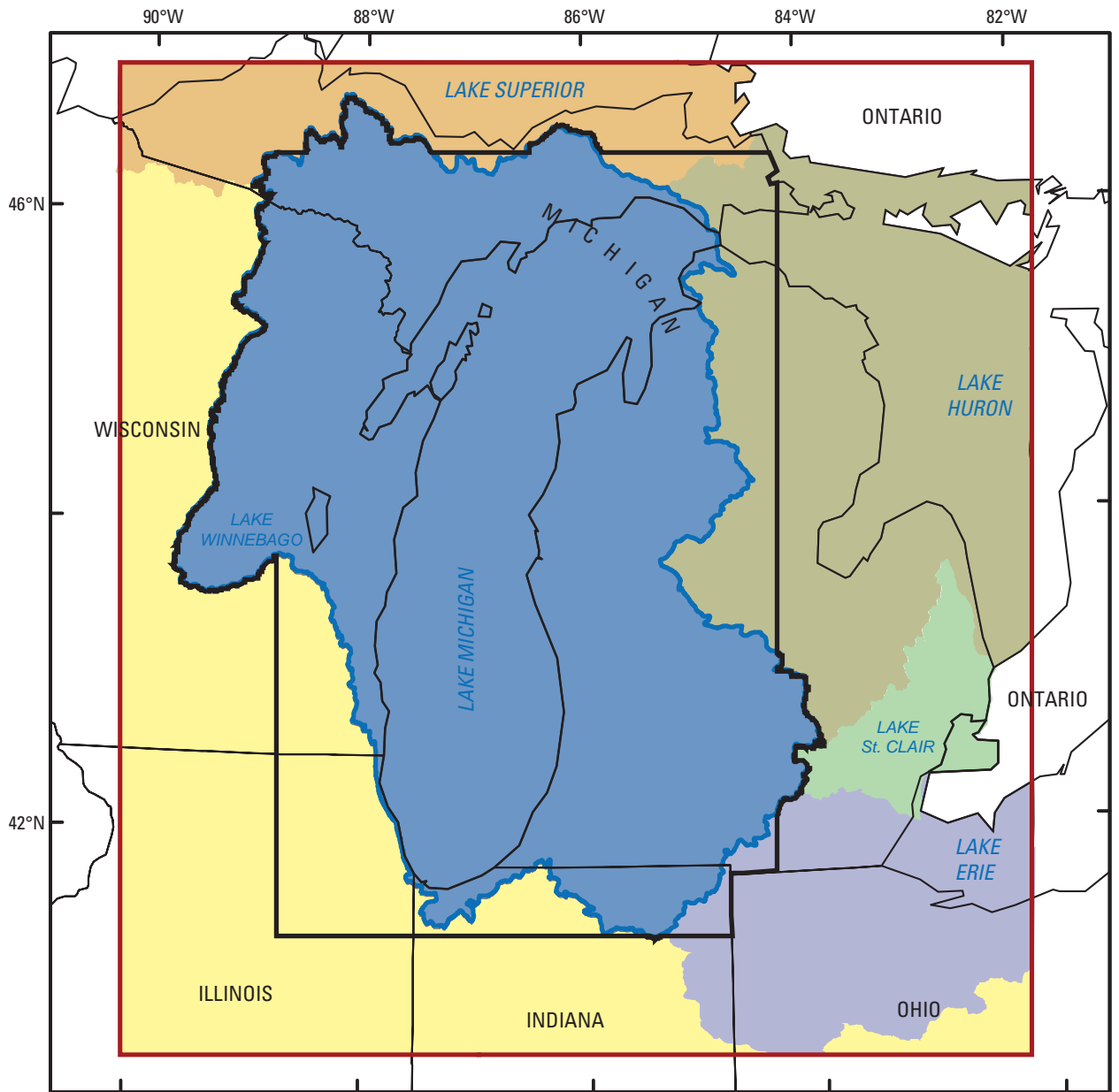
¹ Note that “Lake Michigan Basin” refers to the lake plus its drainage area, whereas “Michigan Basin” refers to the geologic feature.

Other major pumping centers in the model nearfield include the Green Bay and Lake Winnebago area in the Northeastern Wisconsin subregion (NE_WI), the cities of Lansing, Grand Rapids (now mostly supplied by surface water), Jackson, and Kalamazoo in the Southern Lower Peninsula, Michigan subregion (SLP_MI), as well as communities in southern Michigan and in the Northern Indiana (N_IND) subregion such as Michigan City, Elkhart, and South Bend. Changes in pumping through time are a major stress on the groundwater system that cause water levels to fluctuate and groundwater divides to migrate. As a result, historical pumping from high-capacity public-supply, irrigation, and industrial wells is an important input to the LMB groundwater-flow model. High-capacity wells are defined for this study as those that extract on average more than 70 gal/min (100,000 gal/d). Domestic wells commonly extract less than this rate.

1.4 Saline Groundwater in the Lake Michigan Basin

A hydrogeologically important characteristic of the the Lake Michigan Basin area is the presence of saline water² in several of the water-bearing formations. In the Lower Peninsula of Michigan, saline water is present near land surface in lowland areas, particularly on the east side of the Lower Peninsula (Wahrer and others, 1996; Hoaglund, 2004). Shallow bedrock units in some areas are rendered nonpotable by salinity (Meissner and others, 1996; Ging and others, 1996; Westjohn and Weaver, 1996c). Deeper bedrock units in the Michigan Basin host water with specific gravity greater than 1.20, corresponding to dissolved solids (DS) concentrations in excess of 300,000 mg/L (Gupta and Bair, 1997). The high salinity in the Paleozoic bedrock extends into northern Indiana where water in shallow Silurian and Devonian rocks commonly have DS concentrations greater than 10,000 mg/L (Schnoebelen and others, 1998). Under northeastern Illinois, saline water in Cambrian-Ordovician units is commonly present at DS concentrations exceeding 10,000 mg/L at 2,000 ft below sea level (Bond, 1972; Visocky and others, 1985; Nicholas and others, 1987), and upconing of deep saline water toward wells in originally freshwater areas can be a problem around pumping centers withdrawing from the deep sandstone aquifers. In Wisconsin, saline water in bedrock aquifers is more isolated, attaining DS concentrations greater than 1,000 mg/L in pockets between Milwaukee and Green Bay near Lake Michigan (Ryling, 1961).

² Definitions of “salinity” and “saline water” are varied in hydrological literature. For purposes of this report, “saline water” is used to mean water having a dissolved solids concentration greater than 10,000 mg/L, regardless of composition, or a density that can be interpreted as representing a dissolved solids concentration greater than 10,000 mg/L.



Base from ESRI, 2001

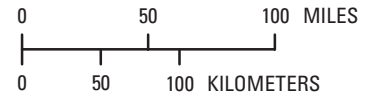
EXPLANATION

- | Surface-water basin | | Model boundary | |
|---|---|---|-----------------|
|  | Lake Superior Basin |  | Model domain |
|  | Lake Michigan Basin |  | Model nearfield |
|  | Lake Huron Basin | | |
|  | Lake St. Clair Subbasin (Lake Erie Basin) | | |
|  | Lake Erie Basin | | |
|  | Upper and Lower Mississippi Basin | | |

Figure 7A. Major surface-water basins in model domain.



Base from ESRI, 2001, National Hydrography Dataset Plus, 2005, and National Atlas of the United States, 2005



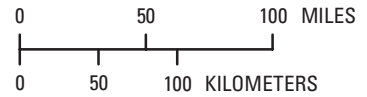
EXPLANATION

Surface-water body		Model or hydrologic boundary	
	Lake		Model domain
	River		Lake Michigan Basin
	Major river		Model nearfield

Figure 7B. Major rivers in model domain.



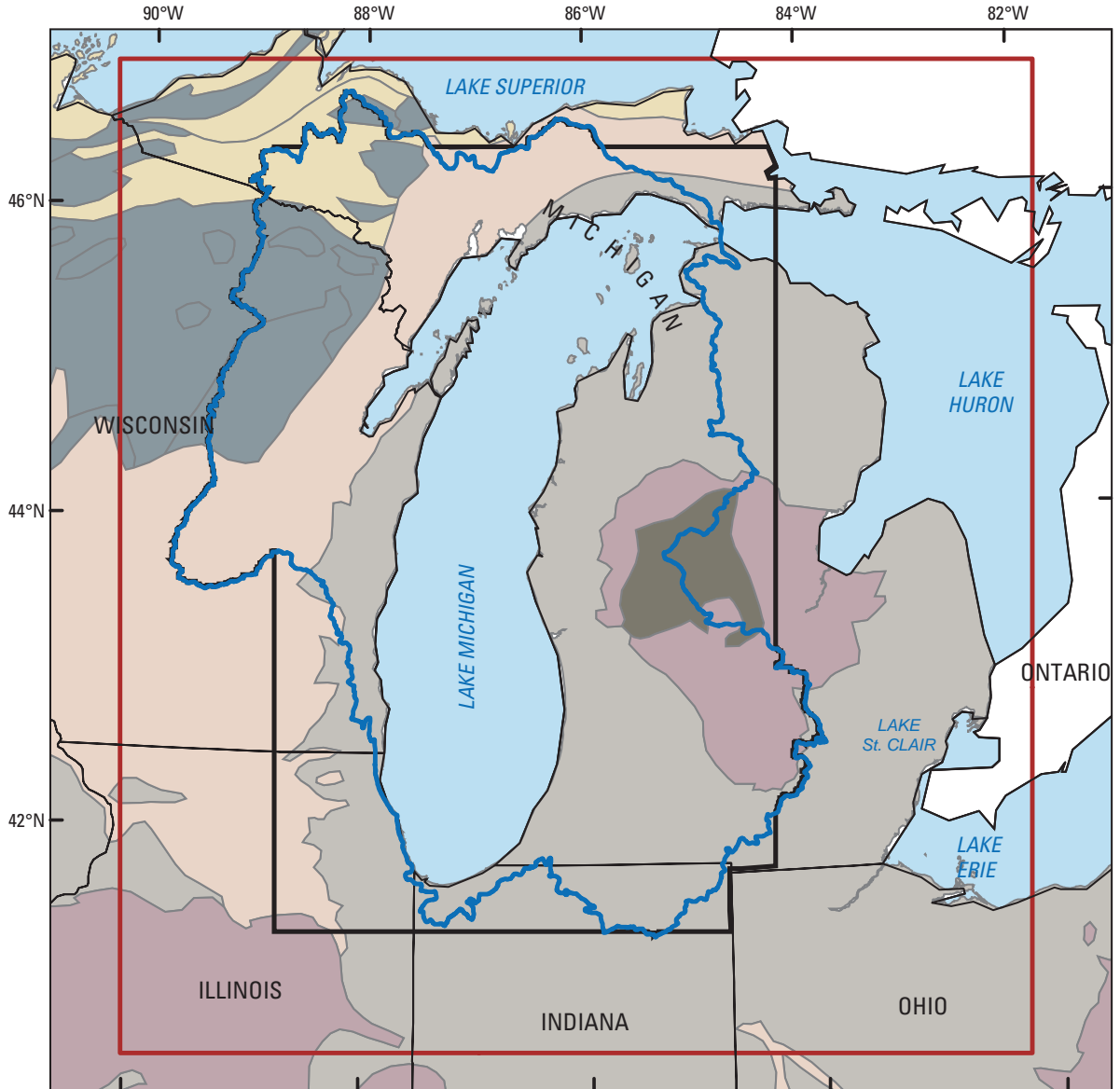
Base from ESRI, 2001, and Hydrologic Unit Boundaries from U.S. Geological Survey, 2005



EXPLANATION

- Geographic or hydrologic boundary**
- Model domain
- Lake Michigan Basin
- Hydrologic unit code (HUC) level 3
- Hydrologic unit code (HUC) level 4

Figure 7C. Major level 3 and 4 hydrologic units in model domain.

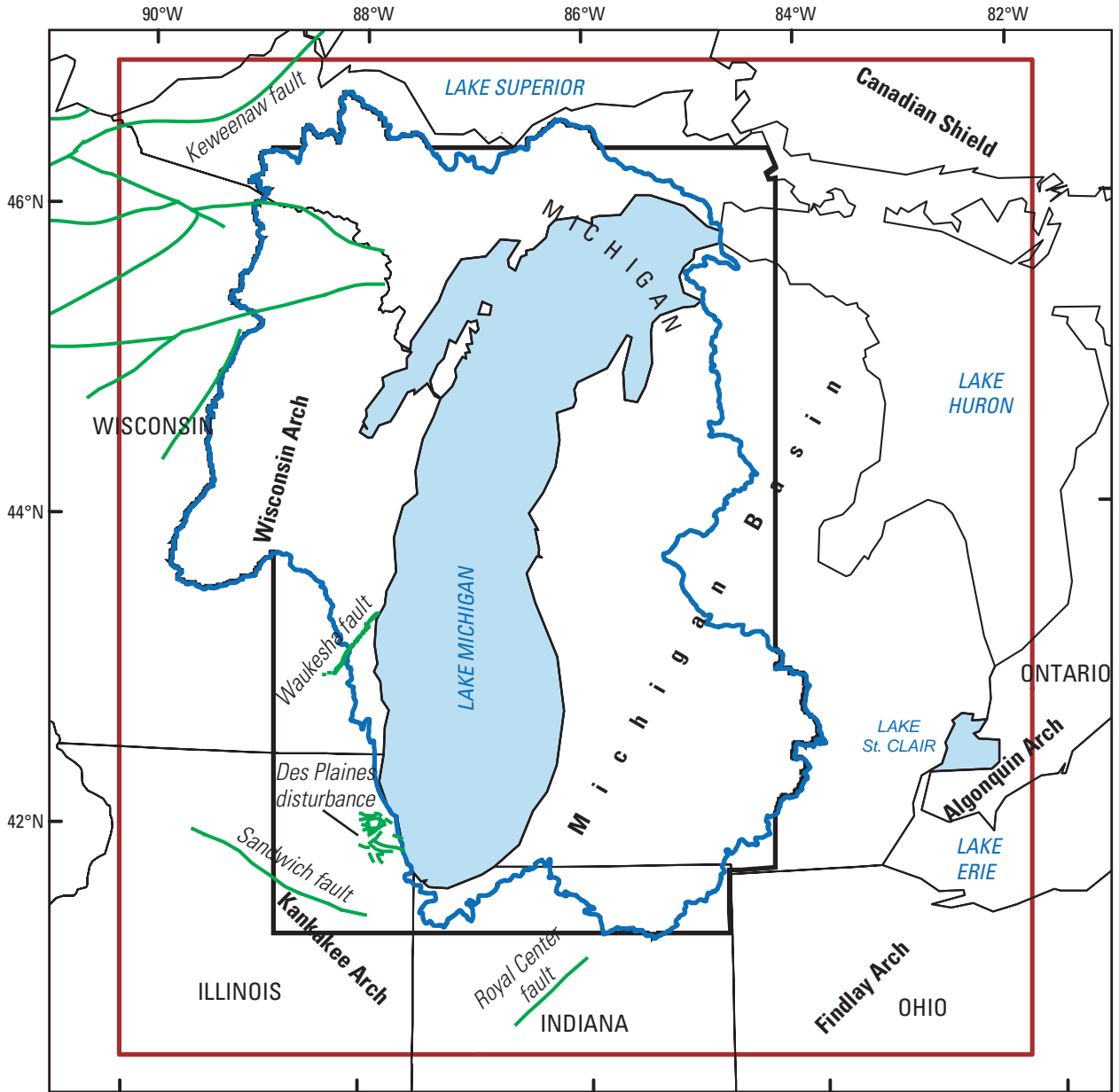


Base from ESRI, 2001; geology from Reed and Bush, 2005

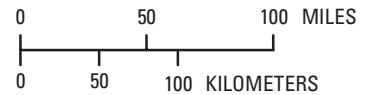
EXPLANATION

- | Bedrock geology | Model or hydrologic boundary |
|--|---|
|  Lower Mesozoic (Triassic and Jurassic) sedimentary rocks |  Model domain |
|  Upper Paleozoic (Pennsylvanian and Permian) sedimentary rocks |  Lake Michigan Basin |
|  Middle Paleozoic (Silurian, Devonian, and Mississippian) sedimentary rocks |  Model nearfield |
|  Lower Paleozoic (Cambrian and Ordovician) sedimentary rocks | |
|  Precambrian sedimentary rocks | |
|  Precambrian igneous and metamorphic rocks | |

Figure 8A. Uppermost bedrock units in the study area.



Base from ESRI, 2001, geology from Reed and Bush, 2005, and faults from U.S. Geological Survey, 2006, and Illinois State Geological Survey, 1995, with the approximate location of the Waukesha fault from Braschayko, 2005



EXPLANATION

- Model domain
- Lake Michigan Basin
- Model nearfield
- Fault

Figure 8B. Uppermost bedrock structural features in the study area.



Figure 9. Estimated 1995 groundwater-withdrawal rates for major metropolitan areas in the U.S. part of the Great Lakes Basin.

Characterization of flow patterns of saline aquifer can be complicated by the effects of the density of the water. Standard methods for hydrogeologic analysis are based on a standard water density of about 1 g/cm^3 . Freshwater with a standard density flows in response to hydraulic pressures. Water with an appreciably higher density due to high DS concentrations (for example, $100,000 \text{ mg/L}$ or greater) will flow in response to hydraulic pressures but will also have a tendency to flow downward because it is heavier, complicating analysis and simulation of water movement. The density of the water also influences the ease with which it can flow horizontally or vertically through subsurface material. The density of saline water, thus, influences the movement of groundwater flow by changing both hydraulic gradients and hydraulic conductivity relative to freshwater conditions. By changing the dynamics of flow, saline conditions also potentially influence the response of aquifers to pumping. Accordingly, one of the chief sets of inputs to the LMB groundwater-flow model is the subsurface distribution of salinity.

1.5 Previous Hydrogeologic Investigations and Modeling Studies

Published studies of groundwater in the Lake Michigan Basin area include surveys of the region's hydrogeology and large-scale modeling efforts by the USGS and state geological agencies.

Within the hydrogeologic literature are comprehensive treatments of the stratigraphic framework for the Great Lakes region, focusing on the occurrence of groundwater and the properties of aquifers and confining units (Allen and Waller, 1975; Weist, 1978; Olcott, 1992). Recent studies of the Great Lakes Basin have also emphasized the connection between geology and water resources (Government of Canada and the U.S. Environmental Protection Agency, 1995; Grannemann and others, 2000; Coon and Sheets, 2006). Most of the work dedicated to regional hydrostratigraphy has been done at the state level.

In Michigan, fundamental investigations targeted the distribution of glacial deposits (Leverett and Taylor, 1915) and the incidence of artesian wells (Allen, 1977), whereas subsequent studies contributed to a better understanding of the hydrogeology (Passero and others, 1981; Westjohn and others, 1994; Westjohn and Weaver, 1996a,b; Westjohn and Weaver, 1998).

In Wisconsin, pioneers in hydrogeology published seminal works (Chamberlin, 1877; Weidman and Schultz, 1915), which were followed by regional studies describing groundwater conditions in areas such as southeastern Wisconsin (for example, Foley and others, 1953) and northeastern Wisconsin (for example, Knowles, 1964). In more recent years, the Wisconsin Geological and Natural History Survey and the USGS published several framework hydrogeologic studies for Wisconsin (Young, 1992; Batten and Bradbury, 1996; Kammerer and others, 1998; Southeastern Wisconsin Regional Planning Commission and Wisconsin Geological and Natural History Survey, 2002).

Hydrologic basin studies published by Indiana state agencies cover a range of hydrogeologic information for the southern part of the Lake Michigan Basin area (Indiana Department of Natural Resources, 1987, 1990, 1994, and 1996). These basin studies are complemented by a series of USGS publications that define the hydrostratigraphy for the northern part of Indiana (Fenelon, Bobay, and others, 1994; Casey, 1997; Fowler and Arihood, 1998; Bugliosi, 1999).

In Illinois, previous hydrologic investigations focused not only on data collection and stratigraphic interpretation (for example, Nicholas and others, 1987) but also on issues arising from the large areas of water-level decline around Chicago, on the source of water to wells, and on the presence of saline conditions in the deep part of the flow system (Suter and others, 1959; Walton, 1960; Walton and Csallany, 1962; Walton, 1965; Visocky and others, 1985).

Some of the earliest groundwater-flow models were developed in the upper Midwest, where electric-analog and analytical techniques were used to forecast drawdown and evaluate sources of water to wells in the Chicago area (Walton, 1964; Prickett, 1967). Applications of numerical groundwater-flow modeling were undertaken in the 1970s and 1980s to test hydrogeologic interpretations and to develop management tools in Illinois (Prickett and Lonquist, 1971), in southeastern Wisconsin (Young, 1976), in Michigan (Fleck and McDonald, 1978), and in northern Indiana (Bailey and others, 1985; Lindgren and others, 1985).

The USGS Regional Aquifer-System Analysis (RASA) program, which spanned 1978–95, enhanced understanding of large-scale groundwater-flow systems in the United States. The RASA studies generated data that increased knowledge of the bedrock and surficial aquifers in the Great Lakes Basin and helped to strengthen interpretations of the subsurface hydrostratigraphy. The program also supported a series of groundwater-flow models that provided a quantitative understanding of subsurface flow at the regional scale. Study areas for three

sets of RASA modeling studies overlap the Lake Michigan Basin model domain.

Mandle and Kontis (1992) constructed a regional model of the aquifers underlying the northern Midwest. The model area extended from central Missouri to the southern shore of Lake Superior and from central Michigan to the South Dakota-Minnesota border, covering 378,880 mi². The computer code used in their study was based on finite-difference programs documented in Trescott (1975) and Trescott and Larson (1976). The application incorporated a uniform grid resolution of 16 mi and used multiple layers to represent major aquifers. Confining units were not included explicitly, but their effect on vertical flow was included by means of a resistance term. The Trescott and Larson code was modified to correct the freshwater heads for the density effects of salinity (without modeling the movement of salinity). The upper boundary of the model was fixed to represent the observed water-table surface, under the assumption that drawdown in the uppermost aquifers was negligible at this scale. Major rivers also were represented with fixed stages. Model simulations showed that groundwater withdrawals had created extensive drawdown in all bedrock aquifer formations under the pumping conditions in 1980, decreasing discharge to rivers and reversing flow across confining units near major pumping centers. Mandle and Kontis (1992) also noted that the grid resolution of the model was too coarse to examine small-scale features of the flow system. A second phase of modeling for the northern Midwest RASA (Young and others, 1989) produced a more detailed transient model of the Chicago-Milwaukee area. It used a version of the computer code MODFLOW developed and documented by McDonald and Harbaugh (1983). The code was modified to include a method developed by Bennett and others (1982) to calculate the approximate withdrawal rates from each aquifer penetrated by a multiaquifer well (Kontis and Mandle, 1988). The Chicago-Milwaukee model featured grid cells as small as 2 mi on a side, allowing for a more refined simulation of the development of the two, large coalescing areas of water-level decline in southeastern Wisconsin and northeastern Illinois.

The separate series of RASA studies devoted to the Lower Peninsula of Michigan included an initial model constructed by Mandle and Westjohn (1989) that simulated the effects of a steady-state water table and salinity on the bedrock hydrology. This model had a horizontal grid spacing on the order of 3 mi over an area of about 22,000 mi². A subsequent model of the same area by Hoagland and others (2002a,b) used estimates of groundwater recharge (Holtzschlag, 1997) to more accurately simulate the shallow and deep parts of the flow system and to estimate direct (riparian) and indirect (base-flow) discharges to the three Great Lakes bounding the Lower Peninsula. The later model used a grid spacing of 3,281 ft (1 km) and individual layers for glaciofluvial sediments, till and red-bed confining units, Pennsylvanian aquifers, Pennsylvanian confining units, and the Marshall aquifer. The underlying Mississippian shale beds were represented by a no-flow boundary. The modelers assumed steady-state

conditions without pumping and did not consider the influence of variable density due to salinity. However, they subjected the model to a rigorous calibration process to improve the reliability of estimates of groundwater discharge to surface-water features in Michigan's Lower Peninsula.

A third series of RASA studies focused on quantifying regional flow in an area just south of the LMB model in northern Indiana, as well as in parts of Ohio and Illinois. The model of the Midwestern Basins and Arches aquifer system by Eberts and George (2000) simulated flow in the water-table aquifer and the underlying areally extensive Silurian-Devonian carbonate-rock aquifer. The model simulated only regional groundwater flow, estimated to be about 10 percent of the total groundwater flow. The model grid consisted of square cells 4 mi on a side and two layers, one for unconsolidated deposits and one for bedrock. The regional flow pattern at the time was not influenced by historical changes in regional pumping, which justified the use of a steady-state model. The simulated flow system showed long flow paths (as much as 50 mi in length) in some areas of the model and indicated that very old water was associated not only with these long flow paths but also with short flow paths where small hydraulic gradients resulted in sluggish flow rates.

Subsequent to the RASA studies, a new generation of regional models was applied to evaluate groundwater flow systems and water budgets in Michigan (for example, Holtschlag and others, 1996; Hoaglund and others, 2002a; Reeves and others, 2004), in eastern Wisconsin (for example, Krohelski, 1986; Conlon, 1998; Krohelski and others, 2000), in northern Indiana (for example, Fenelon and Watson, 1992; Arihood and Basch, 1994; Bayless and Arihood, 1996; Arihood and Cohen, 1998), and in northeastern Illinois (for example, Burch, 1991). Although most of these models were used to develop input datasets and calibration targets for different parts of the LMB model, two additional models were of particular importance in furnishing a variety of inputs for the present study.

Feinstein and others developed a model centered on southeastern Wisconsin (Feinstein, Eaton, and others, 2005; Feinstein, Hart, and others, 2005). The model represented all rock units, including confining beds, from land surface to the top of the Precambrian sequence, by means of 18 layers. Minimum grid resolution was 2,500 ft in the model nearfield of southeastern Wisconsin. The model was calibrated for both predevelopment and pumping conditions by using heads and stream base-flow observations for the period 1864 to 2000. Feinstein, Hart, and others (2005) concluded that nearly 80 percent of water pumped from wells in southeastern Wisconsin is diverted from groundwater that was previously discharged as base flow to streams and lakes. The model indicates that, under 2000 conditions, only a small amount of water replenishing the regional cone of drawdown for the deep part of the flow system was induced from Lake Michigan. In addition, the modeling showed that, between 1864 and 2000, withdrawals from shallow wells open to glacial material and the upper bedrock had reduced shallow groundwater discharge to Lake Michigan by 8.5 percent. Most of this water is probably

returned to the lake through the sewage and water-treatment system, however. Finally, the modeling indicated that, between 1864 and 2000, the western limit of the contributing area for deep wells in pumping centers in southeastern Wisconsin shifted about 10 mi west of the original western boundary of the deep part of the regional groundwater flow system, which discharged toward Lake Michigan under natural conditions.

Meyer and others (2009) constructed and calibrated a regional groundwater-flow model centered in northeastern Illinois. The layering and grid spacing are similar to those in the model centered on southeastern Wisconsin by Feinstein and others (Feinstein, Eaton, and others 2005; Feinstein, Hart, and others, 2005). The model simulates groundwater withdrawals in northeastern Illinois and the surrounding area from 1864 to 2002. As part of the study, the regional model is used to set conditions at the edge of a refined inset model centering on Kane County, an area of special interest because of increasing groundwater withdrawals.

Although many models intersect the LMB model domain, there were several motives for developing a new model as part of the Great Lakes Basin pilot study, which is a part of the National Assessment of Water Availability and Use. The LMB model is based on multiple databases that have been assembled from a variety of sources to represent water use, glacial stratigraphy, bedrock stratigraphy, salinity, recharge, and the surface-water network. Recent advances in groundwater-modeling techniques, particularly in the areas of variable-density modeling and calibration methods, allow some past modeling limitations to be overcome. Faster computers mean that smaller grid sizes for the groundwater model can be used than in the RASA-generation models, allowing for more realistic simulations over the Lake Michigan Basin and adjacent areas. Finally, the sustainability issues that accompany the debate over the Great Lakes Compact³ may best be addressed with a tool that not only incorporates a large regional area corresponding to the western half of the Great Lakes Basin but also is capable of supporting embedded models that can address local management and diversion issues.

³ A major water-availability issue in the Great Lakes Basin for the past decade has been management of Great Lakes water; in particular, control and regulation of diversions of water outside the basin. Decisions regarding regional water management by representatives of the Great Lakes States and Provinces are embodied in the Great Lakes-St. Lawrence River Basin Water Resources Compact (Council of Great Lakes Governors, 2005b) and the Great Lakes-St. Lawrence River Basin Sustainable Water Resources Agreement (Council of Great Lakes Governors, 2005a). In 2008, this interstate compact between the eight Great Lakes States received consent and approval by Congress and was signed into law (U.S. Congress, 2008). The compact is a good-faith agreement by the eight Great Lakes U.S. States and two Great Lakes Canadian Provinces. This compact and agreement build upon the Great Lakes Charter Annex of 2001 (Council of Great Lakes Governors, 2001) and seek to "protect, conserve, restore, improve and effectively manage the Waters and Water Dependent Natural Resources of the Basin." Key features, which have gained significant attention in the region, are regulation of diversions of water outside of the basin and development of water-management goals and policies for the states and provinces within the basin.

2. Data and Methods

Data from many sources contribute to a series of databases that support numerical codes used either to calculate inputs to the LMB model or to run simulations. The data, databases, and numerical codes are summarized in this section.

2.1 Data Sources

2.1.1 Hydrostratigraphic Units and Model Layering

The USGS National Elevation Dataset furnished land surface for the model domain. The initial definition of the sequence of hydrostratigraphic units extending from land surface to the top of Precambrian rocks was derived in part from RASA data (Kontis and Mandel, 1980), supplemented by framework studies in each state. For Michigan, several interpretive compilations target the bedrock stratigraphy (Bricker and others, 1983; Michigan Department of Environmental Quality, 1987; Nadon and others, 2000; Swezey, 2008), whereas others include data for both unconsolidated (mostly glacial) deposits and for Michigan Basin bedrock (Western Michigan University Department of Geology, 1981; Michigan Department of Environmental Quality, 2003). In eastern Wisconsin, county and regional studies were tapped to delineate the model layering (Foley and others, 1953; LeRoux, 1957; Newport, 1962; Knowles, 1964; Knowles and others, 1964; Olcott, 1966; Hutchinson, 1970; Green and Hutchinson, 1965; Krohelski, 1986; Batten, 1987; Conlon, 1998; Batten 2004; Feinstein, Eaton, and others, 2005). Stratigraphic interpretations are based on well data contained in databases compiled by state agencies (Wisconsin Department of Natural Resources, 2006; Wisconsin Geological and Natural History Survey, 2004). Data sources for stratigraphy in northern Indiana include framework studies of bedrock topography and structure (Becker and others, 1978; Bassett and Hasenmueller, 1980; Shaver and others, 1986; Rupp, 1991; Casey, 1992; Bunner, 1993; Casey, 1994; Gray, 2003) and bedrock representations in model studies (for example, Eberts and George, 2000). Local studies focus on the glacial stratigraphy (for example, Bayless and others, 1995). The bedrock stratigraphy and structure of northeastern Illinois are described by many studies (for example, Emrich and Bergstrom, 1962; Buschbach, 1964; Emrich, 1966; Kolata and others, 1978; Kolata and Graese, 1983; Mikulic and others, 1985; Nichols and others, 1987; Brown and others, 2000; Kay and others, 2004). The recent modeling study by the Illinois State Water Survey (Meyer and others, 2009) produced a hydrogeologic

model underlying the groundwater flow model for northeastern Illinois based on many previous studies. It represents the full sequence of stratigraphic units overlying the Precambrian rocks and includes vertical offsets in layer surfaces owing to major faulting. The Illinois State Water Survey generously supplied the USGS with their stratigraphic and structural interpretation, which is directly adapted to the LMB model layering. Finally, the stratigraphy in northwestern Ohio, limited to the model farfield, is available through comprehensive geologic studies (Wickstrom and others, 1992; Ohio Division of Geologic Survey, 2005).

2.1.2 Hydrogeologic Properties of Aquifers and Confining Units

In order to establish initial values for model inputs such as horizontal hydraulic conductivity, vertical hydraulic conductivity, specific storage, and specific yield, data were compiled for both unconsolidated and bedrock deposits. Glacial mapping covering the model domain allowed correlation of hydrogeologic properties with types of glacial deposits (Soller and Packard, 1998; Fullerton and others, 2003). Recent surveys in Michigan yielded estimates of hydrogeologic properties for both glacial and bedrock sediments (Michigan Department of Environmental Quality, 2005, 2006; Apple and Reeves, 2007). For eastern Wisconsin, estimates from many individual studies were compiled, with special attention to results of aquifer tests in bedrock units (Drescher, 1953; Foley and others, 1953; LeRoux, 1957; Newport, 1962; Knowles, 1964; Olcott, 1966; Feinstein and Anderson, 1987; Rovey, 1990; Batten and Conlon, 1993; Jansen, 1995; Stocks, 1998; Muldoon and others, 2001). Existing compilations of subsurface properties were especially helpful (Eaton and others, 1999; Carlson, 2000). Several studies provided information on glacial sediments (Simpkins, 1989; Bradbury and Muldoon, 1990; Rodenback, 1988; Rayne and others, 1996; Clayton, 2001) and on the regional confining unit, the Maquoketa (Eaton, 2002). Overviews of hydrogeologic properties are available for northern Indiana (Indiana Department of Natural Resources, 1987, 1990, 1994, 1996; Fenelon, Bobay, and others, 1994) and are supplemented by estimates contained in studies of particular locations (for example, Lapham, 1981; Fenelon and Watson, 1992; Bayless and Arihood, 1996; Arihood, 1998; Fowler and Arihood, 1998) and by RASA modeling that extends into Ohio (Eberts and George, 2000). The Illinois sources for hydrogeologic-property estimates in the northeast part of the State include hydrogeologic investigations and modeling reports (for example, Walton, 1960; Zeizel and others, 1962; Nicholas and others, 1987; Batten and others, 1999; Walker and others, 2003; Kay and others, 2006).

2.1.3 Recharge

Several studies that combined data collection and some method of estimation linked to the data were used to represent the spatial distribution of recharge in the LMB model for Michigan (Holtschlag, 1996; Neff, Piggott, and Sheets, 2005), for eastern Wisconsin (Cherkauer, 1999; Cherkauer, 2001; Dripps and others, 2001; Cherkauer, 2004; Dripps and Bradbury, 2007; Hart and others, 2008a), for northern Indiana (Rosenshein, 1963; Fowler and Arihood, 1998), and for northeastern Illinois (Hensel, 1992; Arnold and Friedel, 2000). These studies used topography, climate variables, land use, and soil variables to estimate recharge (for example, U.S. Geological Survey, 2000a,b; U.S. Department of Agriculture, 2006). These data were incorporated in a recently developed soil-water-balance (SMB) model used to provide recharge estimates for the LMB model (Westenbroek and others, 2010).

2.1.4 Surface-Water Network

The surficial extent and stages of streams and water bodies (lakes and wetlands)⁴ in the entire LMB model domain were derived from two compilations of data: the National Hydrography Dataset for the United States (U.S. Geological Survey, 2001a, 2005a) and the Great Lakes Aquatic Gap Project (Brenden and others, 2006). These data were used to impose boundary conditions as part of model construction (see section 4) and to define base-flow targets as part of model calibration (see section 5).

2.1.5 Groundwater Withdrawals

Producing a historical database of groundwater withdrawals between 1864 and 2005 for the LMB model required data from many studies, including compilations at the regional scale (Mandle and Kontis, 1992; Solley and others, 1998; Kay, 2002). For Michigan, several reports and databases from comprehensive studies include local information (Michigan Department of Public Health, 1943; Bedell, 1982; Baltusis and others, 1992; Michigan Department of Environmental Quality, Water Bureau, 2006a–e). In Eastern Wisconsin, data from county studies are complemented by compilations in larger surveys that serve as snapshots of water use in time (DeVaul, 1975a,b,c; Lawrence and Ellefson, 1982; Lawrence and others, 1984; Krohelski and others, 1987; Ellefson and others, 1993, 1997; Wisconsin Department of Natural Resources, 1997; Ellefson and others, 2002; Buchwald, 2009). For southeastern Wisconsin, a historical database for withdrawals was incorporated in the most recent model of the area (Feinstein, Eaton, and others, 2005; Feinstein, Hart, and others, 2005).

⁴ Streams are, of course, flowing bodies of water. However, the simplified distinction between “streams” and “water bodies” used in the remainder of this report is similar to and consistent with USGS usage elsewhere—specifically, in the “Streams and Waterbodies” map layer of the National Atlas of the United States (<http://www-atlas.usgs.gov/mld/hydrogm.html>).

The water-use record in northern Indiana is available for much of the historical period through various statewide studies (Indiana Department of Natural Resources, Water Division, 1980; Arvin and Spaeth, 1996), regional studies (Indiana Department of Natural Resources, 1987, 1990, 1994, 1996), and local studies (for example, Stallman and Klaer, 1950). Major compilations are available for groundwater withdrawals in northeastern Illinois for past periods (for example, Suter and others, 1959; Sasman, 1965; Schicht and others, 1976; Avery, 1995; Visocky, 1997), but the main data source is the ongoing Illinois Water Inventory Program of the Illinois State Water Survey begun in 1979 to collect annual pumping rates for high-capacity wells—that is, wells that can produce greater than 70 gal/min. Historical pumping in Ohio, whose area is restricted to the farfield of the model domain, was not examined in this study.

2.1.6 Salinity

Salinity levels within the LMB model domain range from freshwater concentrations (DS less than 1,000 mg/L to saline water (typically defined as DS greater than 10,000 mg/L) to brine (DS greater than 100,000 mg/L). Salinity is highest in the Michigan Basin, where shallow and deep aquifers both contain saline water. The distribution of DS was defined by using data from studies in Michigan (Gupta, 1993; Ging and others, 1996; Meissner and others, 1996; Wahrer and others, 1996; Westjohn and Weaver, 1996; Gupta and Bair, 1997) and in northern Indiana and northwestern Ohio (Gupta, 1993; Schnoebelen and others, 1995; Schnoebelen and others, 1998). On the west side of Lake Michigan, DS concentrations greater than 10,000 mg/L are recorded in deep bedrock aquifers in northeastern Illinois (Bond, 1972; Visocky and others, 1985; Nicholas and others, 1987; Balding, 1991) and more sporadically for rocks underneath parts of Wisconsin near Lake Michigan (Ryling, 1961; Kammerer and others, 1998).

2.1.7 Water Levels

The LMB model was calibrated to reproduce historical groundwater levels throughout the model domain at various depths. The U.S. Geological Survey maintains a historical database from a long-term network of wells that record water levels in various aquifer units (see the U.S. Geological Survey National Water Information System Web site at <http://waterdata.usgs.gov/nwis/gw>). In addition to this national resource, compilations are available for various periods in each of the states within the LMB model domain. For Michigan, they include predevelopment records (Barton and others, 1996), long-term hydrographs of network wells (Cornett and others, 2006), and databases of logs submitted by well drillers that include water levels (Michigan Department of Environmental Quality, 2003).

For eastern Wisconsin, available water-level data include observations and mapped contours derived from observations for the deep bedrock from the early 1900s (Weidman and Schultz, 1915), water levels collected in the early 1980 as part of the RASA studies from intervals in test wells isolated by packers and corresponding to individual hydrostratigraphic units (Young, 1992), contoured representations of the water table at the regional scale (Kammerer, 1995), and a historical compilation of driller-log records (Wisconsin Geological and Natural History Survey, 2004). In addition to the available U.S. Geological Survey network records in northern Indiana, there are early collections of water levels (Capps, 1910) and more recent collections (Crompton and others, 1986; Kay and others, 1996; Eberts, 2000), as well as driller-log databases (Indiana Department of Natural Resources, Division of Water, 2002). Historical compilations in northeastern Illinois record not only the recovery of water levels in deep aquifers after heavy pumping around Chicago diminished in the 1980s when the city converted to Lake Michigan public supply (Visocky and others, 1985; Nicholas and others, 1987; Visocky, 1993), but also the renewed drawdown due to development in areas around Chicago (Visocky, 1997; Burch, 2002).

2.1.8 Groundwater Discharge to Streams and Lake Michigan

The LMB model was also calibrated to reproduce observed groundwater discharge to streams, as base flow. Base flow is sustained or fair-weather streamflow and is composed largely of groundwater discharge. The network of U.S. Geological Survey streamgages provides the data for calculating base flow from streamflow records at the outlet of hydrologic basins (Mason and Yorke, 1997; Rutledge, 1998). Several studies have estimated base-flow characteristics of streams within the LMB model domain (Holmstrom, 1978; Singh and Ramamurthy, 1993; Fowler and Wilson, 1996; Arnold and others, 2000; Neff, Day, and others, 2005). Other studies estimated direct groundwater discharge to Lake Michigan, as well as indirect groundwater discharge to the lake via base flow of streams within the basin (Sellinger, 1995; Grannemann and Weaver, 1999; Holtschlag and Nicholas, 1998). Several geophysical and modeling studies estimated direct groundwater discharge to the west side of Lake Michigan (Bradbury, 1982; Cherkauer and Hensel, 1986; Cherkauer and others, 1987; Nauta, 1987; Craig, 1989; Webb, 1989; Cherkauer and others, 1990; Mueller, 1992).

2.1.9 Lakebed of Lake Michigan

The hydraulic conductivity and thickness of the lakebed of Lake Michigan determines the rate of groundwater discharge to the lake. The bathymetry of the lakebed has been mapped (National Oceanic and Atmospheric Administration, 2005), and geophysical methods have been used to determine the geologic and hydraulic properties of shallow lakebed

sediments (Wold and Hutchinson, 1979; Cherkauer and others, 1987). The Illinois State Geological Survey conducted 400 mi of continuous seismic profiling combined with gravity coring of bottom sediments in southern Lake Michigan (Lineback and others, 1971), the data from which were interpreted as geologic cross sections (Lineback and others, 1972). A second effort under the auspices of the Sea Grant program in Wisconsin used electrical surveys to attempt to evaluate the ease of vertical flow by estimating the vertical hydraulic conductivity of the shoreline lakebed (for example, Cherkauer and others, 1987).

2.2 Databases and Algorithms

The resources of the Great Lakes Basin Pilot program allowed construction of four databases that were used for hydrostratigraphic, water-use, and salinity inputs to the LMB model. Each database is documented in a separate U.S. Geological Survey Scientific Investigations Report. The database work was supplemented by two contracts to state agencies in support of the LMB model databases, one for water-use information and one for mapping of glacial categories. In addition to customized databases, the model relies on particular computer codes to calculate historical recharge, to account for variable-density groundwater flow, and to perform nonlinear regression as part of the calibration process.

2.2.1 Hydrostratigraphic Units

Surface elevations of hydrostratigraphic units were constructed by Lampe (2009) in support of the development of the LMB model. The hydrostratigraphic units were delineated by grouping the bedrock geology within the model domain into aquifers and (or) confining units (fig. 10). In the Lampe study, top and bottom surfaces for 14 hydrostratigraphic bedrock units were constructed over the model domain. The mapped units, in downward order, are as follows:

- Jurassic red beds, under parts of central Michigan (*confining unit*).
- Pennsylvanian sandstones of the Grand River and Saginaw Formations, under parts of the Lower Peninsula of Michigan (*aquifer*).
- Pennsylvanian Saginaw shales and the Parma Sandstone, combined with the Mississippian Bayport Limestone, under parts of the Lower Peninsula of Michigan (*either aquifer or confining unit depending on location*).
- Mississippian shales of the Michigan Formation, under parts of the Lower Peninsula of Michigan (*confining unit*).
- Mississippian Marshall Sandstone, under parts of the Lower Peninsula of Michigan (*aquifer*).

Time-stratigraphic unit		Wisconsin	Illinois	Indiana	Ohio	Michigan	Hydrogeologic unit (model layer)	Aquifer system			
System	Series										
Quaternary		Glacial deposits	Glacial deposits	Glacial deposits	Glacial deposits	Glacial deposits	Quaternary (1-3)	1. QRNR			
Jurassic	Middle	Absent	Absent	Absent	Absent	Ionia Fm	Jurassic (4)	2. PENN			
Pennsylvanian	Upper					Grand River Fm	Upper Pennsylvanian (5)				
	Lower					Saginaw Fm	Lower Pennsylvanian (6)				
Mississippian	Upper					Saginaw Fm (Shale)	Michigan (7)				
	Lower	Parma Sandstone									
Devonian	Upper	Absent	Absent	Absent	Absent	Bayport Ls.	Marshall (8)	4. SLDV			
						Michigan Fm					
	Middle					Marshall Sandstone					
	Lower					Coldwater Shale	Devonian-Mississippian (9)				
Silurian	Upper	Antrim Shale	New Albany Shale Group	Ellsworth Shale	Sunbury Shale	Sunbury Shale	Silurian-Devonian (10)				
	Middle	Milwaukee Fm	Cedar Valley Limestone	Muscatatuck Group	Traverse Group	Traverse Group					
	Lower	Thienville Fm	Wapsipinicon Limestone	Absent	Dundee Formation	Detroit River Group					
Ordovician	Upper	Absent	Absent	Absent	Absent	Detroit River Group	Bass Islands Group				
						Waubakee Fm		Salina Group	Salina Group		
	Middle					Racine Fm	Racine Dolomite	Salomonie Dolomite	Lockport Group	Manistique Group	Silurian-Devonian (11-12)
	Lower					Mayville Fm	Kankakee Dolomite	Brassfield Limestone	Dayton Formation	Burnt Bluff Group	
Cambrian	Upper	Absent	Absent	Absent	Absent	Cataract Group	Cataract Group				
						Maquoketa Fm	Maquoketa Group	Cincinnati group	Richmond Group	Maquoketa (13)	
	Middle					Sinnipee Group	Galena Group	Trenton Limestone	Trenton Limestone	Trenton Fm	Sinnipee (14)
	Lower					Prairie du Chien Gr	Prairie du Chien Gr	Prairie du Chien Gr	Absent	Prairie du Chien Gr	Prairie du Chien-Franconia (16)
Precambrian	Upper	Absent	Absent	Absent	Absent	Black River Limestone	Black River Fm	St. Peter (15)			
						Glenwood Fm	Ancell Group	Ancell Group	Black River Group	Glenwood Fm	
						St. Peter Fm	Wells Creek Fm	Wells Creek Fm	Wells Creek Fm	St. Peter Sandstone	
						Trempealeau Group	Potosi Dolomite	Potosi Dolomite	Knox Dolomite	Trempealeau Fm	
References	Upper	Absent	Absent	Absent	Absent	Black River Group	Glenwood Fm	St. Peter (15)			
						Tunnel City Group	Franconia Fm	Franconia Sandstone	Kerbel Fm	Galesville Sandstone	Ironton-Galesville (17)
						Wonewoc Fm	Ironton Sandstone	Ironton Sandstone	Kerbel Fm	Galesville Sandstone	Eau Claire (18)
						Eau Claire Fm	Eau Claire Fm	Eau Claire Sandstone	Eau Claire Fm	Eau Claire Fm	Mount Simon (19-20)
References	Upper	Absent	Absent	Absent	Absent	Mount Simon Formation	Mount Simon Sandstone	Mount Simon Sandstone			
						Mount Simon Formation	Mount Simon Sandstone	Mount Simon Sandstone of Dresbach Group	Mount Simon Sandstone	Mount Simon Sandstone	
References	Upper	Absent	Absent	Absent	Absent	Jacobsville Sandstone					
						Keweenaw Supergroup	Crystalline Basement Complex	Crystalline Basement Complex	Crystalline Basement Complex	Crystalline Basement Complex	
References		Wisconsin Geological and Natural History Survey, 2006	Buschbach, 1964 Kolata and Graese, 1983 Kolata, 1990 Mikulic and others, 1985 Willman and others, 1975 Young and Siegel, 1992	Gray and others, 1985	Hull, 1990	Catacosinos and others, 2001					

¹Rocks of the Pennsylvanian System were grouped with the Mississippian-Devonian hydrogeologic unit for Illinois

EXPLANATION

- Aquifer
- Aquifer/confining unit
- Confining unit
- Depositional surface
- Erosional surface
- Gr, Group
- Fm, Formation
- Ls, Limestone

Figure 10. Composite section showing time- and rock-stratigraphic framework and nomenclature for the Lake Michigan Basin region correlated with the hydrogeologic units and aquifer systems in the groundwater model. (Aquifer-system abbreviations are defined in table 1.)

- Coldwater Shale and other Mississippian shales, combined with Devonian shales, under the Lower Peninsula of Michigan and extending under parts of northern Indiana and part of Lake Michigan (*confining unit*).
- Silurian and Devonian dolomites, under parts of eastern Wisconsin, northeastern Illinois, and the Upper Peninsula of Michigan and all of the Lower Peninsula of Michigan and northern Indiana (*either aquifer or confining unit depending on location and interval*).
- Ordovician shales of the Maquoketa Group and related groups, under parts of eastern Wisconsin, northeastern Illinois, and the Upper Peninsula of Michigan and all of the Lower Peninsula of Michigan and northern Indiana (*confining unit*).
- Ordovician dolomites of the Sinipee Group and related formations/groups, under parts of eastern Wisconsin, northeastern Illinois, and the Upper Peninsula of Michigan and all of the Lower Peninsula of Michigan and northern Indiana (*either aquifer or confining unit depending on location*).
- Ordovician sandstones of the St. Peter Formation and related formations/groups, under most of eastern Wisconsin, northeastern Illinois, and the Upper Peninsula of Michigan and all of the Lower Peninsula of Michigan and northern Indiana (*aquifer*).
- Ordovician dolomites of the Prairie du Chien Group and upper Cambrian sandstone units including the Franconia Formation and related formations/groups, under parts of eastern Wisconsin, northeastern Illinois, and the Upper Peninsula of Michigan and all of the Lower Peninsula of Michigan and northern Indiana (*either aquifer or confining unit depending on location*).
- Cambrian Ironton and Galesville Sandstones and related formations, under most of eastern Wisconsin, northeastern Illinois, and the Upper Peninsula of Michigan and all of the Lower Peninsula of Michigan and northern Indiana (*aquifer*).
- Cambrian siltstone and sandstone of the Eau Claire Formation, under most of eastern Wisconsin, northeastern Illinois, and the Upper Peninsula of Michigan and all of the Lower Peninsula of Michigan and northern Indiana (*either aquifer or confining unit depending on location*).
- Cambrian Mount Simon Formation, under most of eastern Wisconsin, northeastern Illinois, and the Upper Peninsula of Michigan and all of the Lower Peninsula of Michigan and northern Indiana (*aquifer*). In parts of the Upper Peninsula of Michigan the Mount Simon Formation is underlain by a Precambrian unit—the Jacobsville Sandstone—which acts as an aquifer and is tapped by pumping wells. It is lumped with the Mount Simon Formation to form a single mappable unit in the LMB model framework.

This sequence of units represents the entire bedrock thickness within the model domain. The database report contains isopach (thickness) maps for each hydrostratigraphic unit. Details on the incorporation of the hydrogeologic model into the groundwater-flow model are presented in section 4 of this report (“Model Construction”).

2.2.2 Thickness and Properties of Quaternary Deposits

Unconsolidated sediments overlying the bedrock in the LMB model are largely glacial in origin and Quaternary in age. The thickness and texture of the unconsolidated sediments are described for an area incorporating most of the model domain by Arihood (2009). More than 450,000 water-well driller logs in Michigan, eastern Wisconsin and northern Indiana were used to glean information for mapping the thickness and texture of the unconsolidated material over nearly the entire model domain, as well as to construct a database of water levels for use in model calibration. The hydraulic conductivities representing glacial deposits in the model were computed by using the areal and vertical distribution of the coarse fraction of glacial sediments (silty sand, sand, and gravel) as recorded in driller logs. The method used to convert the coarse-fraction mapping into hydraulic conductivity is presented in section 4 of this report (“Model Construction”). The use of the water levels derived from the water-well driller logs is discussed in section 5 (“Model Calibration”).⁵

The depth of the bedrock surface in parts of the lower peninsula of Michigan, in places exceeding 1,000 ft, required additional analysis to properly map the thickness of the Quaternary deposits. A cooperative study by Michigan State University, the USGS, and the Michigan Department of Environmental Quality (David Lusch, Michigan State University, Department of Geography, RS & GIS Research and Outreach Services, written commun., April 2009; Remote Sensing and Geographic Information Science, 2006) supplemented the information from driller-log data compiled by Arihood (2009).

⁵ Northeastern Illinois was excluded from Arihood’s analysis, so results from other studies, notably Feinstein, Eaton, and others (2005) and Meyer and others (2009), were used to map the thickness, texture, and hydraulic conductivity of the QRNR deposits.

2.2.3 Distribution of Glacial Categories in Wisconsin and Michigan

The calculation of hydraulic conductivity for glacial (Quaternary) deposits in the model domain is a function of not only material texture at a location but also the glacial category mapped for that location. In this study the glacial categories were characterized as

- clayey till,
- loamy till,
- sandy till,
- fine stratified deposits,
- medium and coarse stratified deposits, and
- organic deposits.

The extent of each category corresponds to the distribution of sets of glacial units mapped for USGS regional compilations (Soller and Packard, 1998; Fullerton and others, 2003). Details on the procedure for converting mapped units into glacial categories are given in section 4 of this report (“Model Construction”). One aspect of the procedure required further data collection and interpretation. Because the regional geologic mapping of Quaternary deposits focuses on surficial deposits, the validity of the mapping of glacial categories is increasingly uncertain with depth and is especially uncertain for thick glacial deposits (considered to be sequences greater than 100 ft). In order to extend the mapping in eastern Wisconsin to areas with thicker glacial deposits and also to check the assignments of glacial categories derived from Fullerton and others (2003) for the shallow deposits, a contract was arranged with the Wisconsin Geological and Natural History Survey and with David Mickelson, Professor Emeritus, University of Wisconsin-Madison. The results of these contracts were reinterpretations of the glacial categories for eastern Wisconsin, both for the upper 100 ft of Quaternary-deposit thickness and for areas where the Quaternary-deposit thickness is greater than 100 ft (T. Hooyer, WGNHS, written commun., December 6, 2006).

As part of his contract, Professor Mickelson also studied the assignment of glacial categories in the Lower Peninsula of Michigan and northern Indiana. He indicated areas where the surficial glacial categories derived from Fullerton might not be representative of the upper 100 ft of Quaternary sediment (D. Mickelson, University of Wisconsin, written commun., April 30, 2007).

2.2.4 Groundwater Withdrawals

The historical database for groundwater withdrawals from high-capacity wells within the model domain for the period extending from 1864 to 2005 is described Buchwald

and others (2010). The database details changes in pumping with time and assigns pumping by aquifer and type of end use: public supply, industry, or irrigation. The database contains average pumping rates for more than 13,000 glacial and bedrock high-capacity wells assigned to 12 time intervals (typically 10 years in length). Details on the input of the withdrawal records into the LMB model are presented in section 4 of this report (“Model Construction”).

2.2.5 Illinois Water-Use Information

Part of the groundwater withdrawals record was assembled from databases maintained by the Illinois State Water Survey. It has been collecting water use data for Illinois since at least the early 1940s, primarily in regions where water resources were being extensively developed, such as in the northeastern Illinois area. Documentation of annual groundwater withdrawals for individual high-capacity wells began in 1978 and is available through 2005 through the Illinois Water Inventory Program. Because of the high quality of this historical database for not only municipal but also private industrial and irrigation pumping, the USGS, as part of the Great Lakes Pilot project, contracted with the Illinois State Water Survey to extract information from the database for northeastern Illinois and put it in a form convenient for input to the LMB model. The pumping history that resulted is presented in section 4 of this report (“Model Construction”).

2.2.6 Distribution of Salinity

Maps showing the distribution of DS concentrations were constructed by Lampe (2009). The maps correspond to the Quaternary sediments, the upper Pennsylvanian units, the Marshall aquifer, an interval within the Silurian dolomites containing evaporites (the Salina Group), the Sinipee Group, the Prairie-du-Chien/Franconia layers, and the Mount Simon Formation. Salinity in areas with no data was assumed equal to that in adjacent units or was interpolated vertically by using DS concentrations from units above and below. The maximum DS concentration in the database, approximately 400,000 mg/L, is within the Silurian Salina Group in the Michigan Basin.

The mapped distribution of DS was used to compute the initial density-distribution condition for the LMB model, as discussed in section 4 of this report (“Model Construction”).

2.2.7 Numerical Codes

Several major numerical codes were used to (a) calculate inputs, (b) simulate variable-density groundwater flow, and (c) estimate values of model parameters.

2.2.7.1 Calculation of Historical Recharge

In the Lake Michigan Basin and adjacent areas, recharge is the chief source of water to the groundwater system. Recharge varies spatially as a function of local precipitation patterns, slope of the land surface, and soil conditions. Recharge varies temporally as a function of climatic variation and land-use changes. A soil-water balance model (SWB) that incorporates these spatial and temporal factors was developed for the LMB model as part of the Great Lakes Basin study. The code and method, based on previous work by Thornthwaite and Mather (1957) and Dripps (2003), was developed by Westenbroek and others (2010). The SWB model calculates recharge by using commonly available geographical information system (GIS) data layers (for example, land use, hydrologic soils group, soil available water content, and surface slope as an indication of overland flow direction) in combination with climatological data. The SWB model computes precipitation, evapotranspiration, runoff, infiltration across the land surface, percolation through the unsaturated zone, and recharge to the water table on a daily basis. The daily recharge estimates are then summed to correspond to the time intervals required by the model input. Details on the application of this code to the model nearfield are given in section 4 of this report (“Model Construction”).

2.2.7.2 Simulation of Variable-Density Groundwater Flow

The proximity of saline water to pumping centers both east and west of Lake Michigan requires the use of a variable-density groundwater flow model. The U.S. Geological Survey SEAWAT-2000 code (Langevin and others, 2003) combines the features of MODFLOW-2000 (Harbaugh and others, 2000) developed for groundwater-flow problems under freshwater conditions and the features of the MT3DMS transport code (Zheng and Wang, 1999) developed for simulating the advection, dispersion, retardation, and decay of dissolved constituents in groundwater. The SEAWAT-2000 code solves the variable-density flow equation by formulating the matrix equations in terms of fluid mass and assuming that the fluid density is a linear function of solute concentrations. The application of SEAWAT to the LMB model is described in sections 3 and 4 of this report (“Model conceptualization” and “Model Construction”).

2.2.7.3 Parameter Estimation by Nonlinear Regression

Calibration of the groundwater-flow model requires adjustment of parameter values in order to minimize the difference between observed and simulated heads and flows. The calibration of the LMB model is conditioned by the large number of parameter types and zones, the presence of areas where cell-by-cell variation of parameters is crucial to the solution, the large number and variety of calibration targets, the distinct sensitivity of parameter updates to different target groups, and the need to reconcile parameters that control the predevelopment steady-state solution (for conditions which existed before

large-scale pumping) with parameters that strongly influence the transient historical solution (for the period from 1864 to 2005).

The LMB model was calibrated by using a combination of manual adjustment of parameter values and application of PEST (Doherty, 2008a), a parameter estimation code that uses nonlinear regression. PEST automatically adjusted selected parameters (hydraulic conductivity, recharge, riverbed conductance) through a series of model runs. After each run, simulated groundwater levels, vertical gradients, and base flows were compared to observed values. The runs continued until the differences (residuals) between simulated and observed values were minimized. The calibration processes, as in all studies, depended on subjective choices, such as parameter zonation and target weighting. However, the calibration approach used for the LMB model extends traditional nonlinear regression parameter estimation by employing three advanced tools: (1) *pilot points* (Doherty, 2003; Doherty and others, in press); (2) *Tikhonov regularization* (Tikhonov, 1963a,b; Doherty, 2003; Fienen and others, 2009); and (3) *hybrid singular value decomposition* (Tonkin and Doherty, 2005; Hunt and others, 2007), also referred to as SVD-Assist (SVDA) by Doherty (2008a). An overview on the use of these tools for parameter estimation is provided by Hunt and others (2007) and by Doherty and Hunt (in press); additional information is in section 5 of this report.

3. Conceptual Model of Regional Groundwater System

Developing a conceptual model for the groundwater-flow system in the Lake Michigan Basin requires the definition of the *hydrogeologic framework*: that is, the identification of hydrogeologic units within the glacial and bedrock geology that can be characterized as aquifers or as confining units and grouped into aquifer systems. The second element of the conceptual model consists of the hydrologic behavior of the *regional flow system* in terms of shallow and deep flow, and regional divides. The flow system is also characterized by sources of water (recharge, movement of water from surface water to groundwater, release of water from storage) and sinks (discharge to surface waters, pumping centers, addition of water to storage). The varying strength of sources and sinks (most notably in the case of Lake Michigan itself) has a large influence on water levels and water movement. The third conceptual element is the *interaction between groundwater and surface water*. Discharge of groundwater to surface water affects the location of groundwater divides, whereas the pumping of groundwater can appreciably alter the natural pattern of local and regional discharge. An additional element in this conceptual model is *salinity of water*. High concentrations of dissolved solids, especially in the sedimentary rocks of the Michigan Basin affect the rate and direction of groundwater flow. Finally, attention is paid to the implications of simulating the flow system as *confined* or *unconfined*.

3.1 Hydrogeologic Framework⁶

The study area for the LMB model encompasses most of the Michigan structural basin, which is centered in the Lower Peninsula of Michigan and extends into parts of Illinois, Wisconsin, Indiana, Ohio, and Ontario, Canada. The Michigan Basin is bounded to the north by the Canadian Shield, to the west by the Wisconsin Arch, to the southwest by the Kankakee Arch, to the southeast by the Findlay Arch, and to the east by the Algonquin Arch (Olcott, 1992; Lloyd and Lyke, 1995) (fig. 8). The Kankakee Arch separates the Michigan Basin from the Illinois Basin—part of which is included in the southwest section of the study area. The Findlay Arch separates the Michigan Basin from structural basins to the southeast outside the model domain. Cambrian rocks of the Wisconsin Arch make up the western boundary of the model.

The subsurface stratigraphy varies across the LMB model domain, so a series of stratigraphic columns representing Wisconsin, Illinois, Indiana, Ohio, and Michigan are shown on figure 10. Shallow units along the Wisconsin Arch are correlated stratigraphically with deeper units in areas to the north in the Upper Peninsula of Michigan and to the south in northeastern Illinois, Indiana, and Ohio. Differing depositional environments are reflected by facies changes that result in variations of rock types within a unit. The sedimentary sequence of Cambrian, Ordovician, and Silurian units consists of sandstones, carbonates, and shales that overlie Precambrian basement rock. The sequence ranges in thickness from hundreds to thousands of feet along the Wisconsin/Kankakee Arches to greater than 10,000 ft in the center of the Michigan Basin (Sonnenfeld and Al-Aasm, 1991). The complete rock sequence is not present everywhere within the model domain. On the west, north, and south side of Lake Michigan, the youngest bedrock units are Silurian (except some Devonian rocks near Milwaukee and in northern Indiana); but on the east side, in the Lower Peninsula of Michigan, younger rocks of Mississippian, Pennsylvanian, and Jurassic age exceed 1,000 ft in thickness. Throughout the model domain (except for scattered locations in the northwest corner), the upper bedrock surface is mantled by Quaternary deposits that are mostly glacial in origin but can contain some alluvial deposits.

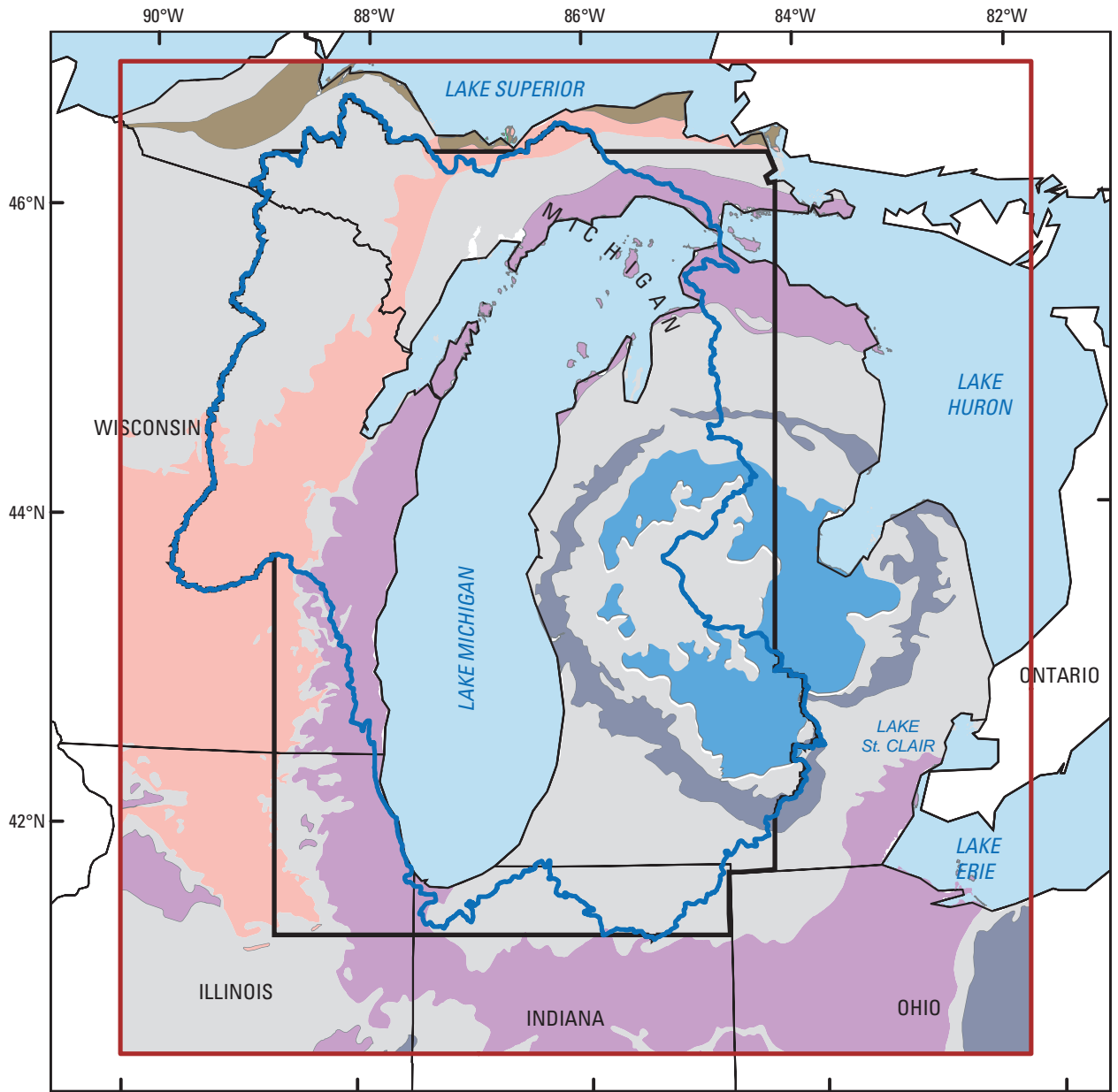
Bedrock aquifers (fig. 11) can contain a variety of conduits subject to preferential flow and associated with fractures, joints, faults, and karst features. For example, carbonate (mostly dolomite) rocks in the model domain commonly contain dissolution and bedding planes that route flow preferentially and, possibly, in a particular direction (see, for example, Bradbury and Muldoon, 1994). However, it is not possible to include these local features in a regional model where the cell size is on the order of a mile in lateral extent and whose layers can be on the order of 1,000 ft thick. Instead, the entire bedrock sequence within the model domain is treated as an

equivalent porous medium whose individual unit hydraulic conductivities are assumed to be bulk properties reflecting the integrated effect of conduits on flow. This approach is common to modeling at the regional scale (Anderson and Woessner, 1992); the omission of relatively small-scale preferential and anisotropic features is expected to have little effect on the results sought from a regional model, such as drawdown patterns around large pumping centers or the pattern of groundwater exchange with Lake Michigan.

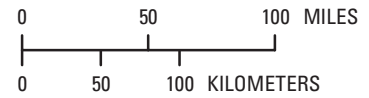
Appendix 1 contains brief descriptions of the geologic framework for the Quaternary deposits at the regional scale and for bedrock units in each subregion of the model. The characteristics of the lithologic units described in the appendix allow the units to be identified as aquifers (defined as geologic formations that contain sufficient saturated permeable material to yield significant quantities of water to springs and wells) or as confining units (defined as bodies of distinctly less permeable material stratigraphically adjacent to one or more aquifers that restrict the movement of water into and out of the aquifers). Some lithologic units are aquifers in some locations and confining units elsewhere. The series of aquifers, confining units, and mixed units define a *hydrogeologic sequence*. The complete order from land surface to crystalline basement for the LMB model is

1. aquifer/confining unit: Quaternary (QRNR)
2. confining unit: Jurassic red beds (JURA)
3. aquifer: Upper Pennsylvanian Grand River and Saginaw Formations (PEN1)
4. aquifer/confining unit: Lower Pennsylvanian Saginaw Formation and Parma Sandstone and Mississippian Bayport Limestone (PEN2)
5. confining unit: Mississippian Michigan Formation (MICH)
6. aquifer: Mississippian Marshall Sandstone (MSHL)
7. confining unit: Devonian/Mississippian shales (DVMS)
8. aquifer/confining unit: Silurian/Devonian carbonates and evaporites (SLDV)
9. confining unit: Ordovician Maquoketa Group/Formation and related units (MAQU)
10. aquifer/confining unit: Ordovician Sinnipee Group and related units (SNNP)
11. aquifer: Ordovician St. Peter Formation/Sandstone and related units (STPT)
12. aquifer/confining unit: Ordovician Prairie du Chien Group and Cambrian Franconia Formation/Sandstone (PCFR), considered part of the Knox Megagroup in some locations (Visocky and others, 1985)
13. aquifer: Cambrian Ironton and Galesville Sandstones and related units (IRGA)
14. aquifer/confining unit: Cambrian Eau Claire Sandstone/Formation (EACL)
15. aquifer: Cambrian Mount Simon Sandstone (MTSM) and, locally, the Precambrian Jacobsville Sandstone.

⁶ For ease of presentation abbreviations are used in this section and in subsequent sections to refer to hydrogeologic units and aquifer systems. They are listed in table 1.



Base from ESRI, 2001; aquifers from U.S. Geological Survey, 2003



EXPLANATION

Principal bedrock aquifers		Model or hydrologic boundary	
	Jacobsville aquifer, Precambrian		Model domain
	Cambrian-Ordovician aquifers		Lake Michigan Basin
	Mississippian (Marshall) aquifers		Model nearfield
	Pennsylvanian aquifers		
	Silurian-Devonian aquifers		
	Confining units		

Figure 11. Principal bedrock aquifers.

In all, the LMB model incorporates five hydrogeologic units defined as aquifers (PEN1, MSHL, STPT, IRGA, and MTSM), six hydrogeologic units defined as mixed aquifer/confining units (QRNR, PEN2, SLDV, SNNP, PCFR, and EACL), and four hydrogeologic units identified as confining units (JURA, MICH, DVMS, and MAQU). The MTSM is described as an aquifer unit even though it commonly contains fine-grained beds several hundred feet below its surface. These beds are incorporated into the bottommost layer of the model, which, in turn, overlies the Precambrian crystalline basement. The crystalline rocks are assumed to be highly resistant to vertical flow, so the interface between sedimentary rocks and the crystalline, Precambrian basement was made the bottom boundary of the flow model.

The sequence of 15 hydrogeologic units is not continuous throughout the model domain. The JURA, PEN1, PEN2, MICH, MSHL, and DVMS units are commonly absent north, west, and south of the Michigan Basin, and other units are absent near the crest of the Wisconsin Arch and toward the western edge of the model. These units, including the SLDV, MAQU and older Paleozoic rocks, were progressively eroded, leaving only thin QRNR deposits and the Mount Simon Sandstone over Precambrian crystalline rock. Bedrock highs can also produce relatively small areas where the QRNR is absent, especially in the northwestern part of the model domain.

Groundwater flows primarily through aquifers and aquifer/confining units, whereas confining units stratify the groundwater-flow system and separate aquifers or aquifer systems. *Aquifer systems* contain one or more aquifers and aquifer/confining units and are typically capped by a confining unit. The hydrogeologic framework of the LMB model consists of five aquifer systems (see also color coding at right side of fig. 10):

1. The Quaternary (QRNR) aquifer system, consisting of one hydrogeologic unit: QRNR
2. The Pennsylvanian (PENN) aquifer system, consisting of three hydrogeologic units: JURA, PEN1, and PEN2
3. The Marshall (MSHL) aquifer system, consisting of two hydrogeologic units: MICH and MSHL
4. The Silurian-Devonian (SLDV) aquifer system, consisting of two hydrogeologic units: DVMS and SLDV
5. The Cambrian-Ordovician (C-O) aquifer system, consisting of seven hydrogeologic units: MAQU, SNNP, STPT, PCFR, IRGA, EACL, and MTSM.

(The vertical extent of the five aquifer systems is shown schematically in fig. 16, discussed in the next section of the report.)

The distribution of groundwater withdrawals is correlated with the aquifer systems. West of Lake Michigan and in the Upper Peninsula of Michigan (where the units composing the PENN and MSHL aquifer systems are almost entirely missing), the major pumping centers withdraw water from the QRNR, SLDV, and C-O aquifer systems. East of Lake

Michigan in the Lower Peninsula of Michigan (where the SLDV and C-O systems are typically too deep and too saline to be exploited), the major pumping centers are in the QRNR, PENN, and MSHL aquifer systems. South of Lake Michigan in northern Indiana and northeastern Ohio (where the PENN and MSHL systems are missing and the C-O system is too deep and saline), the major pumping centers withdraw from the QRNR and, to a much lesser extent, the SLDV aquifer systems. The distribution of wells in the QRNR deposits depends chiefly on the type of glacial material (for example, on the abundance and thickness of outwash deposits), whereas the distribution of wells in bedrock units depends largely on the presence of sandstone or fractured carbonates and their relative thickness.

Another way to characterize the distribution of hydrogeologic units and aquifer systems is by the subregions of the model nearfield. Three of the subregions share a similar geologic framework: NE_WI, SE_WI, and NE_ILL. The sequence of hydrogeologic units and aquifer systems for these subregions is shown in figure 12; it comprises the QRNR, SLDV, and C-O aquifer systems. The entire stack of bedrock slopes gently (on the order of 1° of dip) from the Wisconsin/Kankakee Arches toward the Michigan Basin. Figure 13 shows a similar sequence for the UP_MI, which slopes gently to the south. The Jacobsville Sandstone, which lies between the MTSM and Precambrian sandstone, is an aquifer in this area. The SLDV is present only in the UP_MI in a rim near the Lake Michigan shoreline. To the south of Lake Michigan, in the N_IND subregion, the relatively thin, north-sloping QRNR and SLDV aquifer systems (fig. 14) yield water to wells. The sedimentary sequence for the SLP_MI and NLP_MI subregions (fig. 15) is quite distinct from that of other subregions and includes the PENN and MSHL aquifer systems. The shape of the structural bowl defining the Michigan Basin is distinctive in the section, as are the large number of hydrogeologic units available for water production. Water use from bedrock aquifers, especially in the Michigan Basin, diminishes with depth because the cost of pumping increases and water quality degrades as DS concentrations increase.

Hydraulic gradients and groundwater-flow directions in bedrock on the west and south sides of Lake Michigan tend to align with the dip of bedrock units. On the east side of the lake, however, the hydraulic gradient is west towards the lake and opposite the dip of the bedrock units. Faults generally are not thought to affect the groundwater-flow system in the vicinity of the Lake Michigan basin, with these major exceptions: the Waukesha fault in southeastern Wisconsin, which bounds relatively thin Paleozoic deposits to the west and relatively thick deposits to the east (Feinstein and others, 2005), and the Sandwich fault zone and the probable impact structure known as the Des Plaines Disturbance (Meyer and others, 2009), features which control the thickness of Paleozoic aquifers and confining units in northeastern Illinois.

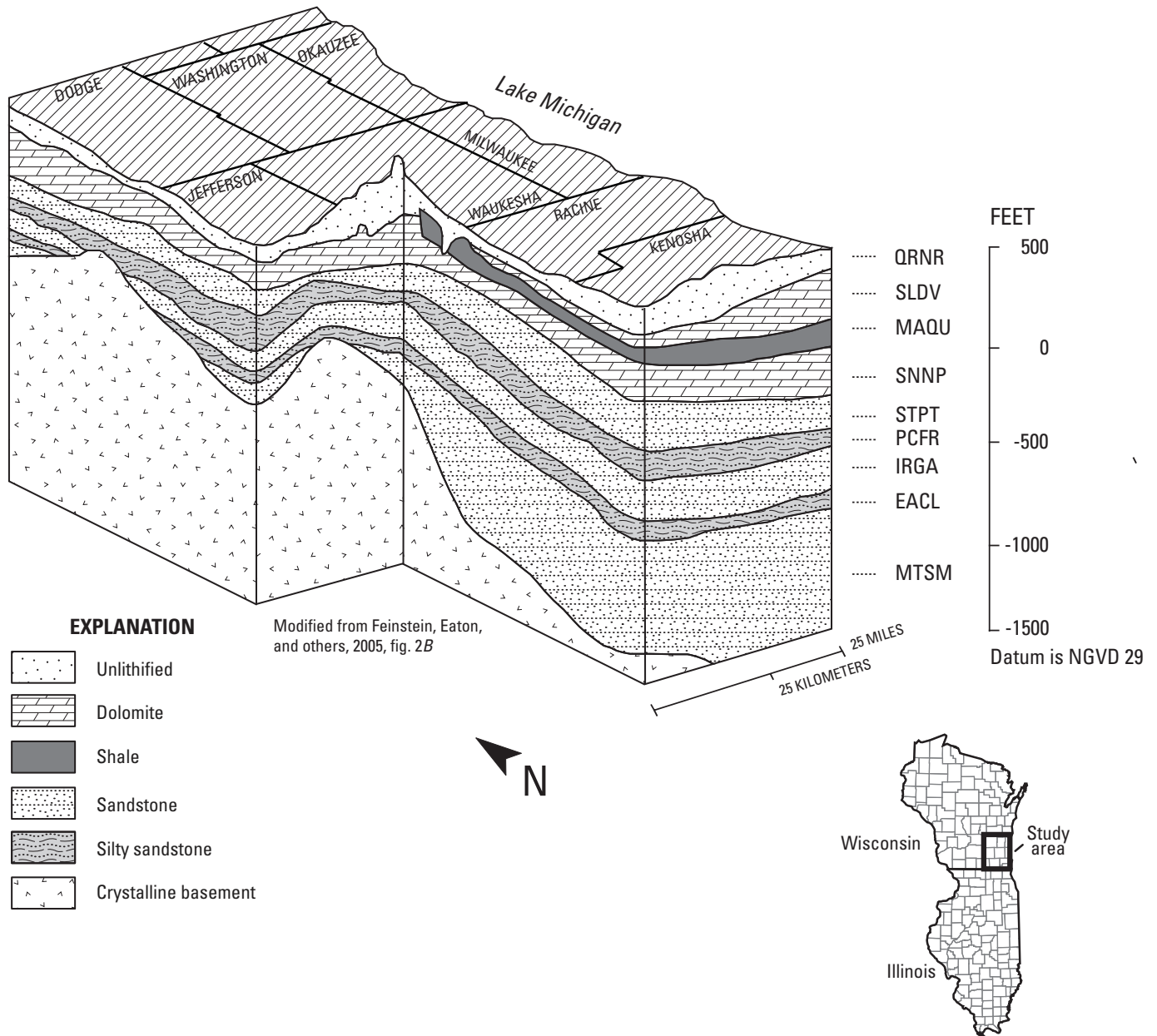


Figure 12. Schematic of hydrostratigraphy in southeastern Wisconsin, northeastern Wisconsin, and northeastern Illinois.

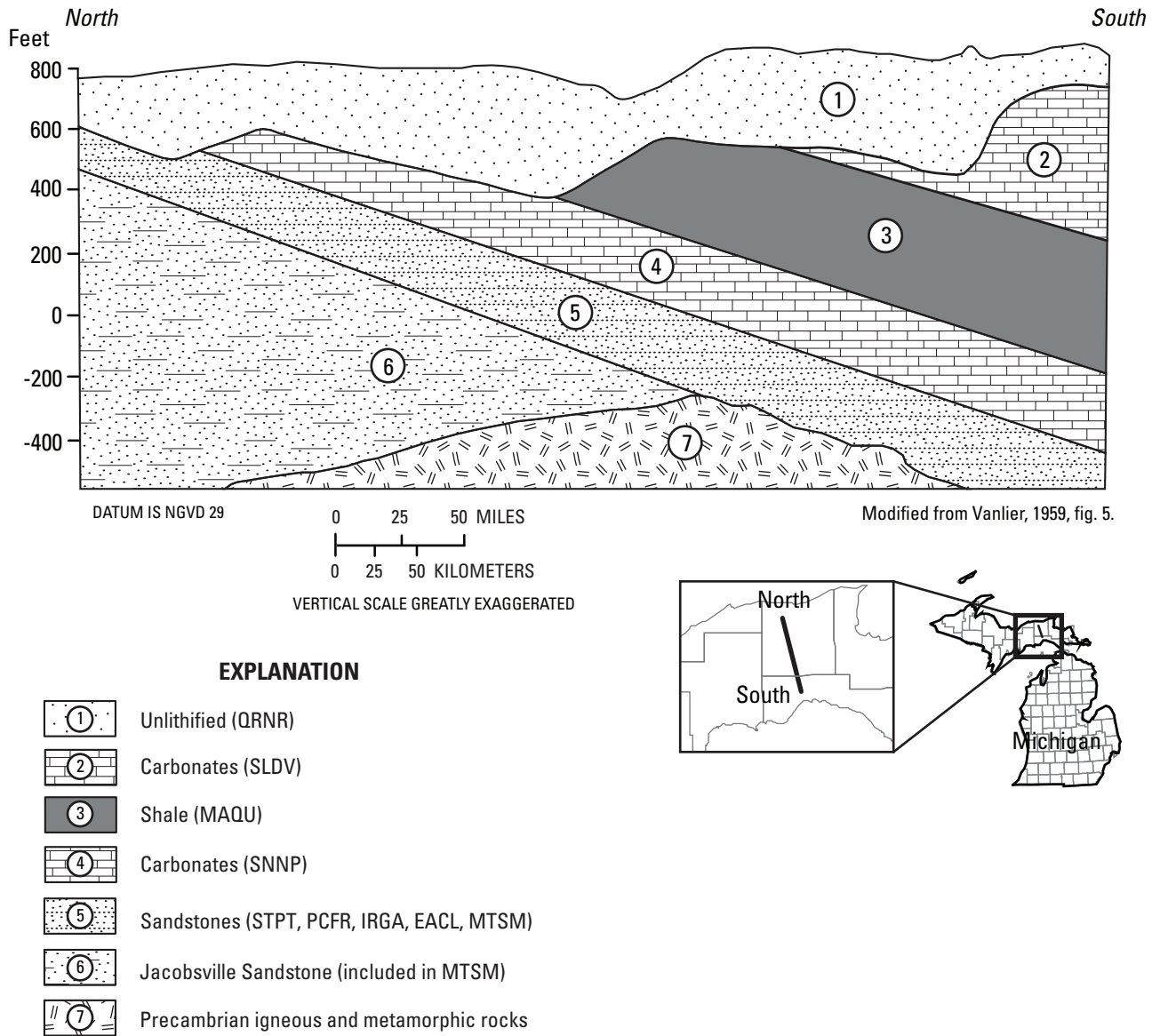


Figure 13. Schematic of hydrostratigraphy in the Upper Peninsula, Michigan.

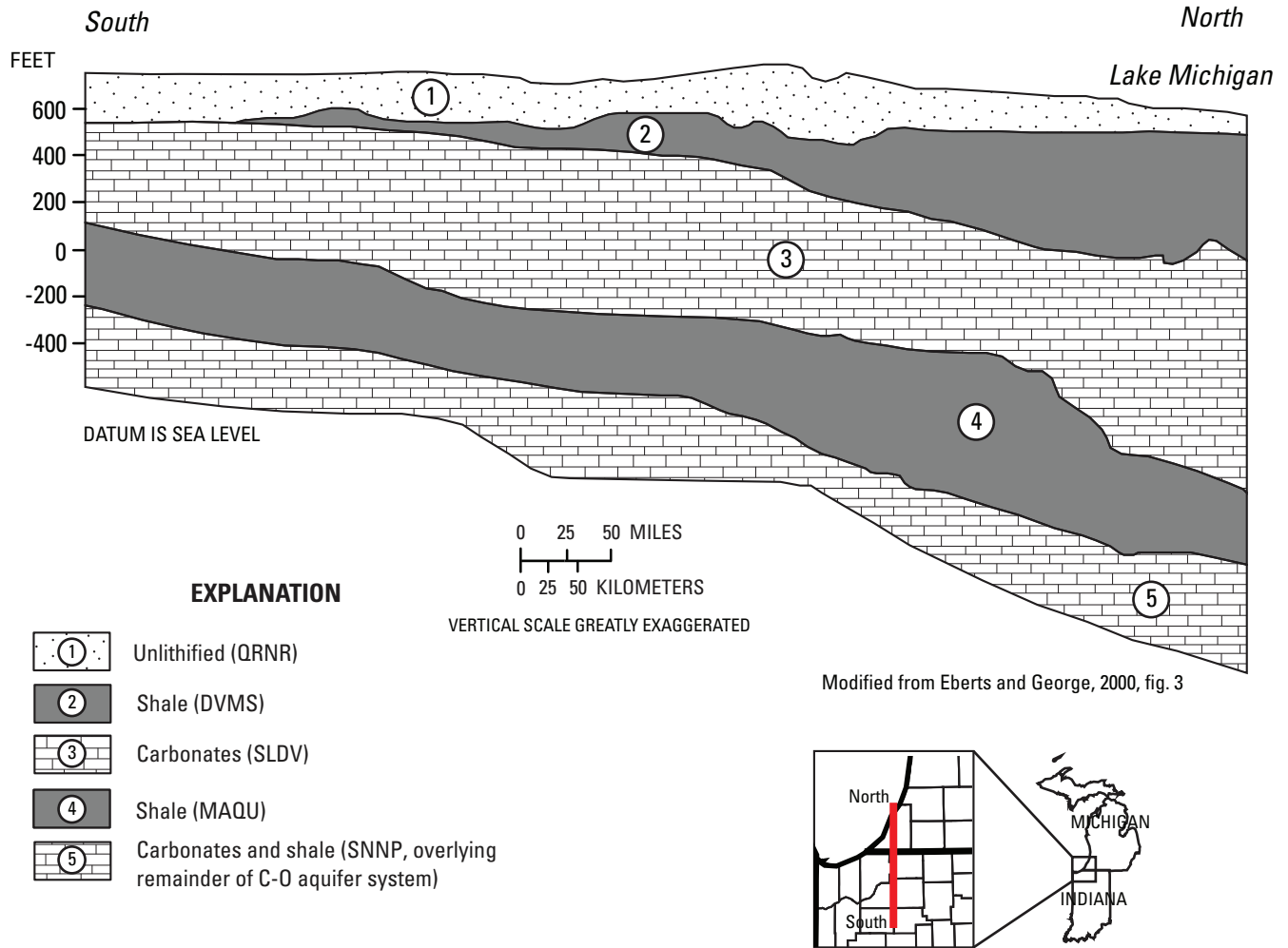


Figure 14. Schematic of hydrostratigraphy in northern Indiana.

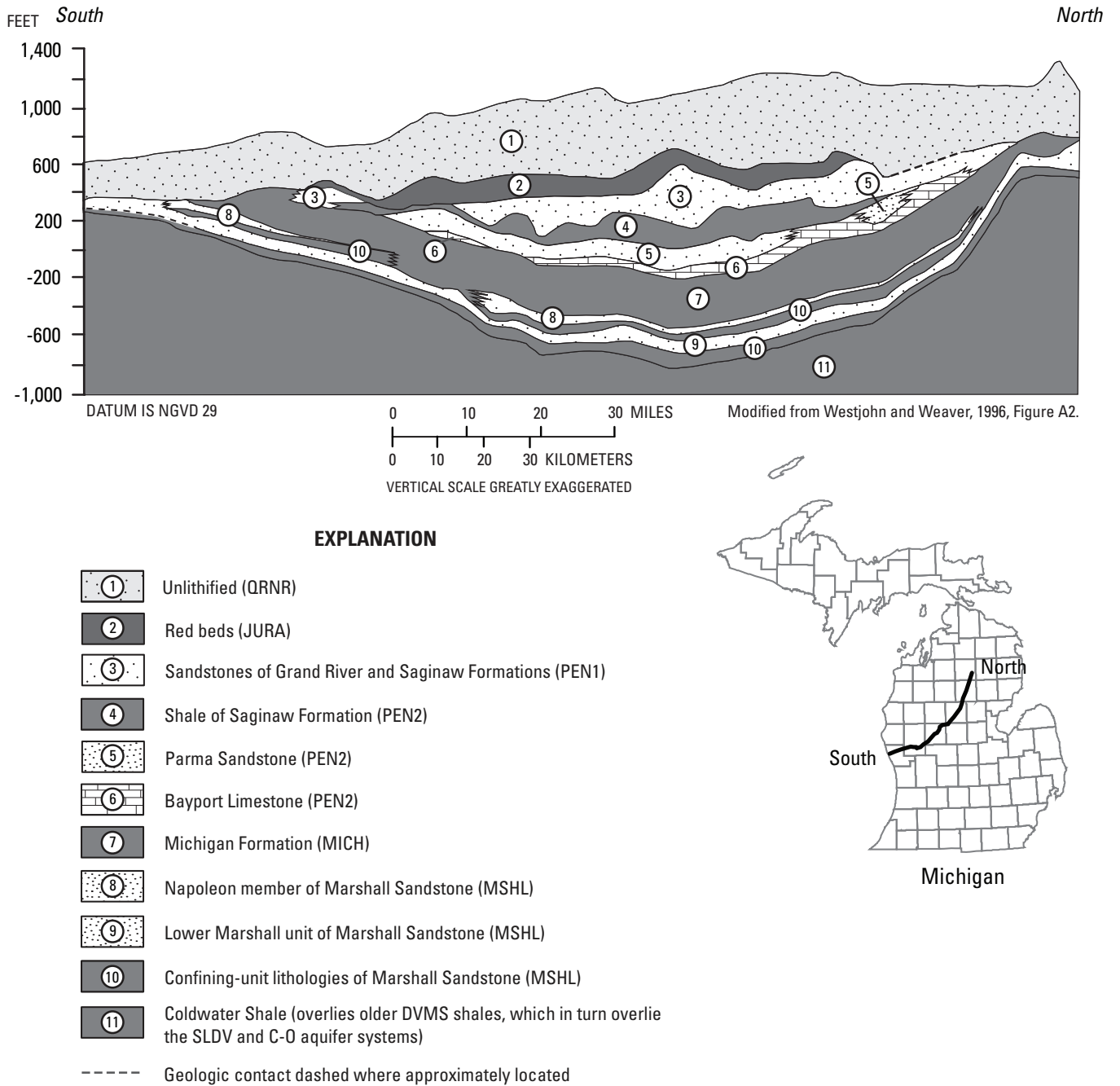


Figure 15. Schematic of hydrostratigraphy in the northern and southern Lower Peninsula, Michigan.

3.2 Regional Flow System

The regional flow system for the LMB model is largely controlled by Lake Michigan in its role as the central discharge location for both surface water and groundwater; it is secondarily controlled by the regional divides that bound the peripheral extent of the Lake Michigan groundwater basin (fig. 16). The regional groundwater divides do not necessarily coincide with the extent of the Lake Michigan drainage basin (that is, the boundaries of the topographic basin that encloses the surface water that ultimately discharges to Lake Michigan). The groundwater regional divides enclose the three-dimensional system of groundwater that discharges (1) directly to Lake Michigan, (2) indirectly to Lake Michigan via discharge to surface-water features tributary to the lake, or (3) to pumping wells inside the Lake Michigan drainage basin. The regional groundwater divides that defined the natural regional groundwater-flow system (that is, the divides that existed before the installation of pumping wells) have shifted over time as a result of pumping (Sheets and Simonson, 2006). For example, a large pumping center near a groundwater divide can move it from its original predevelopment location, enlarging the size of one groundwater basin at the expense of another, particularly if the wells are in confined aquifer systems (Sheets and others, 2005). The locations of groundwater divides vary with depth and do not, in general, correspond to vertical planes (fig. 16). The location of a divide between two groundwater basins near the water table can be very different from the location of the same divide at depth (Feinstein, Eaton, and others, 2005; Feinstein, Hart, and others, 2005; Sheets and Simonson, 2006; Bradbury and others, 2007).

One of the primary applications of the LMB model is to determine how regional divides at different depths within the Lake Michigan groundwater basin have moved through time. The Lake Michigan groundwater basin is surrounded by adjacent regional groundwater basins that are associated with surface-water drainage basins (shown in fig. 7A). They are

- the Mississippi River Basin to the west and south,
- the Lake Superior Basin to the north,
- the Lake Huron Basin to the northeast and east, and
- the Lake St. Clair and Lake Erie Basins to the east.

Regional groundwater divides separate the Lake Michigan groundwater basin from each of the neighboring lake systems to the west, north, and east (figs. 2 and 16). South of Lake Michigan, shallow and deep divides separate subsurface flow that discharges northward to surface-water features tributary to Lake Michigan from subsurface flow that discharges to the south toward the Illinois River Basin.

It is useful to distinguish *shallow* and *deep* groundwater flow within different parts of the Lake Michigan Basin. For this report, the shallow part of the subsurface flow system refers to the circulation of groundwater above the first major and relatively continuous bedrock confining unit, whereas the deep part of the flow system refers to everything below.

Shallow groundwater flow is either unconfined (for example, where flow occurs in coarse-grained QRNR deposits or in bedrock overlain by coarse-grained QRNR deposits) or semi-confined (for example, flow in areas where fine-grained glacial deposits overlie a bedrock aquifer without an intervening bedrock confining unit). Deep groundwater flow is always within bedrock and always confined. Pumping wells and withdrawals can be described as shallow or deep depending on the open interval of the well and its relation to the uppermost bedrock confining unit.

The relative depth referred to by *shallow* and *deep* depends on the continuity of confining units over the area under consideration. West of Lake Michigan, the shallow flow system generally refers to the QRNR and SLDV aquifer systems overlying the Maquoketa confining unit. West of the subcrop of the Maquoketa confining unit, however, the shallow flow system extends deeper and includes the C-O aquifer system. This change in regime is illustrated in figure 17A, where shallow flow in the westernmost part of the Lake Michigan groundwater basin and in the Mississippi River groundwater basin farther to the west extends to deeper units than it does east of the Maquoketa confining unit subcrop. On the east side of the lake, shallow groundwater flow can refer to flow in the QRNR aquifer system only when it is underlain, for example, by Mississippi-Devonian shales; or it can refer, for example, to the combined thickness of the QRNR and PENN aquifer systems overlying the Michigan Formation. Under predevelopment prepumping conditions, the exchange of groundwater between the shallow and deep parts of the flow system is typically small (as illustrated in fig. 17A), but pumping from either shallow or deep wells can induce upward or downward leakage (as illustrated in fig. 17B). These vertical connections between the shallow and deep flow systems have important implications for water availability from the standpoints of quantity and of quality because they control the source areas that contribute water to deep wells. The LMB model was designed to compute estimates of the locations and rates of leakage between the shallow and deep parts of the flow system under both predevelopment and stressed conditions.

3.3 Sources and Sinks

The regional groundwater flow pattern is influenced by the location and strength of sources and sinks of water. Recharge to the water table is the most important source of water for the groundwater system in the Lake Michigan Basin and adjacent areas. The recharge rate varies spatially and depends on factors such as soil type, depth to water table, land slope, and vegetation. Surface-water features such as streams, lakes, and wetlands also can be sources for groundwater, especially in the vicinity of pumping wells. Finally, return by well injection or through leakage from surface impoundments is a potential source of water to the subsurface.

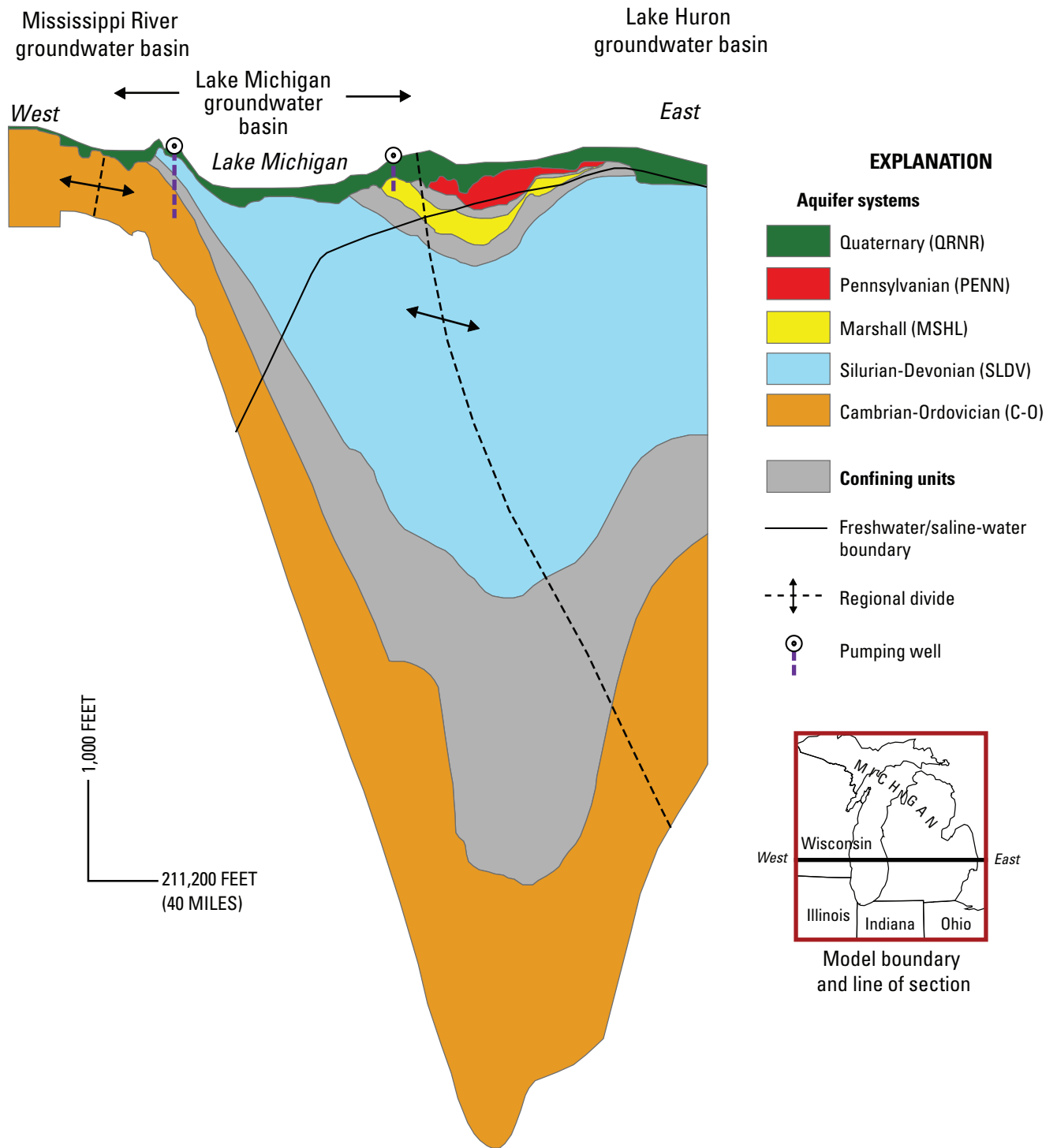


Figure 16. Schematic of flow system and aquifer systems. (Large vertical exaggeration is applied to the schematic section; the true geologic boundaries—without vertical exaggeration—are much more flat-lying than shown, and the aquifer-system thicknesses are small relative to their lateral dimensions.)

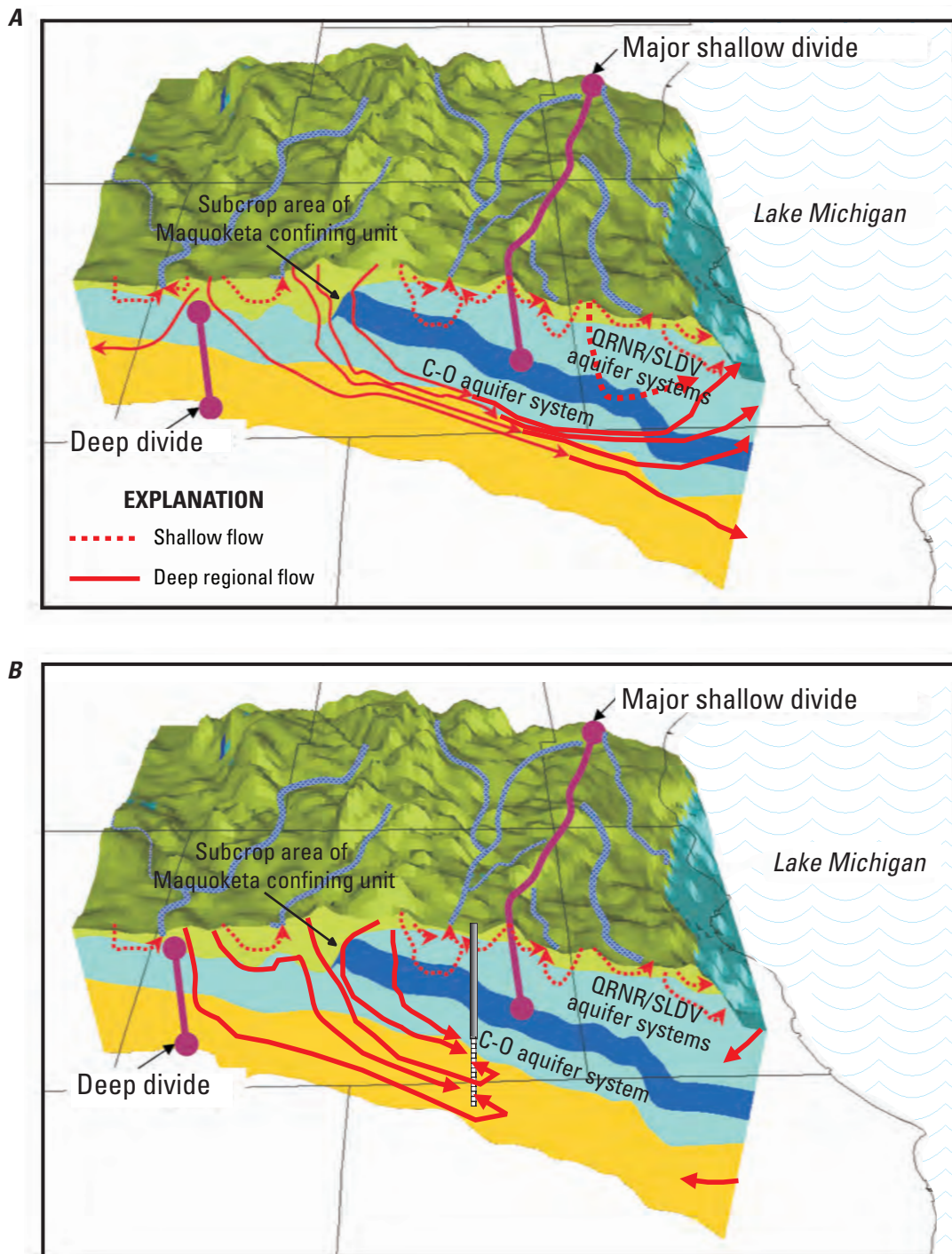


Figure 17. Block schematic of shallow and deep parts of flow system: A, Predevelopment. B, Postdevelopment. (Pumping wells in postdevelopment capture and reverse deep flow that discharged toward Lake Michigan under predevelopment conditions.)

Surface-water bodies and pumping wells usually act as sinks in areas where local or regional groundwater flow systems discharge. Most of the recharge that crosses the water table circulates as groundwater along shallow flow paths back to the surface, where it discharges as *base flow* to streams, lakes, seeps, springs, and wetlands. Shallow wells capture some groundwater that would otherwise discharge to surface-water bodies. Another portion of recharge moves as *leakage* to the deep part of the flow system, following relatively long flow paths that commonly end at regional discharge areas such as Lake Michigan or deep pumping wells. Although Lake Michigan generally serves as a regional sink for both shallow and deep groundwater, it can serve as a source of water for wells, especially near the shoreline.

Besides recharge, exchange with inland surface water and with Lake Michigan, discharge to pumping wells, and infiltration by injection or from impoundments, there are two other source/sink terms that contribute to a groundwater budget analysis for any study area within the model—underflow and storage. *Underflow* refers to the quantity of water that laterally enters or exits the area under consideration at a given time. For example, there is lateral flow into and out of the nearfield area of the LMB model, so the farfield acts as a source or sink with respect to the nearfield. Under pumping conditions, the direction and amount of underflow can change with time. Under both predevelopment and postdevelopment conditions, underflow can cross the vertical projection of topographic boundaries defining a drainage area like the Lake Michigan Basin. The resulting incongruity between groundwater and surface-water divides can be an important issue when estimating and assigning the availability of water resources to distinct geographic regions (be they drainage basins or political jurisdictions).

Changes in pumping from wells can cause regional changes in water levels related to release of water from *storage* (following drawdown) or increase in storage (following recovery). The change in storage reflects the amount of water-level change the drainage and elastic properties of the aquifer material and the unconfined or confined nature of the aquifer. One aim of the LMB model is to simulate the dynamics of groundwater storage in response to changes in recharge and pumping for distinct geographic areas, historical intervals, and aquifer systems.

The LMB model is designed to quantify the water budget associated with the groundwater sources and sinks described above. In some cases the budget components are inputs to the model (for example, spatially and temporally varying recharge rates, time-varying pumping rates); in other cases they are model results (for example, exchange with surface water, storage changes, underflow between basins). The spatial and temporal discretization of the model design can affect the rates of sources and sinks estimated by the model. For example, the simulated amount of storage release around pumping wells is conditioned by the time resolution over which well-withdrawal rates are held stepwise constant (see section 4 of this report, “Model Construction,” and section 8, “Model Limitations and Uncertainty”).

3.4 Groundwater/Surface-Water Interactions

Three types of surface-water features are represented in the LMB model—streams, inland water bodies, and the Great Lakes. Streams input to the model commonly include some first-order, most second-order, and all higher order reaches. (First-order reaches are equivalent to headwaters of streams without tributaries. Second-order reaches begin at the confluence of first-order tributaries. If two second-order reaches flow into each other, they form a third-order reach, and so on.) Inland water bodies include lakes and wetlands more than 20 acres in area (including the largest inland surface-water feature in the model domain, Lake Winnebago, shown in location map in fig. 2). All of Lake Michigan and parts of three other Great Lakes—Lake Superior, Lake Huron and Lake Erie (including Lake St. Clair, which connects the latter two)—are represented in the LMB model. Each set of surface-water features is simulated in the model by a distinct boundary condition (see section 4 of this report, “Model Construction”).

In the LMB model, groundwater discharge to Lake Michigan is estimated as

1. direct discharge through the lakebed, or
2. indirect discharge to streams and water bodies tributary to the lake.

Indirect discharge is computed by summing base flow from the model to inland water bodies and streams within the Lake Michigan drainage basin.

The spatial resolution of the model affects the simulated rate of leakage between groundwater and surface-water features. Cell areas in the LMB model are nearly 1 mi², so multiple surface-water features can be represented by a single cell. The greater the number of surface-water features represented in the model, the more the water-table solution is constrained by these boundary conditions (Feinstein and others, 2006). If all bodies are included in temperate and humid zones like the Lake Michigan Basin, then the water-table surface in many areas is effectively prescribed by boundary-condition inputs, which limits the model’s usefulness; for example, in simulating the response of the shallow groundwater system to pumping. If smaller bodies are omitted to reduce the constraints imposed by boundary conditions, then the model’s nonrepresentation of existing discharge zones can distort the value of other model inputs as the solution seeks to duplicate the observed water-table configuration without the proper distribution of actual sinks (see fig. 18). The tradeoff imposed on a regional model such as the LMB model must be explicitly defined and, where possible, evaluated in terms of the effect on model results (as discussed in section 8 of this report, “Model Limitations and Uncertainty”).

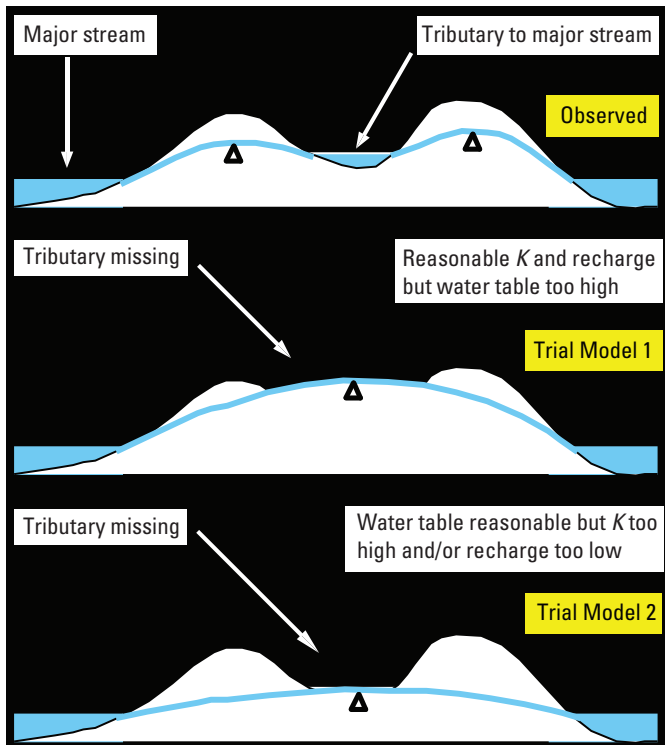


Figure 18. Effect of excluding low-order streams from model input.

3.5 Role of Salinity

A distinctive aspect of the Lake Michigan Basin hydrogeology is the presence of highly concentrated brines in most of the volume of sedimentary rocks dipping into Michigan Basin. Silurian evaporite deposits are the probable source for much of the saline water, although earlier deposits are present in Late Ordovician rocks. Substantial assemblages of halite, gypsum, anhydrite, sylvite, and other evaporite minerals are found in the Salina Group within the SLDV aquifer system, which was deposited during the greatest period of downwarping of the Michigan Basin. Intervals of rapid subsidence are marked by halite precipitation in the center of the basin and anhydrite precipitation toward the basin margins (Sonnenfeld and Al-Aasm, 1991). It is hypothesized that, during downwarping, the evaporite minerals originated from seawater that entered the Michigan Basin from the Kokomo Sea in what is now Indiana and from the Moose River Basin in what is now Lake Huron. The brines were formed in an area roughly circular in shape, and the deposited evaporite beds extend over a radial distance on the order of 100 mi beneath Indiana and Ohio, as well as Michigan.

Salinity associated with the evaporite beds yields DS concentrations greater than 500,000 mg/L in groundwater within the Salina Group (Sonnenfeld and Al-Aasm, 1991) and greater than 10,000 mg/L in several underlying and overlying units

(Westjohn and Weaver, 1996a, b). Saline water extends into Cambrian-Ordovician rocks of northeastern Illinois (Visocky and others, 1985) and parts of the shoreline of Wisconsin (Ryling, 1961), suggesting that much of the groundwater in the Paleozoic rocks under Lake Michigan also is saline (see assumed freshwater/saline-water boundary in fig. 16).

Supply wells are completed in freshwater zones of the deep flow system, but the deep wells in Wisconsin and Illinois create drawdown that probably induces the westward flow of saline water under Lake Michigan toward the pumping centers (Young, 1992; Feinstein, Hart, and others, 2005). The extent to which salinity influences the propagation of water-level drawdown is unknown and the LMB model is used to investigate this issue. SEAWAT-2000 (Langevin and others, 2003), which incorporates the effects of density in the equation of groundwater flow, was used to simulate the effects of salinity on deep flow in the LMB model domain. Although not all the mechanisms associated with brine flow in a deep structural basin can be accommodated in this modeling effort (see section 8, “Model Limitations and Uncertainty”), an attempt was made to take account of the effect of variable density on hydraulic conductivity and gradients within and along the fringes of the Michigan Basin.

The central focus of the modeling effort is to simulate groundwater conditions in the freshwater areas that are important for considerations of water availability. Given this focus, it is appropriate to conceptualize the freshwater/saline-water interface as a kind of model boundary condition that can serve as either a source or a sink of saline water in response to pumping centers on both sides of Lake Michigan. The implementation of this boundary is discussed in report section 4; the effect of the boundary is evaluated in section 7, which compares results of variable-density and uniform-density flow simulations.

3.6 Confined and Unconfined Conditions

The transmissivity of a confined aquifer is independent of the water level (head), whereas that of an unconfined aquifer is a function of the *saturated thickness* of the aquifer, equal to the height of the water-table elevation above the bottom of the aquifer. Storage release in a confined aquifer due to a decline in water levels, which is associated with the elastic compression and expansion of the water and the rock matrix (proportional to the aquifer storage coefficient), is much less than storage release for an equivalent decline in an unconfined aquifer, which is associated with the drainable porosity of the aquifer material (proportional to the aquifer specific yield). Aquifers undergoing water-level decline caused by pumping can transition from confined to unconfined conditions. More than one water table can exist at a single location when unconfined conditions occur not only near the land surface but also in deep aquifers that are partly dewatered owing, for example, to the transient effects of deep pumping.

In general, the more accurate approach is to simulate a shallow flow system as an unconfined aquifer with transmissivity related to the saturated thickness and storage defined by the specific yield; however, treating the entire flow system as a confined aquifer in the LMB model produced a more stable numerical solution, especially during the calibration process. For this reason, multiple models were developed in this study to simulate cells in the flow system as (1) always confined (the “base” model) or (2) either confined or unconfined depending on the position of the water table (an “alternative” model). The properties of the confined-aquifer model were adjusted to account for the effect of saturated thickness on aquifer transmissivity and storage—see section 4 of this report. Model results are reported for the confined-aquifer model in section 6; the unconfined-aquifer model is described and its results compared to the confined-aquifer model in section 7.

4. Model Construction

The LMB model is discretized spatially by use of a finite-difference grid and temporally by use of time periods of constant pumping and recharge (stress). Boundary conditions (specified heads and flows) are specified in the model farfield and control the movement of water into and out of the model nearfield. Head-dependent boundary conditions representing inland surface water and Lake Michigan are specified within the model nearfield. A spatially and temporally variable top model boundary represents the rate of recharge. Finally, the location, depths and withdrawal rates of pumping wells from 1864 through 2005 are also represented as internal model boundaries.

Simulated water levels and flows between adjacent model cells are computed by using assumed subsurface properties of the QRNR and underlying bedrock aquifer systems; for example, the horizontal hydraulic conductivity (K_h) and vertical hydraulic conductivity (K_v) in the unconsolidated QRNR sediments and the bottom sediments of Lake Michigan, as well as by the zones of K_h and K_v assigned to the underlying bedrock sediments. Transmissivities of the aquifer systems represented in the LMB model are computed from the thicknesses and K_h values specified for each system. The response of the system to changing stresses is a function of not only the hydraulic conductivity (K) and thickness distribution but also the assumed storage properties of the sediments. Finally, the LMB model solution in particular depends on the treatment of the variable-density conditions associated with the brines emanating from ancient sediments in the Michigan Basin. All these model elements are discussed in this section.

4.1 Model Grid

The finite-difference grid is composed of rows and columns and a vertical stack of layers. The rows and columns define cells of rectangular or square lateral dimensions. The grid contains 391 rows oriented west to east and 261 columns oriented north to south. The dimensions of both rows and columns form rectangles in the nonuniform outer part of the grid (comprising the farfield and parts of the nearfield mostly outside of the Lake Michigan Basin) and from squares 5,000 ft on a side in the uniform inner part of the grid (comprising most of the model nearfield) (fig. 19). The uniform square cells cover a rectangular area centered on Lake Michigan that extends from row 10 to row 381 and from column 12 to column 248—equivalent to a rectangle 352.3 mi in the north-south directions along rows and 224.4 mi in the west-east direction along columns, summing to an area of about 79,060 mi², and incorporating 88,164 cells per layer out of the model total of 102,051 cells per layer. This inner-mesh area is completely inside the model nearfield, but the nearfield extends beyond it to include some rectangular cells that are inside the Lake Michigan drainage basin (fig. 19).

Outer-mesh rows and columns increase by a factor of 1.3 so that grid cells increase in size from 5,000 ft on a side at each edge of the inner mesh to a maximum size of about 10 mi at the northern edge of the mesh, about 13 mi at the southern edge, about 17 mi at the western edge, and about 22 mi on the eastern edge. The large lateral dimensions of the outer-mesh cells do not compromise the integrity of the finite-difference calculations because the 1.3 enlargement factor has little negative effect on the truncation of the Taylor expansions used in the numerical solution methods of the MODFLOW-2000/SEAWAT-2000 codes (Anderson and Woessner, 1992). Because the outer-mesh cells are more than 10 mi on a side near the northwest, northeast, southwest and southeast corners of the model domain, simulated heads and flows are approximate in these areas. Simulated heads and flows are more accurate in the model nearfield, where cells sizes approach 1 mi².

The model nearfield (composed of all the uniform and some of the nonuniform cells) contains 88,687 cells per layer, including all the Lake Michigan cells. It incorporates an area of 83,263.5 mi² that amounts to 46 percent percent of the model domain. The Lake Michigan Basin (including all of Lake Michigan and its drainage area) covers about 37 percent of the total grid area but 80 percent of the nearfield. Lake Michigan itself covers 12 percent of the total grid area and sums to 27 percent of the nearfield.

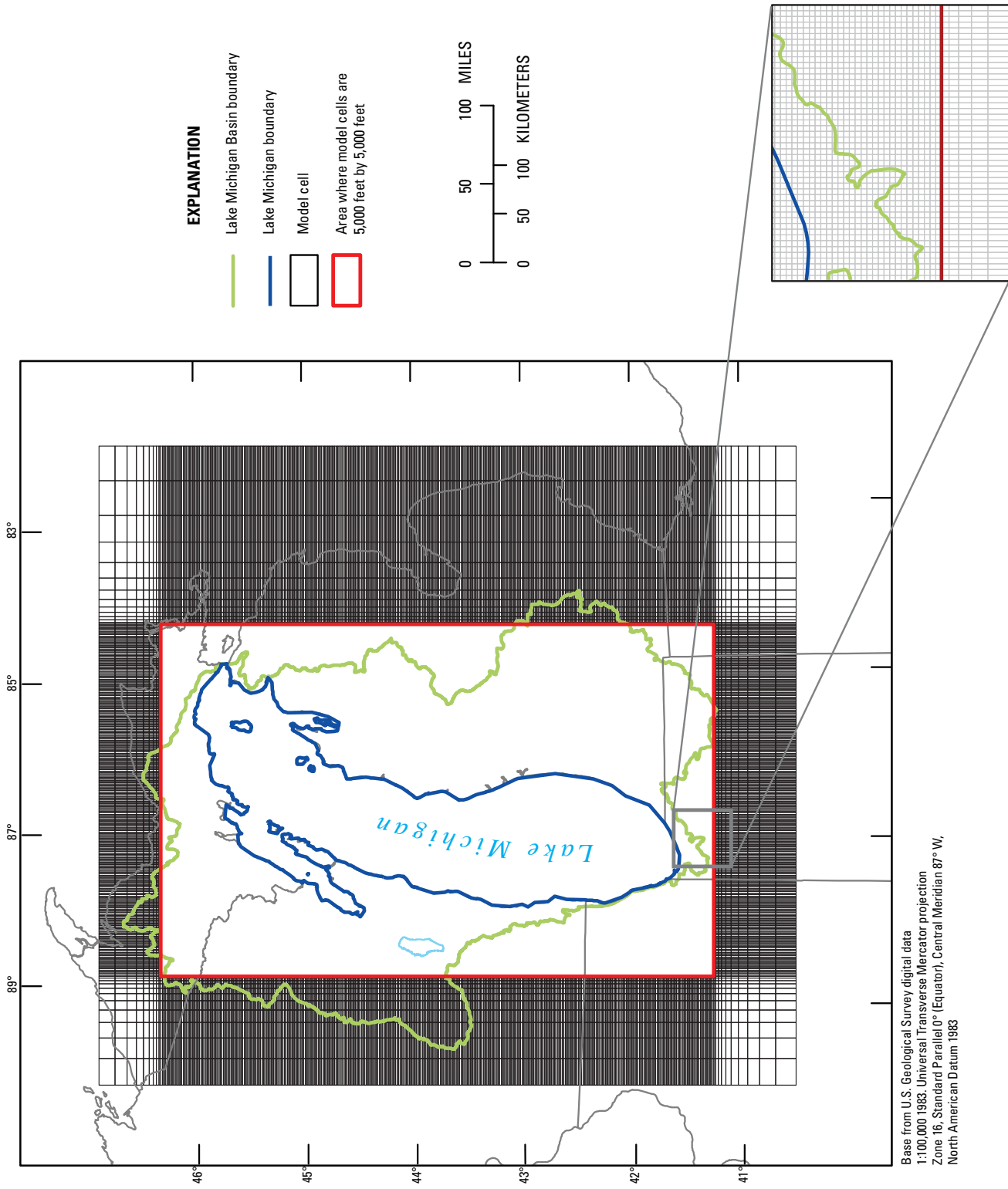


Figure 19. Model grid. (Inset shows example area of transition in northern Indiana from nonuniform grid cells (greater than 5,000 feet on a side) to uniform grid cells (equal to 5,000 feet on a side).)

4.2 Model Layering

The LMB model is a three-dimensional representation of the unconsolidated and sedimentary deposits extending from the water table to the Precambrian bedrock. The model is fully three-dimensional because the entire thickness is incorporated (there are no gaps) and that it includes not only aquifers but also confining units.

The 20 layers in the LMB model are defined in terms of hydrogeologic units. The numbering of layers is from top to bottom. Three hydrogeologic units—the Quaternary, the Silurian-Devonian, and the Mount Simon, are represented by multiple layers, whereas all remaining aquifers and all confining units are represented by a single layer (table 3). The thickness of each layer is variable and computed from elevation surfaces contained in the three-dimensional stratigraphic database prepared to support the LMB model (Lampe, 2009). Where a hydrogeologic unit is missing (that is, “pinched” between overlying and underlying units with thickness), then it is assigned a nominal thickness of 0.2 ft.⁷ The top and bottom of each hydrogeologic unit at a particular row and column location is interpolated from well-log data and contour maps from each of the states covered by the model. The stratigraphic-database report (Lampe, 2009) contains isopach (thickness) maps for all 15 hydrogeologic units incorporated in the LMB model. Thicknesses of units under Lake Michigan were interpolated linearly from stratigraphic data available along the shoreline. However, recent mapping of units in the Michigan Basin was used to configure the thickness of the Devonian-Mississippian confining unit beneath the lake (Lampe, 2009). Unconsolidated material under the lake (lakebed) consists of glacial deposits mantled by recent (Holocene) deposits from the lake itself. Data compiled by Soller (1998) were used to estimate the thickness of unconsolidated sediments beneath the southern half of Lake Michigan (south of a line from Manitowoc, Wis., to Ludington, Mich.; see fig. 2) A shaded

relief map (Colgan and Principato, 1998) and a discussion of the geomorphology of the lakebed (National Oceanic and Atmospheric Administration, 2005) were used to estimate the thickness of the unconsolidated sediments beneath the northern half of Lake Michigan. The median interpolated thickness of the lakebed is 55 ft; the thickness ranges from 8 to 278 ft under 90 percent of the lake; the maximum thickness is 456 ft along a ridge near the center of the water body.

A large proportion of groundwater flow circulates within the unconsolidated deposits, so three model layers are assigned to the QRNR system, rather than just one, to more accurately represent the geology and vertical flow field. Three layers are also assigned to the SLDV system to represent a 50-ft weathered zone at the top surface in thinner parts of the system along the Wisconsin and Kankakee Arches (Meyer and others, 2009) and to account for evaporite deposits in the middle part of the system in the Michigan Basin. The MTSM, which is more than 1,000 ft thick at certain pumping centers west of Lake Michigan, is divided into two layers to allow for a more accurate representation of the drawdown around C-O wells that penetrate as deep as the MTSM but extend only several hundred feet into the unit.

The QRNR, SLDV, and MTSM hydrogeologic units are each assigned multiple layers, but the total thickness of the unit at a given cell location is represented by only the top layer *unless* a threshold thickness value is reached, in which case the excess thickness is assigned to a second layer until (in the case of the QRNR and SLDV units) a second threshold is reached, in which case the additional thickness is assigned to a third layer. If the threshold thickness is not reached at a location, then the cell(s) in the “excess” layer(s) for the unit are assigned a nominal pinched thickness of 0.2 ft. The exact logic and thresholds for dividing the QRNR, SLDV, and MTSM units into multiple layers are presented in table 3. The vertical distribution of the lakebed thickness across model layers generally follows the same logic as the QRNR.

⁷ Pinched layers ordinarily participate in the model simulation; but because they are so thin and because they are assigned the same properties (hydraulic conductivity and storage parameters) as the first unpinched overlying layer, they have negligible effect on the model solution. Numerical experiments were conducted on larger to smaller pinched thicknesses to confirm that the high horizontal to vertical aspect ratios implied by a 0.2 ft pinched thickness in cells do not cause the solution to deteriorate. By using a very small pinched thickness, very little excess thickness is added to the model even in areas where layers are almost missing (for example, toward the northwest of the model domain where QRNR—layer 1—commonly overlies MTSM—layer 19). Infrequently, bedrock layers are at the surface of the model. In such cases, any overlying layers (QRNR plus any missing bedrock) are *inactive* as well as pinched; the layer properties are irrelevant because they do not participate in the model solution.

Table 3. Model layering.**3A.** Correlation between model layers and hydrogeologic units and aquifer systems.

[For correlation between model layers, hydrogeologic units, aquifer systems, and lithostratigraphic units, see fig. 10]

Layer	Abbreviation	Hydrogeologic unit	Aquifer system	System abbreviation
Layer 1	QRNR-upper	Quaternary aquifer/confining unit	Quaternary	QRNR
Layer 2	QRNR-middle	Quaternary aquifer/confining unit	Quaternary	QRNR
Layer 3	QRNR-lower	Quaternary aquifer/confining unit	Quaternary	QRNR
Layer 4	JURA	Jurassic confining unit	Pennsylvanian	PENN
Layer 5	PEN1	Upper Pennsylvanian aquifer	Pennsylvanian	PENN
Layer 6	PEN2	Lower Pennsylvanian aquifer/confining unit	Pennsylvanian	PENN
Layer 7	MICH	Michigan Formation confining unit	Marshall	MSHL
Layer 8	MSHL	Marshall Sandstone aquifer	Marshall	MSHL
Layer 9	DVMS	Devonian-Mississippian confining unit	Silurian-Devonian	SLDV
Layer 10	SLDV-upper	Silurian-Devonian aquifer	Silurian-Devonian	SLDV
Layer 11	SLDV-middle	Silurian-Devonian aquifer/confining unit	Silurian-Devonian	SLDV
Layer 12	SLDV-lower	Silurian-Devonian aquifer/confining unit	Silurian-Devonian	SLDV
Layer 13	MAQU	Maquoketa confining unit	Cambrian-Ordovician	C-O
Layer 14	SNNP	Sinnipee aquifer/confining unit	Cambrian-Ordovician	C-O
Layer 15	STPT	St. Peter sandstone aquifer	Cambrian-Ordovician	C-O
Layer 16	PCFR	Prairie du Chien-Franconia aquifer/ confining unit	Cambrian-Ordovician	C-O
Layer 17	IRGA	Ironton-Galesville aquifer	Cambrian-Ordovician	C-O
Layer 18	EACL	Eau Claire aquifer/confining unit	Cambrian-Ordovician	C-O
Layer 19	MTSM-upper	Mount Simon aquifer	Cambrian-Ordovician	C-O
Layer 20	MTSM-lower	Mount Simon aquifer/confining unit	Cambrian-Ordovician	C-O

Table 3. Model layering.—Continued**3B.** Layering logic for QRNR, SLDV, and MTSM layers.

QRNR
<p>Layer 1 extends from land surface to maximum depth of 100 feet.</p> <p><i>If</i> QRNR is greater than 100 feet thick, then layer 2 extends from 100 feet depth to maximum depth of 300 feet; otherwise, layer 2 is pinched.</p> <p><i>If</i> QRNR is greater than 300 feet thick, then layer 3 extends from 300 feet depth to top of bedrock; otherwise, layer 3 is pinched.</p>
SLDV
<p><i>If</i> the total thickness of the SLDV is less than or equal to 550 feet, then layer 10 extends from top of SLDV to 50 feet below top of SLDV.</p> <p><i>If</i> SLDV is greater than 50 feet thick and less than 550 feet thick, then layer 11 extends from 50 feet below top of SLDV to bottom of SLDV; if SLDV is less than 50 feet thick, layers 11 and 12 are pinched.</p> <p>Layer 12 is pinched.</p> <p><i>If</i> total thickness of SLDV is greater than 550 feet, then</p> <p style="padding-left: 2em;">Layer 10 is upper part of SLDV; its thickness is equal to 50 feet plus total thickness of SLDV less 550 feet, the difference divided by 3.</p> <p style="padding-left: 2em;">Layer 11 is middle part of SLDV; its thickness is equal to 250 feet plus total thickness of SLDV less 550 feet, the difference divided by 3.</p> <p style="padding-left: 2em;">Layer 12 is lower part of SLDV; its thickness is equal to 250 feet plus total thickness of SLDV less 550 feet, the difference divided by 3.</p> <p>For example:</p> <p style="padding-left: 2em;">Suppose the total thickness of the SLDV is equal to 300 feet; then</p> <p style="padding-left: 4em;">Layer 10 is 50 feet thick.</p> <p style="padding-left: 4em;">Layer 11 is 250 feet thick.</p> <p style="padding-left: 4em;">Layer 12 is pinched.</p> <p style="padding-left: 2em;">Suppose the total thickness of the SLDV is equal to 610 feet; then</p> <p style="padding-left: 4em;">Layer 10 is 70 feet thick.</p> <p style="padding-left: 4em;">Layer 11 is 270 feet thick.</p> <p style="padding-left: 4em;">Layer 12 is 270 feet thick.</p> <p style="padding-left: 2em;">Suppose the total thickness of the SLDV is equal to 1,450 feet; then</p> <p style="padding-left: 4em;">Layer 10 is 350 feet thick.</p> <p style="padding-left: 4em;">Layer 11 is 550 thick.</p> <p style="padding-left: 4em;">Layer 12 is 550 thick.</p>
MTSM
<p>Layer 19 extends from top of Mount Simon to maximum depth of 300 feet below top of Mount Simon.</p> <p><i>If</i> MTSM is greater than 300 feet thick, then layer 20 extends from 300 feet below top of Mount Simon to the model basement; otherwise, layer 20 is pinched.</p>

Table 4. Thickness statistics of hydrogeologic units in model nearfield.

[Total number of active nearfield cells = 88,335; total active nearfield area = 82,817 square miles]

Unit	System	Top layer	Bottom layer	Number of cells present	Area (square miles)	Average thickness (feet)	Maximum thickness (feet)
QRNR	QRNR	1	3	84,406	78,787	176	1,107
JURA	PENN	4	4	3,892	3,491	60	195
PEN1	PENN	5	5	9,280	8,656	200	601
PEN2	PENN	6	6	9,917	9,247	163	527
MICH	MSHL	7	7	13,647	12,634	250	720
MSHL	MSHL	8	8	16,864	15,559	193	493
DVMS	SLDV	9	9	40,540	36,791	926	1,940
SLDV	SLDV	10	12	71,807	64,833	1,981	7,148
MAQU	C-O	13	13	73,319	66,189	426	2,162
SNNP	C-O	14	14	79,535	71,929	375	1,400
STPT	C-O	15	15	67,102	60,665	363	1,364
PCFR	C-O	16	16	84,164	78,269	467	1,615
IRGA	C-O	17	17	81,688	75,267	141	543
EACL	C-O	18	18	81,746	75,139	287	1,566
MTSM	C-O	19	20	88,275	82,815	630	2,611

The conversion of the three-dimensional stratigraphic database into the model grid produces hydrogeologic units and model layers with not only distinct thickness characteristics but also widely divergent lateral extent (fig. 20 and table 4). For example, the JURA confining unit in model layer 4 is present over only about 4 percent of the model nearfield, whereas the QRNR and MTSM systems are present over almost the entire nearfield. This complicated stratigraphic pattern is illustrated by selected hydrogeologic sections through the model domain (see fig. 21 for the section traces). Differences in layer thickness along north/south sections that cross the Wisconsin and Kankakee Arches (see fig. 22A, corresponding to column 48) and the Michigan Basin (see fig. 22B, corresponding to column 204) are quite apparent. The first section shows areas where Precambrian bedrock is shallow and overlain by a thin layer of unconsolidated material and sedimentary rock, whereas in the second section sedimentary rocks attain a combined thickness well over 10,000 ft in the center of the Michigan Basin. The west/east sections reveal more of the structure of the Wisconsin and Kankakee Arches and the Michigan Basin. The PENN and MSHL aquifer systems are not present along the northernmost section (fig. 23A, corresponding to row 80), which skirts the southern boundary of the UP_MI and extends into the NLP_MI at the northern edge of the Michigan Basin. The two west/east sections that cross the middle of the Michigan Basin (fig. 23B, corresponding to row 170 and fig. 23C, corresponding to row 260) express its full

bowl-like form, with all or almost all of the 20 model layers present and none or few pinched. The southernmost section, crossing from northeastern Illinois into the northern edge of Indiana (fig. 23D, corresponding to row 350), indicates the presence of the Kankakee Arch to the west and the limited thickness of sedimentary rock at the southern margin of the Michigan Basin to the east.

Grouping model layers into aquifer systems along west/east sections (fig. 24A–D) is a useful way to simplify the visualization of the subsurface geometry. The volume of the Michigan Basin is clearly dominated by the lowermost aquifer systems, the SLDV and C-O, with the QRNR system constituting a thin veneer relative to the overall thickness. In the center of the basin, the PENN and MSHL systems are dominant. The pattern is different west of Lake Michigan, where the QRNR and C-O systems constitute most of the subsurface above the Precambrian bedrock; however, near the lake they are separated by the SLDV system thickening to the east.

Some model layers represent confining units that define the top of aquifer systems:

- JURA (layer 4) at the top of the PENN aquifer system
- MICH (layer 7) at the top of the MSHL aquifer system
- DVMS (layer 9) at the top of the SLDV aquifer system
- MAQU (layer 13) at the top of the C-O aquifer system

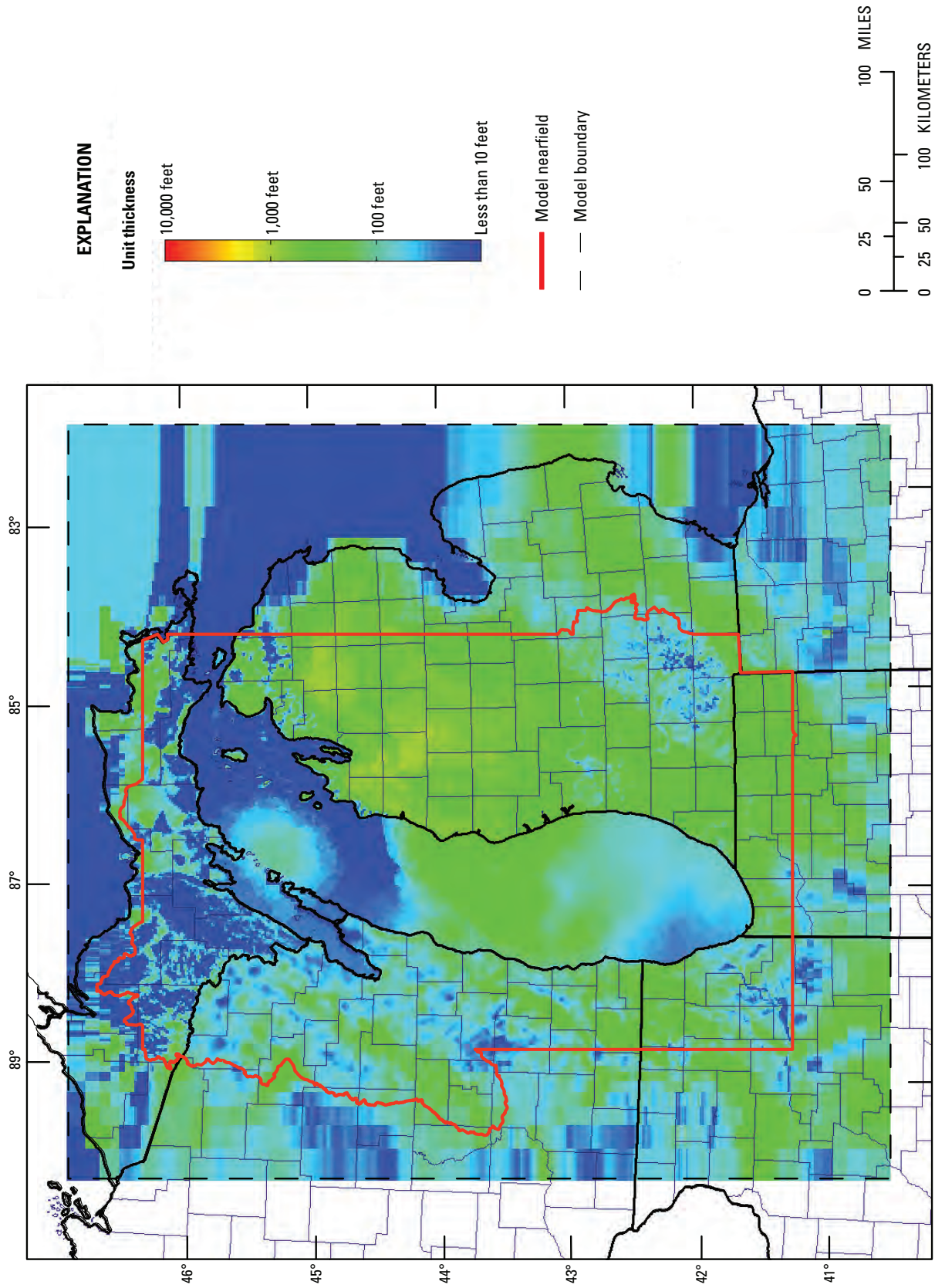


Figure 20A. Thickness of hydrogeologic units: Quaternary deposits (QRNR = layers 1-3).

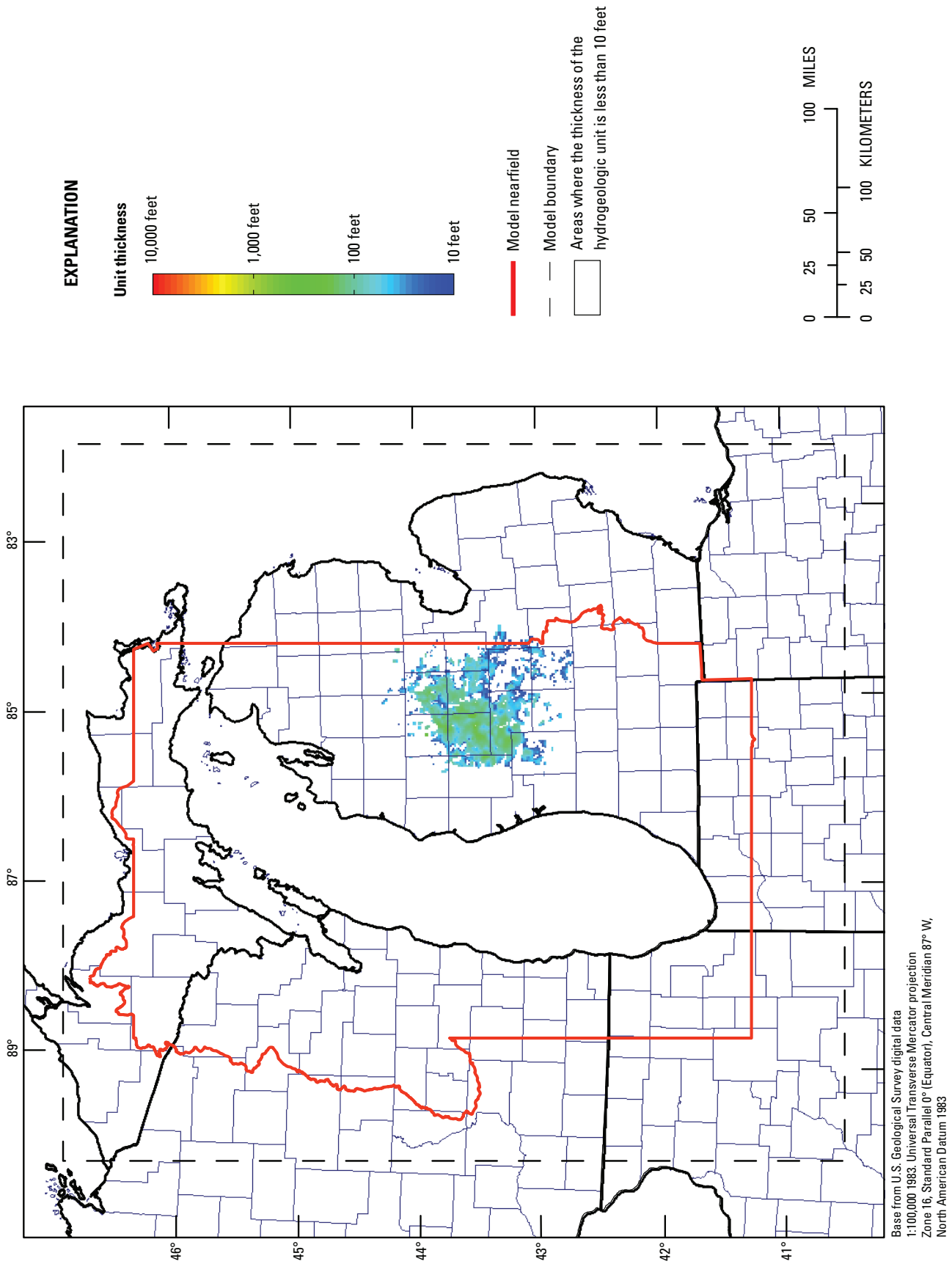


Figure 20B. Thickness of hydrogeologic units: Jurassic red beds (JURA = layer 4).

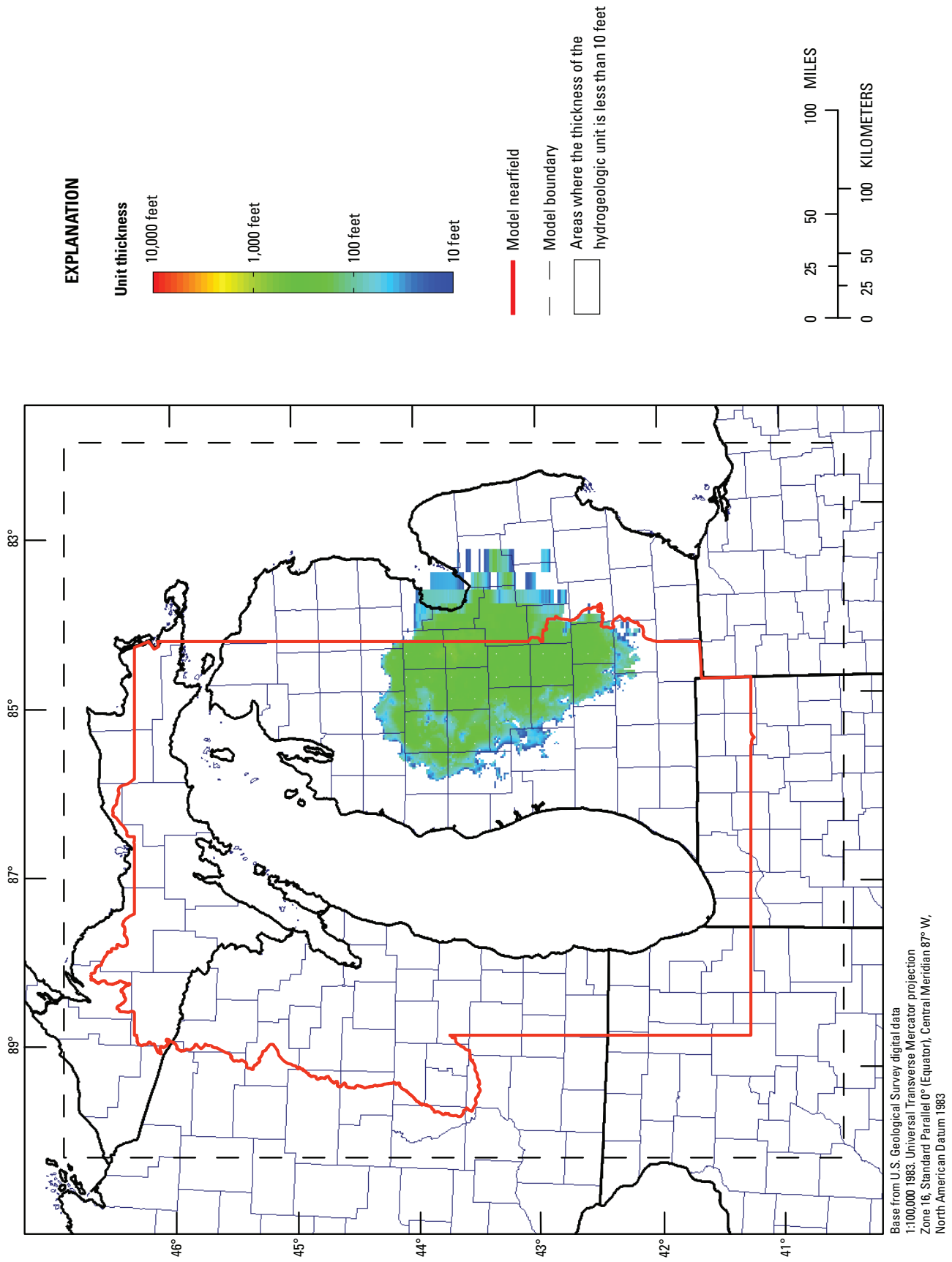


Figure 20C. Thickness of hydrogeologic units: Upper Pennsylvanian sandstone (PEN1 = layer 5).

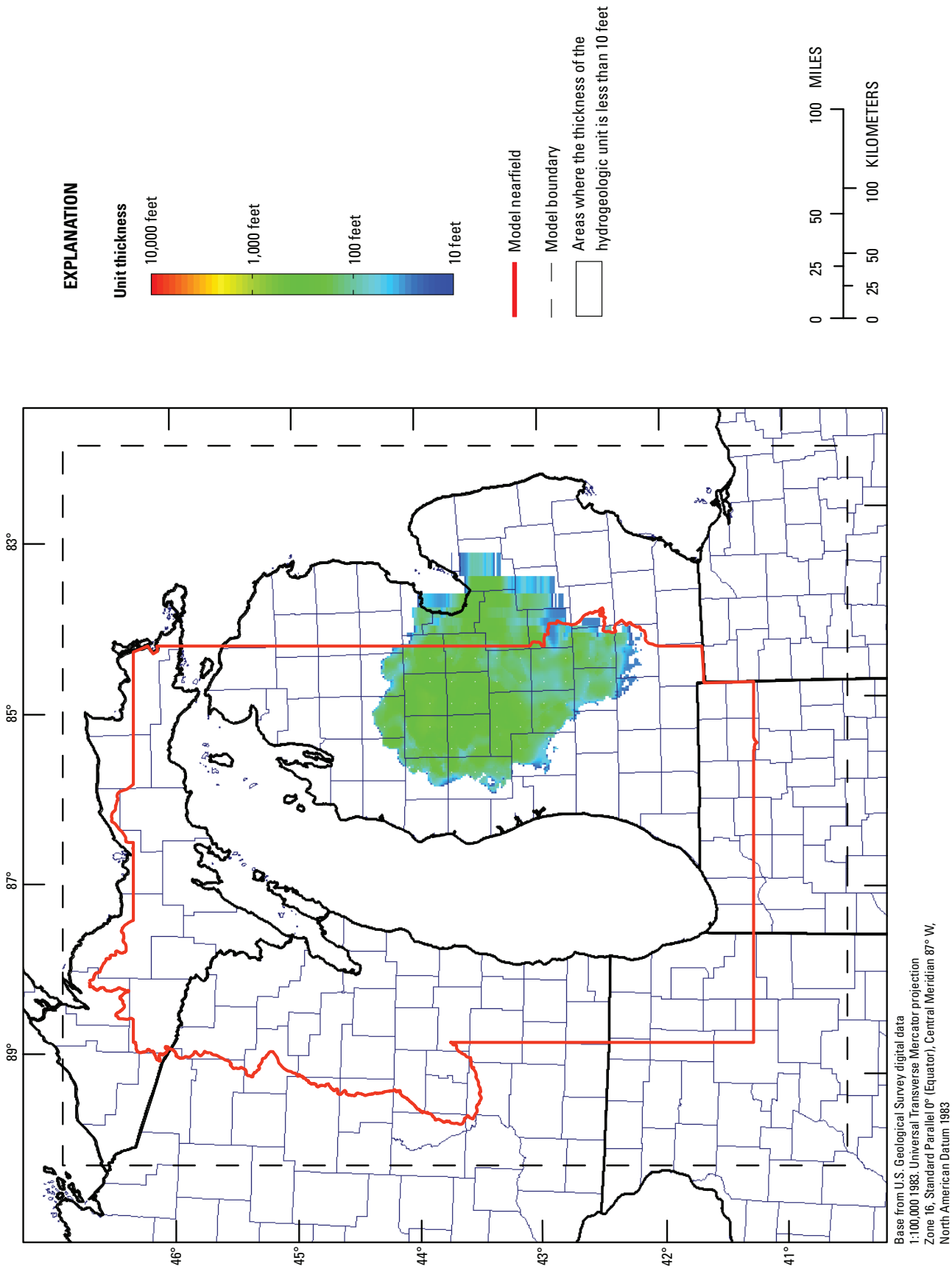


Figure 20D. Thickness of hydrogeologic units: Lower Pennsylvanian sandstone, limestones, and shales (PEN2 = layer 6).

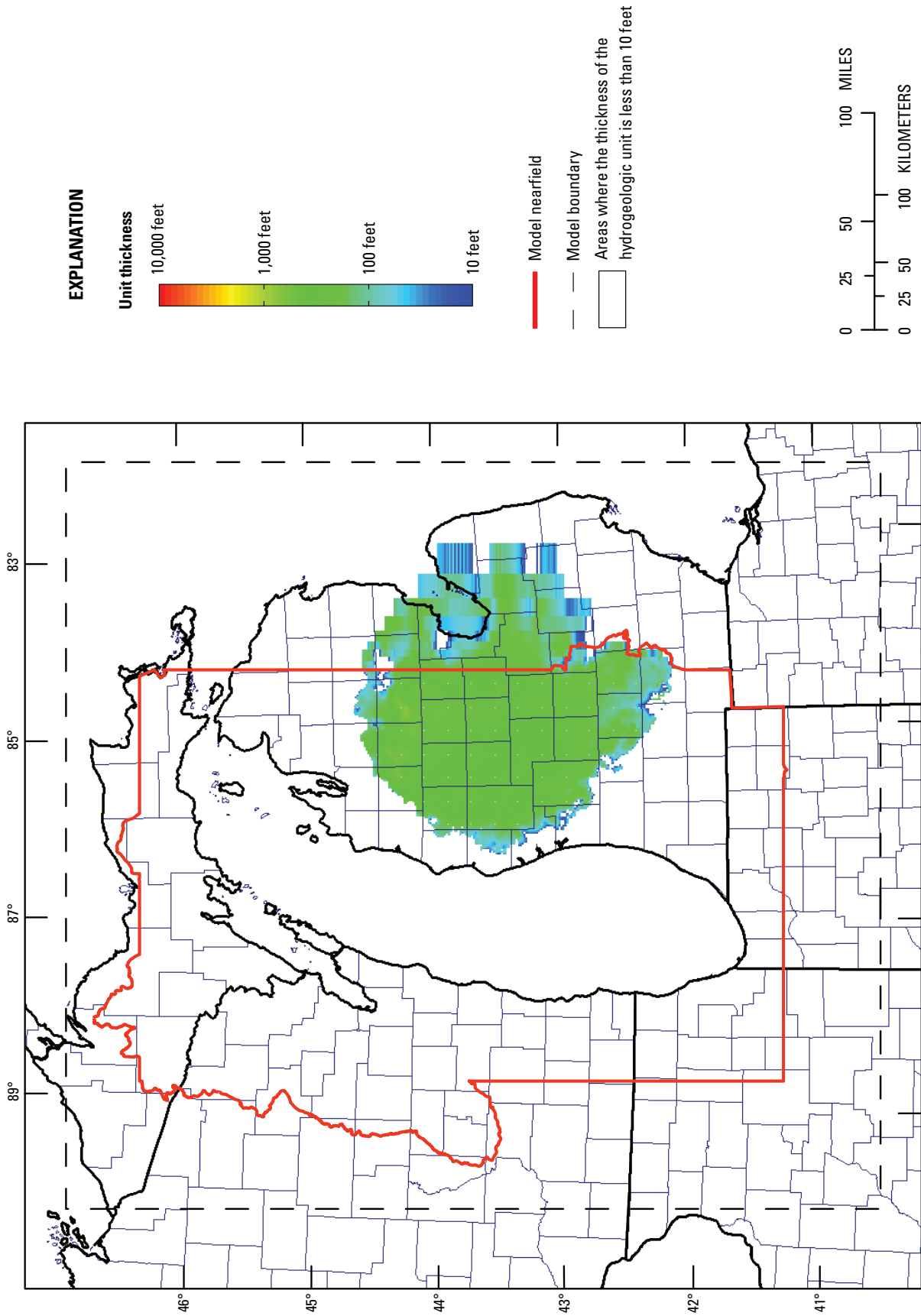


Figure 20E. Thickness of hydrogeologic units: Michigan Formation shale (MICH = layer 7).

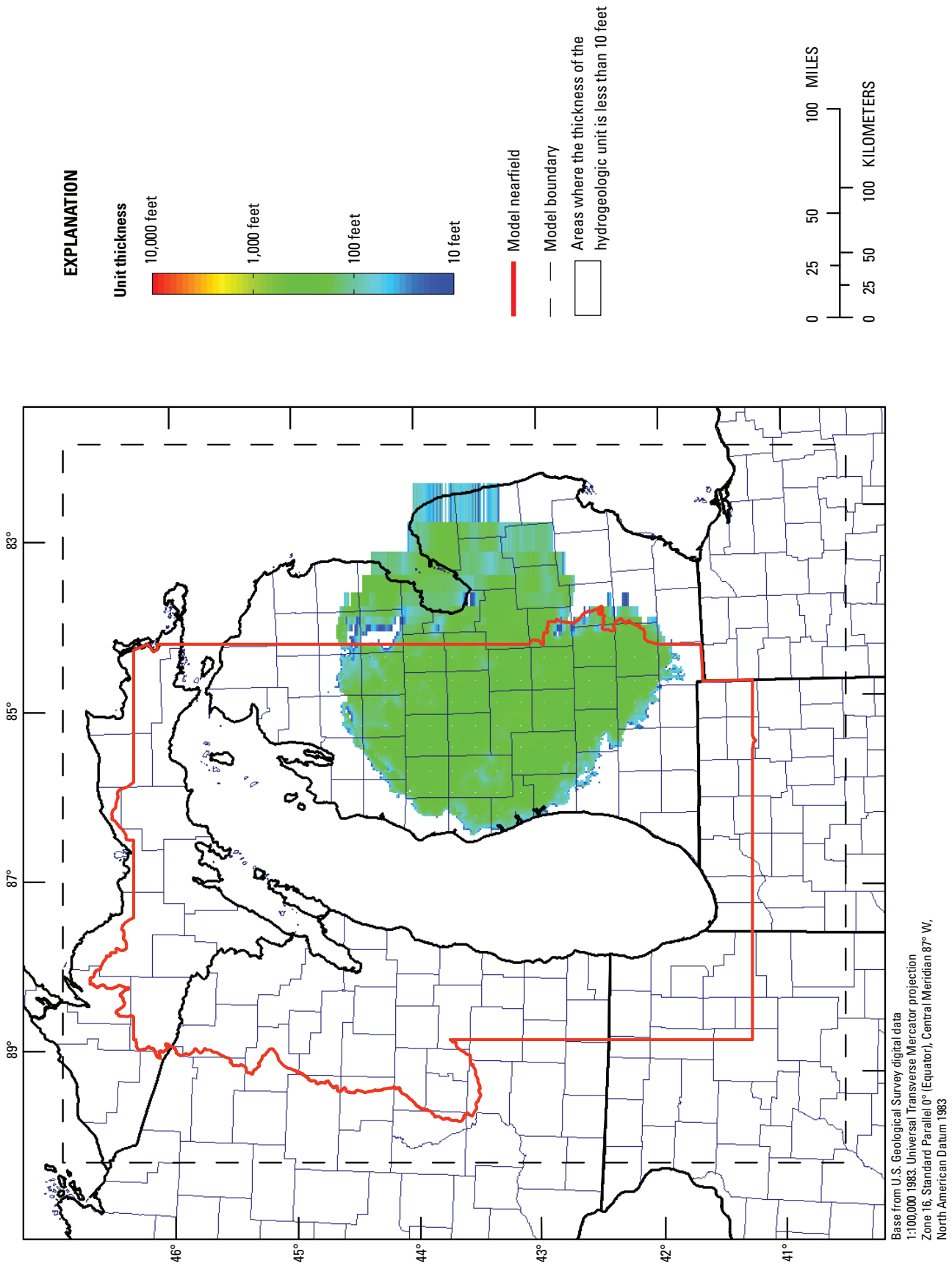


Figure 20F. Thickness of hydrogeologic units: Marshall Sandstone (MSHL = layer 8).

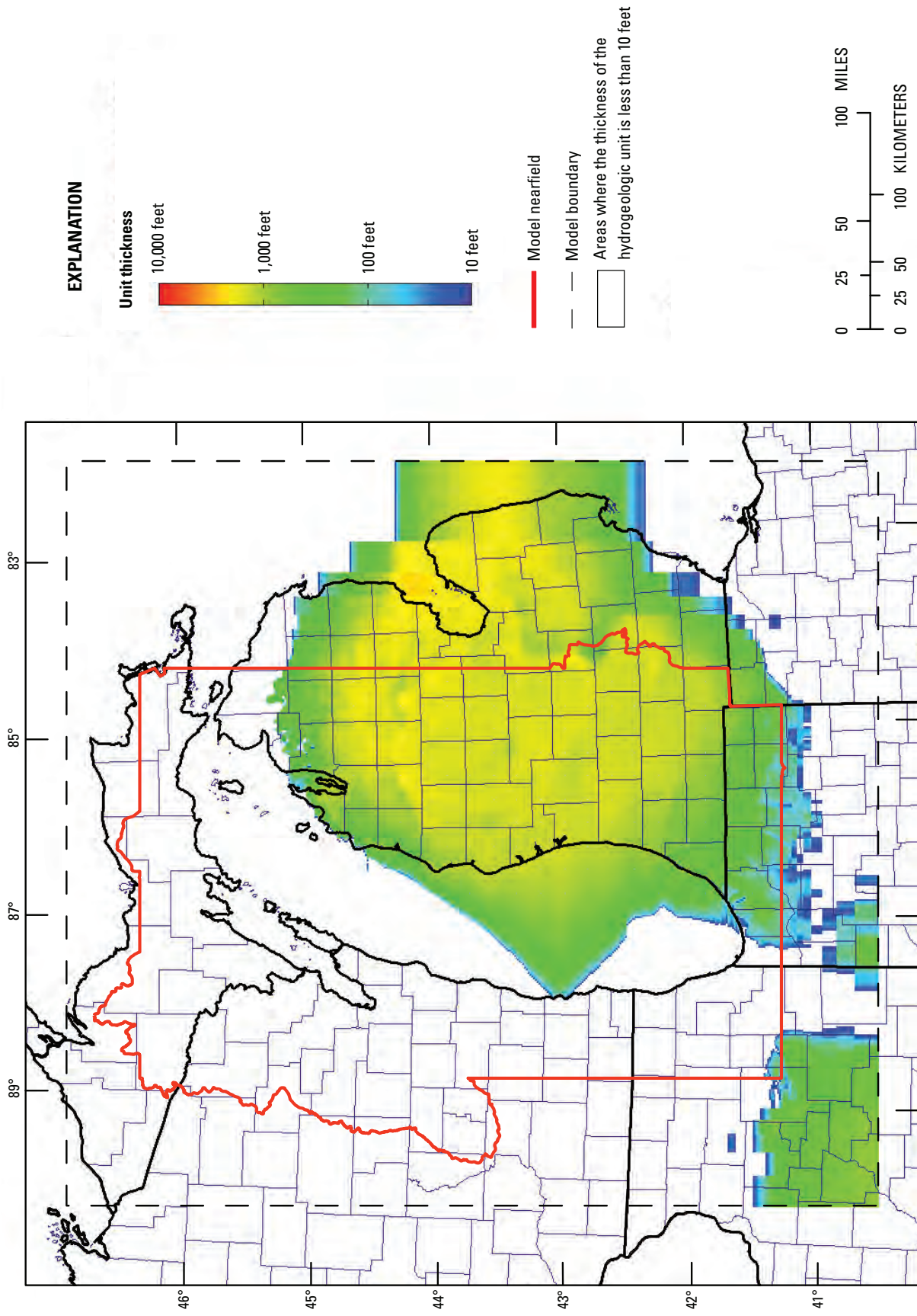


Figure 20G. Thickness of hydrogeologic units: Devonian-Mississippian shale (DVMS = layer 9).

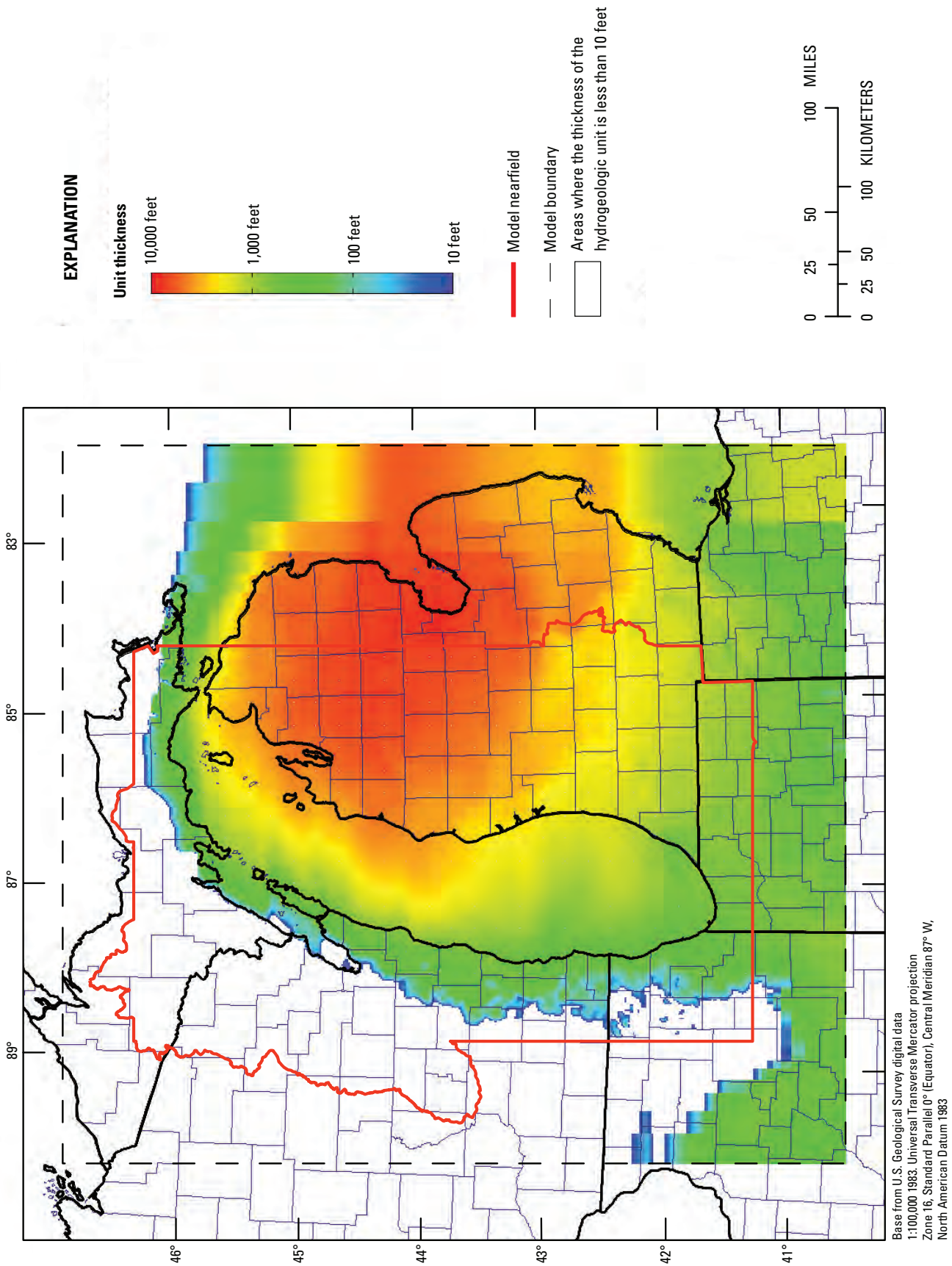


Figure 20/H. Thickness of hydrogeologic units: Silurian-Devonian carbonate and evaporites (SLDV = layers 10-12).

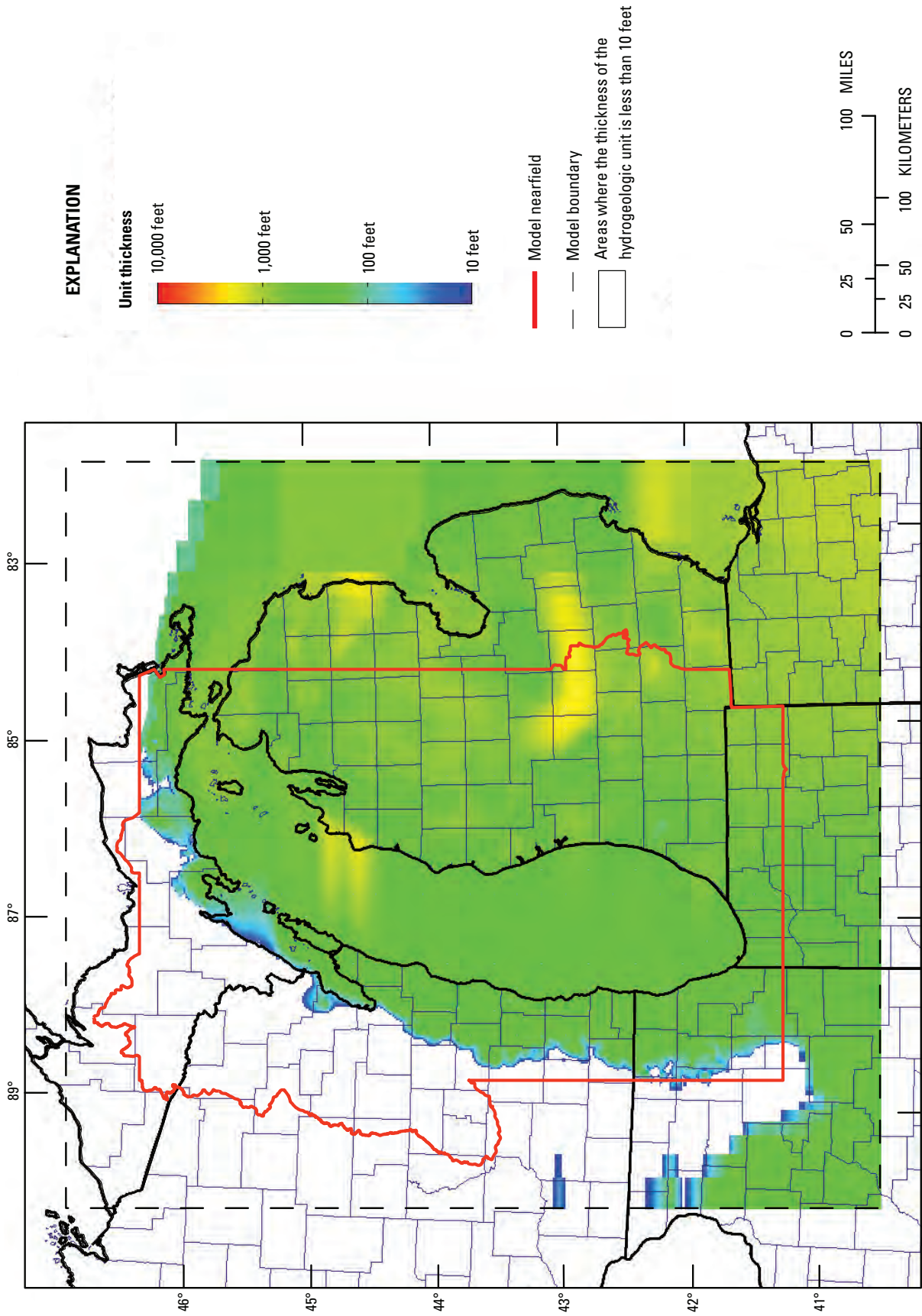


Figure 201. Thickness of hydrogeologic units: Maquoketa shale (MAQU = layer 13).

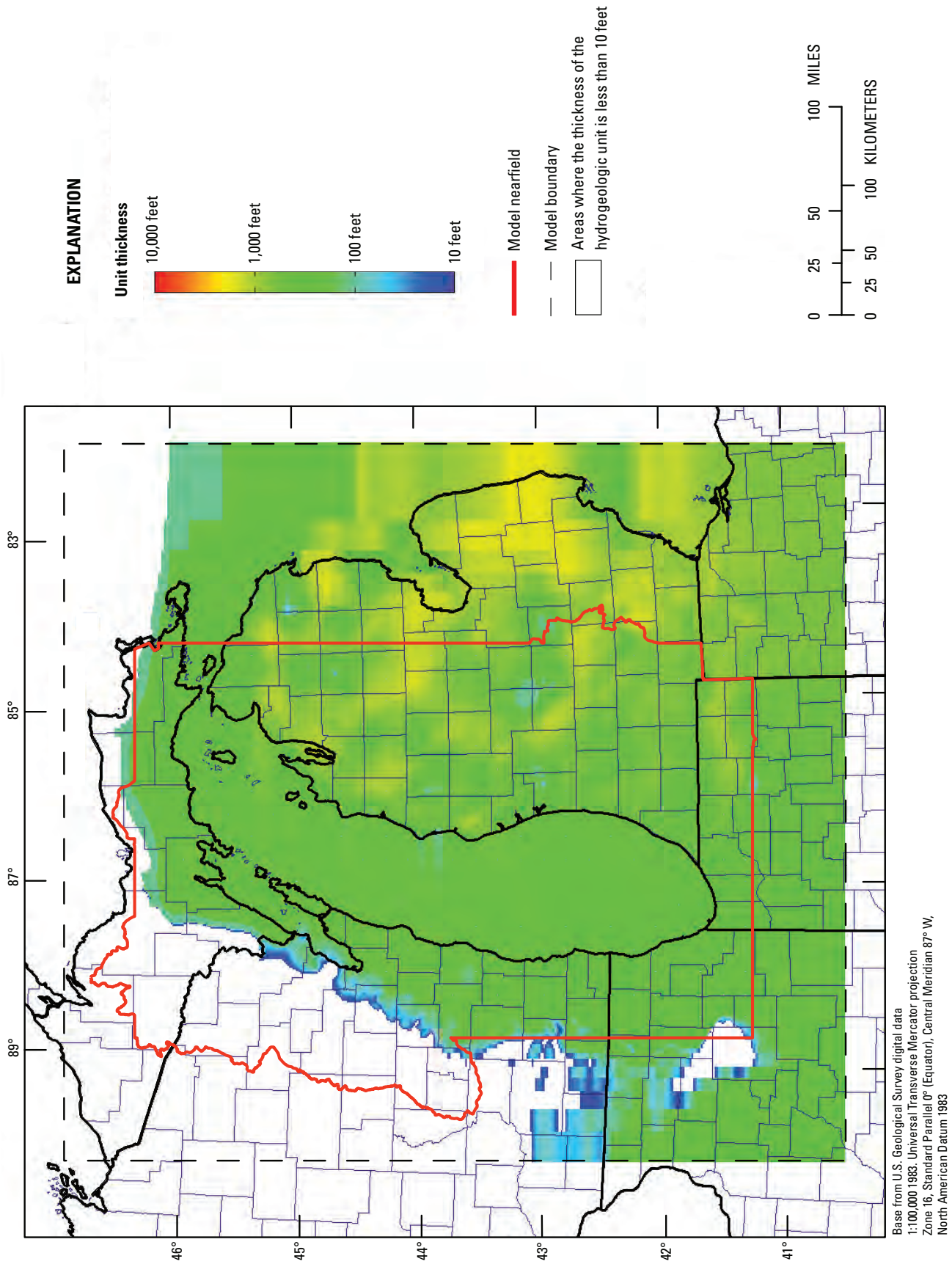


Figure 20J. Thickness of hydrogeologic units: Simipee dolomite (SNNP = layer 14).

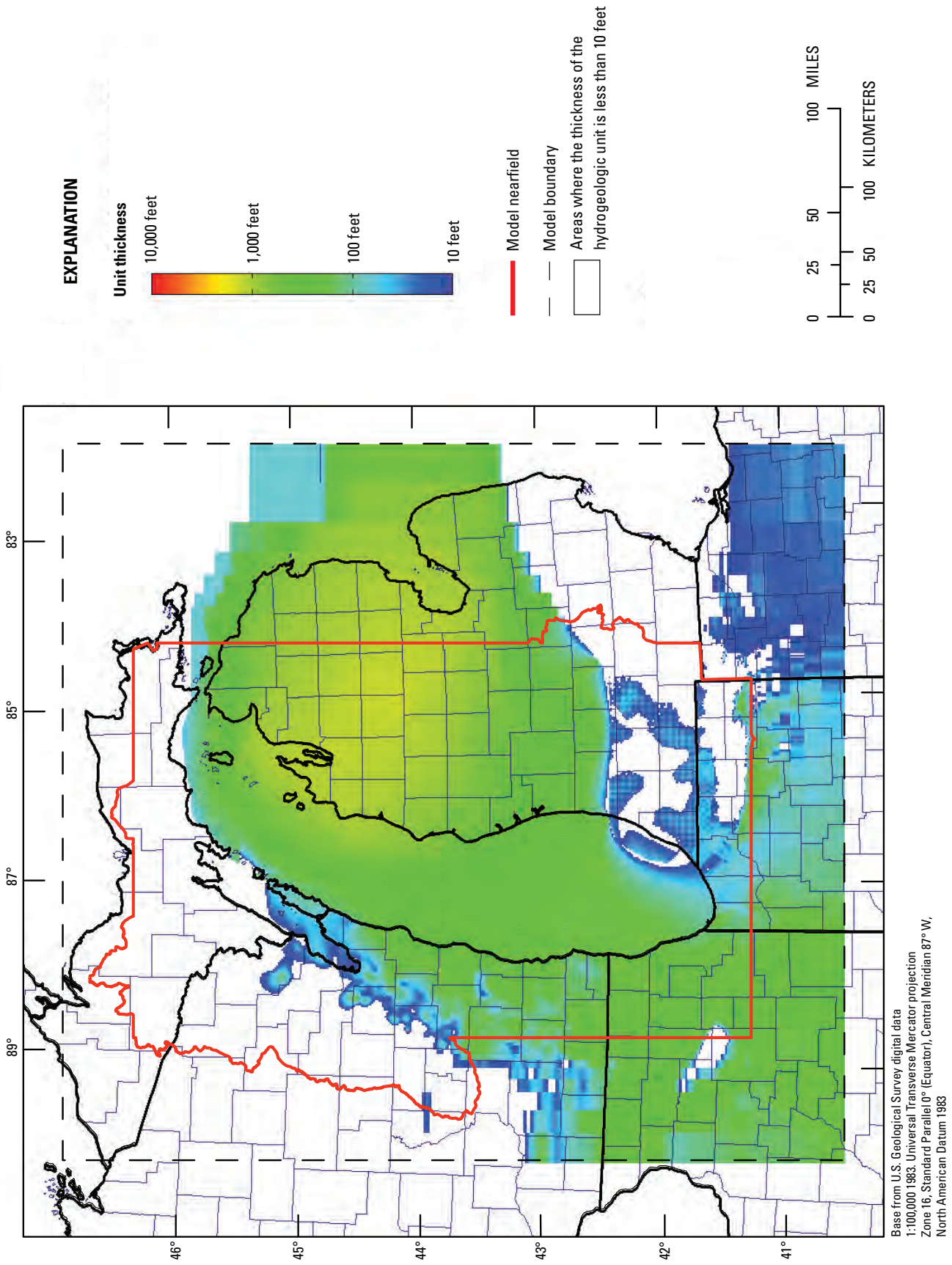


Figure 20K. Thickness of hydrogeologic units: St. Peter sandstone (STPT = layer 15).

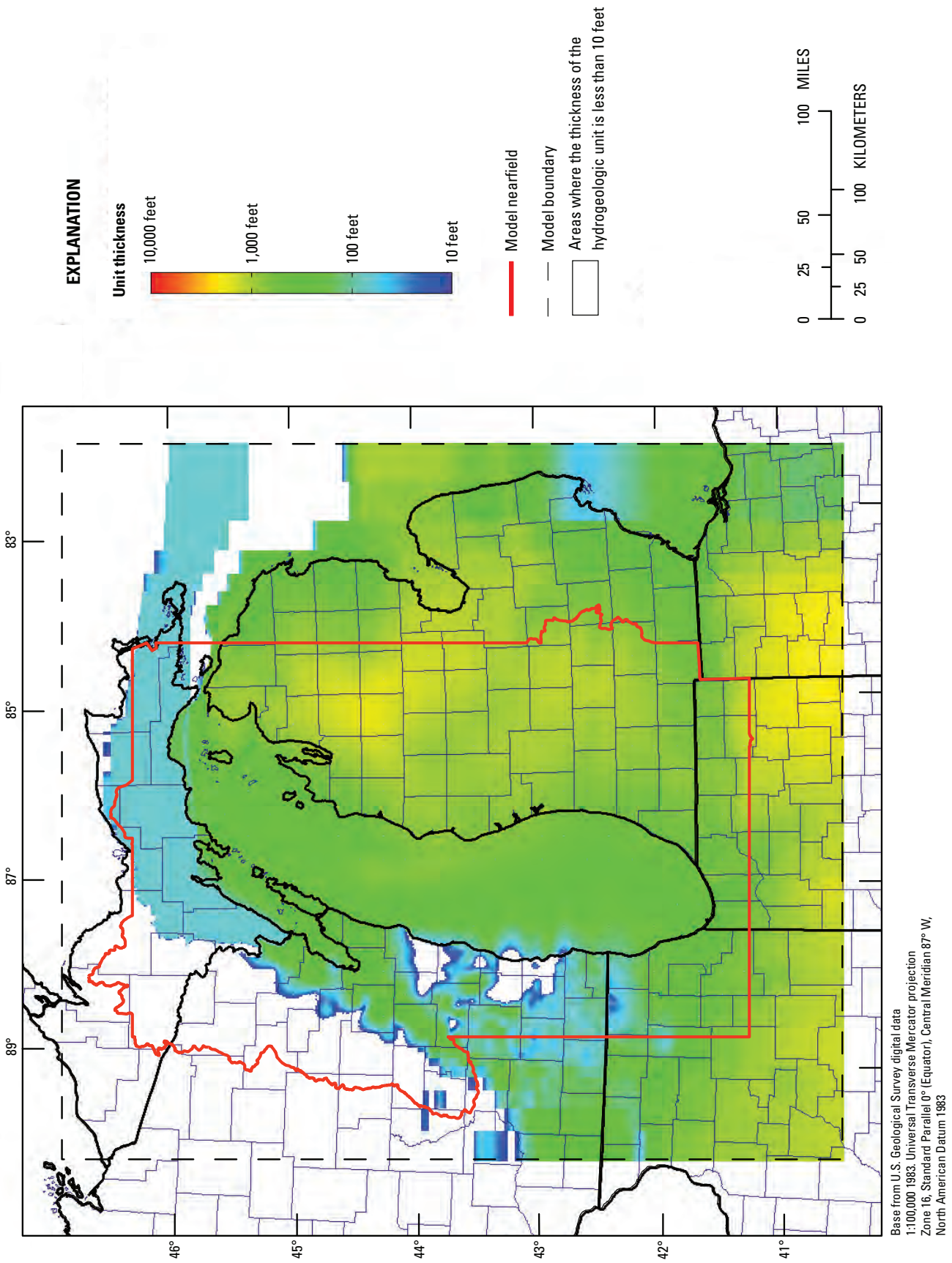


Figure 20L. Thickness of hydrogeologic units: Prairie du Chien dolomite and Franconia sandstone/shale (PCFR = layer 16).

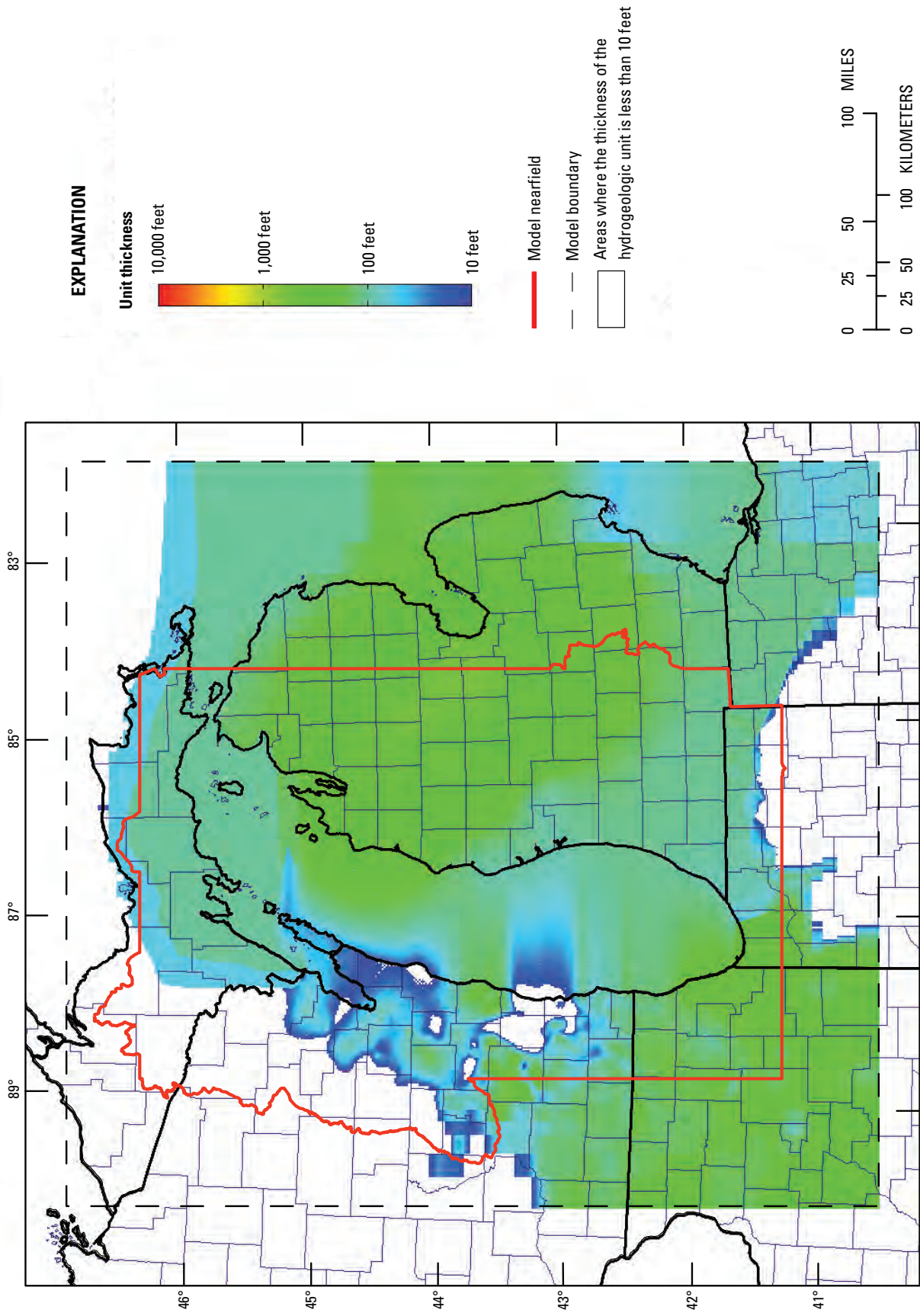


Figure 20M. Thickness of hydrogeologic units: Ironton-Galesville sandstone (IRGA = layer 17).

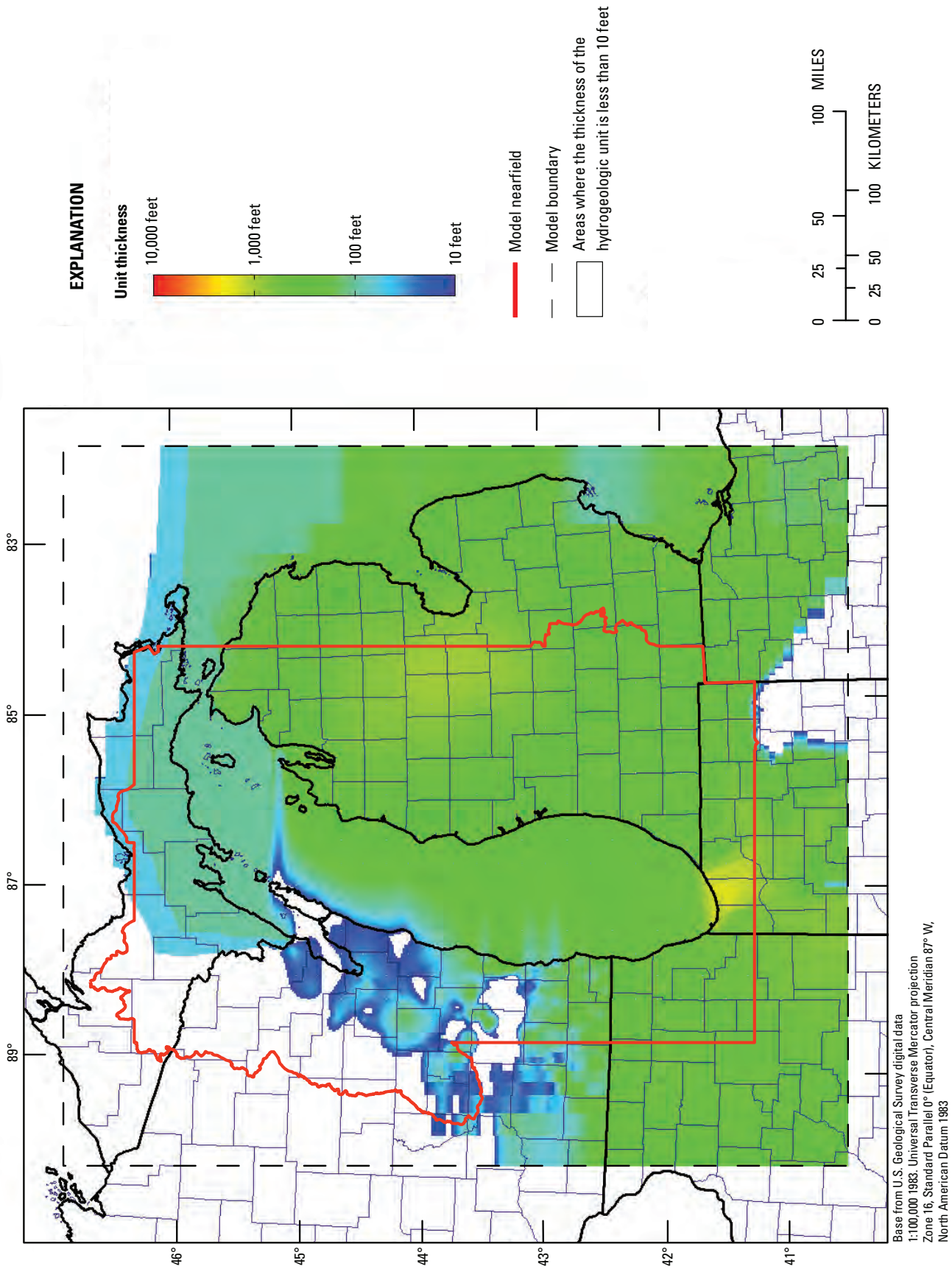


Figure 20M. Thickness of hydrogeologic units: Eau Claire sandstone/shale (EACL = layer 18).

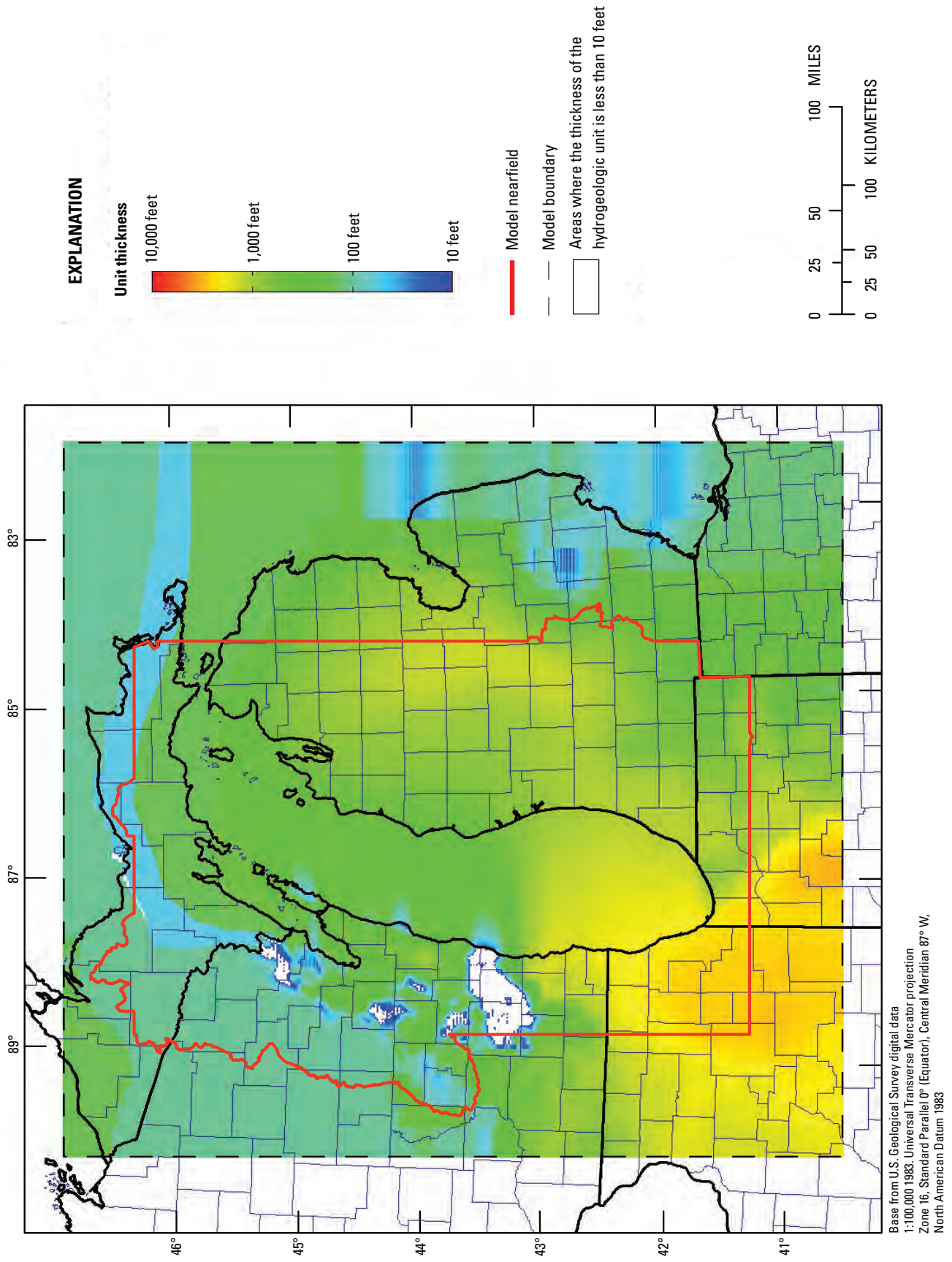


Figure 200. Thickness of hydrogeologic units: Mount Simon sandstone (MTSM = layers 19, 20).

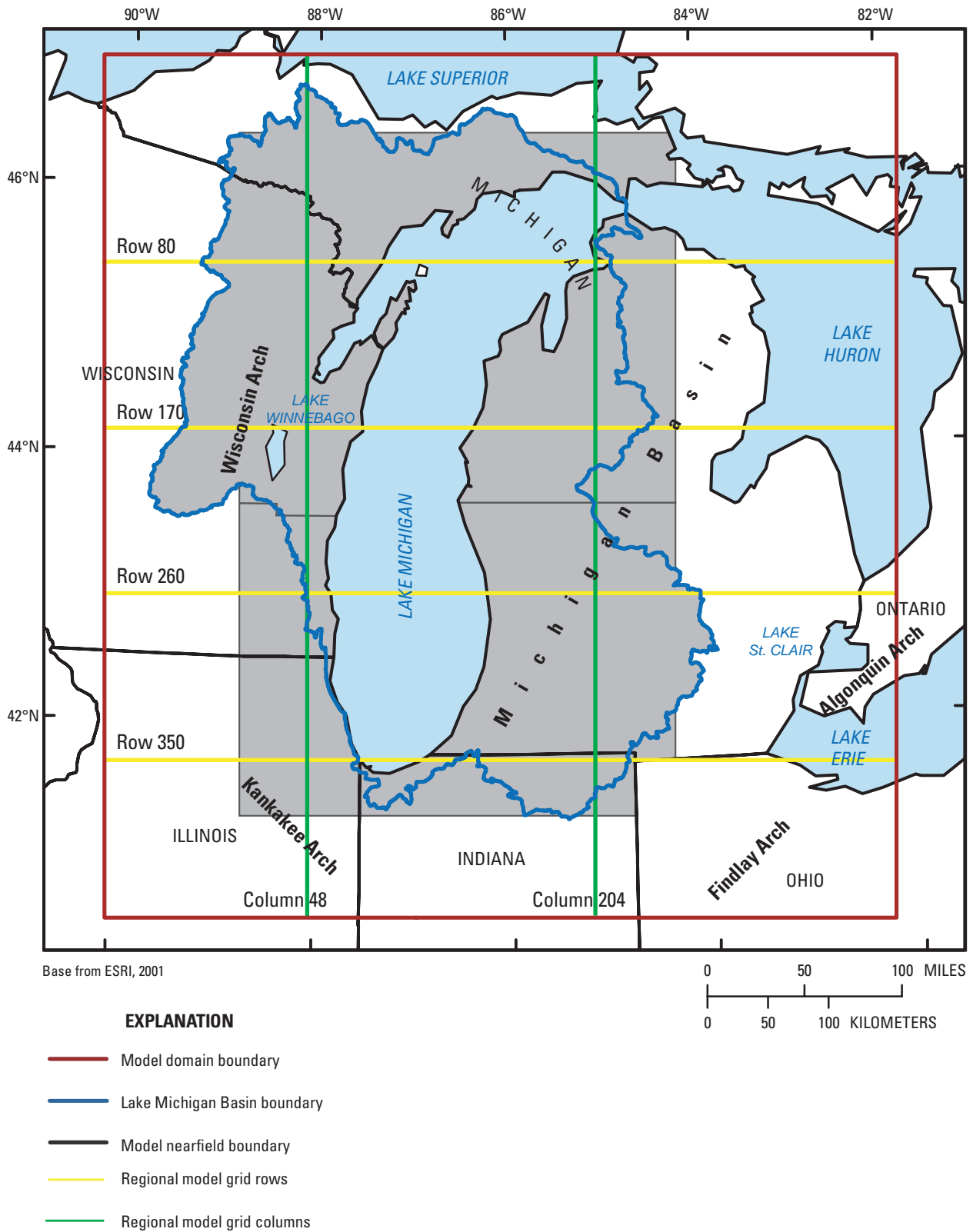


Figure 21. Traces for two north/south and four west/east hydrogeologic cross sections. (North south sections are along model columns. West east sections are along model rows.)

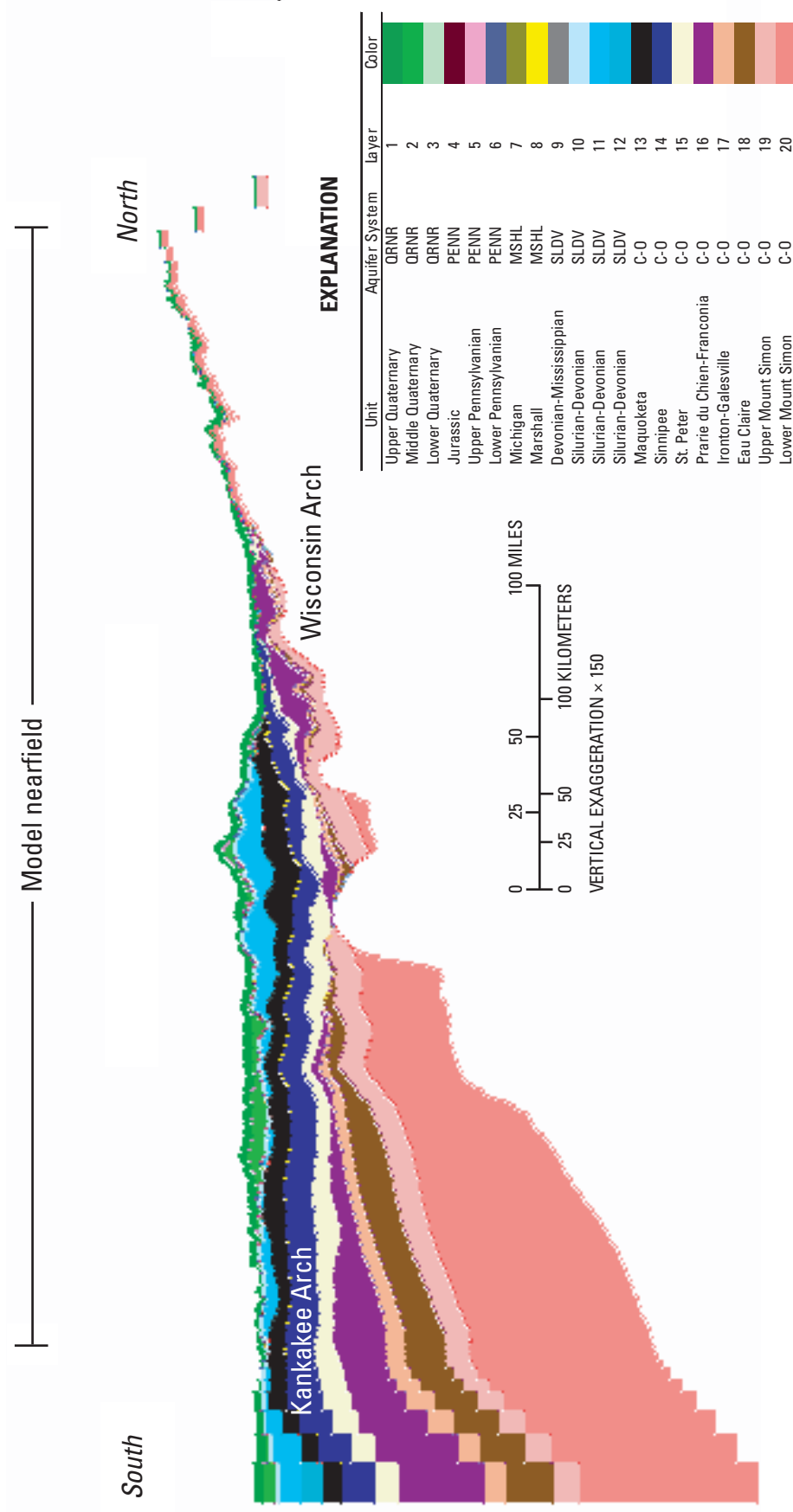


Figure 22A. Layering along model column 48.

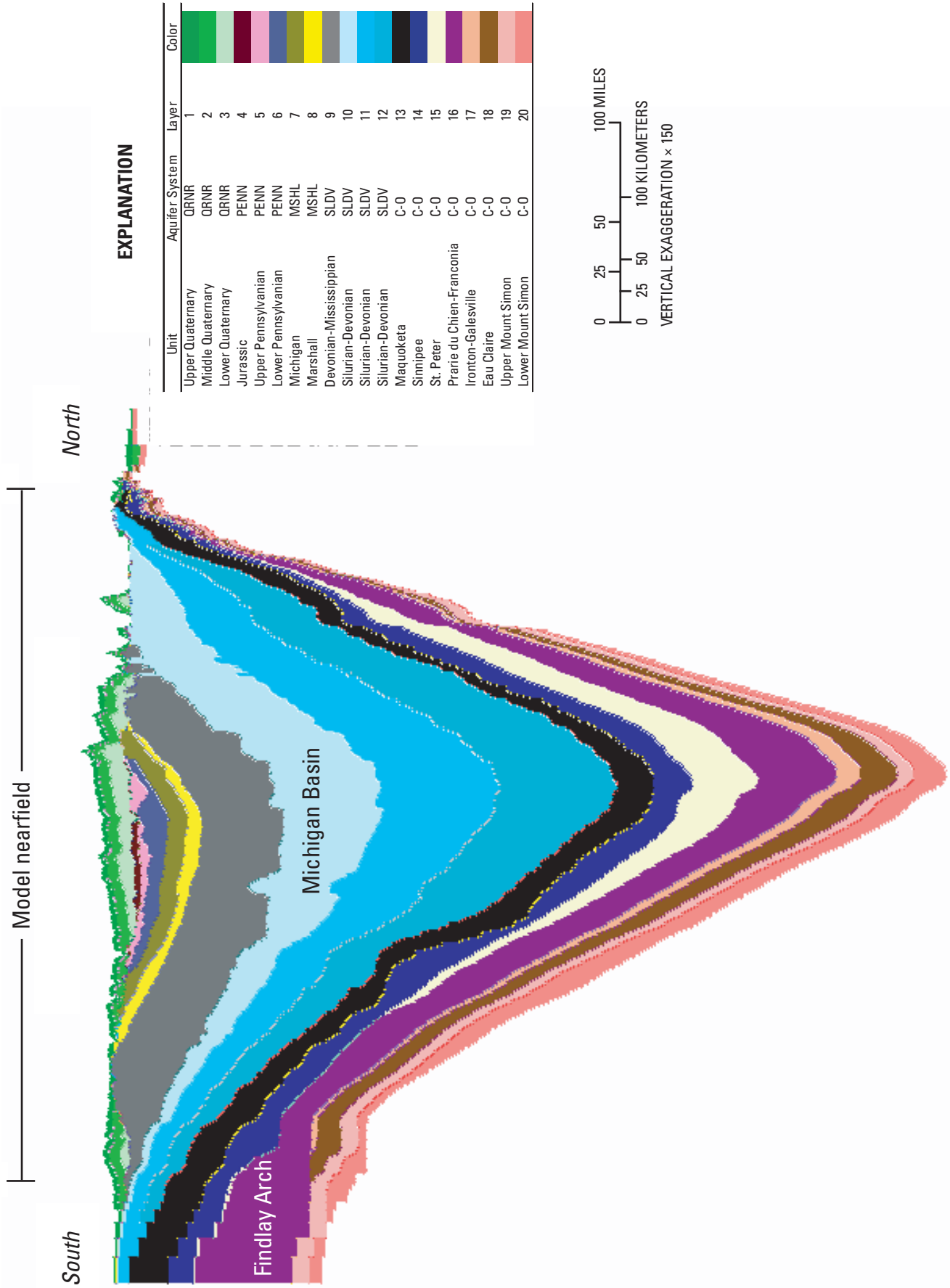


Figure 22B. Layering along model column 204.

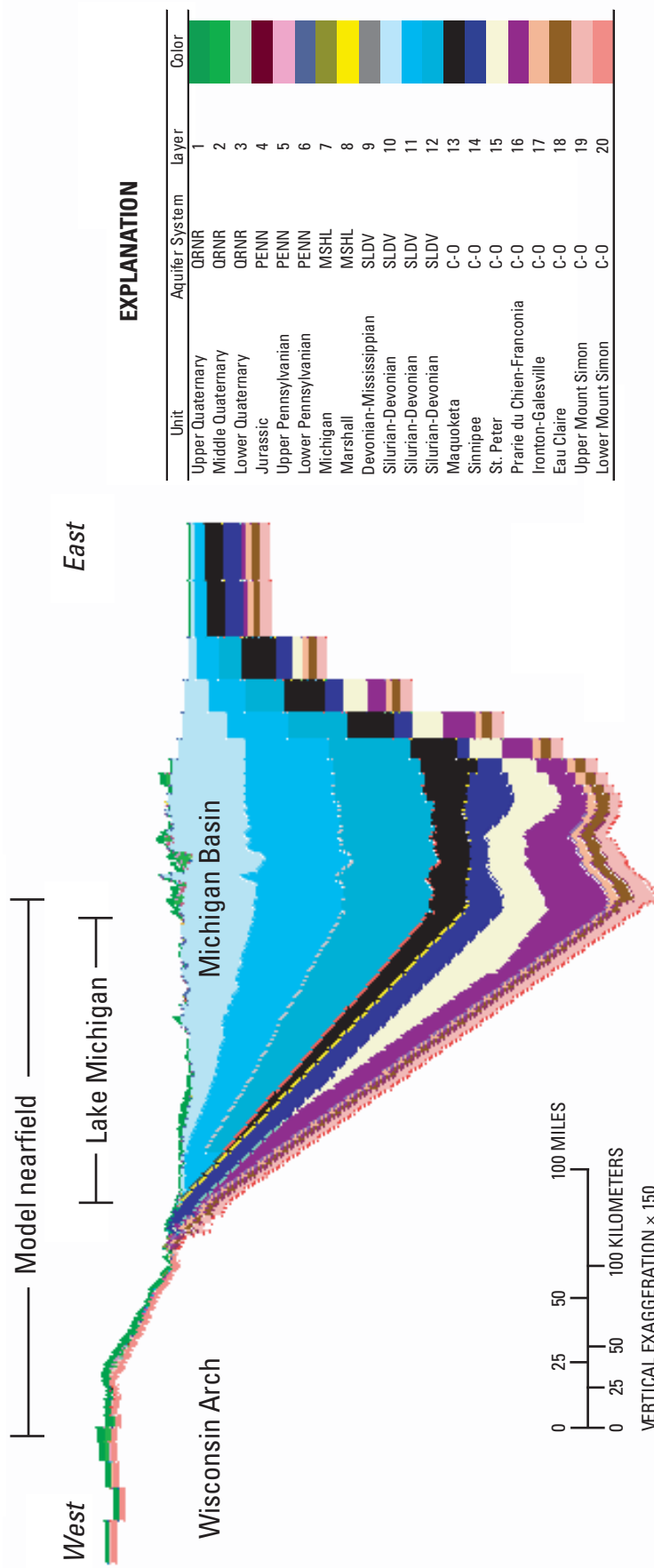


Figure 23A. Layering along model row 80.

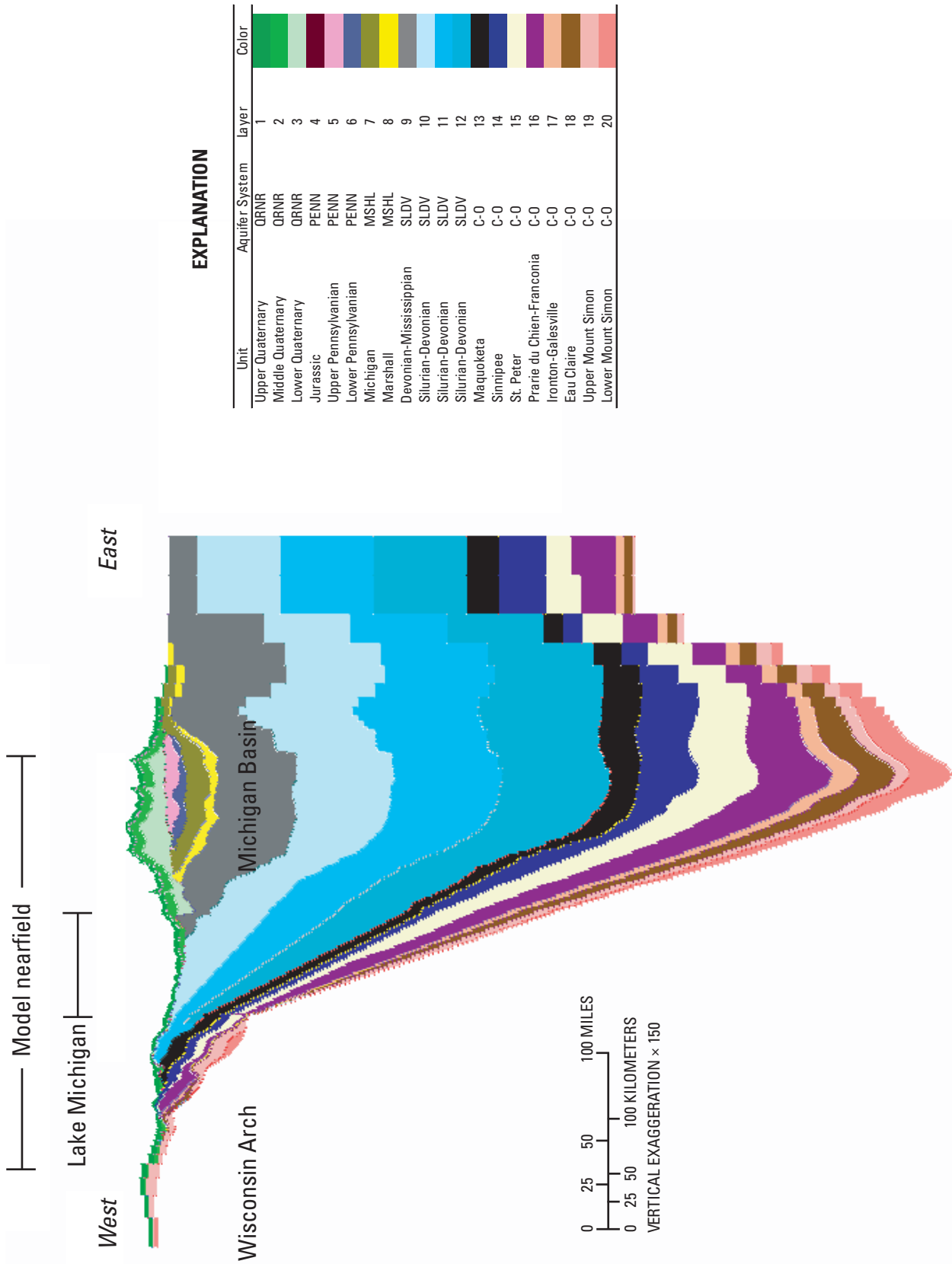


Figure 23B. Layering along model row 170.

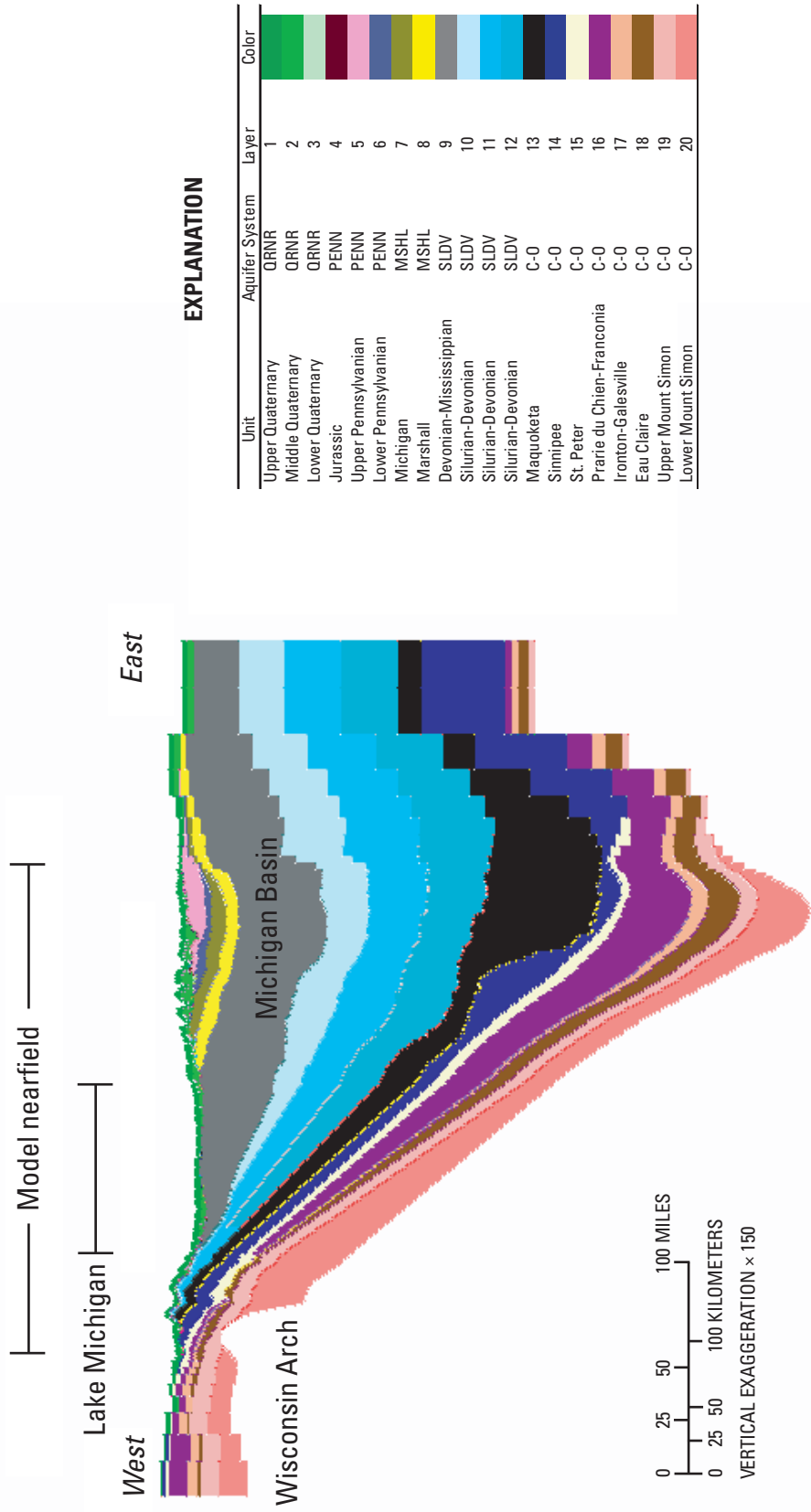


Figure 23C. Layering along model row 260.

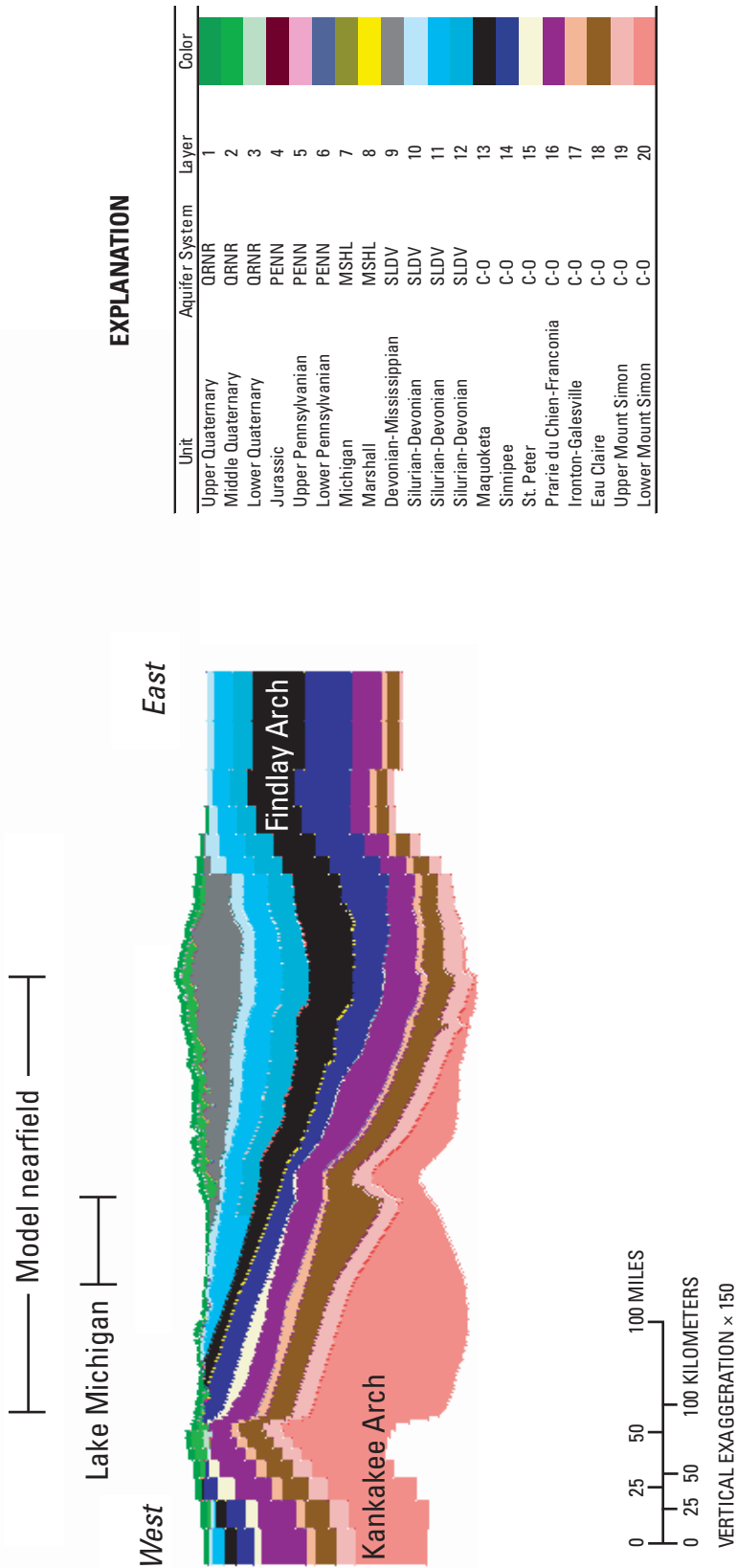


Figure 23D. Layering along model row 350.

Some model layers represent hydrogeologic units that, as a result of lateral facies changes, function as aquifers in some areas and confining units in other areas. The EAACL is a confining unit in the central and southern parts of the model domain, but it functions more as an aquifer in the northern part. Several other units function as confining units only in the Michigan Basin:

- The shale part of the Saginaw Formation (layer 6), a discontinuous body within the PENN system.
- The Salina Group (layer 11) within the SLDV system.
- PCFR (layer 16) within the C-O system.
- Lower MTSM (layer 20) within the C-O system.

Overall, confining units represent a large proportion of the sedimentary bedrock east of Lake Michigan (fig. 25).

The relative thickness of an aquifer system is not always correlated with the amount of water that can be withdrawn from it or the rate of groundwater flow through it. Another major control on flow patterns and water use is the unconfined or confined condition of the aquifer system and, in the case where multiple aquifer systems are present, the degree of separation between relatively shallow unconfined and semiconfined layers and underlying (deeper) confined layers. The boundary between the shallow part of the flow system (consisting potentially of both unconsolidated and bedrock units) and the deep part of the flow system (consisting only of bedrock units) is defined vertically by the elevation of the uppermost unpinched bedrock confining unit (see discussion in section 3.2). The QRNR aquifer system is always shallow, but the other aquifer systems can be either shallow (unconfined or semiconfined) or deep (confined) depending on location. Where present in the nearfield model domain, 62 percent of the PENN aquifer system is shallow and 38 percent is deep; 19 percent of the MSHL system is shallow and 81 percent is deep; 44 percent of the SLDV system is shallow and 56 percent is deep; and 19 percent of the C-O system is shallow and 81 percent is deep. The PENN, MSHL, and SLDV systems tend to be much more heavily used for water supply where they are shallow; in contrast, the sedimentary sequence of the C-O system west of Lake Michigan is heavily pumped both where it is shallow and where it is deep.

4.3 Stress Periods

The time discretization of the model has two purposes:

1. To separate predevelopment conditions, which approximate the natural conditions before the advent of high-capacity pumping wells, from postdevelopment conditions, which have been influenced by variations in pumping and recharge.⁸
2. To simulate changes in recharge and pumping rates at a time scale sufficiently short to incorporate hydrologically important trends (for example, an increase in recharge across the Lake Michigan Basin or water-level recovery in response to shifting the source of an important center's public water supply from wells to surface water).

The first objective was met by constructing a combined steady-state/transient model, with the first stress period devoted to predevelopment conditions: its water-level output serves as the basis for calculating drawdown and recovery in subsequent transient stress periods. The second objective was met by assigning variable stress-period length as a function of the data available (for example, well records and climate and land-use records) and the rapidity of change. The first wells

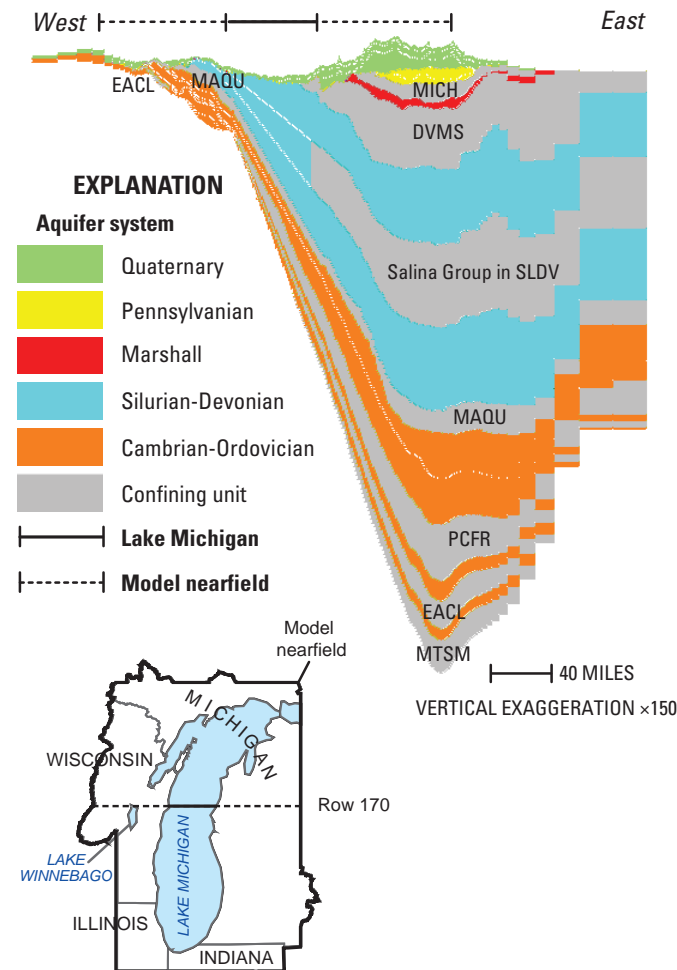


Figure 25. Major confining units along model row 170.

⁸ The terms “predevelopment” and “postdevelopment” distinguish the periods before and after high-capacity pumping started in 1864. However, because development and well discharge accelerated around the onset of World War II, the phrase “predevelopment (pre-1940)” is sometimes used, notably in the treatment of calibration targets, to include the time between 1864 and 1940.

in the Lake Michigan Basin area date to 1864 in the Chicago-Milwaukee area (Feinstein, Eaton, and others, 2005; Feinstein, Hart, and others, 2005). Water-use data over parts of the model domain are sparse until the latter half 20th century (for example, the Illinois water-use database is limited to total amounts from pumping centers before 1964 and only afterwards incorporates discharge from individual wells, whereas the Michigan water-use database contains many gaps before the late 1970s). In the 1970s, climate changes linked to precipitation patterns across much of the eastern United States (Magnuson and others, 2003) gave rise to steplike increase in recharge rates, whereas the most important shift from groundwater to surface water occurred in the early 1980s, when the Chicago area began to supply itself from Lake Michigan. Relatively long stress periods (20 years or more) are used to represent the interval from 1864 to 1940, whereas shorter, 5-year periods represent the 1970s and 1980s, plus the last stress period from 2001 to 2005.

In all, there are 13 stress periods in the model, with the 12 transient stress periods extending over 141 years (table 5). Because the first stress period is steady state, the choice of initial head conditions in the model is arbitrary as long as it causes no part of the model (when in unconfined mode) to dewater and be rendered inactive. Setting the initial head for all layers at a row/column location to the average land-surface elevation over the row/column area fulfilled this requirement.

Table 5. Stress period setup for model.

Stress period	Duration	Time period
1	Steady state	Predevelopment: before Oct. 1864
2	36 years	Oct. 1864–Sept. 1900
3	20 years	Oct. 1900–Sept. 1920
4	20 years	Oct. 1920–Sept. 1940
5	10 years	Oct. 1940–Sept. 1950
6	10 years	Oct. 1950–Sept. 1960
7	10 years	Oct. 1960–Sept. 1970
8	5 years	Oct. 1970–Sept. 1975
9	5 years	Oct. 1975–Sept. 1980
10	5 years	Oct. 1980–Sept. 1985
11	5 years	Oct. 1985–Sept. 1990
12	10 years	Oct. 1990–Sept. 2000
13	5 years	Oct. 2000–Sept. 2005
Total	141 years	Predevelopment–Sept. 2005

The first model stress period consists of one steady-state time step. The subsequent transient stress periods are each divided into five time steps regardless of the stress-period length. All stresses (recharge, pumping, surface-water inputs) are automatically kept constant for the length of the stress period, but the evolution of the response to the continued and changed stresses between periods is influenced by the sequenced solutions for the period. Time-step lengths within each period are increased by a factor of 2 to better simulate changes heads and flows in response to changes in boundary conditions from one stress period to the next. Only the results from the final time step in each stress period are reported.

4.4 Farfield Boundary Conditions

The farfield of the model is composed mostly of cells belong to one of four boundary condition categories: no flow, constant head, general head, and specified non-zero flux.

4.4.1 No Flow

Boundaries at the north, east, south, and west sides of the model are no flow. Although this boundary condition does not reflect actual groundwater conditions at these locations, the effect of the boundary on simulated conditions in the model nearfield is small because (1) the model sides are distant from the model nearfield, (2) other farfield boundary conditions limit its influence, and (3) in some areas, important groundwater divides are present between the model nearfield and the no-flow boundary. The effect of the no-flow side boundaries is assessed in model-sensitivity simulations (see section 7).

No-flow boundaries also define the bottom of the model (at the interface with the Precambrian crystalline rock) and represent inactive areas within the model farfield where the Precambrian bedrock is shallow and the QRNR and bedrock systems are not present (fig. 26). The total area of the farfield inactive zones is 10,741 mi², comprising 5.9 percent of the full model domain. One large zone is in the northwest corner of the model in the Lake Superior Basin; another is in the north-east corner of the model in Ontario, Canada. Neither of these zones participates in the model solution.⁹

⁹ The extent of inactive zones was determined by application of an unpublished U.S. Geologic Survey algorithm written by Arlen Harbaugh (called *MF2KCLST.EXE*, for MODFLOW-2000 Version 1.17.01, dated September 22, 2006) that identifies “islands” of cells in a MODFLOW model that are not in flow connection with the remainder of the domain because too many inactive or dry cells are distributed over one or more areas of the model. In the LMB model, connected clusters of cells in the northwest, northeast, and the far western parts of the model are cut off when Precambrian crystalline bedrock highs render inactive many row/column locations in a neighborhood, causing the entire cluster to become hydraulically isolated.

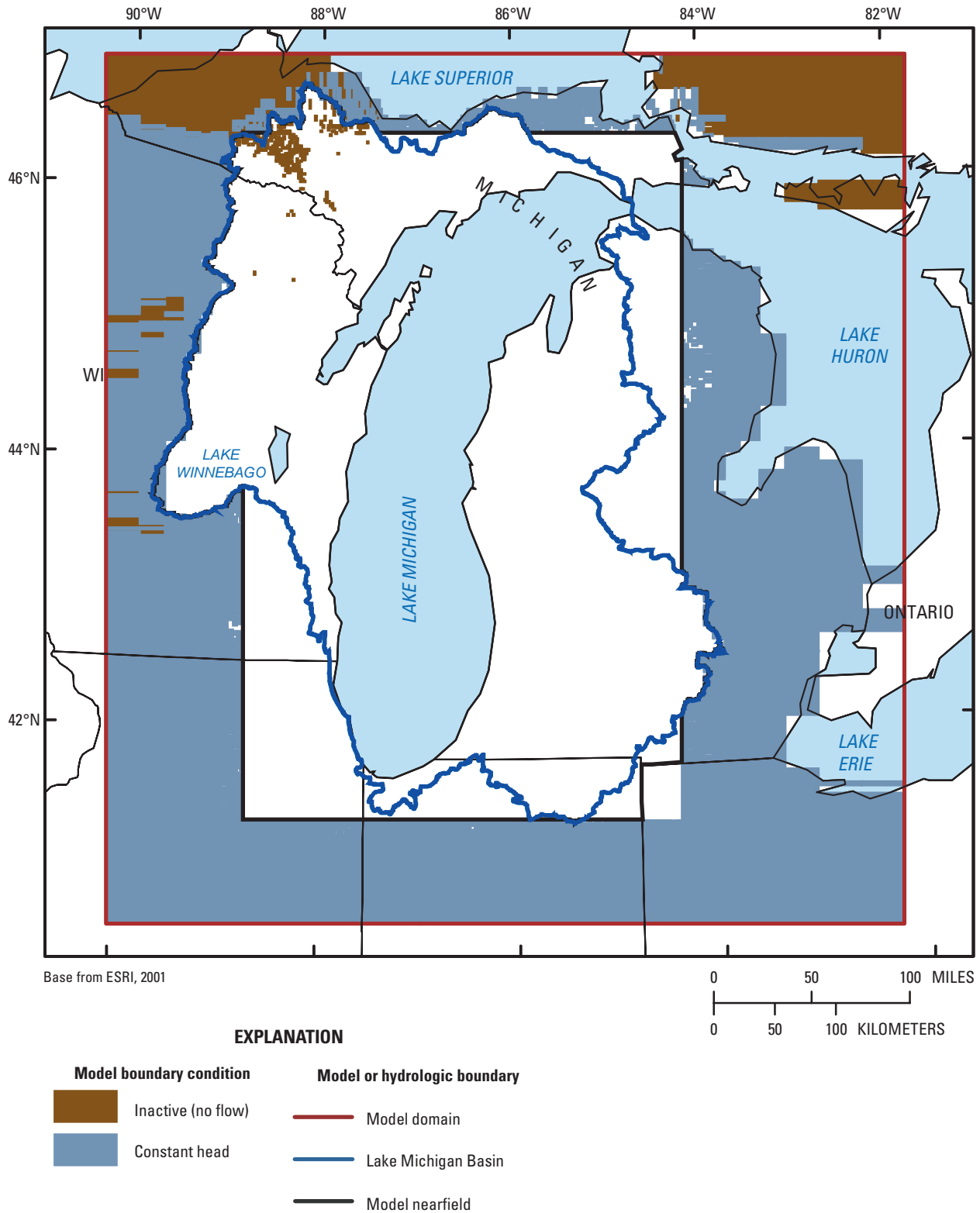


Figure 26. No-flow and constant-head boundary conditions. (The constant-head boundary conditions are applied only to the highest active cell at a row/column location. The inactive (no-flow) boundary conditions are applied to all layers at the row/column location.)

4.4.2 Constant Head

Constant-head (CHD) boundaries were used to specify water-table elevations throughout most of the model farfield (fig. 26). The condition is applied to the highest active cell at a row/column location, which is usually, but not always, model layer 1. The CHD boundaries ensure that regional gradients in the shallow flow system in the model farfield are reasonable and provide a means of computing recharge (through the exchange between constant head and underlying active cells) rather than furnish it as an input. One drawback of this approach is that it is impossible to adjust parameters in the shallow flow system in the model farfield to better match observations of head and flow. Given that the role of the farfield is strictly limited to providing reasonable flux into and out of the nearfield, this constraint is acceptable.

The constant head specified for the topmost active farfield cell corresponds to the average stage in the highest order stream crossing the cell area. If streams are absent, but other surface-water features are present, the constant head equals the elevation of the largest lake in the cell. Because the lateral dimensions of the farfield cells are large (greater than 1 mi on a side, sometimes much greater), the area enclosed by almost all inland farfield cells contain at least one stream or lake. Most (83 percent) of the 8,873 constant-head cells in the model are assigned to layer 1; the remainder correspond to average stage elevations below the bottom of layer 1 and are assigned to lower layers, with all overlying layers converted to inactive cells (that is, they do not participate in the model solution). Constant-head cells in the LMB model are used only in the model farfield and are held constant through all stress periods.

4.4.3 General-Head Conditions

A large part of the model farfield represents Lake Superior, Lake Huron, Lake St. Clair, or Lake Erie (fig. 27). These areas are represented in the LMB model by head-dependent boundaries with the General Head Boundary (GHB) package. Each lake is assigned a constant stage (feet above vertical datum):

- Lake Superior = 601.10
- Lake Huron = 577.50
- Lake St. Clair = 572.33
- Lake Erie = 569.20

The stages for Lake Superior, Lake Huron, and Lake Erie correspond to the National Oceanographic and Atmospheric Administration Low-Water Datum, which is referenced to the International Great Lakes Datum (1985). No low-water datum is reported for Lake St. Clair, however; it is possible to estimate a stage from the historical record (1918–2007) by using the average stage difference between Lake Huron and Lake St. Clair and the average difference between Lake Huron and Lake Erie (U.S. Army Corps of Engineers, Detroit District, 2006).

The fixed farfield lake stages based on the low-water datum nearly equal the average Lake Superior, Lake Huron, and Lake Erie levels measured in 2005, a period of much lower than average stage across the Great Lakes. Section 7 of this report, a discussion of a model sensitivity simulation, describes the effect on model results of using time-dependent lake levels matched to the historical record in place of constant lake stages.

In addition to the stage, the GHB boundary condition for farfield lakes also requires a conductance term that controls the amount of flow entering or leaving the lake for a given hydraulic gradient within a lake cell, based on the specified lake stage and the simulated groundwater level in the same cell. For this application, the conductance term has been set to fairly high values for all the lakes.¹⁰ (The conductance term is equal to the product of the assumed vertical hydraulic conductivity of the lakebed and the area of the cell assumed to transmit flow, divided by the assumed thickness of the lakebed; the resulting units are feet squared per day.) As a result, the GHB cells function in way similar way to constant-head boundary conditions. A comparison run substituting constant heads for GHB conditions produced negligible difference in any nearfield results. The use of a GHB boundary rather than a simpler CHD boundary is intended to keep the accounting of lake flows separate from other flows in the model water budget.

The GHB cells in the model farfield are assigned to layer 1 except in areas where they overlie bedrock, in which case the GHB cells are assigned to a lower layer and all overlying layers at the row/column location are rendered inactive.

4.4.4 Specified Flux

The northern half of the western edge of the model domain lies along the north-south course of the Wisconsin River (shown in fig. 7B) in the model farfield. Most of the northern farfield model edge intersects Lake Superior, and most of the eastern farfield model edge intersects Lake Huron, Lake St. Clair, or Lake Erie. For these sides of the model, the surface-water bodies serve as constant-head boundary conditions. In contrast, the southern side and the southern half of the western side of the farfield model domain do not coincide with surface-water features; instead, the groundwater levels are influenced by deep wells pumped in northeastern Illinois. Pumping has probably caused drawdown on the order of tens of feet in the confined C-O aquifer system in this area, as indicated by a regional model (Meyer and others, 2009) recently constructed by the Illinois State Water Survey (ISWS).

¹⁰ For the farfield lakes, the K_v of the lakebed is assumed to be 1 ft/d, the entire cell surface area is assumed to transmit flow, and the lakebed thickness is assumed to be 1 ft. These values give rise to large conductance values not only because the surface areas of farfield cells are large but also because the assumed lakebed is everywhere set to a very small thickness.

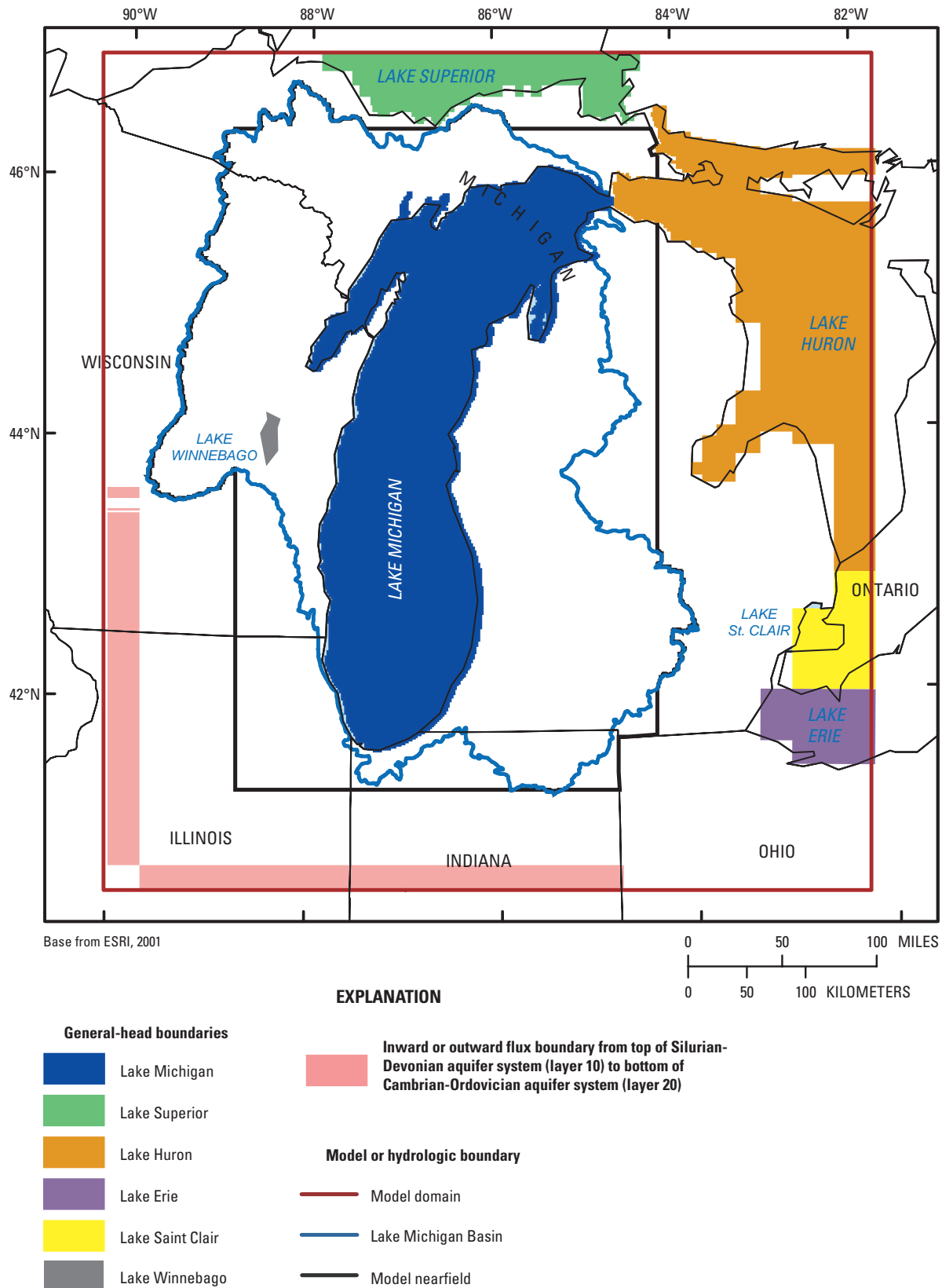


Figure 27. General-head and specified-flux boundary conditions. (The general-head boundary conditions apply to the highest active cell at a row/column location. The specified-flux boundary conditions apply to the bedrock cells in layers 10 to 20.)

Deep pumping is much more active west of Lake Michigan than east of the lake. (See discussion of groundwater withdrawals in this section.) Although shallow pumping centers tapping mostly unconfined aquifers produce restricted drawdown cones bounded by recharge (surface-water) boundaries, deep pumping centers tapping confined aquifers can produce drawdown cones affecting very large areas. Therefore, the possibility that a large drawdown cone associated with confined aquifers will violate the LMB model's edge boundary conditions is essentially limited to Wisconsin and Illinois. The drawdown cones from the major deep pumping centers around Green Bay and Milwaukee, Wis., do not extend beyond the LMB model nearfield (Conlon, 1998; Feinstein, Hart, and others, 2005; also the results from this modeling effort). Only the deep northeastern Illinois pumping center causes appreciable drawdown in the farfield and, therefore, only the farfield boundary conditions connected with this pumping center require special attention.

A constant-flux boundary was used to represent underflow to and from the southern side and the southern half of the western side of the model domain. Fortunately, the ISWS model uses the same pumping database for northeastern Illinois as the LMB model and similar model layers, so results of the ISWS model can be used to specify rates of underflow in the SLDV and C-O aquifer systems in the LMB model. Time periods used in the ISWS model are also similar to stress periods defined for the LMB model. Under predevelopment and early 20th century conditions, the flow simulated by the ISWS model across the LMB model boundary in Illinois, Indiana, and Wisconsin is at some locations inward with respect to the LMB model domain and at some locations outward. However, when increased withdrawals from northeastern Illinois are simulated, flow is almost entirely inward.

A constant-flux boundary was assigned in layers 10 through 20 by using the WEL package. One problem with using flux rates from the ISWS model is that uniform-density flow was assumed, rather than variable-density flow as in the LMB model. The effect of this constant-flux boundary on the LMB model was assessed through model sensitivity simulations (see section 7 of this report).

4.5 Nearfield Surface-Water Network

The nearfield surface-water network consists of

- streams of first order and higher,
- surface-water features designated as lakes or as wetlands, and
- Lake Michigan and Lake Winnebago (the large lake in northeastern Wisconsin; see fig. 1).

The streams, lakes, and wetlands constitute the inland surface-water network. They are represented as RIV cells, whereas GHB cells represent Lake Winnebago and Lake Michigan.

4.5.1 Inland Surface-Water Network

A surface-water database was compiled to represent streams and water bodies for the LMB model. The features of this database and how it is manipulated to generate inputs for both the farfield and nearfield of the model are described in appendix 2. In particular, the database serves to identify the location and quantify the stages and conductance terms used to represent streams and water bodies. The inland surface-water features are represented as RIV cells. The RIV boundaries representing streams are defined so that groundwater can discharge to a stream as base flow when the stream stage is below the simulated water table, and stream water can discharge to groundwater when the stage is above the simulated water table. The RIV boundaries representing lakes and wetlands are defined differently and can act only as discharge areas for groundwater whenever the ambient head is above the stage.¹¹ The treatment of water bodies as DRAIN boundaries was made to prevent one lake from simply routing water to an adjacent lake with a lower stage—an artifact of model construction that can distort the water budget for the model—whereas the ability of streams to lose water was maintained chiefly to allow surface water to act as a source of water to wells under stressed conditions.

The algorithm for assembling the stream input to the model associates a model cell with a stream only if at least part of the stream reach inside the cell (composed of one or more “stream arcs”) is at least 8 ft wide; moreover, it associates a model cell with another water body only if the area of the lake or wetland inside the cell (defined as a “water-body polygon”) is at least 20 acres (see appendix 2). In all, there are 63,398 cells that represent the water-table surface for the inland model nearfield (the remaining 25,289 nearfield cells correspond to Lake Michigan and Lake Winnebago). These width and area thresholds limit the percentage of inland nearfield cells with just streams to 27.5 percent, the percentage with just water bodies to 18.5 percent, and the percentage with both features to 11.1 percent. During model construction, this initial distribution left some areas of the nearfield with too great a distance between discharge points, leading to solutions with water-table elevations above the land surface. In these areas, the thresholds for including surface-water features were relaxed and minor surface-water features were added to the distribution, allowing the percentage of cells representing streams or stream and water bodies to increase to a total of 41.3 percent; the corresponding percentage representing just the water bodies increased to 19.0 percent.

¹¹ When the RIVBOT parameter for a cell in the RIV package input is identical to the STAGE, then the boundary condition in that cell acts the same as an entry in the DRN package and can only accept water. When RIVBOT is below the STAGE, then it can either accept or furnish water depending on the head elevation in the cell. In the LMB model, RIVBOT is set 1 ft below the stage for streams, but for water bodies it is equal to stage.

The distributions of the two types of surface-water features are shown in figures 28 *A* and *B*. As is pointed out elsewhere in this report, setting about 60 percent of the water-table cells to a RIV condition represents a compromise, one intended to insert a surface-water network into the model that is dense enough to prevent spurious water-table mounding with reasonable input parameters, but not so dense that the water-table solution is almost everywhere constrained by boundary conditions.

As in the case of the farfield GHB boundaries, the conductance assigned to any RIV cell is proportional to the assumed hydraulic conductivity of the bed material and the area across which exchange occurs and inversely proportional to the bed thickness. For all features, the bed thickness is assumed to be 1 ft, an arbitrary value. The area term depends on the type of feature. For cells intersecting at least one stream arc assigned at least 8 ft of width, the stream area is equal to the sum of the length of each arc multiplied by its width. The length is provided as a database attribute of the stream arcs, whereas the width is estimated as a function of the upstream distance from the stream arc to the streamhead (see appendix 2). For cells intersecting water bodies, the area assigned the conductance term is limited to a ring defined by the perimeter length of the water body inside the cell multiplied by a 20-ft width, assumed to represent the zone over which there is active exchange between the groundwater and the lake or wetland (see appendix 2).

The specified hydraulic conductivity of lakebeds (set everywhere to 2 ft/d) is assumed to be lower than for streambeds (set to 5 ft/d) but higher than for wetlands (set to 0.5 ft/d). The rationale for this ranking is that the bed materials of streams tend to be coarser than those of lakes, whereas wetlands tend to have the finest beds. The selected conductivity for streambeds is consistent with literature values (see, for example, Krohelski and others, 2000; Calver, 2001), but it is obvious that a single value for the three types of features cannot reproduce field behavior across the regional model nearfield. The extreme simplicity of the approach is mitigated in part by dividing the nearfield into zones based on categories of glacial material (see section 5.2) and adjusting the conductance in each zone during the calibration phase to better match field observations. However, it also must be recognized that the choice of the hydraulic conductivity of the bed exerts limited influence on the overall head and flux solutions (see last section in appendix 2).

The total conductance for any cell is the sum of the conductance terms calculated separately for each surface-water feature included in the model. For cells with both streams and water bodies, both feature types contribute to the total conductance. It is important to avoid assigning multiple RIV conditions to a single cell in a MODFLOW-2000/SEAWAT-2000 model so as to preclude spurious routing of water between them due to unequal stages.

If a water-table cell encloses only one surface-water feature, then the stage assigned the cell is the stage assigned the feature. Owing to the approximately 1-mi² size of the nearfield cells, however, it is very common for more than one surface-water feature to be enclosed. For this reason, it is necessary to derive a representative stage for the entire cell from some or all of the stages of the surface-water elements within it. For cells with only stream arcs or with both stream arcs and water-body polygons, the stage is calculated as the conductance-weighted average of individual stages assigned to the highest order streams in the cell (see appendix 2 for more detail). Because the streams of highest order are generally the biggest streams among the the cells, this method tends to associate the stage with the major stream rather than with its tributaries or adjacent water bodies. For water-table cells enclosing only water bodies, the stage is the conductance-weighted average of their stages.

The elevations of the stages assigned the RIV cells determine the layers to which they belong. If the stage of a particular inland surface-water feature falls below the bottom of layer 1 at a row/column location, then the boundary condition is assigned to the first layer whose bottom at that location is below the stage. In all, 89 percent of the RIV cells belong to layer 1; the rest are distributed mostly among bedrock layers in areas where streams cut through the unconsolidated material. Where the RIV cell is assigned below the top layer, then all overlying layers are inactive.

In the LMB model, the stages assigned the inland nearfield surface-water features are fixed through time. Stream stages, in fact, do change in time, but it is assumed that the water-table solution at the regional scale is not sensitive to this variation. The effect of many other assumptions and simplifications adopted in building the surface-water network are discussed at the end of appendix 2.

To depict more detail in the distribution of streams and water bodies included in the model, we mapped the entire surface-water network in one part of western Michigan (fig. 29A) and superimposed on top of it colored squares representing individual RIV cells, with a code that distinguishes the type of feature and the order of streams enclosed (fig. 29B). This sample area shows the density of the routed surface-water network and the relative frequency of streams, lakes/ponds, and wetlands (swamp/marshes). It demonstrates that all large features—for example, high-order streams—are included, and it indicates the extent to which small features—for example, first-order streams—are included or excluded. It also shows that cells typically contain more than one stream or water body.

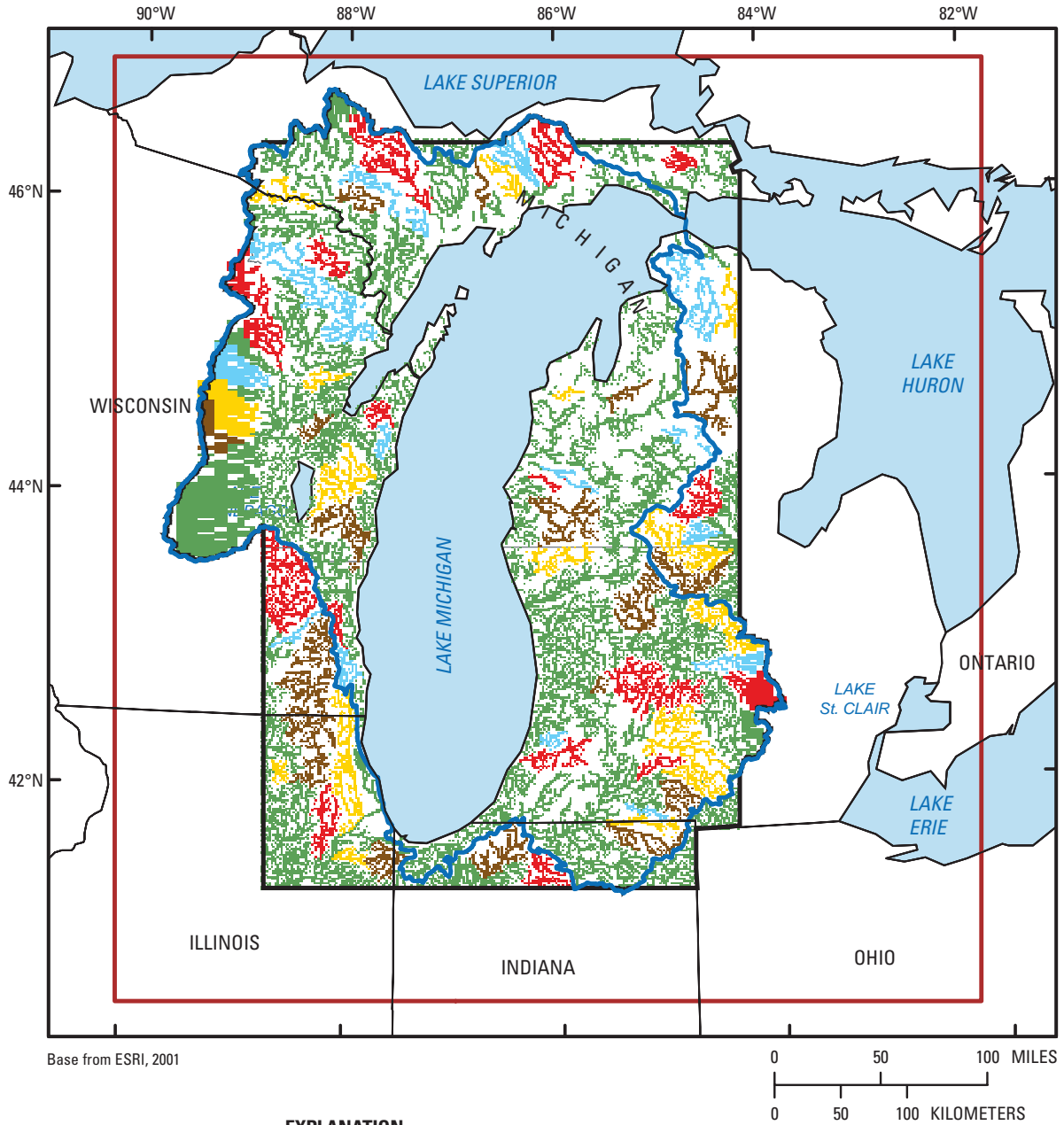
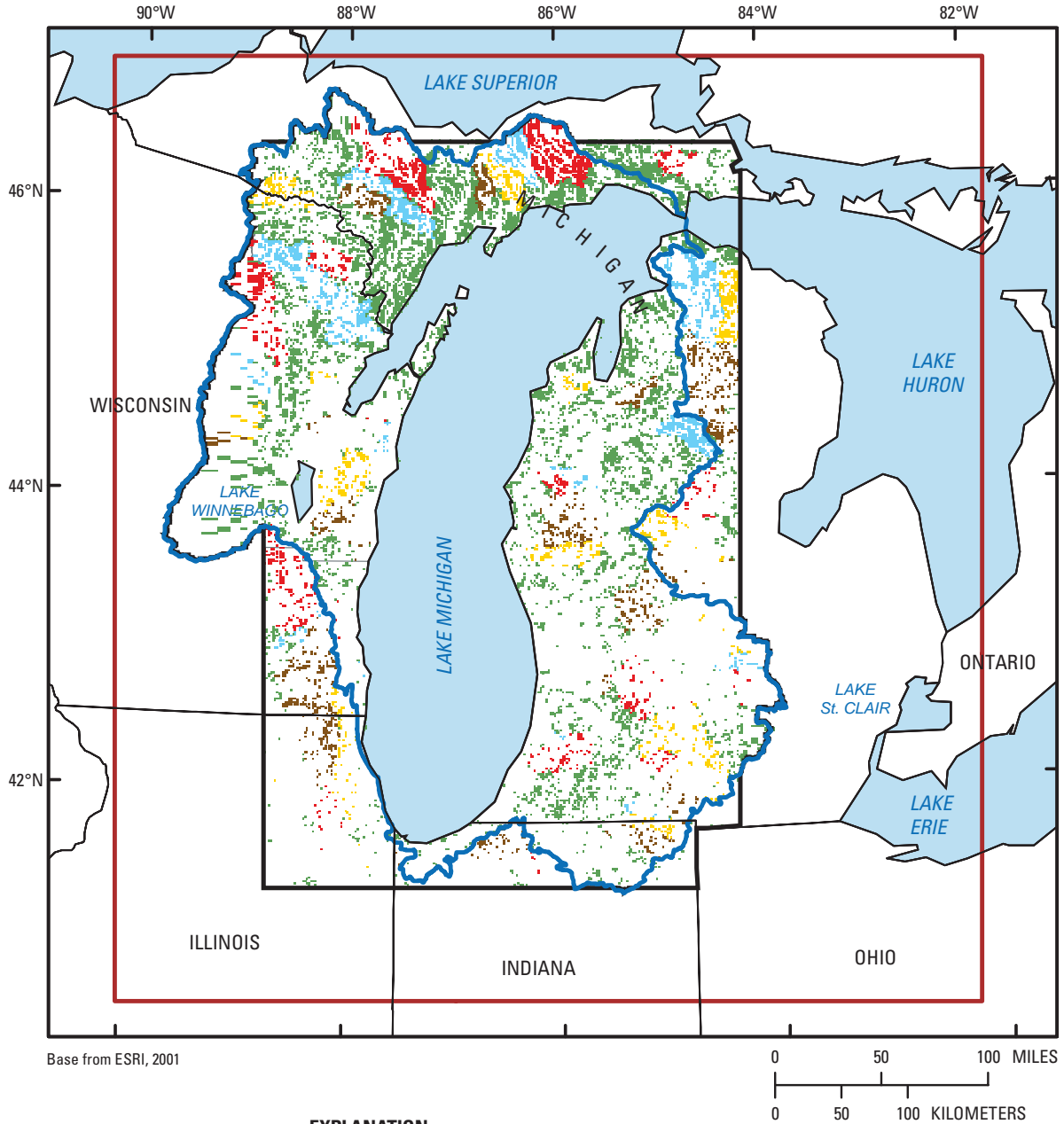


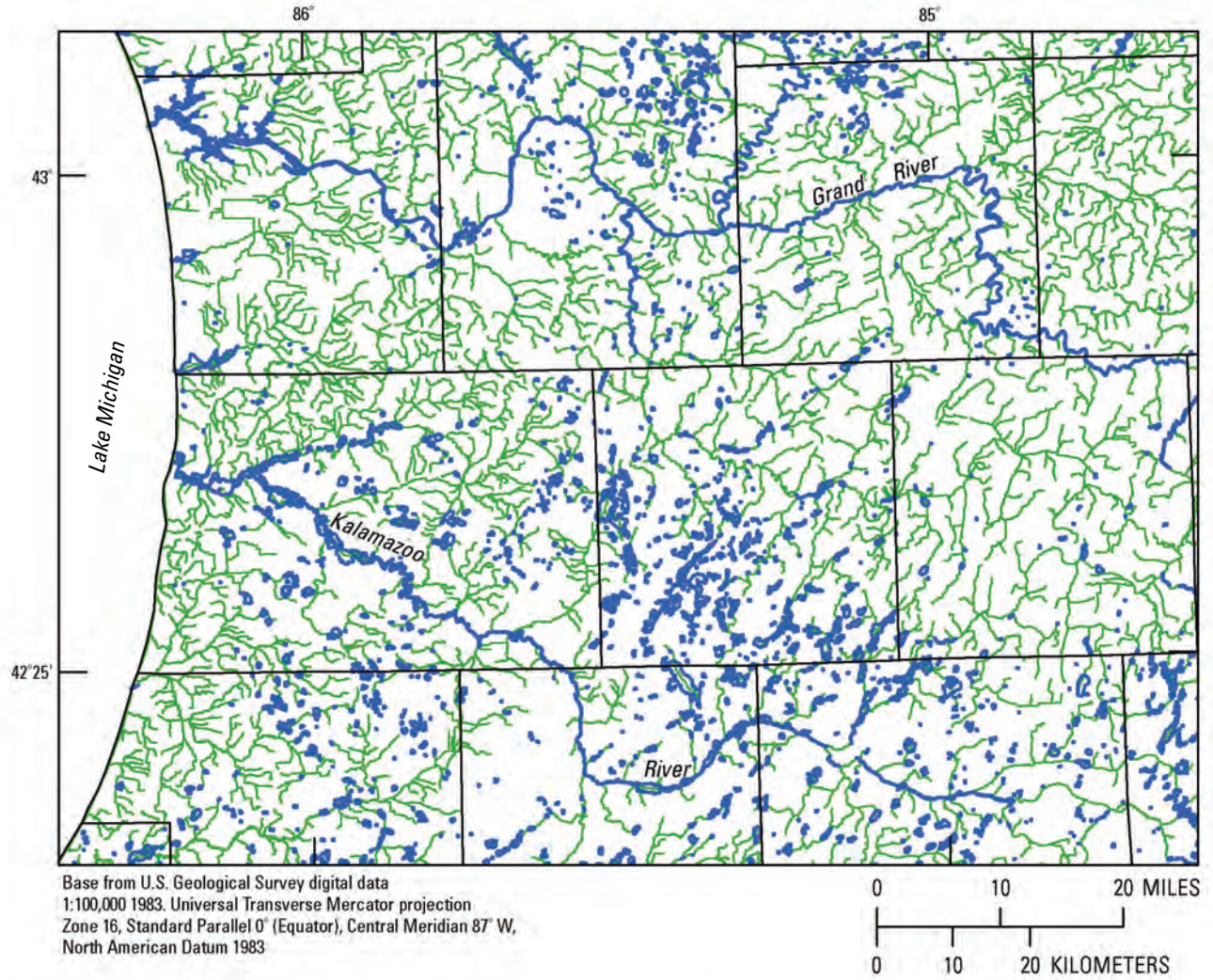
Figure 28A. Streams represented in model.



EXPLANATION

- Water bodies (lakes and wetlands) represented in model, located in basins upstream from gages used for calibration flux targets (multiple colors used only to distinguish between neighboring gaged basins)
- Water bodies (lakes and wetlands) represented in model but not associated with flux targets
- Model or hydrologic boundary**
- Model domain
- Lake Michigan Basin
- Model nearfield

Figure 28B. Water bodies represented in model.



EXPLANATION

- Streams
- Lake or pond

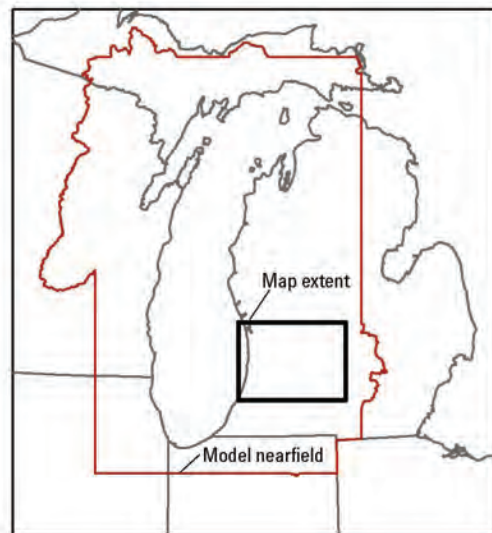
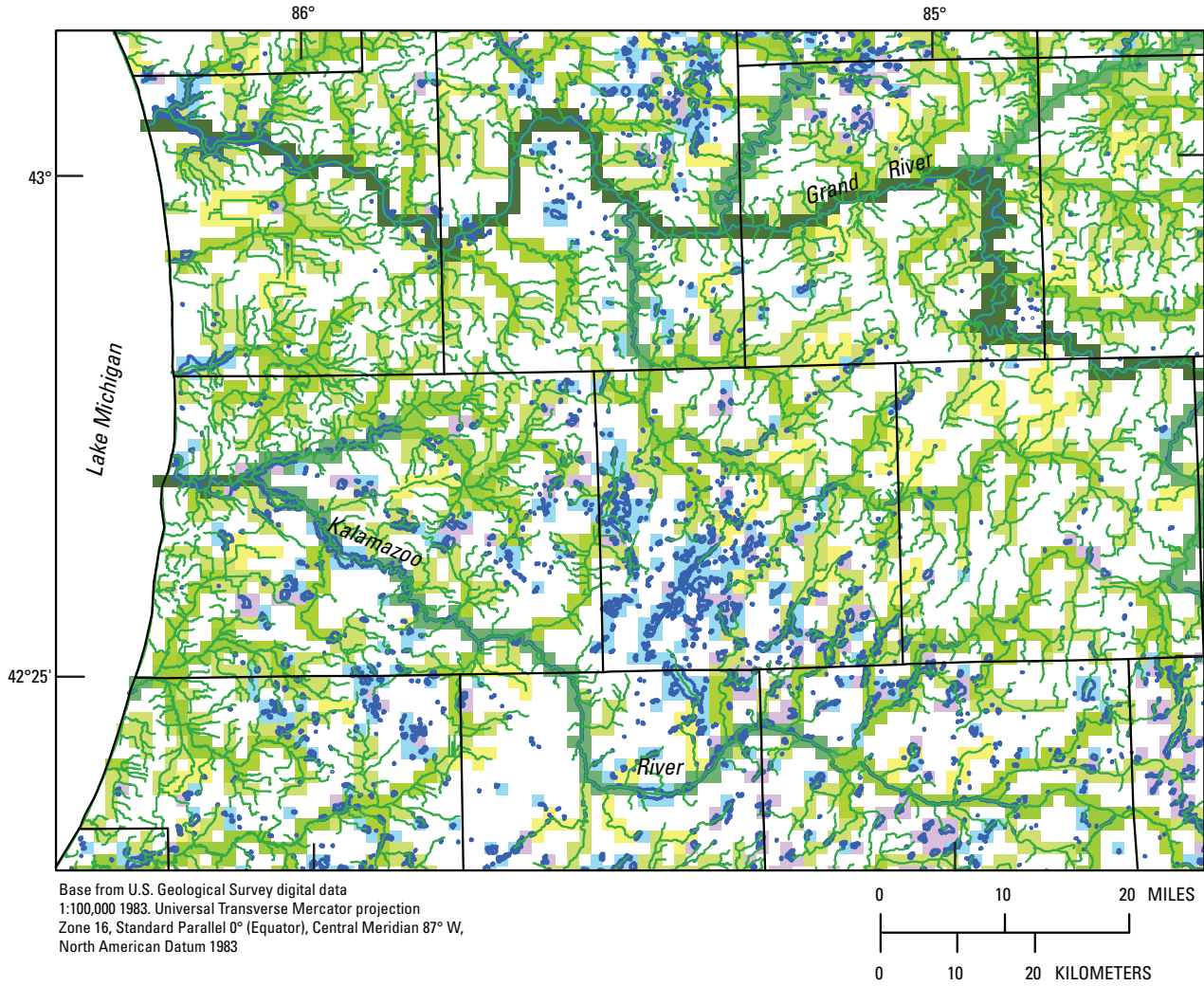


Figure 29A. Example surface-water network without model RIV cells.



- EXPLANATION**
- Stream
 - Lake or pond
- Surface-water type**
- First-order stream
 - Second-order stream
 - Third-order stream
 - Fourth-order stream
 - Fifth-order stream
 - Sixth-order stream
 - Lake or pond
 - Swamp or marsh

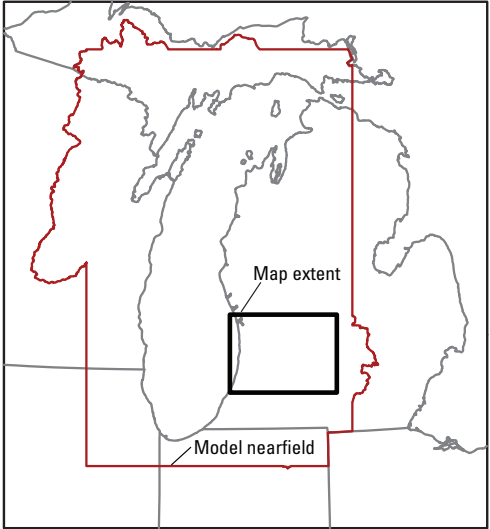


Figure 29B. Example surface-water network with model RIV cells.

4.5.2 Lake Michigan and Lake Winnebago

Lake Michigan and Lake Winnebago are represented as head-dependent boundaries by using GHB cells, similar to the way that Lake Superior, Lake Huron, Lake St. Clair, and Lake Erie are represented in the model farfield (fig. 27). The stage of Lake Winnebago, the largest inland lake in the model domain, is set to 747.0 ft on the basis of information in the surface-water datasets discussed in appendix 2; the conductance of the all its cells is equal to $5.0 \text{ E}7$, based on a surface area of 5,000 by 5,000 ft, a bed thickness of 1 ft, and a bed K_v assumed equal to 2 ft/d. The Lake Michigan stage is set to 577.5 ft, its low-water datum (identical to the stage for Lake Huron because the two lakes are hydraulically connected). As in the case of the farfield Great Lakes, the effect of substituting a time-dependent Lake Michigan stage for a fixed stage was assessed through model sensitivity (see section 7.2). The conductance of cells representing Lake Michigan is set to $2.5 \text{ E}7$, on the basis of a surface area of 5,000 by 5,000 ft, a bed thickness of 1 ft, and a bed K_v assumed equal to 1 ft/d. However, the connection of Lake Michigan to the groundwater system is represented much differently than is the connection in the case of the farfield Great Lakes. The latter function effectively as constant-head boundaries because the GHB conductance is so high. Although the conductance assigned Lake Michigan is also high and, consequently, presents very little resistance to flow across the GHB boundary, much more resistance is imposed by the full bed thickness attributed to the lake. That full thickness corresponds not to the 1-ft thickness of the GHB conductance term but instead to the mapped lakebed deposits of glacial and Holocene origin, discussed above in the “Model Layering” subsection. The greater the thickness and the lower the vertical hydraulic conductivity assigned to layers 1, 2, and 3 under Lake Michigan, the greater is the resistance to vertical flow discharging to the lake. The ease of lake discharge is also affected by the horizontal hydraulic conductivity of the unconsolidated and bedrock deposits underlying and adjacent to the lake. The hydraulic conductivities assigned to the QRNR and bedrock units in connection with the lake are discussed later in this section.

4.5.3 Summary of Farfield and Nearfield Surface-Water Inputs

Streams, water bodies, and the Great Lakes are essentially represented in the model farfield as constant heads that effectively define the water-table surface. In the model nearfield, the surface-water network is represented as head-dependent boundaries by using conductance terms that are related to stream order or to the thickness of underlying materials (as in the case of Lake Michigan). Lakes and wetlands in the model nearfield are effectively represented as drains that allow groundwater discharge but do not permit infiltration of surface water to the aquifer system. Table 6 lists the number of cells belonging to each boundary-condition type,

their distribution in the nearfield/farfield, their distribution in QRNR/bedrock layers, and the number within the model domain.

4.6 Recharge

The LMB model represents the movement of water from the land surface into the groundwater-flow system in two ways. In the model *farfield*, the addition of water is controlled by the gradient between constant head cells at the top of the groundwater flow system and underlying cells deeper in the system. In the model *nearfield*, water is added to the water-table cells at the top of the saturated groundwater flow system at a specified rate in the form of recharge.

Recharge in the model nearfield varies spatially and through time. The rates reflect the evolution of land use, trends in temperature and precipitation, and factors involving hydrologic soil type, land surface slope, and soil-water capacity. Recharge was computed for each model cell and each stress period by using the Thornthwaite-Mather soil-water balance model (SWB) (Westenbroek and others, 2010). As stated by Westenbroek and others, the SWB model calculates spatial and temporal variations in recharge by use of commonly available GIS data layers in combination with tabular climatological data. The code is based on the modified Thornthwaite-Mather soil-water balance approach; components of the soil-water balance are calculated on a daily time step. Recharge calculations are made on a rectangular grid suitable for application to a regional groundwater-flow model.

The SWB model calculates *daily* recharge for each nearfield inland grid cell according to the following equation:

$$\text{recharge} = (\text{precip} + \text{snowmelt}) - (\text{interception} + \text{outflow} + \text{ET}) - \Delta \text{soil moisture}$$

where

<i>precip</i>	is daily precipitation;
<i>snowmelt</i>	is water made available on days when temperatures are high enough to melt accumulated snowpack;
<i>interception</i>	is the amount of daily rainfall trapped by vegetation as a function of land-use type and season;
<i>outflow</i>	is daily surface runoff from a cell according to a curve number rainfall-runoff relation (U.S. Department of Agriculture, 1986) related to soil type, land use, surface condition, and antecedent runoff condition;
<i>ET</i>	is daily evapotranspiration from the root zone of the soil as a function of temperature and vegetation; and
$\Delta \text{soil moisture}$	is the change in the amount of water stored in the root zone calculated according to the method of Thornthwaite (Thornthwaite and Mather, 1955).

Table 6. Surface-water boundary conditions.

River (RIV) cells	Number
Nearfield number	38,237
Farfield number	0
Stream ¹	26,184
Water body ²	12,053
Quaternary	34,218
Bedrock	4,019
Inside Lake Michigan Basin	27,613
Outside Lake Michigan Basin	10,624
General Head Boundary (GHB) cells	Number
Nearfield number	25,290
Farfield number	2,771
Quaternary	27,688
Bedrock	373
Inside Lake Michigan Basin (<i>Lake Michigan, Lake Winnebago</i>)	25,290
Outside Lake Michigan Basin (<i>Lake Superior, Lake Huron, Lake St. Clair, Lake Erie</i>)	2,771
Constant Head (CHD) cells	Number
Nearfield number	0
Farfield number	8,873
Quaternary	7,588
Bedrock	1,285
Inside Lake Michigan Basin	0
Outside Lake Michigan Basin	8,873

¹ RIV cells with stage greater than bed elevation, thereby allowing for outflow from stream to groundwater.

² RIV cells with stage equal to bed elevation, thereby precluding outflow from water body to groundwater.

In using this method, one assumes all the water that percolates on a given day below the rooting depth of vegetation is immediately transferred to the water table as recharge. The method does not account for lags due to movement and storage within the unsaturated zone below the soil root zone and above the water table. This limitation has little importance when daily values are integrated to compute average recharge rates at a cell location over extended periods (for example, for a 10-year model stress period).

The model modules are designed to take advantage of widely available GIS datasets and file structures. Refinements to the SWB recharge model implemented in this study include an algorithm for limiting winter recharge when soils are frozen, based on cumulative days of temperatures below freezing. One option available in the SWB recharge model—the routing of overland flow to allow for focused recharge—is not activated in the LMB application because of the coarse scale

of the model grid. The SWB model is calibrated by adjusting model inputs such as rooting depth of vegetation to produce an improved match between year 2000 recharge and base-flow estimates at the gaged outlets of the watersheds (Westenbroek and others, 2010). More information on the compilation of recharge calibration targets is given in section 5 (and appendix 7) of this report.

For the application of the SWB method to the LMB domain, spatially interpolated arrays of daily minimum temperature, maximum temperature, and precipitation were derived from time series recorded at more than 800 meteorological stations providing data for part or all of the 101-year period from 1900 to 2000. The daily results of the recharge generator were averaged to yield a yearly value for each nearfield model cell. The yearly values were, in turn, averaged over stress-period intervals to produce cell-by-cell arrays for the 10 stress periods extending between 1900 and 2000. The

predevelopment and 1864–1900 stress periods were assigned the same rates as the 1901–1920 stress period, whereas the 2001–5 stress period was assigned the same rate as the 1991–2000 stress period. Because the SWB model calculates recharge partly as a function of land use, and given that only two land-use maps were available for the LMB domain—one for about 1910 and one for 1990, land use was assumed to evolve from the 1910 to the 1990 condition in a linear fashion with respect to time. In effect, recharge arrays were calculated by stress period for both conditions and weighted by time elapsed until or after 1950. In this way, recharge in earlier stress periods more strongly reflect the early-20th-century land use, whereas recharge for later stress periods reflect the late-20th-century land use, and recharge for 1950 is an average of the two.

The results of the SWB recharge model for the LMB nearfield show both temporal and spatial trends. If the recharge rates at all nearfield cells are averaged on a yearly basis and grouped by stress period, it is possible among the upward and downward trends to identify an increase in recharge around 1970 (fig. 30). This increase is consistent with findings of other investigators working at the scale of the Great Lakes Basin (Hodgkins and others, 2007).

The SWB model simulates a range of annual recharge rates within the model nearfield between 3 and 11 in. However, average recharge rates for the 12 stress periods specified in the LMB model range only from 6.80 to 8.84 in. The nearfield-wide average for the stress periods before 1970 is close to 7 in/yr; the average for the stress periods after 1970 is almost 8 in/yr.

In all the nearfield, recharge was computed by the SWB method on a cell-by-cell basis for 10 time intervals. Some intervals correspond to multiple stress periods, but most coincide with a single stress period (fig. 30). The average for any given period hides a fair degree of cell-by-cell spatial variability incorporated into the LMB model. Recharge maps for three sample time intervals—1901 to 1920 (fig. 31A), 1971 to 1975 (fig. 31B), and 1991 to 2005 (fig. 31C)—show an overall spatial range of 0 to 16 in/yr and illustrate areas of consistently higher or lower than average recharge. Higher recharge rates are computed for a north-to-south belt near the eastern shoreline of Lake Michigan that extends from the northern Lower Peninsula of Michigan into Indiana. Recharge in this area is enhanced by moisture from Lake Michigan carried by the prevailing winds from west to east, sometimes also by areas of coarse soil underlain predominantly by glacial outwash. Lower recharge rates are computed for a belt along the western side of Lake Michigan in Wisconsin and Illinois, which is associated with generally fine soils underlain by clayey tills. The maps also show a few zones of very low recharge (for example, a north-to-south span in the Upper Peninsula of Michigan north of Green Bay and an area in southern Michigan). The shallow unconsolidated part of the flow system is very thin in these areas and, on the assumption that the near-surface bedrock severely limits infiltration, the recharge rates are assumed to be small and were reduced to 0.5 in/yr. Recharge also was reduced to 0.5 in/yr in the urbanized vicinity of Chicago. These combined changes caused the global average nearfield recharge rate to decrease by 3 percent relative to the original average rate generated by the SWB recharge model.

The recharge rates computed by the SWB model adjusted through model calibration are described in section 5.

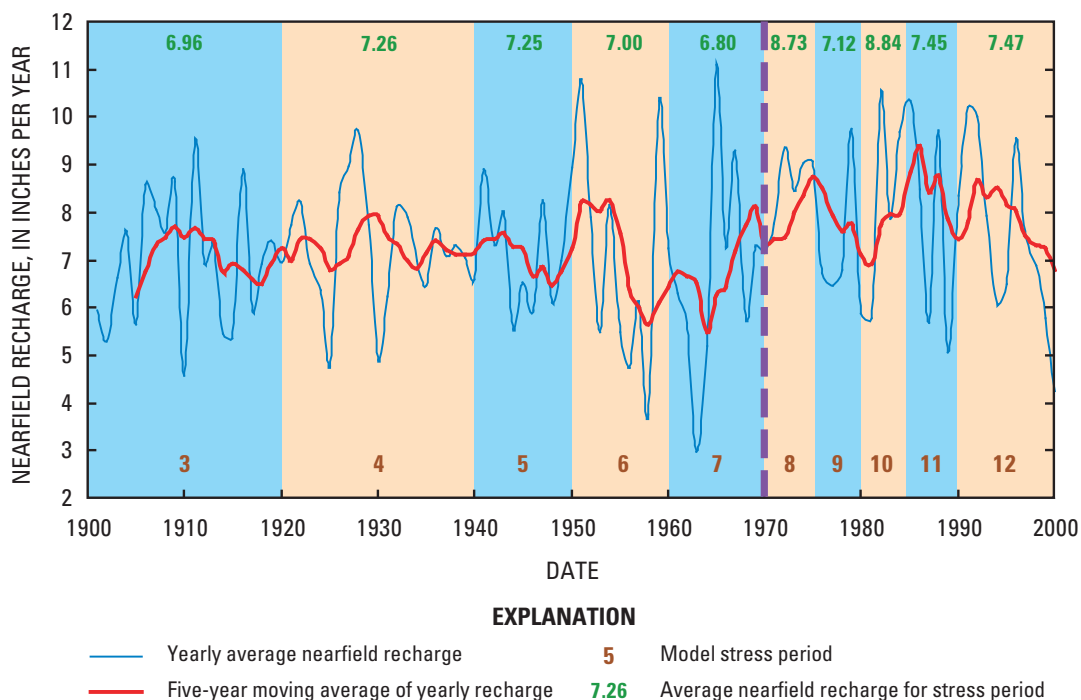


Figure 30. Recharge trends for the inland nearfield area of the model.

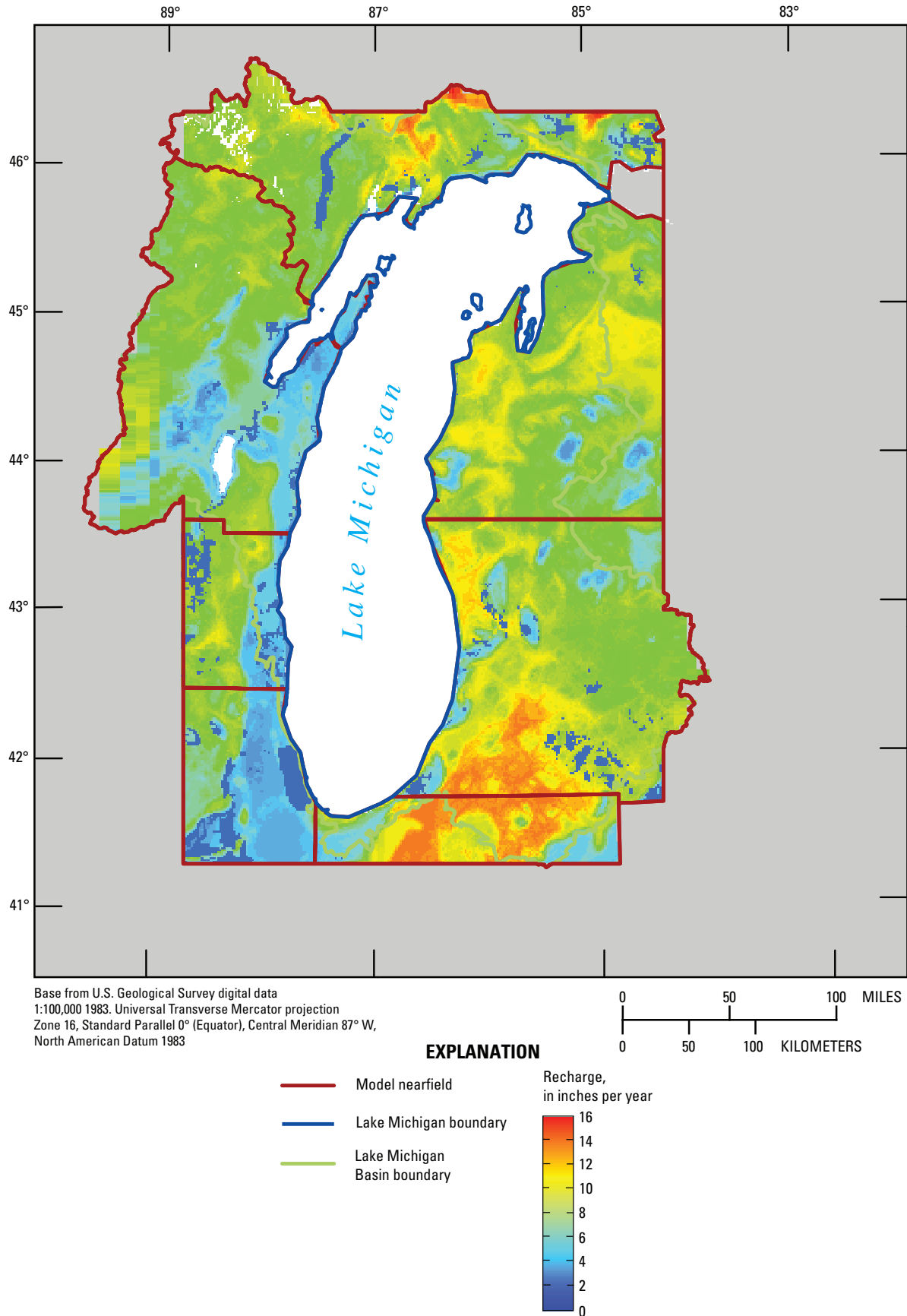


Figure 31A. Recharge distribution: 1901–20.

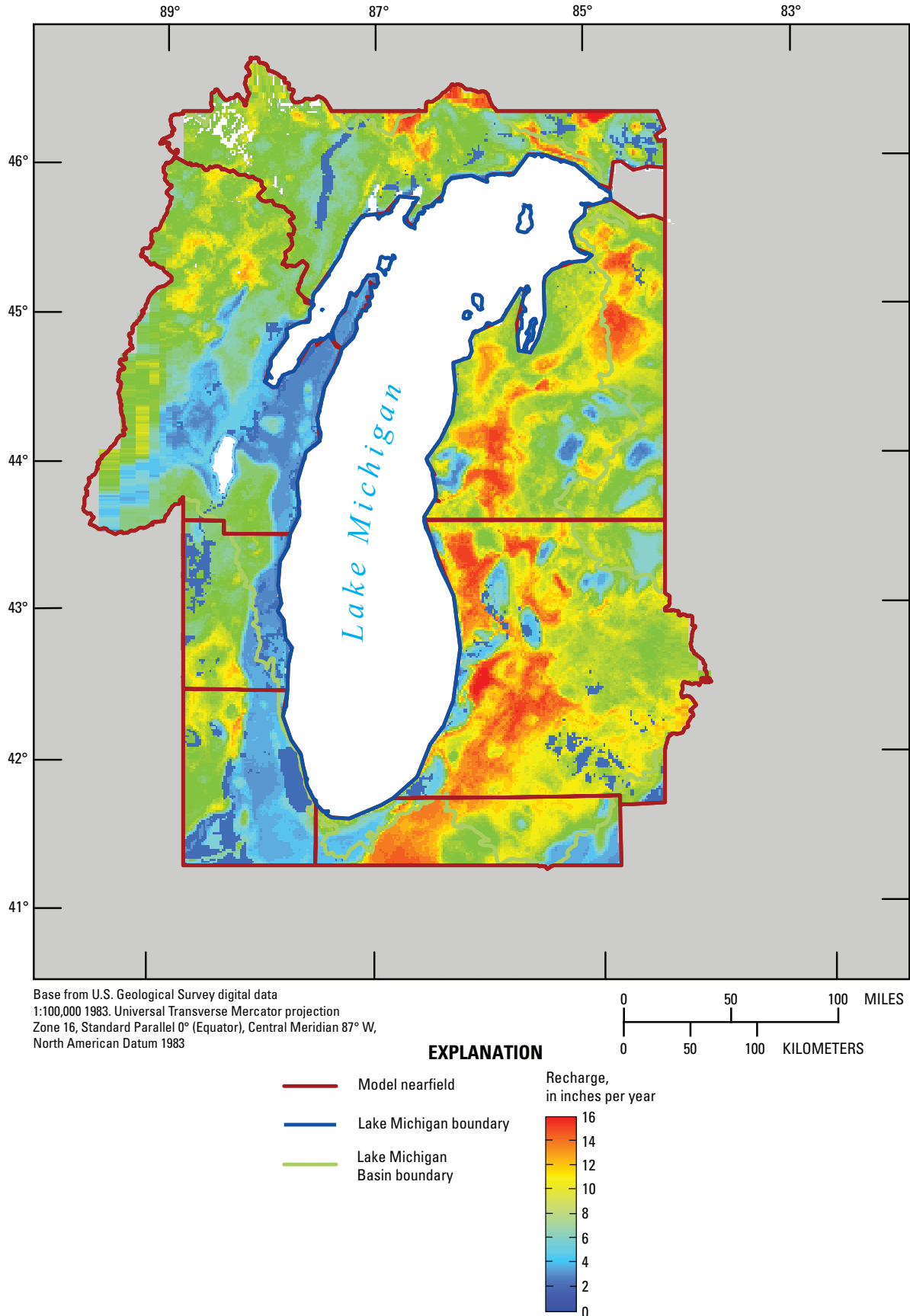


Figure 31B. Recharge distribution: 1971–75.

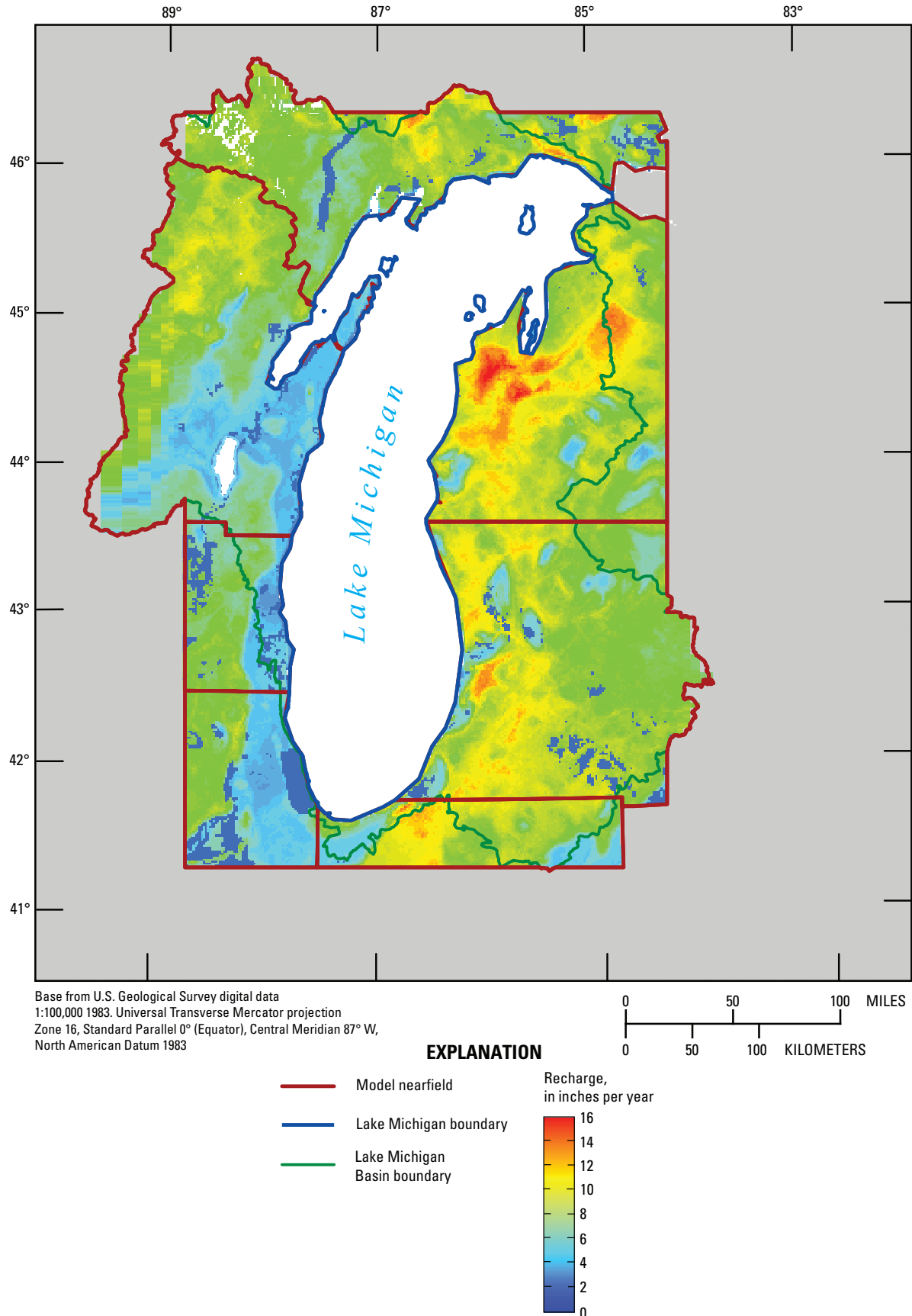


Figure 31C. Recharge distribution: 1991–2005.

4.7 Well Withdrawals

Three types of stresses in the LMB model change through time: boundary fluxes in the southwestern corner of the grid, recharge, and well withdrawals. Boundary fluxes function as sources or sinks of water depending on location and depth. Recharge is a source of water that is spatially distributed and applied to the water table. Well withdrawals are point sinks that can draw from any layer or combination of layers in the model and from any model cell as long as it is not assigned a constant head and as long as it is not pinched (that is, the unit it represents has some thickness).

A database of historical pumping constructed for the LMB model is described in Buchwald and others (2010). It documents the range of methods that support the tabulations of pumping by individual wells for all the nearfield and part of the farfield from 1864 through 2005. Four water-use categories are considered in the database: public supply, industrial/commercial, irrigation/golf course, and aquaculture. The well withdrawals are located by subregion and by depth according to what aquifer system or systems are pumped.

4.7.1 Database Limitations

The compilation of historical pumping rates for the LMB model has several limitations. Domestic pumping is not included because, although the number of domestic wells is large compared to those in other water-use categories, households generally use relatively small amounts of groundwater and pump it from shallow aquifers; the drawdown cone around each well is commonly buffered by nearby surface water unless recharge is very small (Bradbury and Rayne, 2009). In addition, most of the pumped water is returned to groundwater through onsite septic systems. In Wisconsin, it is estimated that domestic wells account for 23 percent of total groundwater withdrawals (Lawrence and Ellefson, 1982), but less than half the amount is thought to be consumed (Solley and others, 1998); estimates of return rate have been as high as 80 to 90 percent (Topper, 2007; Cherkauer, 2007). Together these estimates of extraction and return suggest that omission of domestic wells from the database underestimates total withdrawals by 5 percent.¹²

Pumping from the other water-use categories is typically almost all consumed rather than returned to the groundwater system. Even for irrigation, between 70 and 100 percent of the pumped water is estimated to be consumed by evapotranspiration (Shaffer and Runkle, 2007), so gross rates of withdrawals for irrigation can be fairly equated in most cases with net rates. In this study, the term “high-capacity wells” refers to those pumped at rates greater than 70 gal/min—equal to 0.1 Mgal/d—whereas low-capacity wells are those pumped at rates less than 70 gal/min. Although there are more low-capacity than high-capacity wells in the LMB model, high-capacity wells account for most of the total discharge. For 2001 to 2005, the model database contains 6,764 low-capacity wells and 2,381 high-capacity wells, but the combined discharge from the former is only 200.50 Mgal/d, whereas the discharge from the latter is 892.86 Mgal/d.

A second limitation of the LMB water-use database is that coverage of the model farfield is incomplete. Pumping information in these areas was only collected for high-capacity wells that pump from deep, confined aquifers that typically give rise to regional cones of depression. Pumping from the shallow flow system in the model farfield was assumed to have a negligible effect on flow between the nearfield and farfield. Given the hydrogeology of the model domain and the patterns of water use, it is reasonable to conclude that deep, confined pumping since 1864 is much more likely to have occurred west of Lake Michigan in Wisconsin and Illinois than east of the lake in Michigan and Indiana. To test this assumption, a survey of both shallow and deep pumping wells was done for the year 2004 in parts of Michigan and Indiana within the model farfield. In Michigan, 745 wells pumped a total of about 48 Mgal/d, and only 7.5 percent discharged from deep wells. In Indiana, 954 wells pumped about 42 Mgal/d, and 10 percent discharged from deep wells. On the basis of these findings, the error in omitting pumping from the deep flow system in the model farfield in Michigan and Indiana is acceptable. However, in order to minimize any error from omitting farfield pumping east of Lake Michigan, historical pumping was tabulated for the farfield area of all Michigan and Indiana counties that straddle the farfield/nearfield boundary, as well as for the Monroe County industrial pumping center near Lake Erie in southwestern Michigan.¹³ It should be noted that farfield pumping in the entire model domain west of Lake Michigan (that is, in Illinois and Wisconsin) was included by using the same database coverage applied to the nearfield.

¹² The most likely areas where omission of domestic pumping can lead to simulation errors are around high-density residential communities served by both domestic wells and by sewers or holding tanks. There are few examples in the LMB model domain. One is the city of Mequon north of Milwaukee, which before 2000 is estimated to have pumped 3 Mgal/d from domestic wells, but this water was not returned to the subsurface (Feinstein, Eaton, and others, 2005). Since 2000, some of that pumping has been replaced with Lake Michigan supply.

¹³ No water-use data at all were compiled for Ohio. The state is outside the Lake Michigan Basin, and pumping is limited and mostly from shallow aquifers; accordingly, it is expected that the drawdown cones would be restricted in size and have little influence on the exchange of water between the model farfield and nearfield.

As expected, the entries to the water-use database become gradually more complete with time after 1864. For example, data sources for public-supply withdrawals in Michigan are sparse before the late 1970s, whereas the detailed Illinois surveys of public-supply, industrial-commercial, and irrigation discharge only begin in the early 1960s. The Illinois pumping before then was approximated by assigning all estimated discharge to only seven pumping centers. Some of the inevitable gaps in spatial and withdrawal information were handled by special estimation methods¹⁴ so that, on balance, the inputs to the model are believed to accurately reflect overall historical trends with respect to amounts withdrawn from each aquifer system (Buchwald and others, 2010).

4.7.2 Transfer of Database to Model

Not all the entries in the water-use database have been transferred to the model. Some farfield wells in inactive and constant-head cells are excluded because they would have no effect on the model simulation. In addition a small number of farfield and nearfield wells that, according to the model stratigraphy, are in pinched units also are omitted. The elimination of all these wells reduces the pumping tabulated in the original database by about 13 percent for the last stress period, a decrease that is representative of the reductions for other stress periods and which mostly affects withdrawal rates in the farfield. The total number of individual pumping wells active in at least one model stress period is 13,312.

Pumping for each stress period is input to the LMB model by means of two SEAWAT-2000 packages. For wells that penetrate only one layer, the WEL package is employed. For wells that penetrate multiple model layers, the Multi-Node Well (MNW) package is used to divide the total withdrawal among layers on the basis of transmissivity and the hydraulic gradient between the well and the aquifer (Halford and Hanson, 2002). Two additional inputs are required by the MNW package for each well: the borehole radius and the “skin” resistance, the latter referring to the disturbed interval around the well. They are set, respectively, to 0.5 ft and to 5 ft²/d for all multilayer wells to promote numerical stability. The MNW package allows for circulation through the pumped borehole (water can exit some layers penetrated by the well while entering others, but the prescribed sink discharge is maintained). Whenever input of horizontal hydraulic conductivity to the model is modified, the MNW package also automatically resets the exchange between the well and the penetrated model layers as a function of the resulting aquifer transmissivity. This recalculation of pumping rates internal to the MNW package is a significant advantage because it eliminates the need for any manual updating of rates during the automated calibration process described in section 5.

¹⁴ For example, in Wisconsin, pumping from industrial wells was estimated as a function of one or more of the following: pump capacity, approved normal daily pumpage, and an industry-specific withdrawal coefficient. Details on all estimation methods are given in Buchwald and others (2010).

In addition to the 1,306 pumping wells represented in the model, 4 injection wells are represented near Kalamazoo in the southern Lower Peninsula of Michigan. These wells are used in the model to account for the return of cooling water from pharmaceutical plants, water which is pumped from and then infiltrated back the QRNR aquifer system through constructed wetlands, ponds, or lakes (Luukkonen and others, 2004). The return infiltration began in the 1960s and continued through 2005, varying in quantity from 5.7 to 10.1 Mgal/d.

One other sink is also represented by the WEL input package: the Deep Sewer Tunnel System under Milwaukee, Wis. The 19.4-mi-long tunnel was installed in the early 1990s through the shallow Silurian dolomite in the SLDV aquifer system, some of which is highly fractured. The installation collects combined-sewer overflow during rainstorms and stores it for later treatment. Studies by the Milwaukee Metropolitan Sewage District estimate average groundwater discharge to the Deep Tunnel as 2.8 Mgal/d during dry periods (Dunning and others, 2004; Feinstein and others, 2003). The water is subsequently treated and pumped into Lake Michigan. In the LMB model, the groundwater discharge at the 2.8 Mgal/d rate is withdrawn for the 1991–2000 and 2001–5 stress periods from the Silurian bedrock (layer 11) over 20 cells that coincide with the tunnel geometry. Although Chicago is also underlain by a deep-tunnel system, that tunnel intersects mostly competent dolomite and is thoroughly grouted where rock is fractured (Knoerle, Bender, Stone & Associates, 1977), so little or no groundwater discharges to the tunnel.

4.7.3 Pumping Totals in Model

The 1,306 pumping wells in the model are distributed between the nearfield (77 percent) and the farfield (23 percent). The subregion with the largest number of wells is North-eastern Illinois; the smallest number is in the Upper Peninsula of Michigan (table 7). Over 40 percent of the nearfield wells are public supply; nearly all the remainder is split evenly between the industrial/commercial and irrigation/golf course categories. The QRNR system contains the most nearfield wells, followed by the C-O and SLDV systems.

The number of active wells and their pumping vary greatly by stress period and by aquifer system (table 8). For example, around 1900, the model database contains only 108 active nearfield wells pumping 16 Mgal/d, more than half of which is drawn from the C-O aquifer system. By 2000 there are 7,252 active nearfield wells pumping 841 Mgal/d, more than half of which is drawn from the QRNR aquifer system. The total nearfield pumping increased for each stress period through the early 1980s, when the Chicago diversion of Lake Michigan replaced groundwater extraction and caused a dip in use. The upward trend resumed in the 1990s but reached a plateau in the last stress period (2001–5), due in part to decreased withdrawals in southeastern Wisconsin (fig. 32). The trend of farfield withdrawals entered in the model is consistently upward for the entire simulation period.

Table 7. Number of pumping wells by subregion, water-use category, and aquifer system.

[Wells active for any model stress period are counted in totals]

Nearfield totals	
Total =10,255	
Number by subregion	
1,384	SLP_MI
333	NLP_MI
79	UP_MI
1,808	NE_WI
1,180	SE_WI
1,784	N_IND
3,687	NE_ILL
Number by water-use category	
4,431	Public supply
2,877	Irrigation/golf courses
2,896	Industrial/commercial
51	Aquiculture
Number by aquifer system (assigned to aquifer system of lowest layer penetrated)	
4,971	QRNR
144	PENN
153	MSHL
2,042	SLDV
2,945	C-O
Farfield totals	
Total = 3,051	
Number by subregion	
3,051	Farfield
Number by water-use category	
1,003	Public supply
1,444	Irrigation/golf courses
596	Industrial/commercial
8	Aquiculture
Number by aquifer system (assigned to aquifer system of lowest layer penetrated)	
1,119	QRNR
10	PENN
21	MSHL
231	SLDV
1,670	C-O

Table 8. Pumping by stress period and aquifer system.

[Table includes only pumping from wells; it excludes injection wells and inflow to the Milwaukee Deep Tunnel. Mgal/d, million gallons per day]

Aquifer system	Number of wells	Pumping (Mgal/d)
Predevelopment (stress period 1)		
QRNR nearfield	0	0
PENN nearfield	0	0
MSHL nearfield	0	0
SLDV nearfield	0	0
C-O nearfield	0	0
Total nearfield	0	0
Farfield	0	0
Oct. 1864–Oct. 1900 (stress period 2)		
QRNR nearfield	39	4.77
PENN nearfield	9	.97
MSHL nearfield	4	1.70
SLDV nearfield	0	.00
C-O nearfield	56	8.59
Total nearfield	108	16.04
Farfield	14	1.35
Oct. 1900–Oct. 1920 (stress period 3)		
QRNR nearfield	69	8.98
PENN nearfield	16	4.17
MSHL nearfield	7	2.69
SLDV nearfield	16	.50
C-O nearfield	144	39.88
Total nearfield	252	56.22
Farfield	38	6.17
Oct. 1920–Oct. 1940 (stress period 4)		
QRNR nearfield	135	19.40
PENN nearfield	30	10.05
MSHL nearfield	12	11.64
SLDV nearfield	46	1.99
C-O nearfield	298	71.60
Total nearfield	521	114.68
Farfield	86	12.02

Table 8. Pumping by stress period and aquifer system.—
Continued

[Table includes only pumping from wells; it excludes injection wells and inflow to the Milwaukee Deep Tunnel. Mgal/d, million gallons per day]

Aquifer system	Number of wells	Pumping (Mgal/d)
Oct. 1940–Oct. 1950 (stress period 5)		
QRNR nearfield	335	51.66
PENN nearfield	32	17.31
MSHL nearfield	20	16.43
SLDV nearfield	126	7.83
C-O nearfield	408	101.14
Total nearfield	921	194.37
Farfield	141	29.81
Oct. 1950–Oct. 1960 (stress period 6)		
QRNR nearfield	482	91.07
PENN nearfield	45	23.68
MSHL nearfield	27	26.91
SLDV nearfield	191	12.23
C-O nearfield	487	127.14
Total nearfield	1,232	281.04
Farfield	265	46.25
Oct. 1960–Oct. 1970 (stress period 7)		
QRNR nearfield	999	183.20
PENN nearfield	54	31.74
MSHL nearfield	34	35.28
SLDV nearfield	1,322	60.34
C-O nearfield	1,081	172.27
Total nearfield	3,490	482.82
Farfield	984	122.72
Oct. 1970–Oct. 1975 (stress period 8)		
QRNR nearfield	1,276	228.09
PENN nearfield	83	41.21
MSHL nearfield	46	30.01
SLDV nearfield	1,494	104.83
C-O nearfield	1,159	234.48
Total nearfield	4,058	638.61
Farfield	1,186	176.48

Table 8. Pumping by stress period and aquifer system.—
Continued

[Table includes only pumping from wells; it excludes injection wells and inflow to the Milwaukee Deep Tunnel. Mgal/d, million gallons per day]

Aquifer system	Number of wells	Pumping (Mgal/d)
Oct. 1975–Oct. 1980 (stress period 9)		
QRNR nearfield	1,778	276.55
PENN nearfield	83	41.21
MSHL nearfield	58	31.68
SLDV nearfield	1,695	118.18
C-O nearfield	1,346	266.58
Total nearfield	4,960	734.19
Farfield	1,670	197.09
Oct. 1980–Oct. 1985 (stress period 10)		
QRNR nearfield	2,578	332.38
PENN nearfield	109	39.99
MSHL nearfield	83	32.16
SLDV nearfield	1,499	119.36
C-O nearfield	1,311	272.05
Total nearfield	5,580	795.94
Farfield	1,851	220.00
Oct. 1985–Oct. 1990 (stress period 11)		
QRNR nearfield	2,945	340.95
PENN nearfield	110	40.07
MSHL nearfield	83	31.83
SLDV nearfield	1,635	119.70
C-O nearfield	1,338	223.59
Total nearfield	6,111	756.14
Farfield	2,049	234.37
Oct. 1990–Oct. 2000 (stress period 12)		
QRNR nearfield	3,787	465.87
PENN nearfield	123	38.17
MSHL nearfield	127	45.47
SLDV nearfield	1,705	104.25
C-O nearfield	1,510	187.10
Total nearfield	7,252	840.85
Farfield	2,419	264.48

Table 8. Pumping by stress period and aquifer system.—
Continued

[Table includes only pumping from wells; it excludes injection wells and inflow to the Milwaukee Deep Tunnel. Mgal/d, million gallons per day]

Aquifer system	Number of wells	Pumping (Mgal/d)
Oct. 2000–Oct. 2005 (stress period 13)		
QRNR nearfield	3,704	465.69
PENN nearfield	130	40.58
MSHL nearfield	130	41.37
SLDV nearfield	1,360	91.38
C-O nearfield	1,416	191.78
Total nearfield	6,740	830.79
Farfield	2,407	262.57

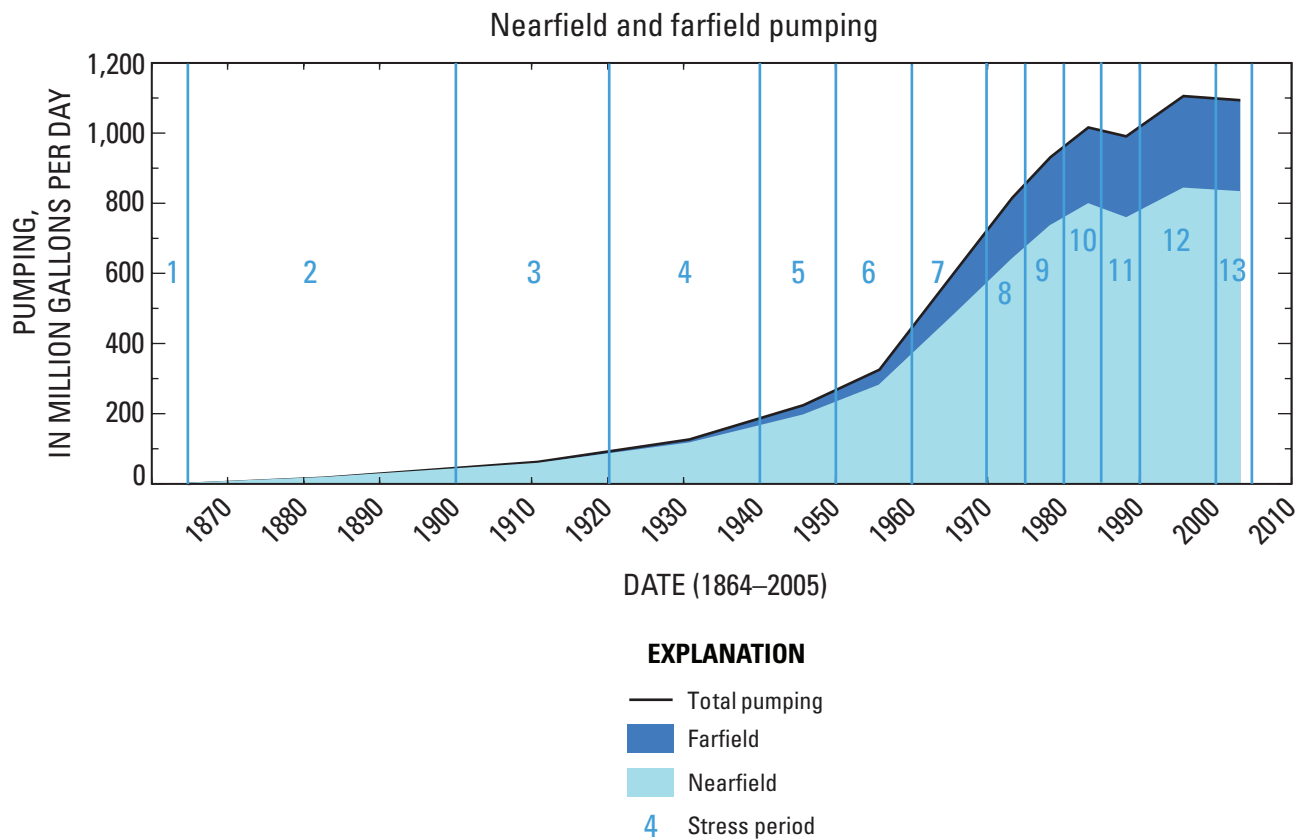


Figure 32. Total nearfield and farfield pumping through time.

The withdrawal trends by model subregion (fig. 33A) show that the share of nearfield pumping attributable to northeastern Illinois dropped sharply around 1980, whereas the share attributable to the southern Lower Peninsula of Michigan increased sharply, especially in the 1980s and 1990s. Other regions show subtle inflections over time. For example, the increased use in northeastern Wisconsin slowed in the 1950s because the city of Green Bay public water supply switched sources from well water to Lake Michigan water. The withdrawal trends by water-use category in the model nearfield (fig. 33B) show the predominance of the public-supply category; pumping for irrigation exceeds industrial withdrawal around 1990. The trends by aquifer system (fig. 33C) show that the effect of the Chicago lake diversion for water supply was to reduce C-O withdrawals relative to QRNR pumping. The contribution of the SLDV system rose abruptly around 1960, whereas the PENN and MSHL share remains small and stable through time.

The spatial distribution of groundwater withdrawals by water-use category is illustrated for the periods 1941 to 1950 (fig. 34A), 1976 to 1980 (fig. 34B), and 2001 to 2005 (fig. 34C). The large circles in the public-supply and industrial/commercial categories coincide with the major pumping centers in the SLP_MI (for example, around Lansing, Kalamazoo, and Grand Rapids), in NE_WI (around the city of Green Bay), in SE_WI (near and west of Milwaukee), and in NE_ILL (communities bordering Chicago).

The distribution of pumping wells indicates a widespread distribution of shallow wells throughout the model domain and concentrated areas of deep wells in areas west of Lake Michigan. In general, the number of wells drawing from both unconfined/semiconfined aquifers and from confined aquifers increases over time, although local trends in the spatial distribution of shallow and deep pumping are highly variable (figs. 35A–C). However, when the number and discharge of shallow versus deep pumping is tabulated not only by aquifer system (table 9A) but also by state (table 9B), it is evident how different is the water use in Michigan and Indiana is from that in Wisconsin and Illinois. The states east of Lake Michigan depend on pumping from the shallow part of the flow system, largely from the QRNR aquifer system. The states west of the lake utilize both shallow and deep wells. The deep pumping centered around Green Bay in NE_WI, around Milwaukee in SE_WI, and outside Chicago in NE_ILL acts to generate large interfering cones of depression that extend far under Lake Michigan. The pumping input to the LMB model allows the propagation of the stresses to be followed through time and across a very large area.

4.8 Hydraulic Conductivity

Every cell in the model is assigned a value for horizontal and for vertical hydraulic conductivity. For the QRNR aquifer system in the upper three upper model layers, values of K_h and K_v vary by cell. In contrast, for bedrock aquifer systems in

layers 4–20, the K_h and K_v vary by zones, with blocks of cells sharing a common value. The methods for selecting K values also differ for the QRNR and bedrock aquifer systems. In addition, different methods are used to estimate the K of inland QRNR deposits and QRNR deposits under Lake Michigan and the farfield Great Lakes.

4.8.1 QRNR Deposits Below Inland Areas

The hydraulic conductivity assigned to QRNR deposits in inland areas is based on the type of glacial material and the granular texture of the material—its “coarse fraction.” The coarse fraction is defined as the proportion of a depth interval for which the driller descriptions in well logs gives precedence to sand and gravel (or related terms such as “cobbles”) over silt and clay (or related terms such as “hardpan”).

The QRNR deposits in the LMB model are divided into six categories: clayey till, loamy till, sandy till, fine stratified deposits (often derived from lake sediments), medium and coarse stratified deposits (associated with outwash sediments), and organic deposits. The distribution of glacial categories is based on surficial mapping by Fullerton and others (2003)¹⁵ and supplemented by unpublished mapping in support the LMB model in 2006 by the Wisconsin Geological and Natural History Survey and David Mickelson, emeritus professor of glacial geology at the University of Wisconsin-Madison.¹⁶ The distribution of glacial categories in the top layer (extending to a maximum depth of 100 ft from land surface) is complex (fig. 36A) and reflects the movements of different lobes of the Laurentian ice sheet (see appendix 1, section 1). The glacial categories of the second layer (from 100 to 300 ft below land surface) and third layer (more than 300 ft below land surface) reflect bedrock valleys in Wisconsin and are often filled with fine-grained deposits (figs. 36B and C). Outside of Wisconsin, the type of glacial material at depths below 100 ft has not been mapped at the LMB model regional scale.

¹⁵ The surficial units present in the LMB model domain in the map prepared by Fullerton and others, 2003, were assigned to model glacial categories according to the following scheme approved by Professor Mickelson:

Clayey till = 3 units (ta, tc, td); Loamy till = 5 units (tb, tj, tk, tl, tm);
Sandy till = 0 units (none present);
Fine stratified = 3 units (EL, lc, la); Medium stratified = 7 units (al, ag, ed, es, gs, ca, Lu);
Coarse stratified = 7 units (gg, gl, lk, ls, kg, kt, ci); Organic = 7 units (ha, hb, hc, hd, he, hp, hs).

¹⁶ The supplemental mapping satisfies two objectives: (1) to extend the mapping of glacial categories to layers 2 and 3 in Wisconsin and (2) to confirm across the model domain that the surficial glacial categories corresponding to the surficial units mapped by Fullerton are characteristic of the full 100-ft thickness of layer 1, and, if not, to assign the predominant categories that apply for the layer 1 thickness. For example, the remapping of layer 1 accounts for the substitution of sandy till for other surficial deposits in parts of northern Wisconsin and the substitution of clayey till for surficial fine-stratified deposits near Saginaw Bay area in eastern Michigan.

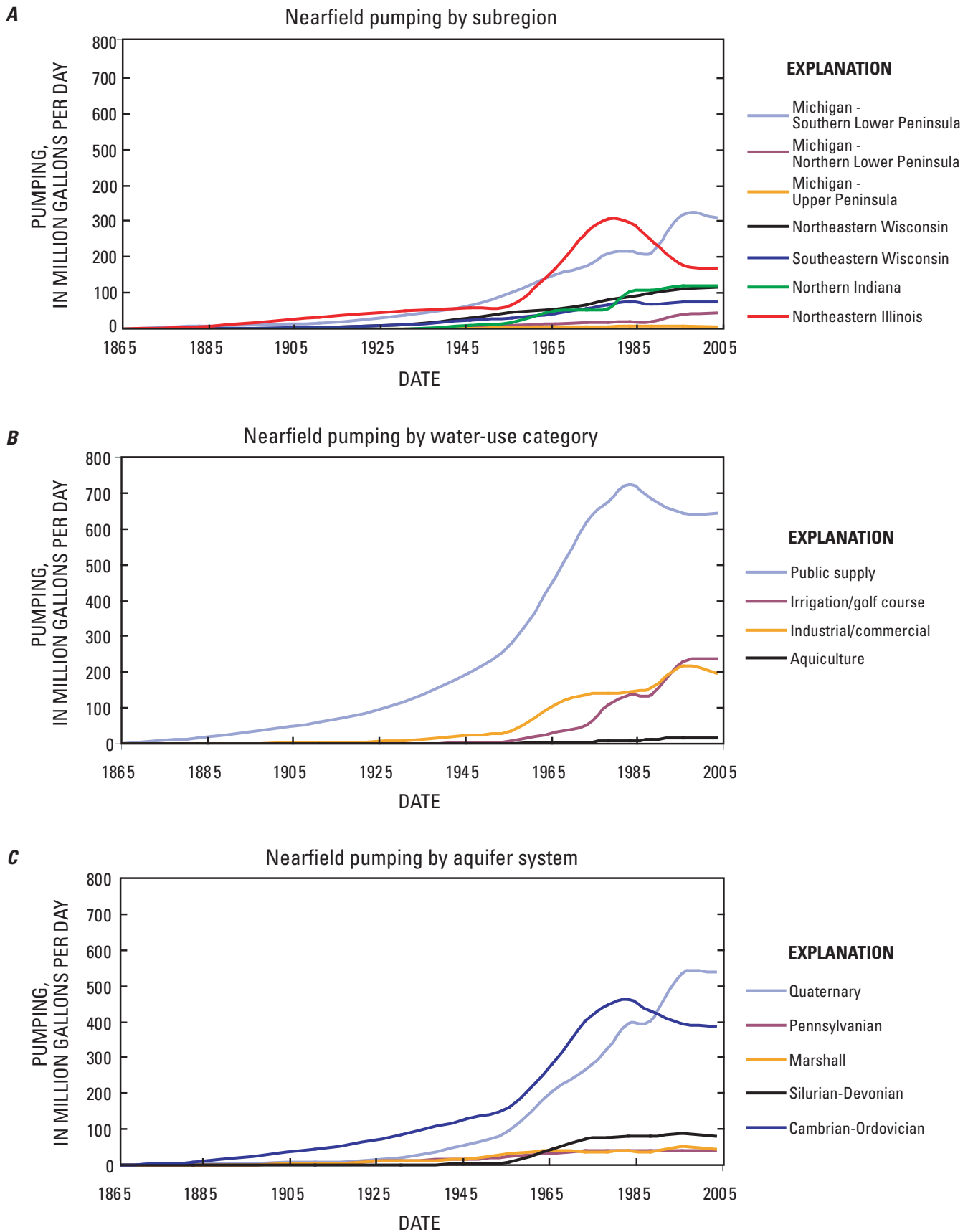
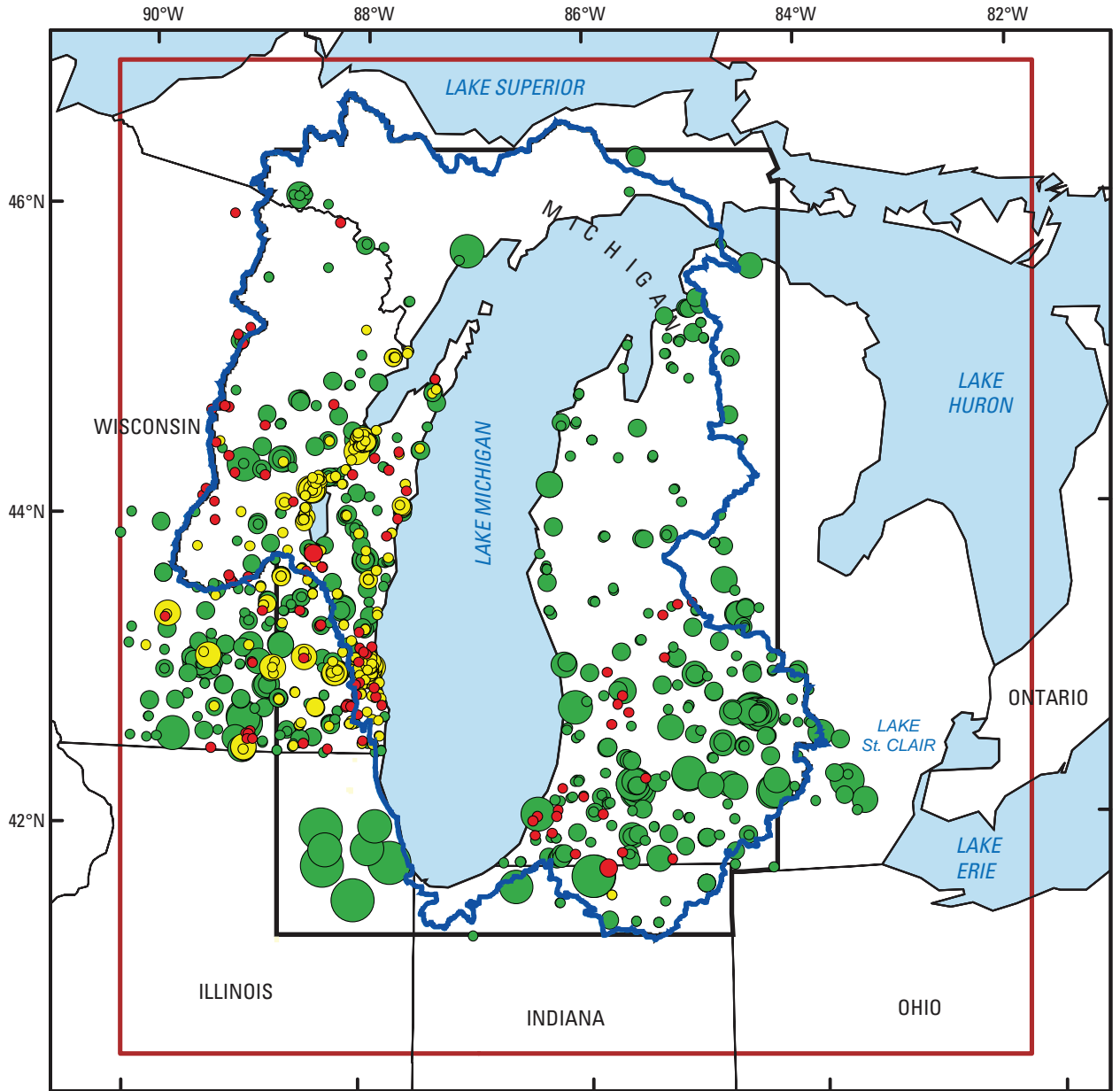
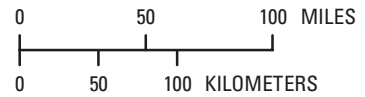


Figure 33. Nearfield pumping through time by A, subregion; B, water-use category; and C, aquifer system.

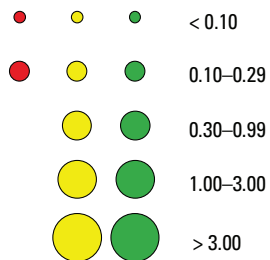


Base from ESRI, 2001



EXPLANATION

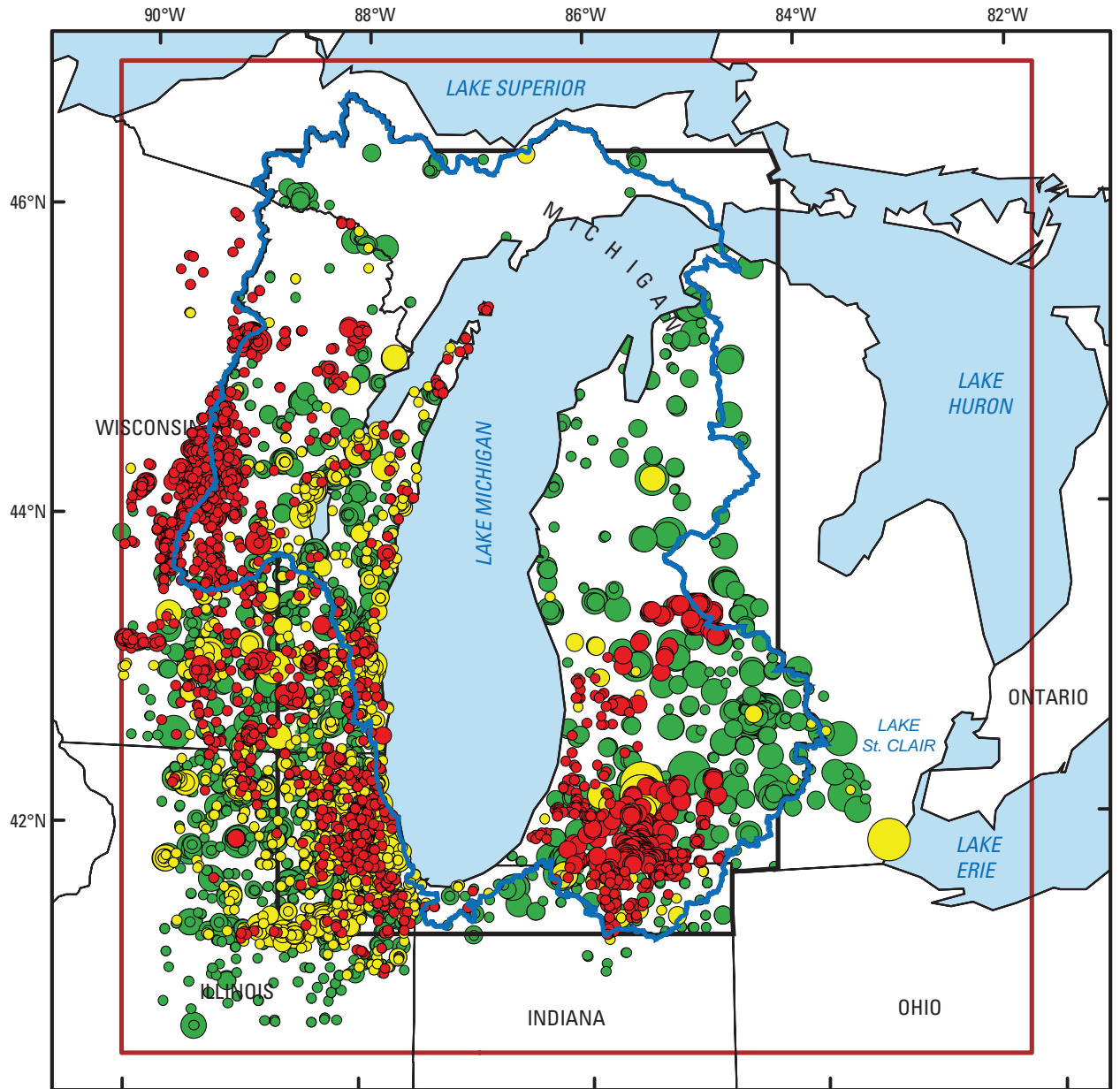
**Water use for stress period from 1941 through 1950
(million gallons per day)**



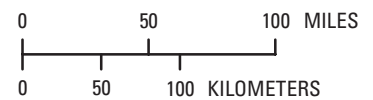
Model or hydrologic boundary



Figure 34A. Spatial distribution of pumping by water-use category: 1941–50.

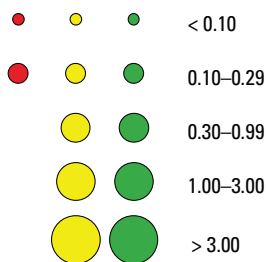


Base from ESRI, 2001



EXPLANATION

**Water use for stress period from 1976 through 1980
(million gallons per day)**

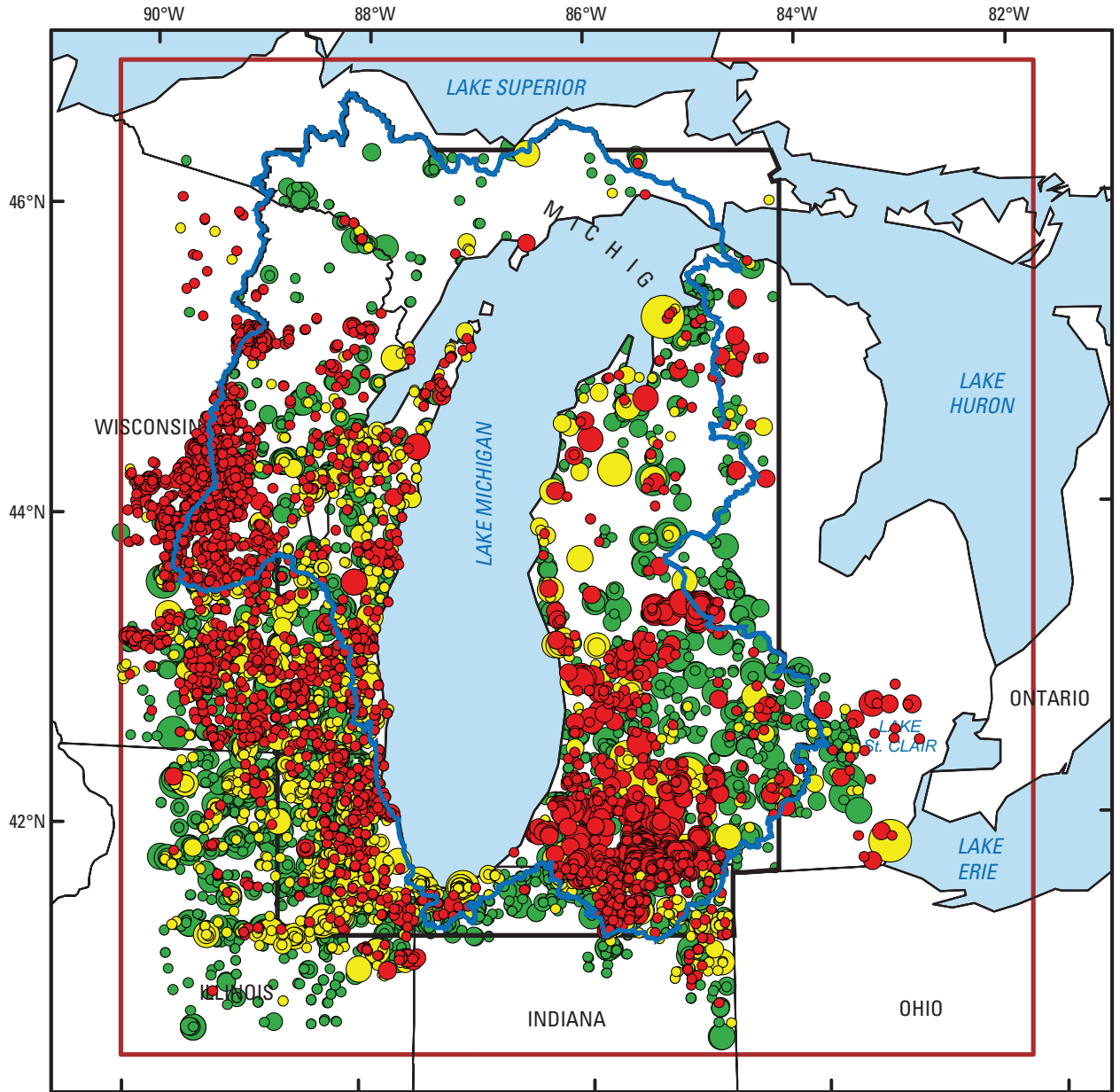


●	Irrigation
●	Industrial
●	Public supply

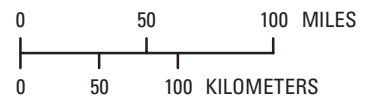
Model or hydrologic boundary



Figure 34B. Spatial distribution of pumping by water-use category: 1976–80.

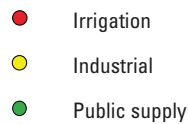
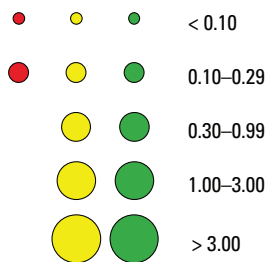


Base from ESRI, 2001



EXPLANATION

**Water use for stress period from 2001 through 2005
(million gallons per day)**



Model or hydrologic boundary



Figure 34C. Spatial distribution of pumping by water-use category: 2001–5.

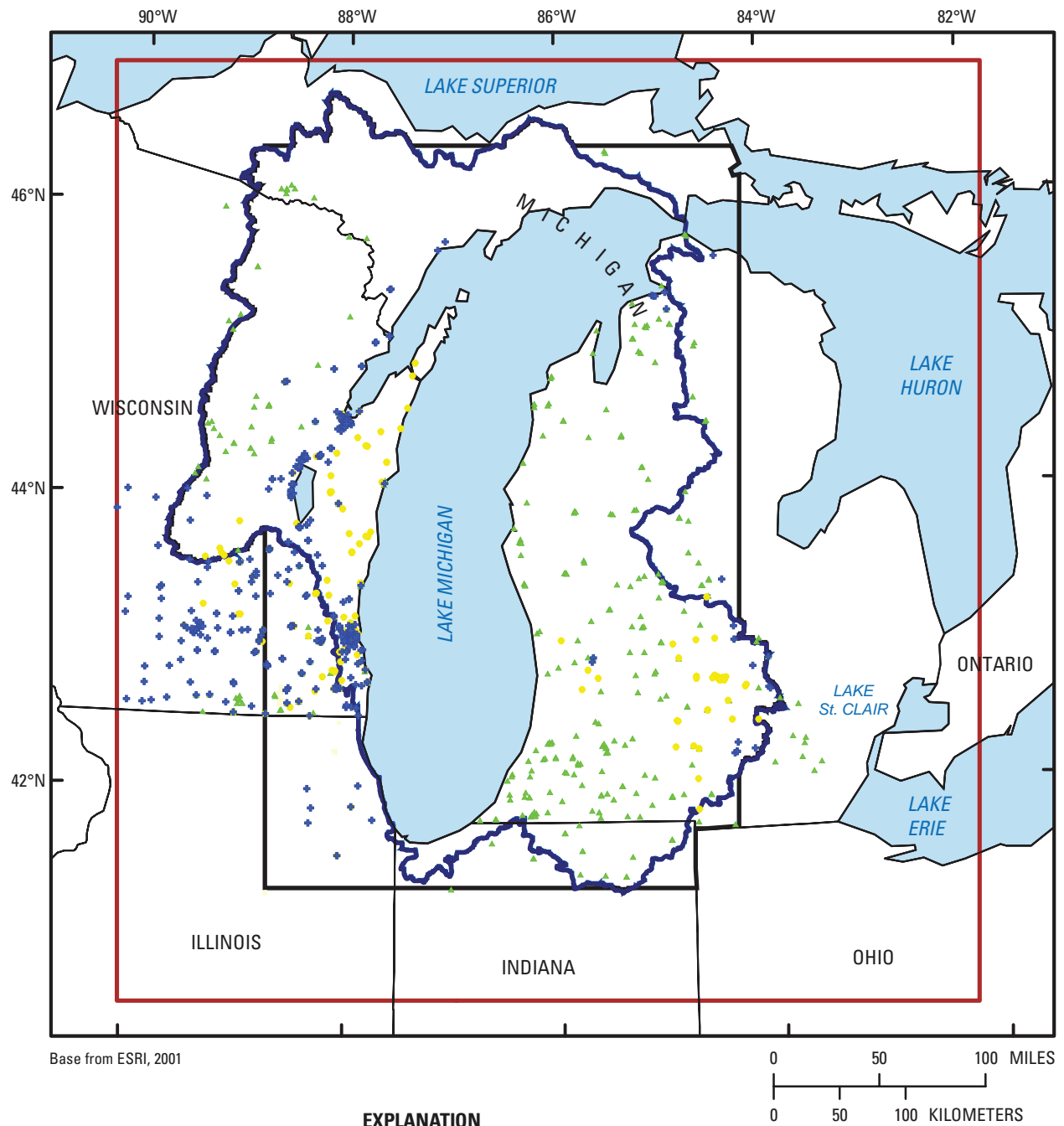


Figure 35A. Spatial distribution of shallow Quaternary, shallow bedrock, and deep bedrock wells: 1941–50.

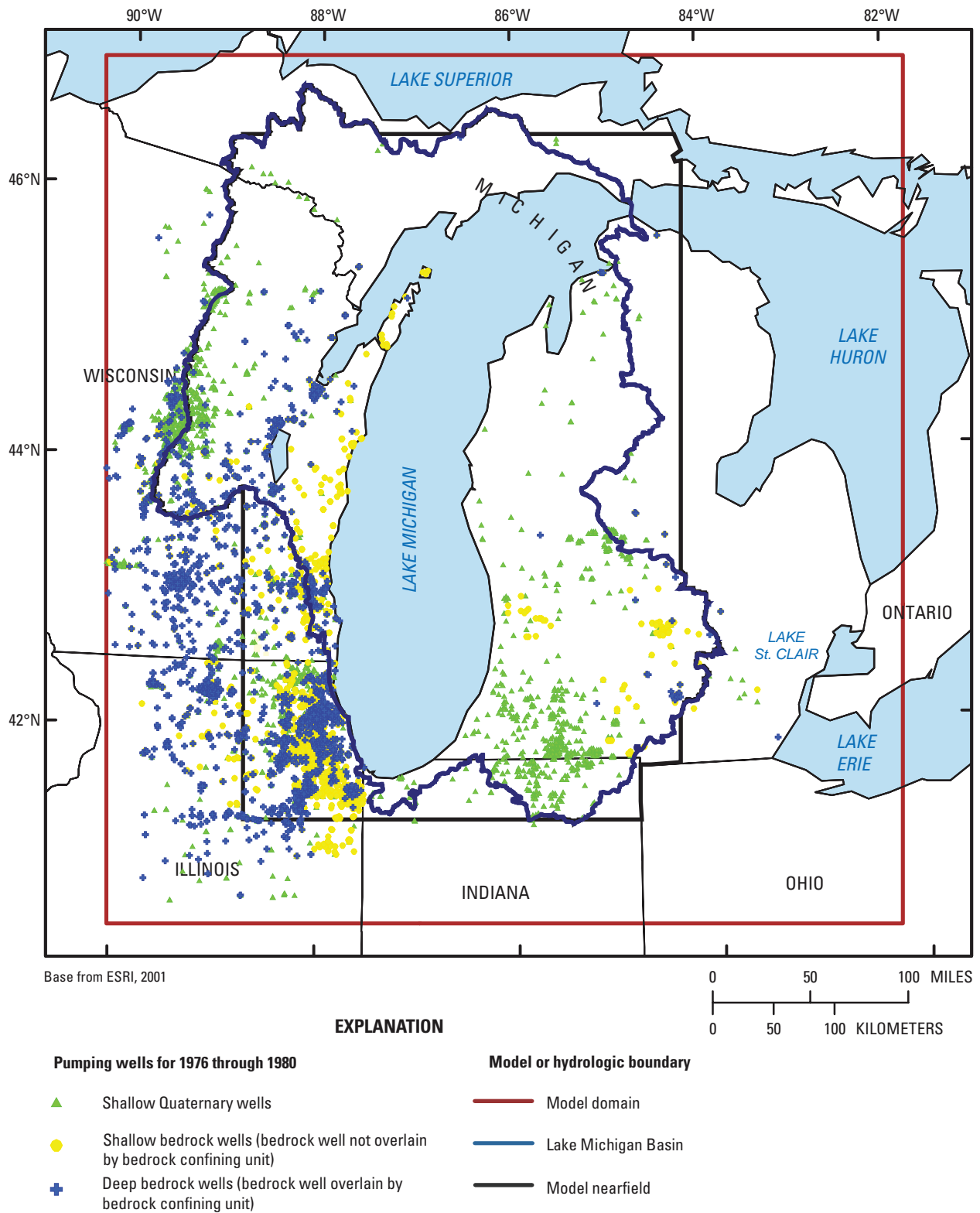


Figure 35B. Spatial distribution of shallow Quaternary, shallow bedrock, and deep bedrock wells: 1976–80.

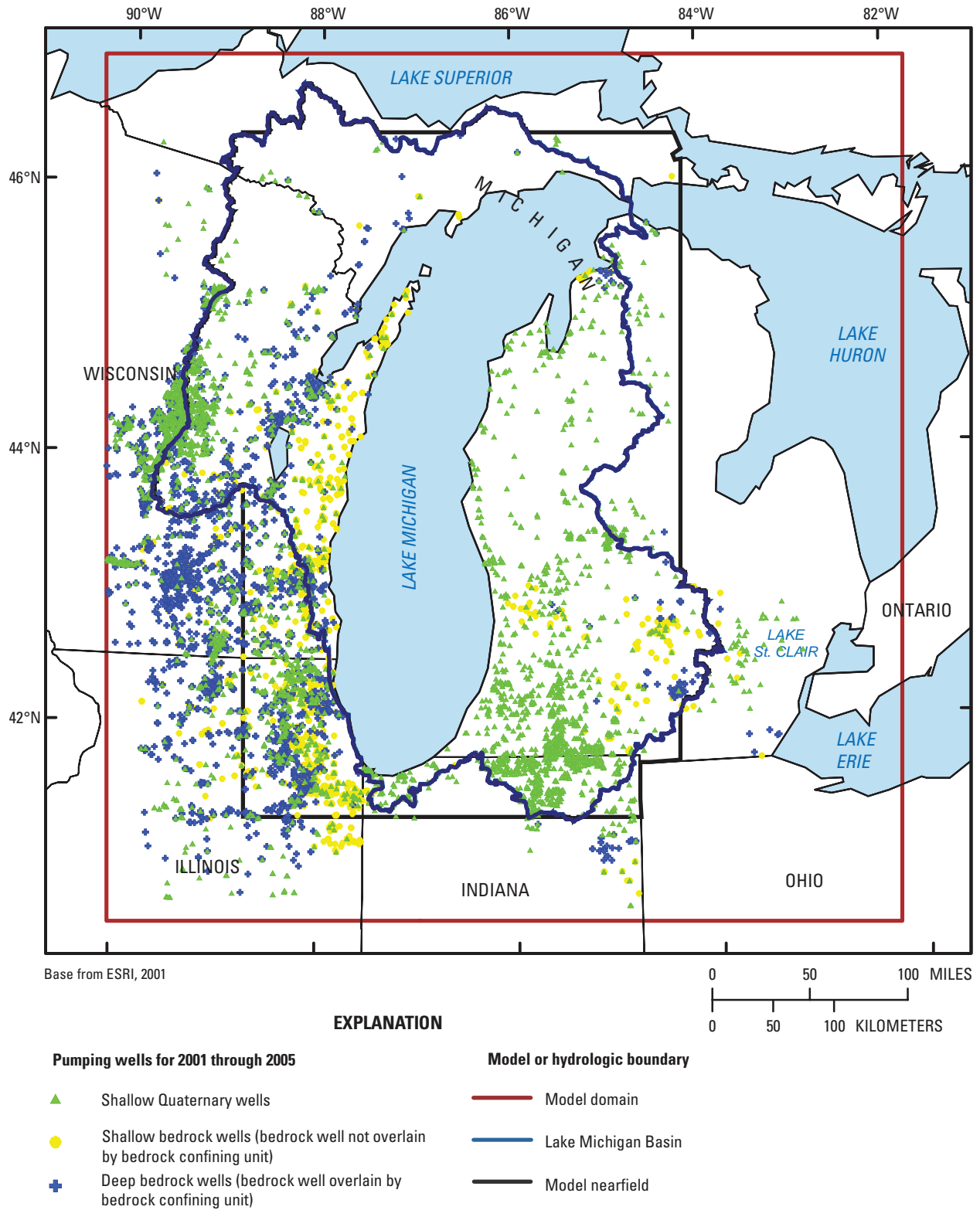


Figure 35C. Spatial distribution of shallow Quaternary, shallow bedrock, and deep bedrock wells: 2001–5.

Table 9. Shallow compared to deep withdrawals.

Shallow withdrawals include pumping from wells that penetrate unlithified Quaternary deposits plus pumping from shallow bedrock. Shallow bedrock withdrawals are from wells open to aquifers above the uppermost bedrock confining unit. Deep withdrawals are from wells that penetrate to bedrock aquifers that are below the uppermost bedrock confining unit. The uppermost bedrock confining unit at any row or column location in the model corresponds to the most shallow layer that is more than 5 feet thick and is assigned a vertical hydraulic conductivity less than or equal to 0.001 foot per day. If no bedrock confining unit is encountered, then the entire

model thickness falls within the shallow part of the flow system at that location.

Shallow wells can be considered to pump under unconfined conditions when at the water table or when any overlying QRNR deposits are coarse grained, or under semiconfined conditions when any overlying QRNR deposits are fine grained. Deep wells all pump under confined conditions.

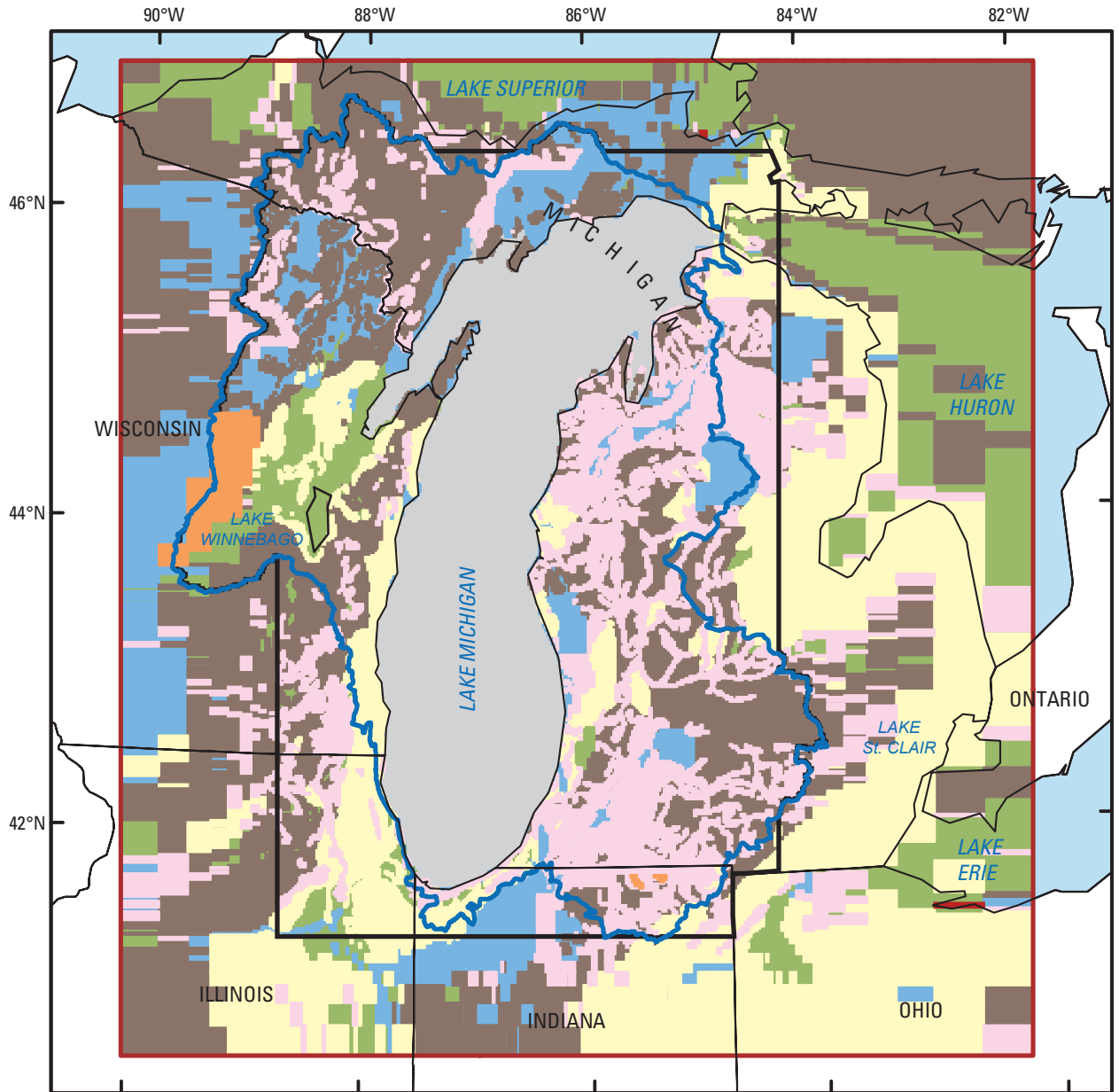
Mgal/d, million gallons per day.

9A. Shallow and deep withdrawals through time for entire model domain.

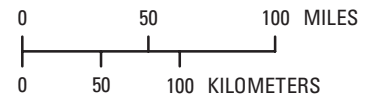
Withdrawal zone	Number of wells in model	Percentage of total number	Withdrawal in model (Mgal/d)	Percentage of total withdrawals
1941–50				
Shallow QRNR	366	34	56.5	25
Shallow bedrock	192	18	34.1	15
Deep bedrock	504	48	133.5	60
1976–80				
Shallow QRNR	2,449	37	322.8	35
Shallow bedrock	2,029	31	185.4	20
Deep bedrock	2,152	32	423.1	45
2001–5				
Shallow QRNR	4,694	51	537.8	49
Shallow bedrock	1,841	20	173.3	16
Deep bedrock	2,612	29	382.3	35

9B. Percentages of withdrawals by state for 2001–5 in model nearfield.

State	Withdrawal (Mgal/d)	Shallow QRNR (percent)	Shallow bedrock (percent)	Deep bedrock (percent)
Michigan	348	72.3	22.2	5.5
Indiana	117	98.9	1.1	.0
Wisconsin	193	27.3	20.5	52.2
Illinois	167	23.4	16.4	60.2



Base from ESRI, 2001



EXPLANATION

Glacial categories in layer 1

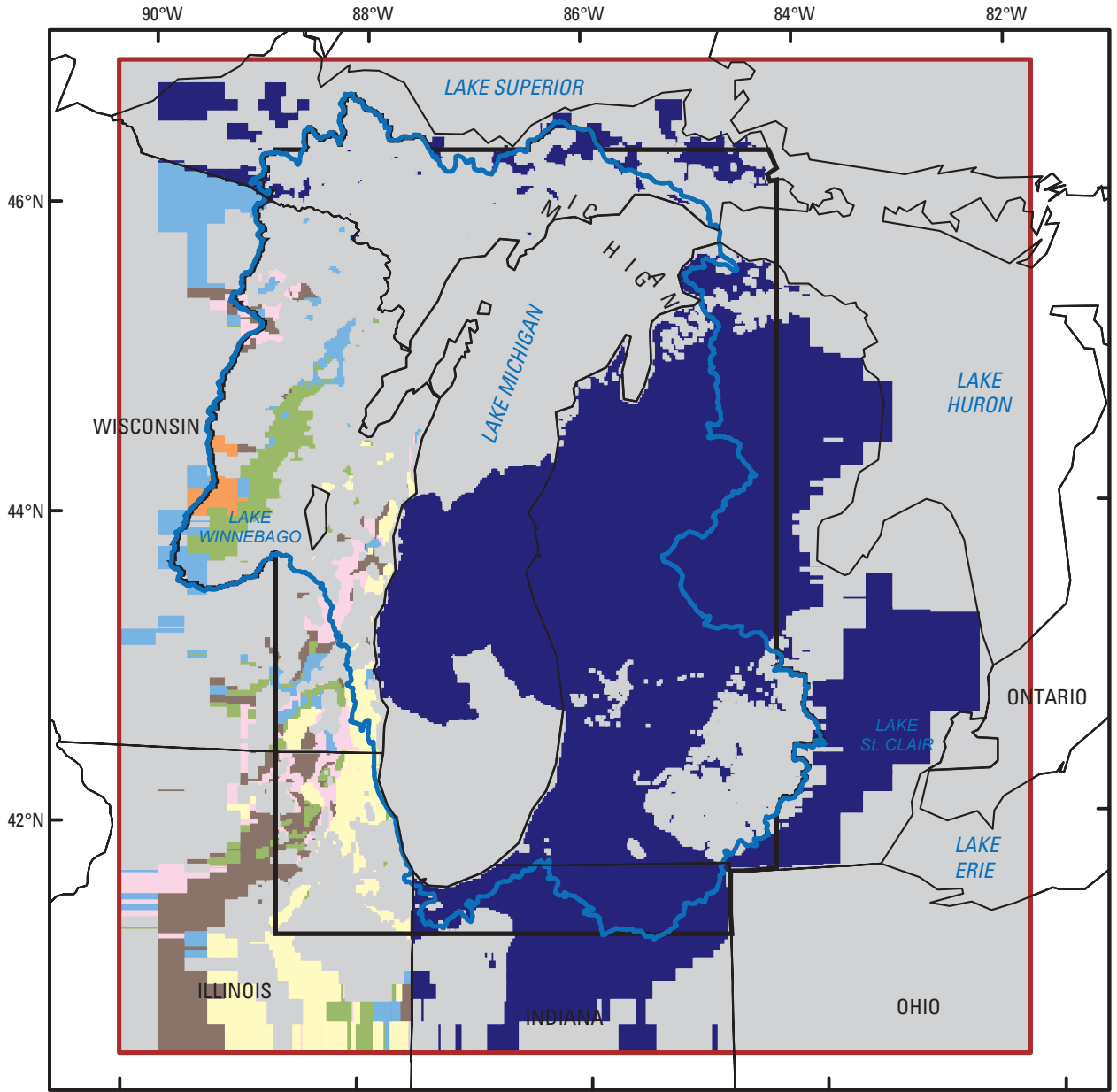
(Fullerton and others, 2003; Soller and Packard, 1998)



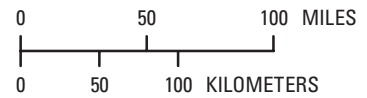
Model or hydrologic boundary



Figure 36A. Glacial categories in model layer 1.



Base from ESRI, 2001



EXPLANATION

**Glacial categories in layer 2
(Fullerton and others, 2003; Soller and Packard, 1998)**

 Clayey till	 Fine stratified
 Loamy till	 Medium stratified
 Sandy till	 Coarse stratified
 Unknown	 Quaternary absent

Model or hydrologic boundary

 Model domain
 Lake Michigan Basin
 Model nearfield

Figure 36B. Glacial categories in model layer 2.

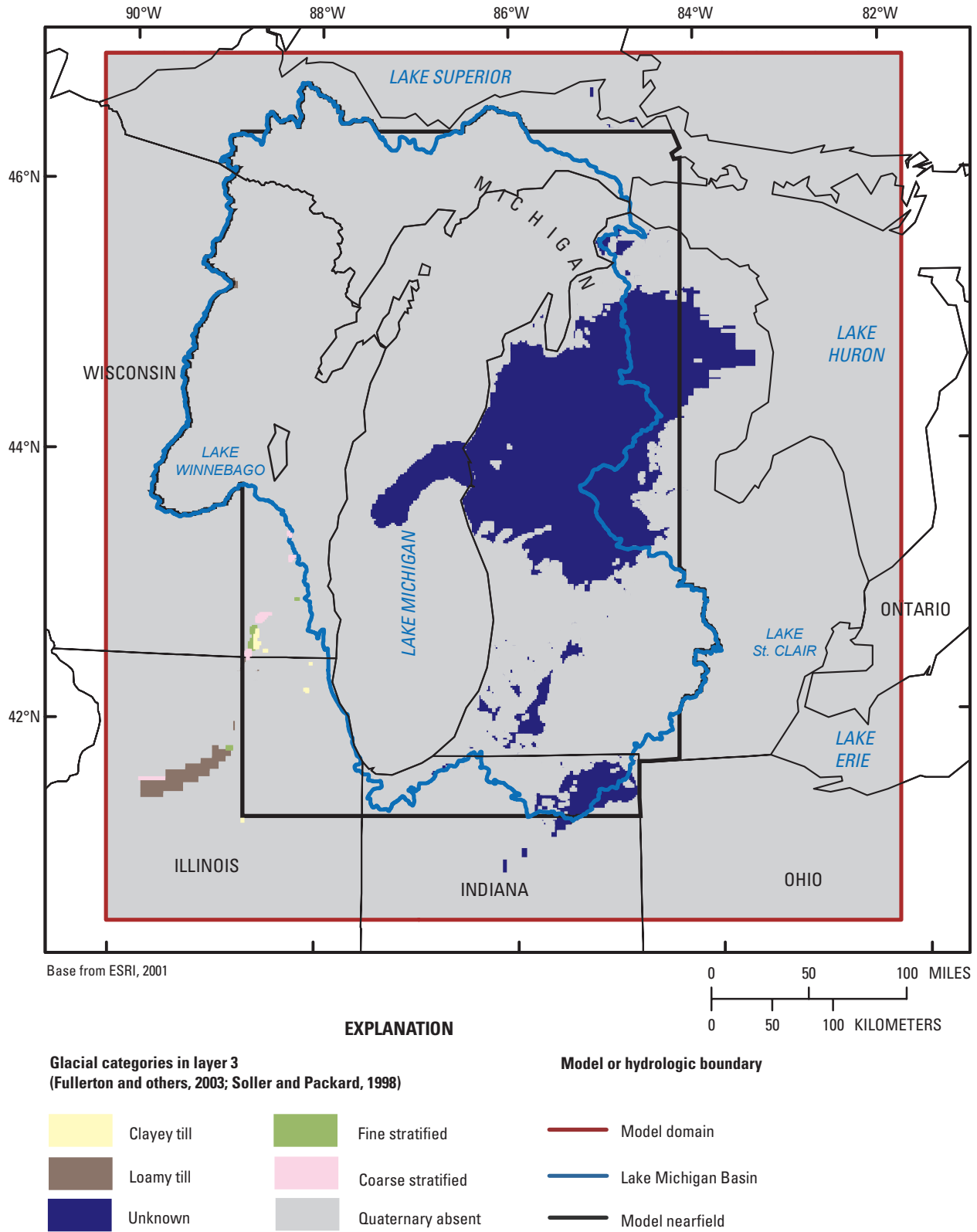


Figure 36C. Glacial categories in model layer 3.

The distribution of the coarse fraction in QRNR deposits is mapped for the depth intervals associated with each of the top three model layers from hundreds of thousands of well logs assembled in support of the LMB model (Arihood, 2009). The texture of glacial deposits was mapped in Michigan, Indiana, and Wisconsin but not in Ohio or Illinois.

The pattern of the coarse fraction in layer 1 (fig. 37A) correlates with the map of glacial categories (fig. 36A) except in outwash areas where drillers have encountered predominantly fine-grained deposits and areas of clayey till or fine stratified deposits where drillers encountered predominantly coarse-grained deposits. The pattern of the coarse fraction in layer 2 (fig. 37B) and especially layer 3 (fig. 37C) is more approximate than in layer 1, owing to the relative scarcity of boreholes (Arihood, 2009).

The initial hydraulic-conductivity assignment to the inland QRNR deposits is a function of not only the glacial category but also the coarse fraction attributed to an inland nearfield or farfield model cell in layers 1, 2, and 3. The two variables are combined by means of an empirical “power law” that uses an expected K_h value and an allowable range based on the glacial category and then computes K_h values within the allowable range based on the coarse fraction (appendix 3). The power law yields K_h values with assumed expected ranking of K_h (clayey till < fine stratified < loamy till and organic < sandy till < medium and coarse stratified). Where coarse-fraction information is missing (for example, in northeastern Illinois and northeastern Ohio), the expected value of K_h for the mapped glacial categories is assigned directly to all cells. Where the glacial category is unknown (parts of layer 2 and most of layer 3), parameters corresponding to fine stratified deposits are assumed (see appendix 3).

Plots of the power-law relations between the coarse fraction and the estimated K_h for different glacial materials (fig. 38A–C) show the expected K_h (based on the average coarse fraction encountered in QRNR cells), as well as the possible range of values. For example, the K_h that corresponds to the average coarse fraction for clayey till is around 1 ft/d, but the allowable range is from 0.1 to 10 ft/d. This procedure yields the nearfield distribution of initial K_h for layer 1 shown in figure 39.

The initial value of K_v for any given inland QRNR cell is derived from the computed K_h by means of a single vertical anisotropy factor set at 20 to 1. Accordingly, an initial K_h of 100 ft/d automatically yields an initial K_v of 5 ft/d, and an initial K_h of 1 ft/d yields an initial K_v of 0.05 ft/d.

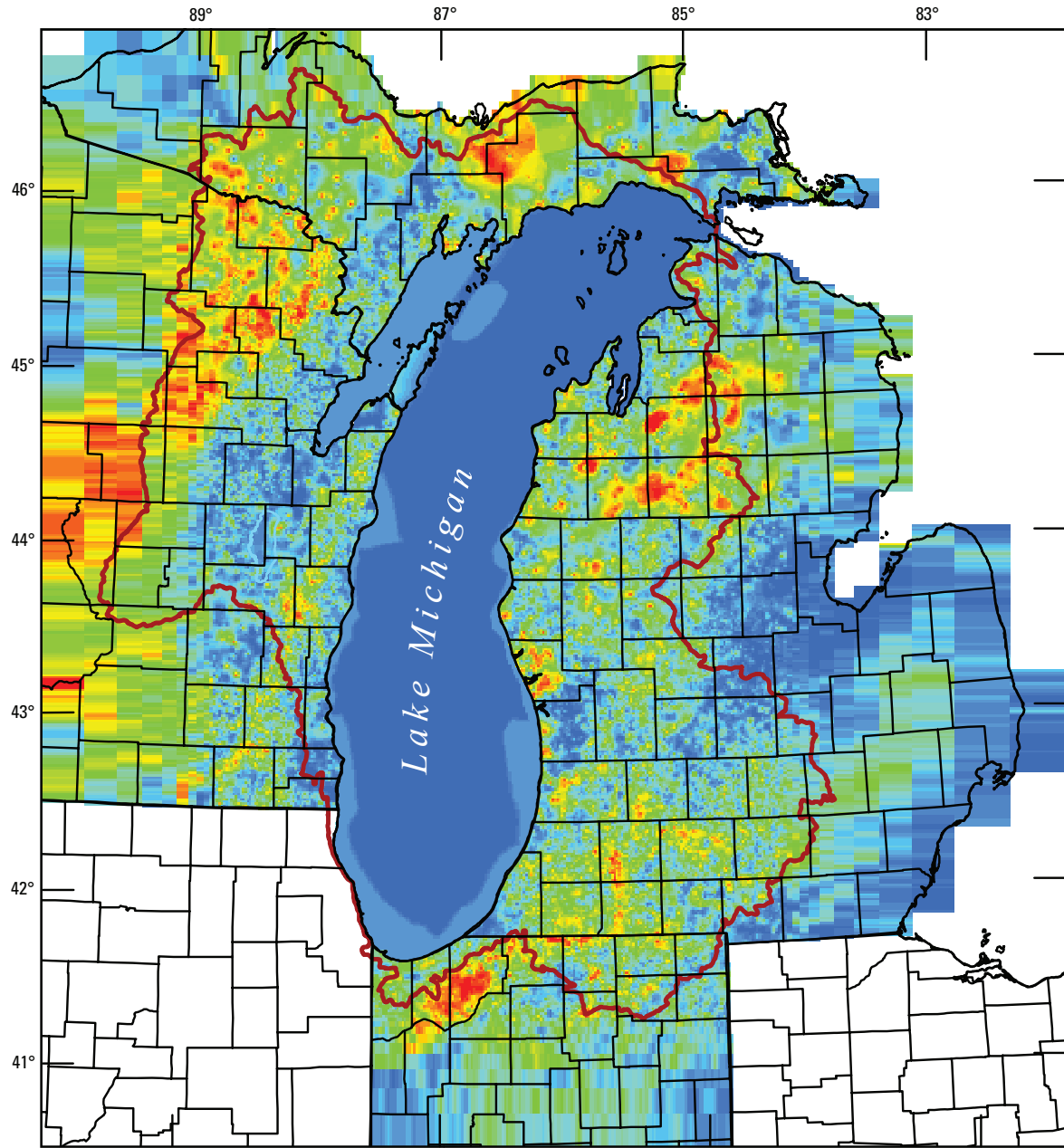
The arrays of initial K_h and initial K_v are both subject to calibration and sensitivity analysis. The calibration is not performed individually for each cell; rather, a single K_h and a single K_v multiplier is estimated for each glacial category across all three QRNR layers as a way to improve the agreement between observed field conditions and the model simulation. The updated postcalibration values are discussed in section 5. In section 7, the sensitivity of the model results to the method for estimating QRNR K is evaluated by comparing

the base model to a simplified simulation in which one average value for K_h and one average value for K_v represent all the cells belonging to a single glacial category.

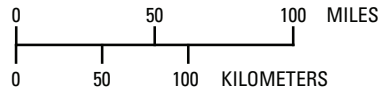
4.8.2 QRNR Layers Below Lake Michigan and Farfield Lakes

The distribution and rate at which groundwater discharges directly to Lake Michigan is, in part, a function of the horizontal and, more especially, the vertical hydraulic conductivity of the glacial and recent sediments that underlie the lake. A number of resource-assessment, geomorphological, and geophysical investigations provide insight into the texture and permeability of the lakebed material. One set of studies identified mappable sand bodies in the lakebed sediment, which are assumed to be zones of relatively high hydraulic conductivity (Ayers and Chandler, 1967; Meisburger and others, 1979; Eadie and Lozano, 1999; Ayers, unpublished report for the NOAA Great Lakes Environmental Research Laboratory). Some of these investigations employed gravity and seismic methods along multiple transects (for example, Lineback and others, 1971). Other studies used geomorphological methods to identify the proximal (nearshore) sections of ancient deltas that prograded into the lake at low stage (Colgan and Principiato, 1998; Soller, 1998; National Oceanic and Atmospheric Administration, 2005). These deltas, which overlap with the distribution of sand bodies, are likely sites for the accumulation of sediment with enhanced coarse fraction. One delta extends about 12 mi into Lake Michigan northeast of Green Bay, Wis.; others are located where ancient rivers emptied into the lake north and south of Grand Rapids, Mich. The final source used to map the texture of lakebed sediments was results from geophysical studies along the Wisconsin shoreline (Cherkauer and others, 1990). The investigators converted measurements of electric conductance into estimates of hydraulic conductance terms, which, when paired with thickness estimates, allow the nearshore to be segmented into texture zones.

By combining the available data sources, it is possible to assemble a map for the nearshore that categorizes hydraulic conductivity into areas of low, middle, and high for the Lake Michigan lakebed (fig. 40). Nearshore sediments (corresponding to a lateral distance of three model cell widths, or about 3 mi) are assigned to the middle K zone unless evidence from sand-body studies, geomorphology, or the electric conductance records indicates that the sediments have coarser or finer texture. Most of the interior of the lakebed is assumed to be composed of fine-grained sediments, except where data suggest otherwise. The values applied to layer 1 are extended to layer 2 where the estimated unconsolidated thickness exceeds 100 ft and to layer 3 where it exceeds 300 ft. In terms of proportion, 73 percent of the lakebed area is assigned to the interior, 1 percent to the low, 24 percent to the middle, and only 2 percent to the high K zones. However, in some areas along the shoreline, the high K zone is notable.



Base from U.S. Geological Survey digital data
 1:100,000 1983. Universal Transverse Mercator projection
 Zone 16, Standard Parallel 0° (Equator), Central Meridian 87° W,
 North American Datum 1983



EXPLANATION

— Lake Michigan Basin boundary

Percentage of coarse material

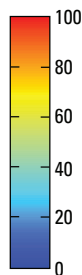
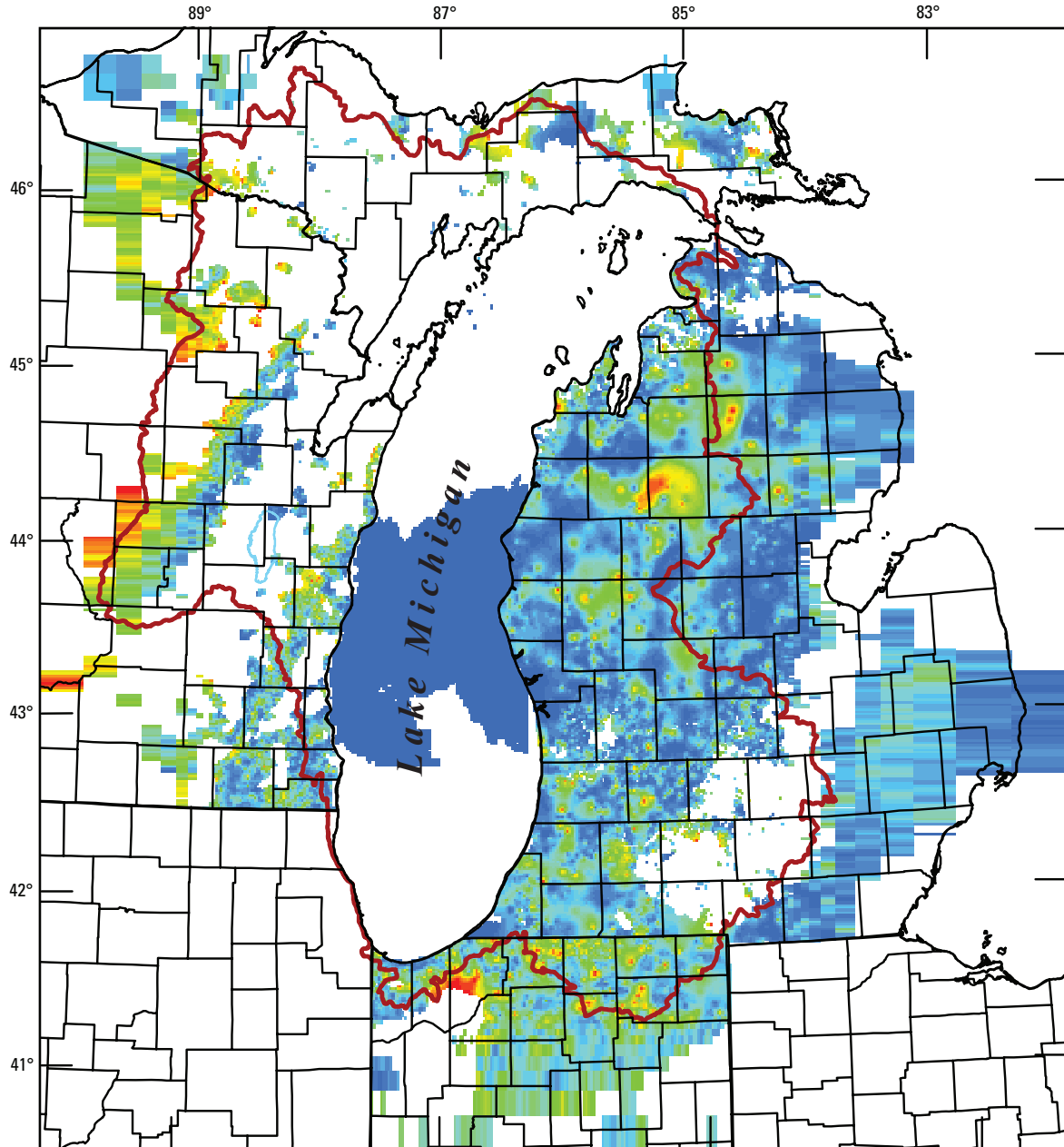


Figure 37A. Coarse fraction in model layer 1.



Base from U.S. Geological Survey digital data
 1:100,000 1983. Universal Transverse Mercator projection
 Zone 16, Standard Parallel 0° (Equator), Central Meridian 87° W,
 North American Datum 1983

0 50 100 MILES
 0 50 100 KILOMETERS

EXPLANATION

— Lake Michigan Basin boundary

Percentage of coarse material

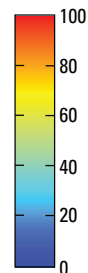


Figure 37B. Coarse fraction in model layer 2.

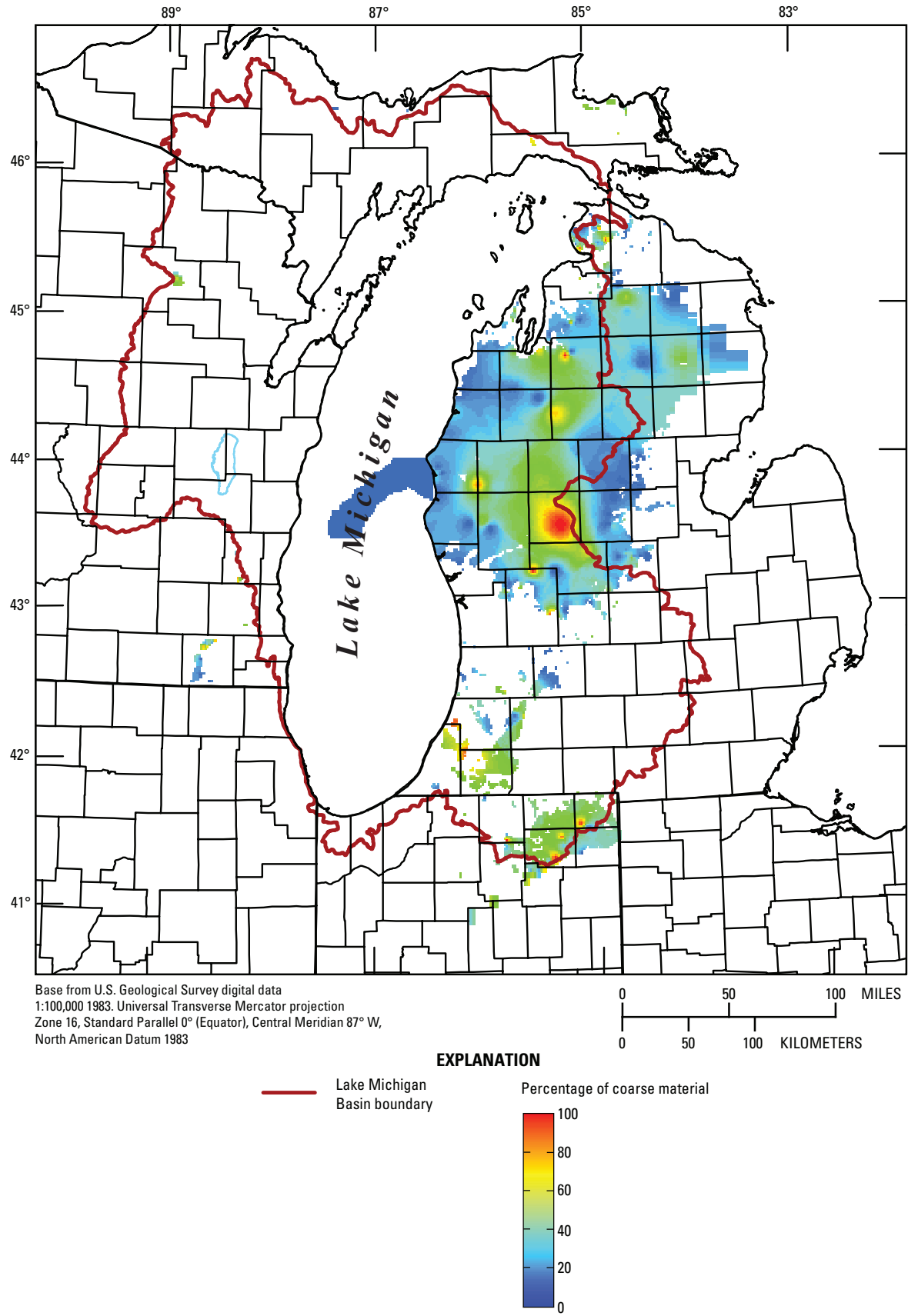


Figure 37C. Coarse fraction in model layer 3.

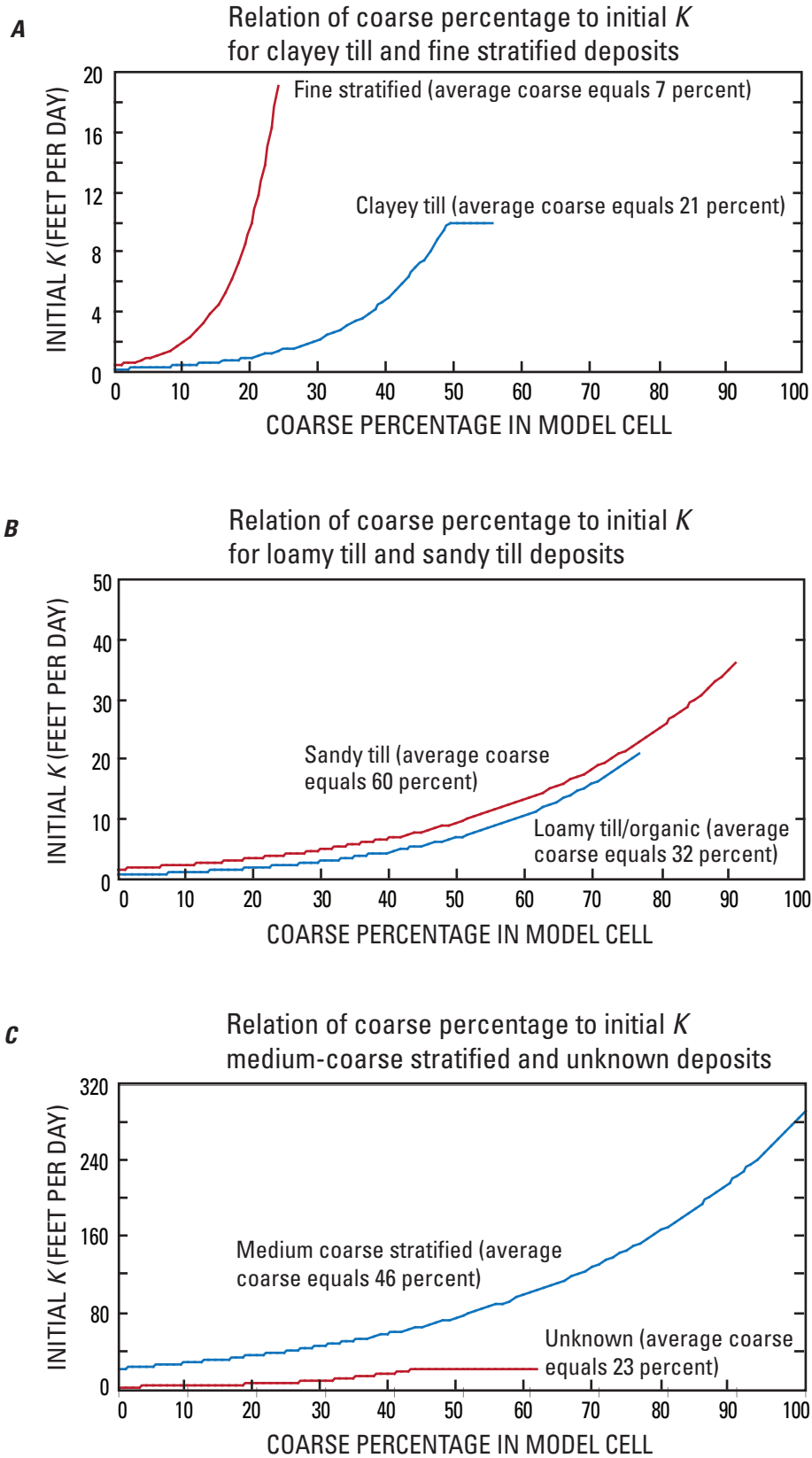


Figure 38. Relation of initial hydraulic conductivity values to coarse fraction, by glacial category.

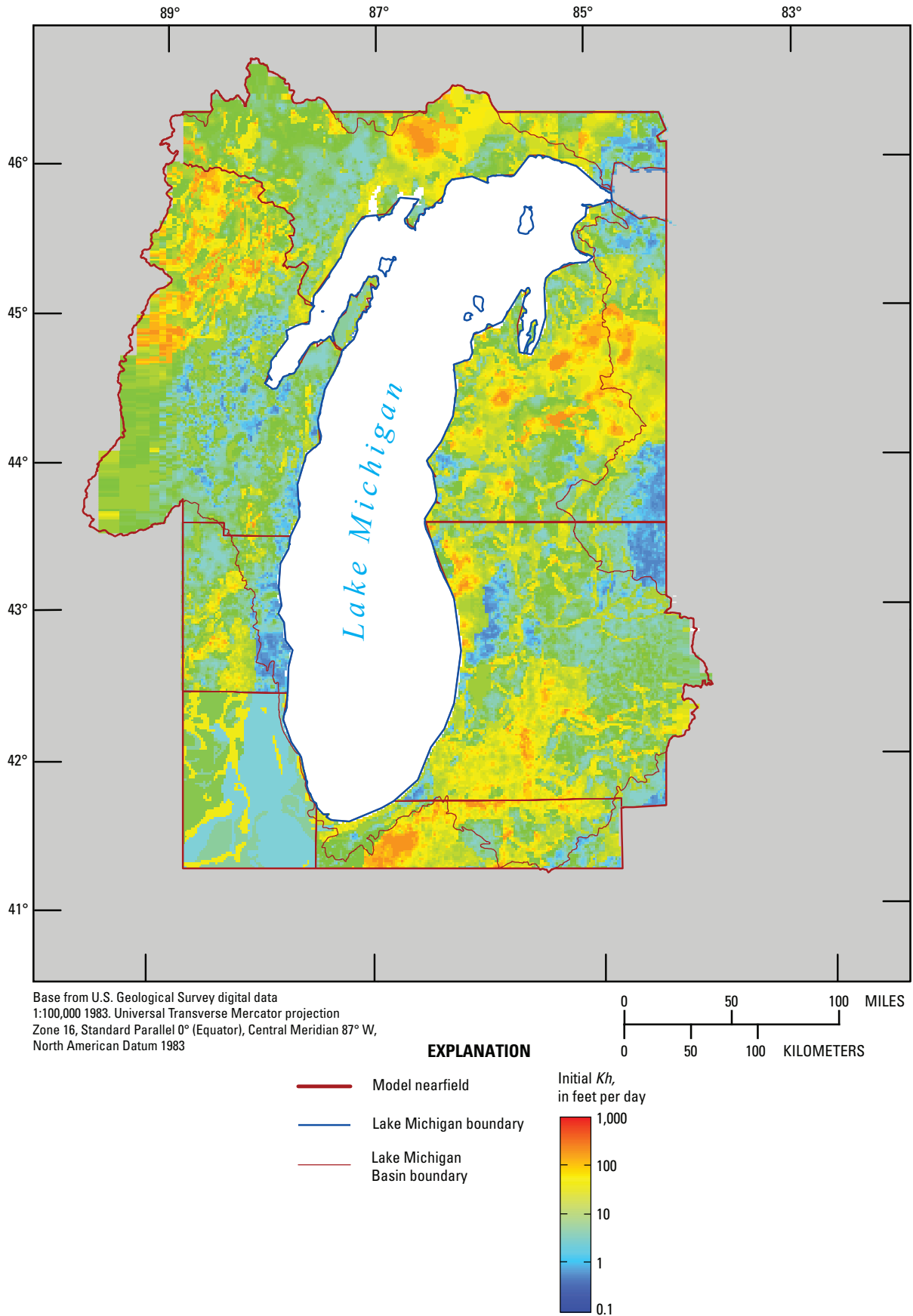


Figure 39. Initial horizontal hydraulic conductivity distribution in nearfield area of model layer 1.

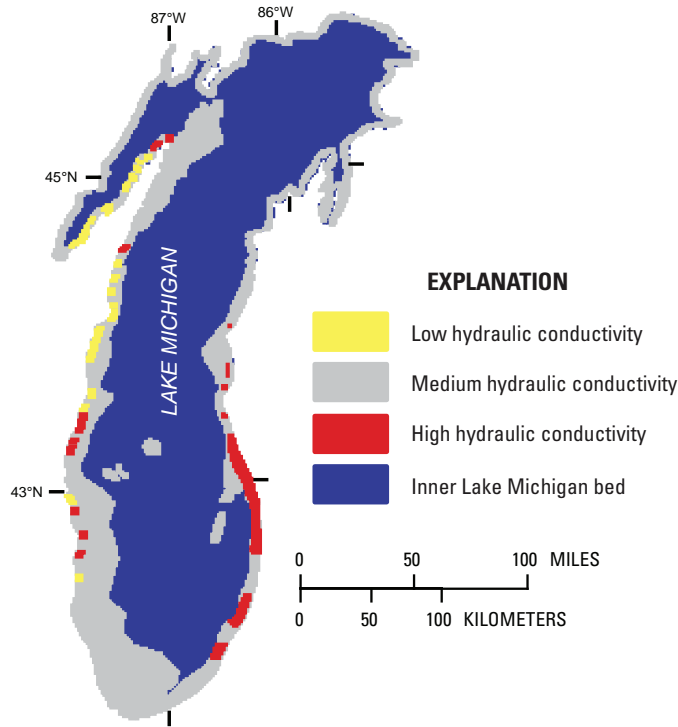


Figure 40. Hydraulic conductivity zones under Lake Michigan.

Because direct discharge of groundwater to Lake Michigan is controlled largely by the upward vertical component of the hydraulic gradient, the K_v values assigned the lakebed zones are of particular importance. Calculations based on the geophysical study along the Wisconsin shoreline (Cherkauer and others, 1990) suggest that values in the range of 0.001 to 0.1 ft/d are reasonable starting estimates. Accordingly, the high end of the expected range was assigned to the high K zones, the low end was assigned to the low and interior K zones, and an intermediate value was assigned to the middle K zone. The K_v zones were adjusted during model calibration (appendix 5, table A5–2). The K_h values for the same sediments range from 0.1 to 1 ft/d and were fixed during the calibration. Both K_h and K_v were modified during model sensitivity analysis (see section 7).

The K_v values specified for QRNR sediments in the model farfield under Lakes Superior, Huron, St. Clair, and Erie were based on the mapped glacial categories because no drilling logs were available. The glacial categories were not derived from the Fullerton compilation (which is limited to inland areas) but from a map of Quaternary sediments in the eastern United States prepared by Soller and Packard (1998).¹⁷

¹⁷ This map employs only a few unconsolidated units, which are equated to the model glacial categories as follows:

Glacial Units in Soller and Packard map	Glacial categories in LMB model
Coarse stratified	Medium/Coarse stratified
Fine stratified	Fine stratified
Till	Loamy till
Patchy QRNR	Loamy till
Organic	Organic

The resulting zonation of the QRNR sediments under the farfield lakes is shown in figure 36A. During the calibration process, their K_h and K_v values are subject to the same multiplier parameters as the inland cells grouped in the same glacial category.

4.8.3 Bedrock Hydraulic Conductivity and Transmissivity of Aquifer Systems

Horizontal and vertical hydraulic-conductivity values are assigned to the model bedrock layers (4 to 20) in *blocks* of cells. The increasing scarcity of hydraulic-conductivity data with depth make it unreasonable to vary bedrock K_h and K_v on a cell-by-cell basis; instead these parameters are varied in a piecewise constant manner (that is, by blocks).¹⁸

The assignment of K_h and K_v block values draws on four types of sources: results of aquifer tests, specific-capacity calculations based on water-well driller logs, published reports that analyze hydrogeology at the county or subregional scale, and interpretations from published groundwater-flow models. The mix of sources is presented by state in appendix 4A.

Appendix 4B contains a detailed description of the *initial* block K_h and K_v assignments to bedrock aquifer systems, organized by layer. The transmissivities of bedrock aquifer systems are calculated by multiplying the K_h values by the layer thickness (transmissivity units: ft²/d). Pinched cells are excluded, as well as cells for which the head solution with the initial input falls below the bottom of the cell. The results for each of the five aquifer systems are displayed in figure 41 according to a log scale. For completeness, the initial transmissivities for the unconsolidated units in the QRNR aquifer system are compared to the distribution in the bedrock systems.

The initial transmissivity for the topmost QRNR aquifer system (fig. 41A) reflects the underlying geology of the deposits. The highest transmissivities are clustered where outwash deposits are thick in the NLP_MI subregion and to a lesser extent in N_IND, the western part of NE_WI, and the so-called kettle moraine area some distance inland in SE_WI. The lowest transmissivity is associated with the clayey tills commonly found along the Lake Michigan shoreline in the subregions of NE_WI, SE_WI, and NE_ILL. Values are also very low in parts of the UP_MI where glacial deposits are very thin and under Lake Michigan where the system is dominated by fine-grained deposits.

¹⁸ During the calibration process, a single multiplier is applied either to the value assigned to one block of cells or, alternatively, the multiplier is applied to the multiple values in multiple blocks. The cells in one or more blocks subject to a single calibration multiplier constitute a zone. In this section, only the block assignments are discussed; the calibration zones are described in section 5.

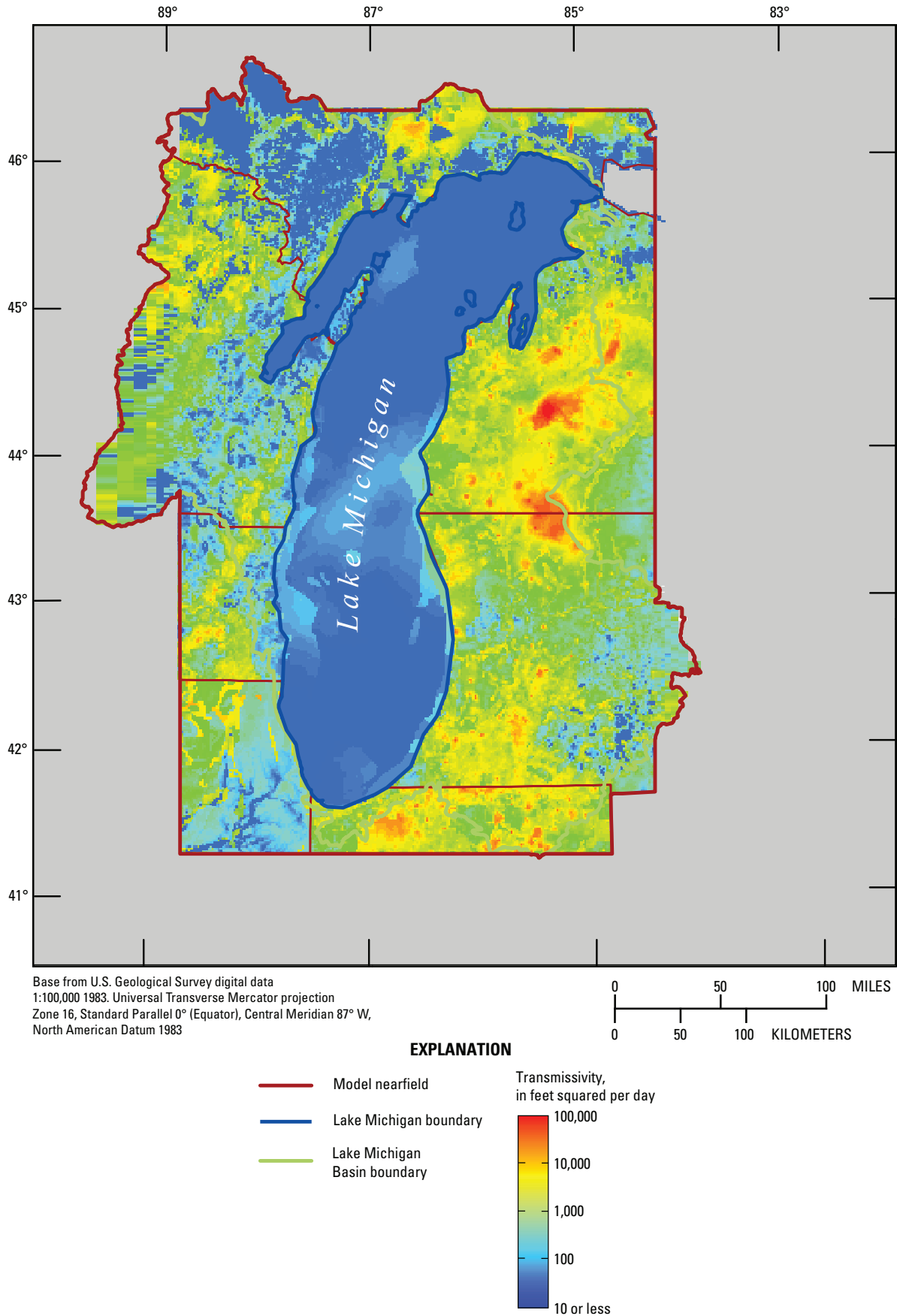


Figure 41A. Initial transmissivity distribution in aquifer system QRNR.

The two aquifer systems limited to the NLP_MI and SLP_MI subregions show small transmissivity trends. For the PENN aquifer system (fig. 41B), transmissivities tend to decrease from north to south with some local variations. For the MSHL aquifer system (fig. 41C), transmissivities tend to increase from north to south.

The SLDV aquifer system thickens appreciably in the center of the Michigan Basin, and this thickening influences the pattern of transmissivity (fig. 41D). The lowest transmissivities are found in areas to the west where the rocks subcrop beneath QRNR deposits.

Available data from well logs and pumping tests indicate that the transmissivity for the C-O aquifer decreases from north to south, owing to a greater fraction of fine-grained clastics (for example, siltstone) relative to sandstone (Feinstein, and others, 2005). However, increasing thickness of deposits causes transmissivity to increase for some hydrostratigraphic units toward the middle of the Michigan Basin (fig. 41E). Transmissivities are lowest in the northwest farfield part of the model domain, where the C-O rocks are thin and chiefly restricted to the MTSM unit.

The K_v assignments for confining units control the rate deep regional flow. Values generally range between $1.0 \text{ E}-3$ and $1.0 \text{ E}-7$ ft/d, as shown in a representative west/east section (fig. 42). The lowest values are associated with the evaporites in the SLDV aquifer system, followed by the shales in the DVMS system and at the top of the C-O system (the Maquoketa unit). Note that the K_v for SLDV aquifer increases as you move out of the Michigan Basin and away from the evaporite deposits in the Salina Group.

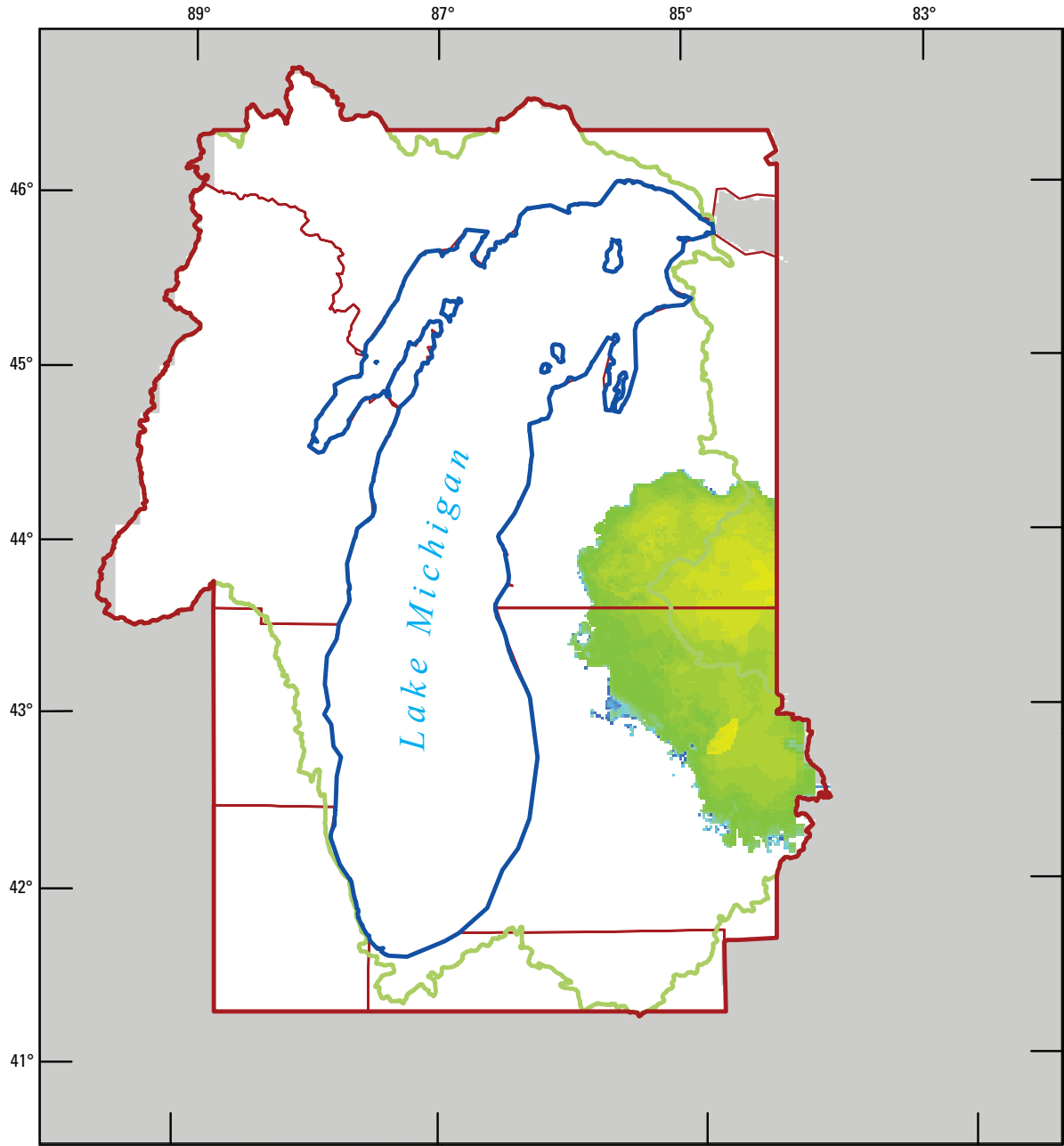
The K_h and K_v values assigned to bedrock aquifer systems for layers 4 to 20 produce a range of vertical anisotropy values. For layers defined as aquifers, the ratio of K_h to K_v varies between 50 to 1 and 2,000 to 1. For layers defined as confining units, the ratio varies between 1,000 to 1 and 20,000 to 1. The large ratios reflect the low K_v associated with confining shale beds and evaporites. The vertical anisotropy ratios reflect the presence of fractured or permeable beds inside the confining units (which increase the ease of horizontal flow) alternating with shale beds (which produce high resistance to vertical flow). This condition, for example, is well documented for shales in the Maquoketa hydrogeologic unit (Eaton, 2002). The biggest range in anisotropy is for layers defined as both aquifers and confining units, owing to the occurrence of high- and low-permeability material in the same unit. The vertical anisotropy ratios for these units vary between 50 to 1 and 10,000 to 1.

4.9 Storage

Storage parameters control the release or gain of water within the groundwater-flow system that accompany water-level changes in response to pumping and recharge. Different storage parameters are assigned for unconfined and confined aquifers. In confined aquifers, the specific storage (S_s , units of

ft^{-1}) reflects both the elasticity of the aquifer material and the expansion or contraction of the groundwater. The specific storage is multiplied by thickness to yield the storage coefficient (S , dimensionless). In unconfined aquifers, the specific yield (S_y , dimensionless) reflects the draining or filling of pores and partings. A confined aquifer can be converted to an unconfined aquifer if the hydraulic head falls below the aquifer top elevation; in that case, changes in storage changes are controlled by the specific yield rather than the specific storage. The opposite can occur when the water table rises above the aquifer top.

There are limited sources of data that quantify storage parameters in the LMB model domain, so zonation of storage parameters is much simpler than the zonation for other parameters such as recharge and hydraulic conductivity. A single S_s value of $2.6 \text{ E}-7 \text{ ft}^{-1}$ is specified for all bedrock aquifers in the model. This value is based on pumping-test information from Wisconsin and Illinois and reflects conditions in the C-O aquifer system (Foley and others, 1953; Mandle and Kontis, 1992; Feinstein, Eaton, and others, 2005; Feinstein, Hart, and others, 2005). A larger S_s value of $5.7 \text{ E}-6 \text{ ft}^{-1}$ is assigned the QRNR system in the three top unconsolidated layers to account for their more compressible material. It is worth noting, however, that because the water table generally (although not always) resides in the top model layer, the parameter that more heavily influences storage change in layer 1 is typically the specific yield. The S_y values input to the model for unconfined cells are much higher than the product of S_s and thickness for confined cells; this imbalance indicates the powerful effect on storage release exercised by dewatering of pores compared to the weak storage effect produced by elastic responses for the same change in water level. Cells in layers 1 to 3 within the QRNR system are initially assigned a single S_y value equal to 0.15, a typical average (Anderson and Woessner, 1992) used in place of a possible range from below 0.05 to above 0.40, depending on grain-size distribution and resulting porosity and packing (Morris and Johnson, 1967). The S_y of layers in the PENN and MSHL aquifers systems are assumed equal to 0.05, which reflects the predominance of clastic material in these rocks and the limited availability of pore space between the grains of the matrix. The initial specific yield of layers in the SLDV aquifer system is set even lower, to 0.005, because the porosity in these carbonate rocks is largely derived from joints and fractures. Finally, S_y in the C-O aquifer system is assumed to be either 0.05 to reflect porosity in the units dominated by sandstone (STPT through MTSM units) or 0.005 to reflect predominant fracture porosity in shale and carbonate-dominated rocks (MAQU and SNNP units). The bedrock S_y values influence the simulated solution only when the water table fluctuates in bedrock layers, which can occur in isolated areas of bedrock highs or in places where deep withdrawals cause dewatering of a zone at the top of an aquifer and the presence of an underlying deep water table. The latter mechanism is documented in parts of the LMB model domain where deep pumping centers penetrate the C-O aquifer system (see section 7).



Base from U.S. Geological Survey digital data
 1:100,000 1983. Universal Transverse Mercator projection
 Zone 16, Standard Parallel 0° (Equator), Central Meridian 87° W,
 North American Datum 1983

EXPLANATION

- Model nearfield
- Lake Michigan boundary
- Lake Michigan Basin boundary

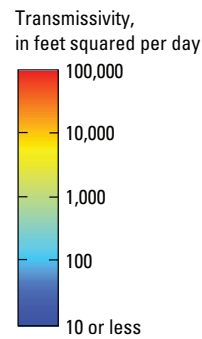


Figure 41B. Initial transmissivity distribution in aquifer system PENN.

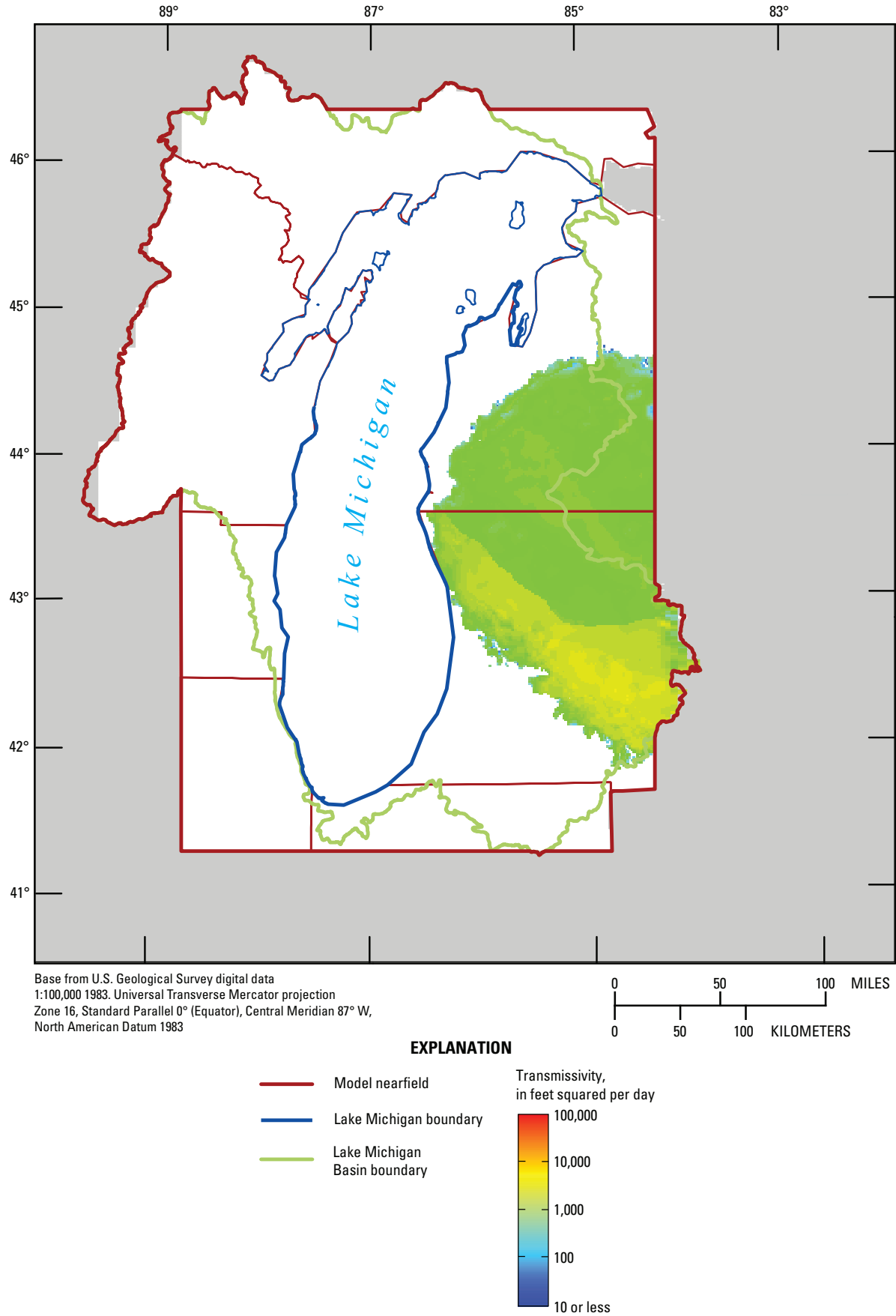
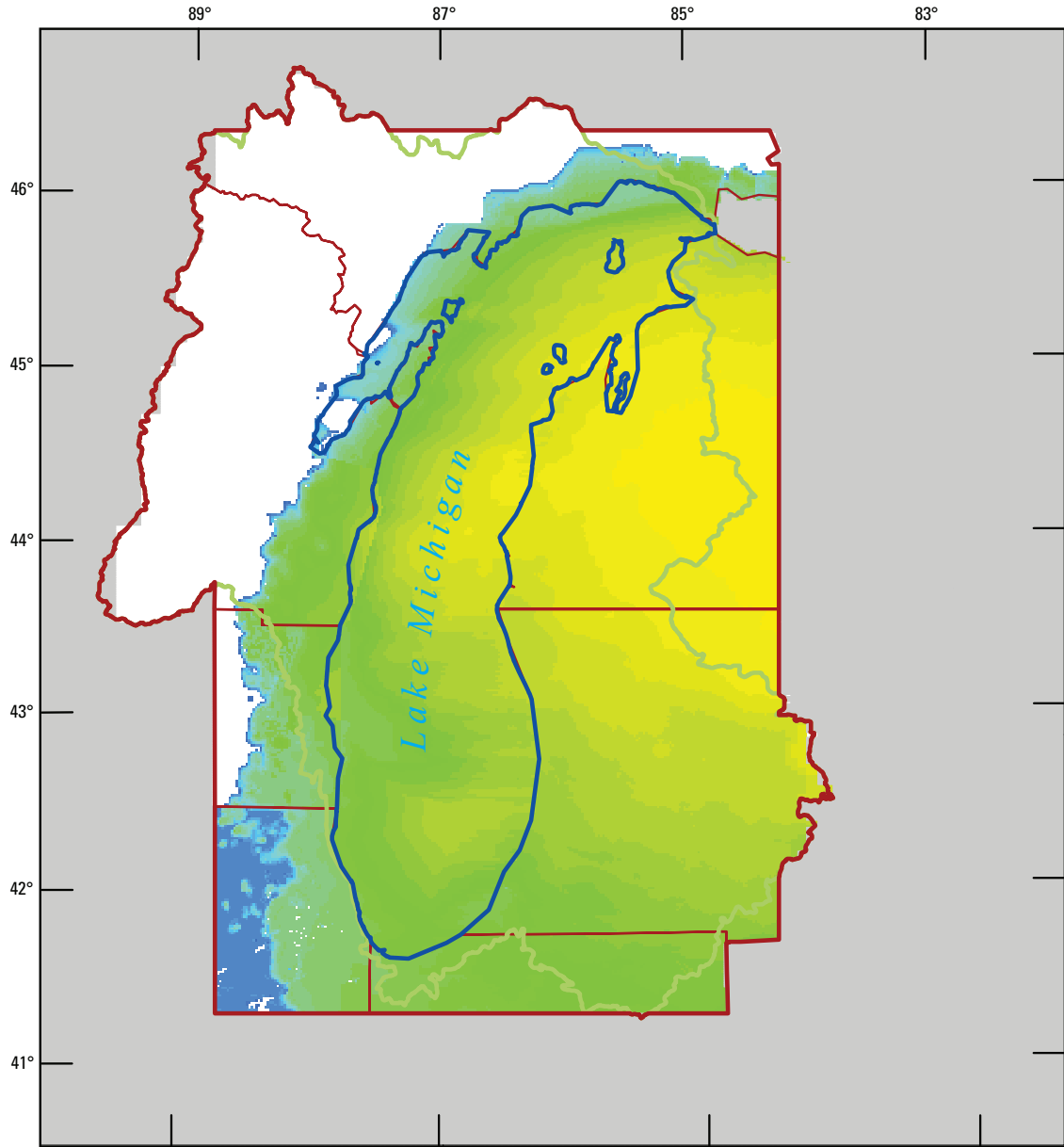


Figure 41C. Initial transmissivity distribution in aquifer system MSHL.



Base from U.S. Geological Survey digital data
 1:100,000 1983. Universal Transverse Mercator projection
 Zone 16, Standard Parallel 0° (Equator), Central Meridian 87° W,
 North American Datum 1983

EXPLANATION

- Model nearfield
- Lake Michigan boundary
- Lake Michigan Basin boundary

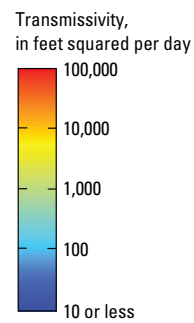


Figure 41D. Initial transmissivity distribution in aquifer system SLDV.

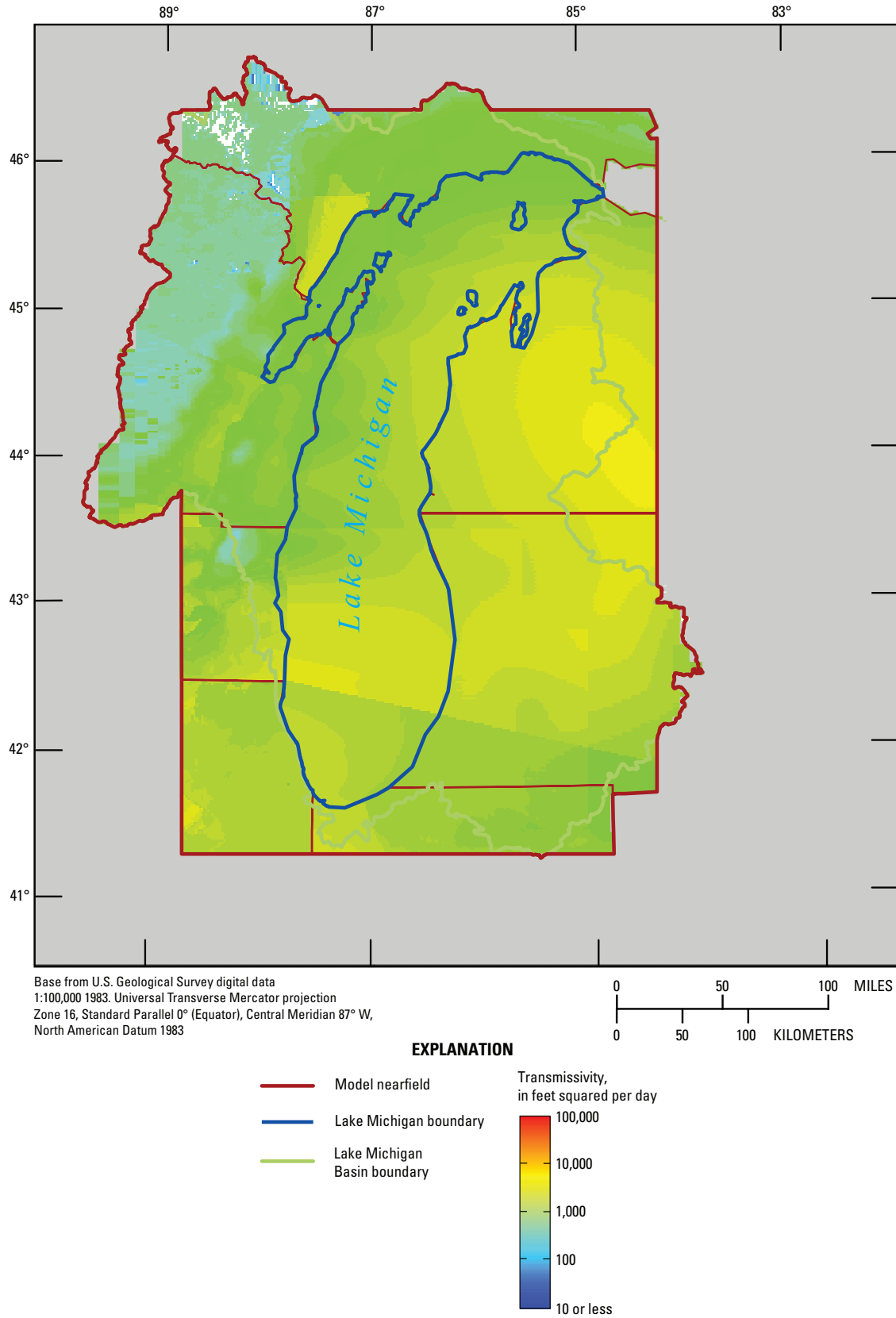


Figure 41E. Initial transmissivity distribution in aquifer system C-O.

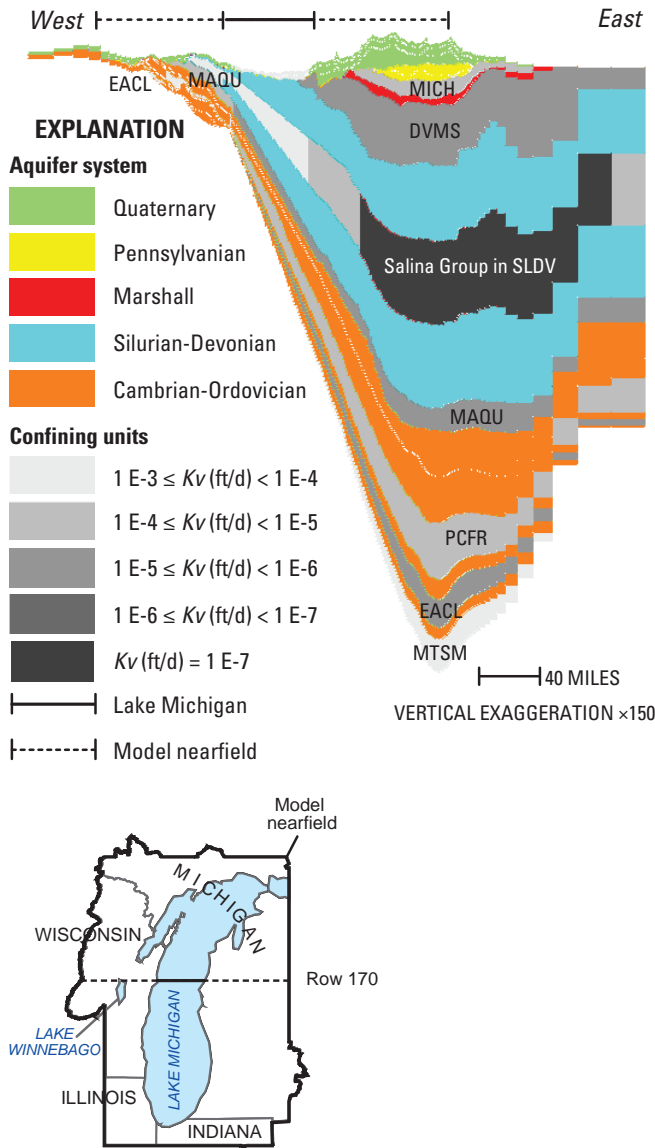


Figure 42. Initial vertical hydraulic conductivities in major confining units, row 170.

4.10 Salinity

The presence of saline water (including brines with concentrations greater than 100,000 mg/L) in the Michigan Basin and the potential interaction of the drawdown cones of pumping centers in freshwater zones with surrounding saline water motivate the use of the variable-density groundwater-flow model SEAWAT (Guo and Langevin, 2002; Langevin and others, 2003). SEAWAT is an adaptation of the USGS groundwater-flow model MODFLOW; it incorporates extra terms in the governing groundwater-flow equation to account for variable density and utilizes the transport code MT3D to simulate the movement of salinity as a solute. SEAWAT-2000 version 4 (Langevin and others, 2007) allows density to be a function of multiple dissolved species and the groundwater-flow equation

to respond to viscosity and temperature as well as density variations. The coupled flow and transport model invokes an equation of state that describes how fluid density varies with changes in solute concentration or fluid temperature.

For the Lake Michigan Basin model, the main interest from a water-availability viewpoint is the freshwater part of the system and its water levels, drawdown, and flow patterns. As a result, the saline water in other parts of the flow system can be viewed as boundary that influences the movement of groundwater toward surface-water features and pumping wells in the freshwater areas. Accordingly, the details of the circulation in the most saline part of the system are of secondary importance. The freshwater focus of the study leads to a simplification of SEAWAT whereby the water density in the system is fixed to always correspond to the salinity input to the model on the basis of available data. The density-dependent groundwater flow equation within SEAWAT is solved and the influence of saline water on the magnitude and direction of flow is simulated, but transport is not represented; thus, the density conditions within the saline water remain constant. The major assumptions implicit in this approximation are that pumping from deep wells does not significantly alter the salinity distribution and that the salinity distribution is stable during the 141-year transient simulations. These assumptions are tested and supported with an alternative fully coupled flow and transport model, which does simulate changes in density and concentration over time (presented in section 7). Additional work could be done to assess the effects of temperature and viscosity on the response of the system to pumping.¹⁹ Despite these omissions, it is posited that the consideration of fixed saline conditions by itself improves the ability of the simulation to approximate real processes when compared to a model that considers only freshwater conditions, because the SEAWAT solution more accurately simulates the response of the variable-density system to stresses, particularly to deep pumping.

The estimated density of the groundwater in areas of saline water is based on both dissolved solids concentration and density information (Lampe, 2009). Concentration data representing salinity can be converted to density with a simple linear equation of state (Baxter and Wallace, 1916):

$$\rho = \rho_o + EC$$

where

- ρ_o is the reference density,
- E is the density-concentration slope, and
- C is the concentration of the fluid.

To compute density from concentration, a reference density, corresponding to freshwater conditions (62.44 lb/ft³) is assumed, salinity is defined in dissolved solids concentration units of milligrams per liter (mg/L), and the density-concentration slope factor is set to 4.46 E-5 (lb/ft³)/(mg/L).

¹⁹ It also is unclear whether isostatic rebound induced by glacial unloading persists in the deep part of the Michigan Basin and whether it affects fluid movement in the saline waters of the Michigan Basin.

For example, a salinity of 10,000 mg/L corresponds to a fluid density of 62.78 lb/ft³, and a salinity of 400,000 mg/L corresponds to a fluid density of 80.28 lb/ft³. This linear equation is an approximation of the true relation between density and concentration, but it appears to hold even at brine concentrations close to halite saturation (Yager and others, 2007).

The distribution of dissolved solids concentrations for the LMB model domain presented by Lampe (2009) is interpolated from available data sources for the following units:

- QRNR in layer 1 (Waherer and others, 1996),
- PEN1 in layer 5 (Meissner and others, 1996),
- MSHL in layer 8 (Ging and others, 1996),
- SLDV in layer 11 (Gupta, 1993; Eberts and George, 2000; Schnoebelen and others, 1998),
- SNNP in layer 14 (Gupta, 1993; Visocky and others, 1985; Kammerer and others, 1998),
- PCFR in layer 16 (Gupta, 1993; Young, 1992; Kammerer and others, 1998), and
- MTSM in layer 19 (Gupta, 1993; Bond, 1972; Kammerer and others, 1998).

The concentrations in the remaining units are derived from layers presented above as follows:

- QRNR in layers 2 and 3 is equated with layer 1,
- JURA in layer 4 is the average of corresponding cells in layers 1 and 5,
- PEN2 in layer 6 is equated with layer 5,
- MICH in layer 7 is the average of corresponding cells in layers 5 and 8,
- DVMS in layer 9 and SLDV in layer 10 are the average of corresponding cells in layers 8 and 11,
- SLDV in layer 12 is equated with layer 11,
- MAQU in layer 13 is the average of corresponding cells in layers 11 and 14,
- STPT in layer 15 is the average of corresponding cells in layers 14 and 16,
- IRGA in layer 17 is equated with layer 16,
- EACL in layer 18 is the average of corresponding cells in layers 16 and 19,
- MTSM in layer 20 is equated with layer 19.

Sources of water in the model (recharge, the water induced from surface-water features and infiltrated water) are assigned salinities equal to zero. The only boundary that is

potentially affected by salinity is the constant-flow boundary representing underflow through bedrock systems along the southwestern part of the model. Even though it is not correct, the salinity of this flow is also assumed to be zero. However, the effect on simulated water levels is likely to be very small and localized (Christian Langevin, U.S. Geological Survey, written commun., February 12, 2009).

In order to be certain that mapped concentration transitions from layer to layer are stable, a 100-year transport simulation was run with the initial parameter assignments and steady-state conditions assumed (that is, no pumping). Assumed values for dispersivities in this transport simulation were 10 ft (longitudinal), 1 ft (transverse horizontal), and 0.1 ft (transverse vertical); the assumed value for molecular diffusion was 1.0 E-5 ft²/d; the assumed value for porosity and effective porosity was 0.2. The maximum transport time step was 1 year. After 100 years of coupled flow and transport simulation, less than 0.1 percent of the mass represented by the initial salinity distribution was lost by moving across the sides of the model. Within the domain, changes in concentration were extremely small, suggesting that the mapped concentrations are relatively stable. The transport simulation was eventually repeated by using calibrated parameter values (see section 5) with the same stable result. It is unlikely that changes in the initial concentration (density) distribution affect the results of the 141-year simulations described later in the report. For the final model runs, salinities were fixed to equal the results of the 100-year transport run with calibrated parameter values.

In general, salinity levels are much higher on the east side than the west side of Lake Michigan (table 10). There is also a striking vertical segmentation, with high salinity levels appearing only in the MSHL hydrogeologic unit and below (table 10). The spatial pattern is shown for four west/east hydrogeologic sections in figure 43. Dissolved solids concentrations in the Michigan Basin approach 500,000 mg/L in the evaporite-rich areas of the SLDV and in some underlying units, but concentrations are less than 10,000 mg/L west of Lake Michigan except in isolated parts of Wisconsin (see row 170) and in northeastern Illinois (see row 350). Concentrations in shallow units are highest to the east toward Lake Huron (row 170). The four sections also indicate saline conditions under Lake Michigan. Interpolation between available data points near the east and west shores of the lake indicates that concentrations can exceed 100,000 mg/L in bedrock units under the lake. The high density associated with such saline levels could affect the propagation of drawdown around deep pumping centers along the west shore of Lake Michigan, and, consequently, could distort the shape of source areas of water to these wells. One objective of the LMB model construction is to assess this possibility.

Table 10. Percentage of model nearfield that is saline west and east of Lake Michigan.

[Saline conditions correspond to model cells with concentrations greater than 10,000 milligrams per liter]

Layer	Aquifer system	Saline area west of Lake Michigan (percent)	Saline area east of Lake Michigan (percent)
1	QRNR	0.00	0.03
2	QRNR	.00	.05
3	QRNR	.00	.69
4	PENN	.00	.00
5	PENN	.00	.01
6	PENN	.00	.12
7	MSHL	.00	66.82
8	MSHL	.00	59.70
9	SLDV	.00	92.58
10	SLDV	.00	88.03
11	SLDV	.00	89.67
12	SLDV	.00	91.35
13	C-O	1.65	99.39
14	C-O	2.32	99.59
15	C-O	2.14	100.00
16	C-O	.46	99.15
17	C-O	.53	99.13
18	C-O	8.72	100.00
19	C-O	10.38	100.00
20	C-O	13.59	100.00

4.11 Model Input Packages, Program Executable, and Graphical Interface

The LMB model uses the following MODFLOW and MODFLOW-2000 packages:

- Basic (BAS6)
- Block-Centered Flow (BCF6)
- Recharge (RCH6)
- River (RIV6)
- General Head (GHB6)

- Well (WEL6)
- Multi-Node Well (MNW1)
- Discretization (DIS)
- Output Control (OC)
- Preconditioned Conjugate Gradient 2 (PCG2)

The Block-Centered Flow (BCF) package is used instead of the Layer Property Flow (LPF) package because with the BCF package the vertical conductance between layers is independent of the saturated thickness of each layer; this makes the numerical solution more stable, particularly in the case where deep layers dewater in response to pumping. The RIV package simulates exchange between the groundwater and surface-water systems. As explained above, in the case of water bodies (lakes and wetlands), the input to this package is adjusted so that it mimics the MODFLOW Drain package and only allows exchange to occur from the groundwater to the surface water. The WEL package is used for flux boundary conditions and for pumping wells (or for injection wells used to represent infiltration from surface impoundments) that penetrate a single layer. The MNW package is used for pumping wells that penetrate multiple layers. The MNW package is able to simulate flow through boreholes for both pumped and passive conditions, but it is invoked in the LMB model only for actively pumped wells. A special option in the OC package is invoked to reference simulated drawdown to the end of the first stress period; that is, to predevelopment conditions. The PCG2 solver package controls the path to convergence for each of the 61 model time steps. For example, it allows the user to dampen the maximum amount of head change allowed during iterations within a time step. Convergence is reached only when the maximum head change and flux change in all cells satisfy tolerance criteria. Discussion of the damping and tolerance criteria selected for this application is postponed to section 5 because these criteria are important elements of the calibration process.

One package called by the LMB model is specific to SEAWAT—the Variable Density Flow (or VDF) package. It depends on a file that contains cell-by-cell fixed densities converted from salinity concentrations by using the linear constitutive equation discussed above. Simulations are executed with version 4 of SEAWAT-2000, compiled by the USGS in November 2007. The internal calculations of SEAWAT-2000 are in double precision, but the output is in single precision. The platform used to visualize input and output is Ground Water Vistas version 5 (Rumbaugh and Rumbaugh, 2004, 2007).